



# **Exploring mTOR Signalling as a Targeted Approach Against Ovarian Cancer**

A thesis submitted for the degree of Doctor of Philosophy

by

**Karly-Rai Rogers-Broadway**

Department of Life Sciences

College of Health and Life Sciences

Brunel University

September 2015

## **Declaration**

I hereby declare that the research presented in this thesis is my own work, except where otherwise specified, and has not been submitted for any other degree.

Karly-Rai Rogers-Broadway

## **Dedication**

For Doug Brawley, who started it all.

And for Julie Davies, through whom all things are possible.

## Abstract

Ovarian cancer is the second most common gynaecological malignancy and was diagnosed in over 7000 women in 2011 in the UK. There are currently no reliable biomarkers available for use in a regular screening assay for ovarian cancer and due to characteristic late presentation (78% in stages III and IV) ovarian cancer suffers from a low survival rate (35% after 10 years). The mTOR pathway is a central regulator of growth, proliferation, apoptosis and angiogenesis; providing balance between available resources such as amino acids and growth factors, and stresses such as hypoxia, to control cellular behaviour accordingly. Emerging data links mTOR with the aetiopathogenesis of ovarian cancer. We hypothesised that mTOR inhibitors could play a therapeutic role in ovarian cancer treatment.

In this study we began by validating the expression of four main mTOR pathway components, mTOR, DEPTOR, rictor and raptor, at gene and protein level in *in vitro* models of endometrioid (MDAH-2774) and clear cell (SKOV3) ovarian cancer using qPCR and ImageStream technology. We demonstrate that MDAH-2774 cells have higher proliferative capacity than SKOV3 cells, suggesting different inherent signalling capacities. Using a wound healing assay we show that inhibition of the mTOR pathway using Rapamycin, rapalogues, Resveratrol and NVP BEZ-235 induces a cytostatic and not cytotoxic response up to 18 hours in these cell lines. We extended these findings up to 72 hours with a proliferation assay and show that the effects of inhibition of the mTOR pathway are primarily mediated by the dephosphorylation of p70S6 kinase. We show that mTOR inhibition does not involve alteration of mTOR pathway components or induce caspase 9 or 3 cleavage. Preclinical studies including ovarian tissue of ovarian cancer patients, unaffected controls and patients with unrelated gynaecological conditions show that DEPTOR is reliably upregulated in ovarian cancer. We also show that increased DEPTOR is a positive prognostic predictor in ovarian cancer and is decreased in later stage disease. Finally, we demonstrate that DEPTOR upregulation is mirrored in RNA extracted from whole blood of ovarian cancer patients. This in conjunction with the development of ultra-fast qPCR instrumentation can provide a valuable point of care testing platform for non-invasive diagnostics. A screening method that could provide early detection of ovarian cancer would represent a sea change in the diagnosis and treatment of this commonly lethal disease.

## Acknowledgments

Πρώτον, ένα μεγάλο ευχαριστώ στον Δρ. "αφεντικό" Καρτέρη, για την εποπτεία, την καθοδήγηση και την κατανόησή του. Δεν πίστευα ότι θα μπορούσα να το κάνω όλο αυτό, ευχαριστώ πολύ που το πιστέψατε για μένα.

(Firstly, thank you to Dr. Manos "The Boss" Karteris, for your supervision, guidance and understanding. I didn't know I could do this, thank you for knowing for me.)

To Richard Lewis, Nick Burroughs, Ian Gunter, Neil Mallon, Mark Otridge and Mike Nash at BJS Biotechnologies, thank you so much for all of your support. Who would have imagined that we would end up here?

Thank you to Dr. Julie Davies and Georgios Sotiriadis, you guys know what you mean to me, don't make me say it. And to Amanda Rozeik and Dimple Chudasama for all of your help. Thank you to Dr. Amanda Harvey, for being the mediating voice through all my head-spins. I appreciate what you've done.

A special thank you to Edward Pendragon Knowler and Sarah Driver, for being my connection to the real world of hospitals and medicine and reminding me that I don't operate in a vacuum.

Thank you to my wonderful family, I know you haven't always understood why I wanted to do this but you've never shown me anything but total love and support and I couldn't be more grateful. To my mum and dad, Leigh Stent and Dennis Broadway, your unending support means the world to me, I couldn't have done this without you. Also, to my step-dad Adrian, I promise to never tell mum where you hide the chocolate biscuits. To my beautiful siblings, Adam, Jessica and George, thank you for your encouragement and your acceptance, it means the world to me. And especially to George, my amazing little brother, always remember that you are much more intelligent than I am and I'm okay with that. To my Grandma Joanie and Grandad Bob, thank you for all of your support. And to my most excellent godmother, Helen Rowley, if I am half as kind and generous as you I'll consider myself a good person.

A special thank you to Dee Mann and Suzi Robertson, who listened and never doubted.

And to Joyce Sharpe, who knew I'd finish before I started, I miss you every day.

## Contents

Declaration	ii
Abstract	iv
Acknowledgments	v
Table of Contents	vi
List of Figures	xi
List of Tables	xv
List of Abbreviations	xvii
Publications Resulting From This Work	xx
Aims and Objectives	xxi
<b>1: Prolegomenon</b>	<b>1</b>
1.1: Ovarian Cancer	1
1.1.1: The Ovaries	1
1.1.2: Incidence of Ovarian Cancer	3
1.1.3: Severity and Advancement of Ovarian Cancer	4
1.1.4: Ovarian Cancer Survival	6
1.1.5: Ovarian Cancer Subtypes	8
1.1.6: Diagnosis of Ovarian Cancer	12
1.1.7: Ovarian Cancer Risk Factors	13
1.1.8: Treating Ovarian Cancer	15
1.1.8.1: Chemotherapy	15
1.2: Endometriosis	17
1.2.1: Diagnosing Endometriosis	19
1.2.2: Pathogenesis of Endometriosis	20
1.2.3: Treating Endometriosis	22
1.3: Endometriosis and Ovarian Cancer: The Connection	23
1.4: The mTOR Pathway	23
1.4.1: mTOR Complexes	24
1.4.1.1: mTOR	24
1.4.1.2: DEPTOR	25
1.4.1.3: GβL	25
1.4.1.4: Raptor	26
1.4.1.5: PRAS40	26
1.4.1.6: Rictor	26
1.4.1.7: mSIN1	26
1.4.1.8: Protor	27
1.4.2: Downstream of mTOR Complexes	30
1.4.2.1: mTORC1	30
1.4.2.2: mTORC2	31
1.4.3: Upstream of mTOR Complexes	33
1.4.3.1: mTORC1	33
1.4.3.1.1: TSC1/TSC2	33
1.4.3.1.2: The PI3 Kinase/Akt/mTOR Axis	33
1.4.3.1.3: The Ras/MAP Kinase Pathway	34
1.4.3.1.4: Stress Signals: Energy, Hypoxia and DNA Damage	34

1.4.3.1.5: Growth Signals: Nutrients and Amino Acids	36
1.4.3.2: mTORC2	37
1.5: Ovarian Cancer, Endometriosis and the mTOR Pathway	37
1.6: mTOR Pathway Inhibitors	40
1.6.1: Rapamycin and the Rapalogues	40
1.6.1.1: Rapamycin: Mechanism of Action	41
1.6.2: Dual mTOR and PI3 Kinase Inhibitors	42
1.7: Point of Care Diagnostics	47
1.7.1: qPCR	47
1.7.2: Thermal Cyclers	48
1.7.3: Point of Care Testing	49
<b>2: Methodology</b>	51
2.1: Tissue Culture	51
2.1.1: Cell Lines	51
2.1.2: Tissue Culture Practice	52
2.1.3: Thawing Cryopreserved Cells	52
2.1.4: Subculturing Cells	53
2.1.5: Cryopreserving Cells	53
2.2: Cell Treatments	53
2.2.1: Seeding Cells	53
2.2.2: Treating Cells	54
2.3: Proliferation Assay	55
2.4: Wound Healing Assay	55
2.5: Clinical Samples	56
2.5.1: Fresh Ovarian Tissues	56
2.5.2: Paraffin Embedded Ovarian Tissues	56
2.5.3: Whole Blood	60
2.6: RNA Extraction	60
2.6.1: RNA Extraction from Cultured Cells	60
2.6.1.1: GenElute™	60
2.6.1.2: Nucleospin®	61
2.6.2: RNA Extraction from Tissue Samples	62
2.6.3: RNA Extraction from Whole Blood	62
2.6.4: RNA Quantification	63
2.7: cDNA Synthesis	63
2.7.1: SuperScript® II	64
2.7.2: nanoScript™ 2	65
2.8: Protein Extraction	65
2.8.1: Laemmli Buffer	65
2.9: Reference Gene Assessment	66
2.9.1: geNorm	67
2.9.2: geNorm Analysis	69
2.10: qPCR	69
2.10.1: Primers	69
2.10.2: Gel Electrophoresis	70
2.10.3: Power SYBR® Master Mix	71

2.10.4: KAPA SYBR® Fast Universal Master Mix	72
2.10.5: qPCR Analysis	74
2.11: Western Blotting	75
2.11.1: Western Blot Analysis	81
2.12: ImageStream	81
2.12.1: Fixing Cells	81
2.12.2: Staining Cells	82
2.13: Immunohistochemistry	83
2.14: Statistical Analysis	85
<b>3: mTOR, DEPTOR, rictor and raptor expression in ovarian cancer models and in response to mTOR pathway inhibition</b>	<b>86</b>
3.1: Introduction	86
3.2: Objectives	87
3.3: Results	88
3.3.1: Confirmation of mTOR pathway component expression in SKOV3 and MDAH-2774 ovarian cancer cell lines	88
3.3.2: Gene expression of mTOR pathway components and mTOR pathway inhibition	90
3.3.2.1: mTOR Expression in SKOV3 Cells	93
3.3.2.2: mTOR Expression in MDAH-2774 Cells	95
3.3.2.3: DEPTOR Expression in SKOV3 Cells	98
3.3.2.4: DEPTOR Expression in MDAH-2774 Cells	100
3.3.2.5: Rictor Expression in SKOV3 Cells	103
3.3.2.6: Rictor Expression in MDAH-2774 Cells	105
3.3.2.7: Raptor Expression in SKOV3 Cells	108
3.3.2.8: Raptor Expression in MDAH-2774 Cells	110
3.3.3: Summary	113
3.4: Discussion	113
<b>4: The effects of mTOR pathway inhibition in <i>in vitro</i> models of ovarian cancer</b>	<b>115</b>
4.1: Introduction	115
4.2: Objectives	116
4.3: Results	116
4.3.1: Proliferation and migration of SKOV3 and MDAH-2774 cells in a wound healing scenario	116
4.3.1.1: SKOV3	117
4.3.1.2: MDAH-2774	118
4.3.2: Proliferative capacity of SKOV3 and MDAH-2774 cells after mTOR pathway inhibition	119
4.3.2.1: SKOV3	120
4.3.2.2: MDAH-2774	122
4.3.3: Activity of mTOR and caspase pathways after mTOR pathway inhibition	125
4.3.3.1: Caspase 9	125
4.3.3.1.1: SKOV3	126
4.3.3.1.2: MDAH-2774	128
4.3.3.2: Caspase 3	130



4.3.3.3: p70S6 Kinase	131
4.4: Discussion	132
<b>5: Mapping of mTOR, DEPTOR, rictor, raptor and p70S6 kinase at gene and protein level in ovarian cancer clinical samples</b>	137
5.1: Introduction	137
5.2: Objectives	138
5.3: Results	138
5.3.1: Analysis of reference gene stability in ovarian clinical tissue samples using the geNorm™ 12 gene kit	139
5.3.2: Gene expression analysis of mTOR, DEPTOR, rictor and raptor in ovarian tissue clinical samples from patients with ovarian cancer, endometrial cancer, endometriosis and fibroids	142
5.3.3: <i>In silico</i> analysis of mTOR pathway component gene expression levels in unaffected and ovarian cancer patients	145
5.3.3.1: mTOR	146
5.3.3.2: DEPTOR	147
5.3.3.3: Raptor	147
5.3.4: Protein expression analysis of mTOR, DEPTOR, rictor, raptor and p70S6 kinase in paraffin embedded ovarian tissue clinical samples from patients with ovarian cancer	148
5.3.4.1: mTOR	149
5.3.4.2: DEPTOR	152
5.3.4.3: Rictor	155
5.3.4.4: Raptor	156
5.3.4.5: p70S6 Kinase	158
5.3.5: <i>In silico</i> analysis of survival in relation to mTOR pathway component biomarker expression	161
5.3.5.1: mTOR Overall Survival	162
5.3.5.2: DEPTOR Overall Survival	163
5.4: Discussion	164
<b>6: Development of a PoCT platform for ovarian cancer</b>	169
6.1: Introduction	169
6.2: Objectives	173
6.3: Results	173
6.3.1: Reaction Efficiency and Time	173
6.3.2: Reaction Uniformity	176
6.3.3: Biomarker Detection in Whole Blood	180
6.4: Discussion	181
<b>7: General Discussion</b>	185
7.1: Why is this research important?	185
7.2: How is the mTOR pathway implicated in ovarian cancer?	185
7.3: What role does mTOR pathway inhibition play in the treatment of ovarian cancer?	186
7.4: How could CTCs form the basis of a PoCT for ovarian cancer?	187
7.5: What are the limitations of this research?	188
7.6: Future Directions	190

7.6.1: Increase sample size	190
7.6.2: Optimise PoC blood assay	191
7.6.3: Further elucidate the cytostatic effects of mTOR pathway inhibition	191
7.6.4: Use additional <i>in vitro</i> models to study the effects of mTOR pathway inhibition	192
7.6.5: Investigate the role of MAP kinase signalling in ovarian cancer	192
7.6.6: Elucidate the subcellular localisation of mTOR complexes	193
7.6.7: Investigate the stoichiometry of the DEPTOR/mTOR interaction	193
7.7: Concluding Remarks	194
<b>8: Bibliography</b>	196
<b>9: Appendix 1 - qPCR</b>	233
9.1: qPCR	233
9.2: Experimental Design	233
9.3: Amplification	235
9.4: Post-Amplification Controls	239

## List of Figures

### 1: Prolegomenon

1.1: Diagram of the ovary	2
1.2: Cases and rate of ovarian cancer diagnosis in the UK	3
1.3: The location and metastasis of ovarian cancer and the corresponding stage	5
1.4: Examples of high and low grade serous ovarian carcinoma	6
1.5: Ovarian cancer survival	7
1.6: Ovarian cancer survival by stage at diagnosis	8
1.7: Examples of serous, mucinous, endometrioid and clear cell carcinoma	8
1.8: New cases and deaths of ovarian cancer	12
1.9: Lifestyle and health related risk factors for ovarian cancer	14
1.10: Chemical structures of Carboplatin and Paclitaxel	16
1.11: The endometrium throughout the menstrual cycle	18
1.12: The common sites of ectopic endometrium implantation	19
1.13: Retrograde menstruation	21
1.14: The mTOR pathway	28
1.15: Inputs and outputs of mTORC1 signalling	36
1.16: The mTOR pathway in cancer	38
1.17: The mechanism of action of Rapamycin	42

### 3: mTOR, DEPTOR, rictor and raptor expression in ovarian cancer models and in response to mTOR pathway inhibition

3.1: Relative mTOR, DEPTOR, rictor and raptor gene expression in SKOV3 and MDAH-2774 cell lines	89
3.2: Representative images of mTOR, DEPTOR, rictor and raptor protein expression in SKOV3 and MDAH-2774 cell lines	90
3.3: Relative mTOR expression in SKOV3 cells following treatment with Rap, Eve and Def	93
3.4: Relative mTOR expression in SKOV3 cells following treatment with Tem, Res and BEZ	94
3.5: Relative mTOR expression in MDAH-2774 cells following treatment with Rap, Eve and Def	95
3.6: Relative mTOR expression in MDAH-2774 cells following treatment with Tem, Res and BEZ	96
3.7: Relative DEPTOR expression in SKOV3 cells following treatment with Rap, Eve and Def	98
3.8: Relative DEPTOR expression in SKOV3 cells following treatment with Tem, Res and BEZ	99
3.9: Relative DEPTOR expression in MDAH-2774 cells following treatment with Rap, Eve and Def	100
3.10: Relative DEPTOR expression in MDAH-2774 cells following treatment with Tem, Res and BEZ	101
3.11: Relative rictor expression in SKOV3 cells following treatment with Rap, Eve and Def	103
3.12: Relative rictor expression in SKOV3 cells following Tem, Res and	104

BEZ treatment	
3.13: Relative rictor expression in MDAH-2774 cells following Rap, Eve and Def treatment	105
3.14: Relative rictor expression in MDAH-2774 cells following Tem, Res and BEZ treatment	106
3.15: Relative raptor expression in SKOV3 cells following Rap, Eve and Def treatment	108
3.16: Relative raptor expression in SKOV3 cells following Tem, Res and BEZ treatment	109
3.17: Relative raptor expression in MDAH-2774 cells following Rap, Eve and Def treatment	110
3.18: Relative raptor expression in MDAH-2774 cells following Tem, Res and BEZ treatment	111
<b>4: The effects of mTOR pathway inhibition in <i>in vitro</i> models of ovarian cancer</b>	
4.1: Representative images of wound healing assay in SKOV3 cells	117
4.2: Representative images of wound healing assay in MDAH-2774 cells	118
4.3: Proliferation assay graph for SKOV3 cells following Rap, Eve and Def treatment	120
4.4: Proliferation assay graph for SKOV3 cells following Tem, Res and BEZ treatment	121
4.5: Proliferation assay graph for MDAH-2774 cells following Rap, Eve and Def treatment	122
4.6: Proliferation assay graph for MDAH-2774 cells following Tem, Res and BEZ treatment	123
4.7: Average viable cell increase of SKOV3 and MDAH-2774 cells after 72 hours	124
4.8: Representative images of western blots for caspase 9 in SKOV3 and MDAH-2774 cells	125
4.9: Densitometric analysis of western blots for caspase 9 in SKOV3 cells following Rap, Eve and Def treatment	126
4.10: Densitometric analysis of western blots for caspase 9 in SKOV3 cells following Tem, Res and BEZ treatment	127
4.11: Densitometric analysis of western blots for caspase 9 in MDAH-2774 cells following Rap, Eve and Def treatment	128
4.12: Densitometric analysis of western blots for caspase 9 in MDAH-2774 cells following Tem, Res and BEZ treatment	129
4.13: Representative images of western blots for caspase 3 in SKOV3 and MDAH-2774 cells	130
4.14: Representative images of western blots for p70S6 kinase in SKOV3 and MDAH-2774 cells	131
<b>5: Mapping of mTOR, DEPTOR, rictor, raptor and p70S6 kinase at gene and protein level in ovarian cancer clinical samples</b>	
5.1: geNorm M values for reference gene panel	140
5.2: geNorm V values for reference gene panel	141
5.3: Relative mTOR, DEPTOR, rictor and raptor gene expression in	142

ovarian cancer clinical samples	
5.4: Relative mTOR, DEPTOR, rictor and raptor gene expression in endometriosis clinical samples	143
5.5: Relative mTOR, DEPTOR, rictor and raptor gene expression in fibroids clinical samples	144
5.6: Relative mTOR, DEPTOR, rictor and raptor gene expression endometrial cancer clinical samples	145
5.7: Oncomine analysis of mTOR gene expression in ovarian carcinoma	146
5.8: Oncomine analysis of mTOR gene expression in ovarian serous cystadenocarcinoma	146
5.9: Oncomine analysis of DEPTOR gene expression in ovarian serous adenocarcinoma	147
5.10: Oncomine analysis of raptor gene expression in ovarian serous adenocarcinoma	147
5.11: Immunohistochemical analysis of mTOR expression in epithelial and germ cell tumours and representative images of staining	149
5.12: Immunohistochemical analysis of mTOR expression in grade I, II and III tumours and representative images of staining	150
5.13: Immunohistochemical analysis of mTOR expression in stage I, II, III and IV tumours and representative images of staining	151
5.14: Immunohistochemical analysis of DEPTOR expression in epithelial and germ cell tumours and representative images of staining	152
5.15: Immunohistochemical analysis of DEPTOR expression in grade I, II and III tumours and representative images of staining	153
5.16: Immunohistochemical analysis of DEPTOR expression in stage I, II, III and IV tumours and representative images of staining	154
5.17: Immunohistochemical analysis of rictor expression in grade I, II and III tumours and representative images of staining	155
5.18: Immunohistochemical analysis of raptor expression in epithelial and germ cell tumours and representative images of staining	156
5.19: Immunohistochemical analysis of raptor expression in grade I, II and III, and stage I, II, III and IV tumours and representative images of staining	157
5.20: Immunohistochemical analysis of phosphorylated p70S6 kinase expression in epithelial and germ cell tumours and representative images of staining	158
5.21: Immunohistochemical analysis of phosphorylated p70S6 kinase expression in grade I, II and III tumours and representative images of staining	159
5.22: Immunohistochemical analysis of phosphorylated p70S6 kinase expression in stage I, II, III and IV tumours and representative images of staining	160
5.23: Kaplan-Meier plot of overall survival and mTOR expression in ovarian cancer patients	162
5.24: Kaplan-Meier plot of overall survival and mTOR expression in	162

ovarian cancer patients with <i>TP53</i> mutation	
5.25: Kaplan-Meier plot of overall survival and DEPTOR expression in ovarian cancer patients	163
5.26: Kaplan-Meier plot of overall survival and DEPTOR expression in stage III and IV ovarian cancer patients	163
<b>6: Development of a PoCT platform for ovarian cancer</b>	
6.1: Three xxplate™ well configurations	170
6.2: xxplate™ electrical contact points	172
6.3: Heatmap images of two different xxplate™ current pathways	172
6.4: Standard curves of comparative qPCR experiments	175
6.5: Fluorescence uniformity of CFX96™ and 7900HT Fast thermal cyclers	177
6.6: Fluorescence uniformity of xxpress® and Rotor-Gene Q thermal cyclers	178
6.7: Average C <sub>q</sub> values of fluorescence uniformity qPCRs	179
6.8: Relative DEPTOR expression in whole blood and ovarian tissue of ovarian cancer patients	180
<b>7: General discussion and concluding remarks</b>	
7.1: Proposed patient screening stream	191
<b>9: Appendix – qPCR</b>	
9.1: Schematic representation of a typical three-step qPCR thermal protocol	237
9.2: Schematic representation of the stages of a qPCR reaction	238
9.3: An example of an amplification curve	239
9.4: An example of a dissociation curve	240

## List of Tables

### 1: Prolegomenon

1.1: Ovarian cancer staging parameters	4
1.2: Ovarian cancer grading parameters	5
1.3: Clinical details of the subtypes of ovarian cancer	11
1.4: Endometriosis staging parameters	20
1.5: mTOR pathway inhibitors	45

### Chapter 2: Methodology

2.1: Characteristics of SKOV3 and MDAH-2774 cell lines	52
2.2: mTOR pathway inhibitor concentrations	54
2.3: Details of clinical tissue samples	56
2.4: Details of paraffin embedded clinical tissue samples (20)	57
2.5: Details of paraffin embedded clinical tissue samples (70)	60
2.6: Primer/dNTP mix (Superscript® II)	64
2.7: First Strand Buffer mix (Superscript® II)	64
2.8: Extension buffer (nanoScript™ 2)	65
2.9: Laemmli buffer	66
2.10: Details of reference gene panel	66
2.11: Components of a qPCR reaction (geNorm)	68
2.12: The thermal protocol of qPCR experiment (geNorm)	68
2.13: Details of primers used in qPCR	70
2.14: Components of a qPCR reaction (Power SYBR® Master Mix)	71
2.15: The thermal protocol of a qPCR experiment (Power SYBR® Master Mix)	72
2.16: Components of a qPCR reaction (Kapa SYBR® Fast Master Mix)	73
2.17: The thermal protocol of a qPCR experiment (Kapa SYBR® Fast Master Mix)	73
2.18: Formulations of resolving and stacking gels	75
2.19: Formulation of 10X running buffer	76
2.20: Formulation of 1X wet-transfer buffer	77
2.21: Formulation of 10X TBS	77
2.22: Formulation of 1X TBS Tween	77
2.23: Details of antibodies used in western blotting	80
2.24: Formulation of solutions for enhanced chemiluminescence	80
2.25: Details of antibodies used in ImageStream	82
2.26: Incubations to deparaffinise and rehydrate paraffin embedded tissue	83
2.27: Formulation of antigen retrieval solution	83
2.28: Incubations to dehydrate stained tissue samples	85
2.29: The asterisk denotations of <i>p</i> values	85

### 3: mTOR, DEPTOR, rictor and raptor expression in ovarian cancer models and in response to mTOR pathway inhibition

3.1: Details of mTOR pathway inhibitors	91
3.2: Summary of gene expression changes	113

### 5: Mapping of mTOR, DEPTOR, rictor, raptor and p70S6 kinase at gene and protein level in ovarian cancer clinical samples

5.1: A summary of clinical samples	139
<b>6: Development of a PoCT platform for ovarian cancer</b>	
6.1: A summary of thermal cyclers compared	173
6.2: The thermal profile of comparative qPCR experiments	174
6.3: Summary of comparative qPCR experiments	176
<b>7: General discussion and concluding remarks</b>	
7.1: Examples of currently active clinical trials involving rapalogues	187
<b>9: Appendix – qPCR</b>	
9.1: A typical qPCR reaction formulation	235
9.2: A typical two-step qPCR thermal protocol	236
9.3: A typical three-step qPCR thermal protocol	237



## Abbreviations

<b>4EBP1</b>	4E binding protein 1	<b>DNA</b>	Deoxyribonucleic acid
<b>AMPK</b>	AMP-responsive protein kinase	<b>dNTP</b>	Deoxynucleoside triphosphate
<b>ARID1A</b>	AT rich interactive domain 1A	<b>DPX</b>	Di-N-butyl phthalate in xylene
<b>Atg13</b>	Autophagy related 13	<b>DTT</b>	Dithiothreitol
<b>ATP</b>	Adenosine triphosphate	<b>ECL</b>	Enhanced chemiluminescence
<b>BEZ</b>	NVP BEZ-235	<b>EDTA</b>	Ethylenediaminetetraacetic acid
<b>BMI</b>	Body mass index	<b>EGA</b>	European Genome-phenome Archive
<b>bp</b>	Base pairs	<b>EGF</b>	Epidermal growth factor
<b>BRAF</b>	B-Raf proto-oncogene, serine threonine kinase	<b>ELMO3</b>	Engulfment and cell motility 3
<b>BRCA</b>	Breast cancer, early onset	<b>EMA</b>	European Medicines Agency
<b>CA125</b>	Cancer antigen 125	<b>EMT</b>	Epithelial-mesenchymal transition
<b>CCC</b>	Clear cell carcinoma	<b>EIF-4E</b>	Eukaryotic translation initiation factor 4E
<b>CCDN1</b>	Cyclin D1	<b>EIF-4G</b>	Eukaryotic translation initiation factor 4G
<b>CDK1</b>	Cyclin dependent kinase 1	<b>EIF-4EBP1</b>	Eukaryotic translation initiation factor 4E binding protein 1
<b>CDKN2A</b>	Cyclin-dependent kinase inhibitor 2A	<b>EU</b>	European Union
<b>cDNA</b>	Complementary DNA	<b>Eve</b>	Everolimus
<b>CO<sub>2</sub></b>	Carbon dioxide	<b>FBS</b>	Foetal bovine serum
<b>C<sub>q</sub></b>	Quantification cycle	<b>FIGO</b>	International Federation of Gynecology and Obstetrics
<b>CTCs</b>	Circulating tumour cells	<b>FIP200</b>	FAK family kinase-interacting protein of 200 kDa
<b>CTNNB1</b>	Catenin beta 1	<b>FKBP12</b>	FK-506 binding protein 12
<b>DAB</b>	3,3'-Diaminobenzidine	<b>FRAP</b>	FK-506 binding protein 12- rapamycin-associated protein
<b>DAPI</b>	4',6-diamidino-2-phenylindole	<b>FRB</b>	- FKBP12 Rapamycin binding
<b>Def</b>	Deforolimus		
<b>DIE</b>	Deep infiltrating endometriosis		
<b>DMEM</b>	Dulbecco's Modified Eagle's Medium		
<b>DMSO</b>	Dimethyl sulfoxide		

**GAP** - GTPase activating protein

**GEO** - Gene Expression Omnibus

**GnRH** Gonadotrophin releasing hormone

**GOI** Gene of interest

**Grb10** Growth factor receptor-bound protein 10

**GTP** Guanosine triphosphate

**GβL** G protein beta subunit-like

**HGSC** High grade serous carcinoma

**HIF-1α** Hypoxia inducible factor 1 alpha

**HR** Hazard ratio

**HRP** Horseradish peroxidase

**HRT** Hormone replacement therapy

**IOSE** Immortalised ovarian surface epithelial

**IRS** Insulin receptor substrate

**KRAS** Kirsten rat sarcoma viral oncogene homologue

**LGSC** Low grade serous carcinoma

**LKB1** Liver kinase B1

**MAP** Mitogen activated protein

**MAPKAP1** Mitogen activated protein kinase associated protein 1

**MIQE** Minimum Information for the publication of Quantitative Real-Time PCR Experiments

**miRNA** MicroRNA

**mLST8** Mammalian lethal with SEC13 protein 8

**MMP** Matrix metalloproteinase

**mRNA** Messenger ribonucleic acid

**mSIN1** Mammalian stress-activated MAP kinase-interacting protein 1

**mTOR** Mechanistic target of Rapamycin

**mTORC** Mechanistic target of Rapamycin complex

**NHS** National Health Service

**NICE** National Institute for Health and Care Excellence

**NSAID** Non-steroidal anti-inflammatory drug

**NSCLC** Non-small cell lung cancer

**NTC** Non-template control

**OD** Optical density

**OS** Overall survival

**PBS** Phosphate buffered saline

**PCNA** Proliferating cell nuclear antigen

**PK1** PIP<sub>3</sub> dependent protein kinase 1

**PFA** Paraformaldehyde

**PFS** Progression free survival

**PI3 kinase** Phosphoinositide 3-kinase

**PIK3CA** Phosphatidylinositol-4,5-bisphosphate 3-kinase, catalytic subunit alpha

**PIP<sub>2</sub>** PtdIns 4,5-bisphosphate (PtdIns(4,5)P<sub>2</sub>)

**PIP<sub>3</sub>** PtdIns 4,5-bisphosphate (PtdIns(3,4,5)P<sub>3</sub>)

**PKB** Protein kinase B

**PKCα** Protein kinase C alpha

<b>PoC</b> Point of Care	<b>SD</b> Standard deviation
<b>PoCT</b> Point of Care Test(ing)	<b>SDS</b> Sodium dodecyl sulphate
<b>PPAR<math>\gamma</math></b> Peroxisome proliferator-activated receptor gamma	<b>SEER</b> Surveillance, Epidemiology and End Results Program
<b>PRAS40</b> Proline rich Akt substrate of 40kDa	<b>SREBP</b> Sterol regulatory element-binding protein
<b>Protor</b> Protein observed with rictor	<b>ST13</b> Suppression of tumorigenicity 13
<b>PRR5L</b> Proline rich 5 like	<b>TBE</b> Tris borate EDTA
<b>PtdIns</b> Phosphatidylinositide	<b>TBS</b> Tris buffered saline
<b>PTEN</b> Phosphatase and tensin homologue on chromosome ten	<b>TCC</b> Transitional cell carcinoma
<b>qPCR</b> Quantitative polymerase chain reaction	<b>TCGA</b> The Cancer Genome Atlas
<b>RAF1</b> Raf-1 proto-oncogene, serine/threonine kinase	<b>Tem</b> Temsirolimus
<b>Rap</b> Rapamycin	<b>TEMED</b> Tetramethylethylenediamine
<b>Raptor</b> Regulatory associated protein of TOR	<b>TERT</b> Telomerase reverse transcriptase
<b>Res</b> Resveratrol	<b>TIOSE</b> Telomerase immortalised ovarian surface epithelial
<b>Rheb</b> Ras homologue enriched in brain	<b>TP53</b> Tumour protein 53
<b>Rictor</b> Rapamycin insensitive companion of mTOR	<b>TSC1</b> Tuberous sclerosis complex 1
<b>RNA</b> Ribonucleic acid	<b>TSC2</b> Tuberous sclerosis complex 2
<b>RNF43</b> Ring finger protein 43	<b>ULK1</b> Unc-51 like autophagy activating kinase 1
<b>RQ</b> Relative quantity	<b>VEGF</b> Vascular endothelial growth factor

## Publications Resulting From This Work

- Amplification efficiency and thermal stability of qPCR instrumentation: Current landscape and future perspectives. **Rogers-Broadway KR**, Karteris E. *Exp Ther Med*. 2015 Oct;10(4):1261-1264.
- Differential effects of rapalogues, dual kinase inhibitors on human ovarian carcinoma cells in vitro. **Rogers-Broadway KR**, Chudasama D, Pados G, Tsolakidis D, Goumenou A, Hall M, Karteris E. *Int J Oncol*. 2016 May.

## Aims and Objectives

- To validate gene and protein expression of four key mTOR complex components (mTOR, DEPTOR, rictor and raptor) in two ovarian cancer cell lines as *in vitro* models of ovarian cancer.
- To investigate the effects of differential mTOR pathway inhibition on the wound healing capability, proliferative capacity, and markers of cell death and mTOR pathway activity to assess suitability as an ovarian cancer treatment.
- To investigate changes in gene and protein expression of key mTOR pathway components (mTOR, DEPTOR, rictor, raptor and phosphorylated p70S6 kinase) with a view to assessing their suitability as a biomarker of ovarian cancer disease.
- To assess the prognostic effects of mTOR pathway component expression using *in silico* Kaplan-Meier analysis.
- To assess four commercially available thermal cyclers for efficiency, correlation coefficient, speed and usability to evaluate their suitability as a point of care testing device.

# ***Chapter 1***

## ***Prolegomenon***

Despite the many medical advances made in the past 40 years, cancer still remains the most distressing diagnosis to receive. This is particularly true for ovarian cancer, where the 5 year survival rate remains alarmingly low at 46% and whose death rate has scarcely improved since the 1970s (Figure 1.8) (SEER, 2015c; CRUK, 2015h). Two main limitations of the treatment of all human disease are the time taken for diagnosis and the lack of insight into the interpatient variability that modulates response to therapeutics; to remedy this, much interest is now being taken in point of care (PoC) diagnostics. Point of Care Testing (PoCT), where a full diagnostic test is carried out in a single visit to a healthcare provider, is able to reduce the delay in central laboratory based assessment and improve patient outcomes through earlier and more appropriate commencement of treatment. PoCT is not currently a reality for ovarian cancer due to the lack of reliable biomarkers of disease. This is worsened by the mild and ambiguous symptoms associated with ovarian cancer which often go unnoticed or misdiagnosed. Here we discuss PoCT by quantitative polymerase chain reaction (qPCR), ovarian cancer and its strongly related risk factor, endometriosis, and how the mTOR (mechanistic target of Rapamycin) signaling pathway may be a useful bridge to connect ovarian cancer to a reliable PoCT.

### **1.1 Ovarian Cancer**

#### **1.1.1 The Ovaries**

The ovaries are female reproductive organs which sit bilateral to the uterus and superior to the vagina in the pelvic cavity. They are responsible for the development and release of ova, or female germ cells, into the fallopian tubes during ovulation and the release of the sex hormones oestrogens and

progesterone. Mammals have two ovaries which are encapsulated in an epithelial layer and alternate the release of an ova with each ~28 day menstrual cycle. Follicular cells in the ovary form a follicle containing a single germ cell in a process called folliculogenesis. As the germ cell matures, the follicular cells increase in number and develop into granulosa cells which nourish the germ cell. When the follicle has matured, it ruptures and releases the germ cell to the fallopian tube in a process called ovulation. This leaves an empty follicle known as a corpus luteum which continues to secrete sex hormones throughout the menstrual cycle (Tortora and Derrickson, 2005) (Figure 1.1).

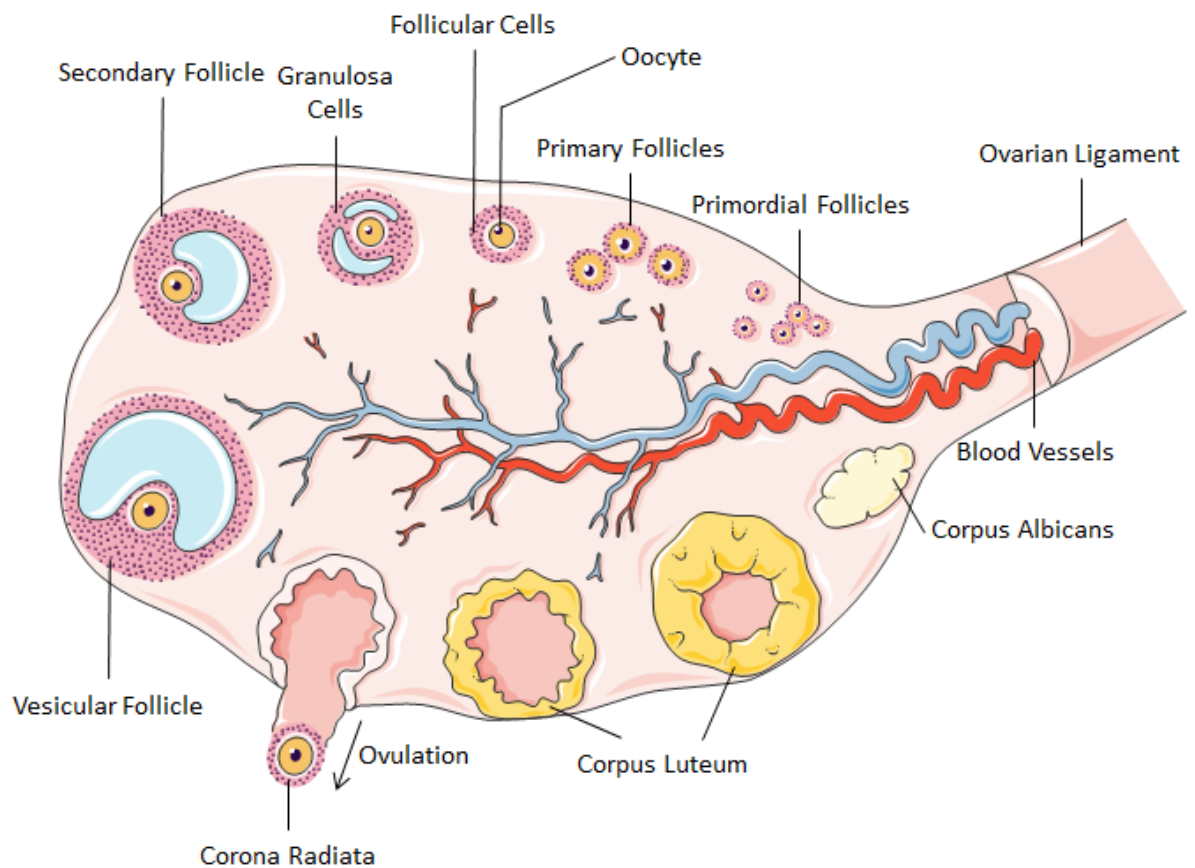


**Figure 1.1** - Diagram of the ovary showing the stages of follicular development (image adapted from Servier Medical Art, with permission).

Oestrogen and progesterone levels change throughout the menstrual cycle with oestrogen peaking just before ovulation and progesterone steadily increasing after ovulation has occurred. If fertilisation does not take place, oestrogen and progesterone return to basal levels and menstruation occurs. The ovaries cease to

produce oestrogen and progesterone at menopause, at which time menstruation and fertility terminates (Tortora and Derrickson, 2005).

### 1.1.2 Incidence of Ovarian Cancer

Ovarian cancer is the fifth most common female cancer and is diagnosed in more than 7,000 people in the UK every year (NHS Choices, 2013). Risk of ovarian cancer is increased when a first degree relative is affected, particularly in cases of serous disease and if presentation occurs under 50 years of age (Jervis *et al.*, 2014). Most commonly, ovarian cancer is epithelial in origin with other types accounting for only 10% of cases (CRUK, 2014b). Ovarian cancer is primarily a post-menopausal disease with the majority of cases occurring in patients over 60 years of age (Figure 1.2).

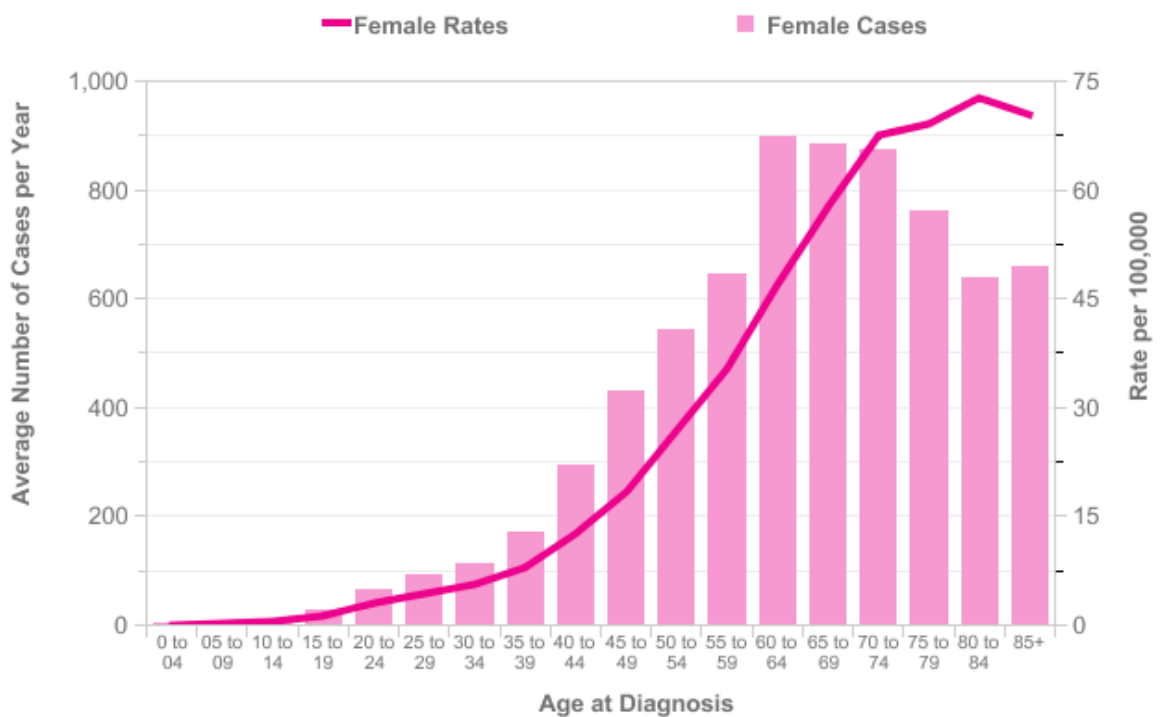


**Figure 1.2** - The average number of ovarian cancer cases diagnosed and the rate per 100,000 people in the UK in relation to age at diagnosis (CRUK, 2012, with permission). Ovarian cancer is primarily a post-menopausal condition with the majority of cases diagnosed in patients over 60 years of age.



### 1.1.3 Severity and Advancement of Ovarian Cancer

The severity of ovarian cancer metastasis is currently assessed using the International Federation of Gynecology and Obstetrics (FIGO) staging system detailed below (Table 1.1, Figure 1.3):

Stage	Substage	Description
<b>I</b>	Ia	The tumour is confined to one ovary with no signs of tumour on the surface.
	Ib	As Ia but involving both ovaries.
	Ic	The tumour is confined to one or both ovaries with either or all of the following: signs of the tumour on the surface of the ovary, rupture of tumour capsule before or during surgery, malignant cells found in ascites.
<b>II</b>	Ila	Metastasis outside the ovaries in the uterus or fallopian tubes.
	Ilb	Metastasis to pelvic cavity organs for example the bladder.
<b>III</b>	IIIa	Metastasis to retroperitoneal lymph nodes or microscopic malignancy found outside the pelvis.
	IIIb	Tumour smaller than or equal to 2cm found outside the pelvic cavity including surface of liver and/or spleen.
	IIIc	Tumour bigger than 2cm found outside the pelvic cavity including surface of liver and/or spleen.
<b>IV</b>	IVa	Pleural effusion (fluid around the lungs) positive for malignant cells.
	IVb	Metastasis to distant sites including extra-abdominal and parenchymal liver or spleen involvement.

**Table 1.1** - Ovarian cancer staging parameters as defined by FIGO (Society for Gynecologic Oncology, 2014).

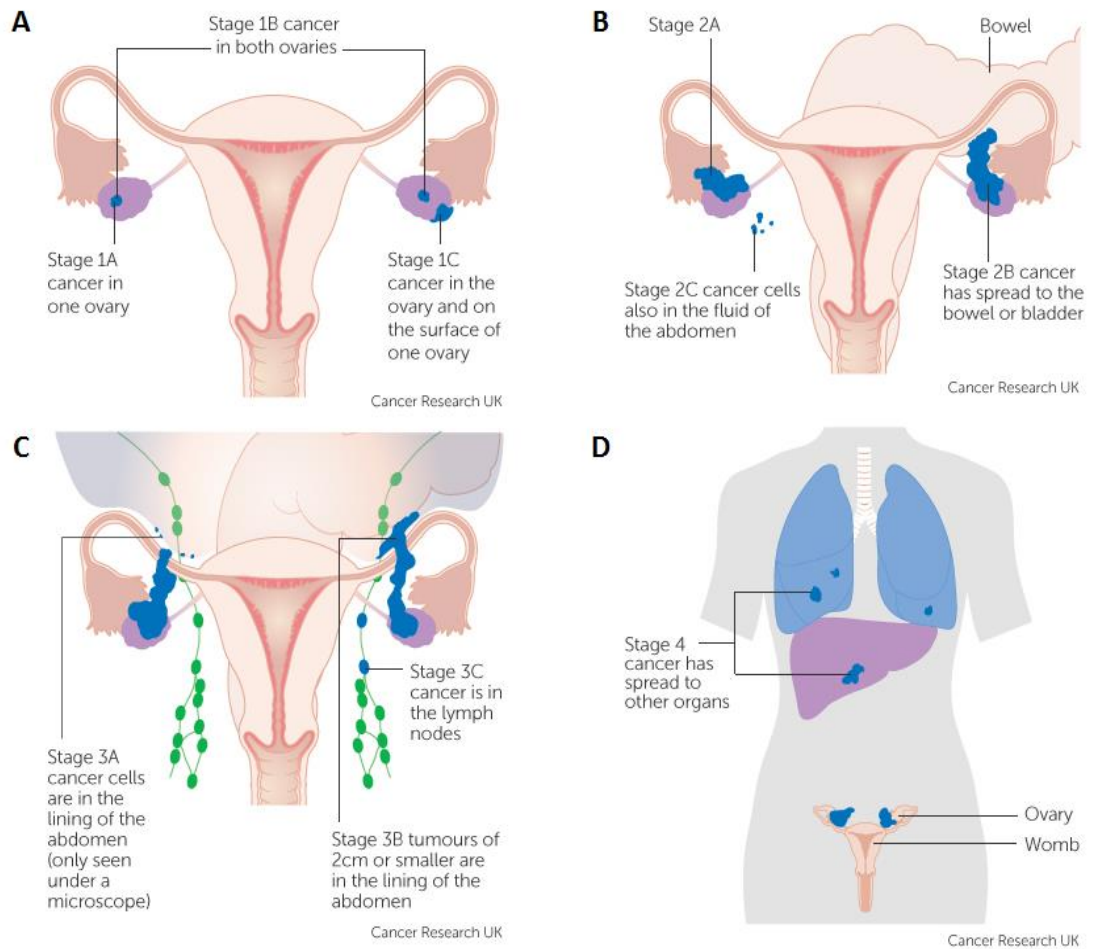


**Figure 1.3 - The location and metastasis of ovarian cancer and the corresponding stage. (A) Stage I ovarian cancer is confined to the ovaries. (B) Stage II ovarian cancer has metastasised to near locations within the pelvic cavity such as the fallopian tubes or bladder, (C) Stage III ovarian cancer has metastasised to the retroperitoneal lymph nodes or outside of the pelvic cavity, (D) Stage IV ovarian cancer involves malignant cells in pleural effusion and metastasis to distant sites. Diagram adapted from Cancer Research UK (CRUK, 2014a, with permission).**

In addition to stage, a patient can also be given a grade defining the level of differentiation of the tumour cells. Grades are defined as follows (Table 1.2):

Grade	Description
I	Well differentiated
II	Moderately differentiated
III	Poorly differentiated

**Table 1.2 - Ovarian cancer grading parameters (Table adapted from CRUK, 2014a, with permission).**

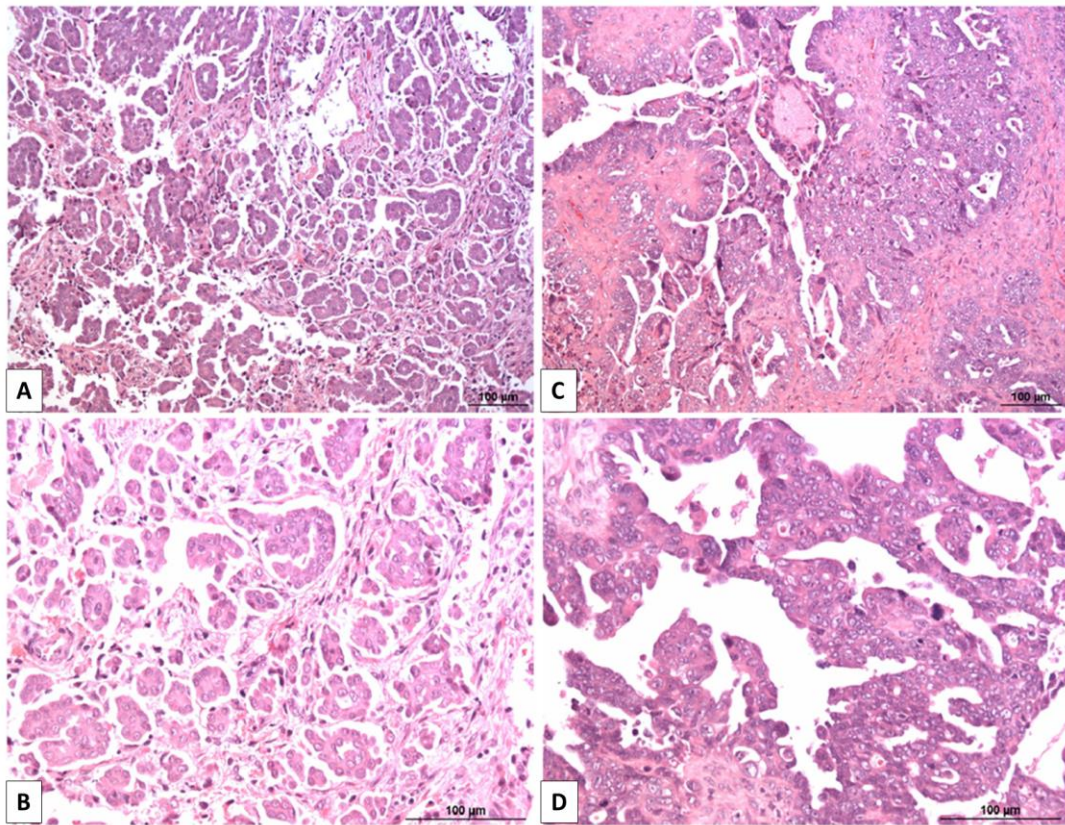


**Figure 1.4** - Haematoxylin and eosin stained examples of low grade (**A** [100X], **B** [200X]) and high grade (**C** [100X], **D** [200X]) serous ovarian carcinoma. High grade carcinomas show higher nuclear atypia and loss of papillary structure in comparison to low grade tumours (Image adapted from Smolle et al., with permission).

High grade tumours show a higher rate of nuclear atypia and proliferative rate in comparison to low grade tumours (Figure 1.4) (Smolle et al., 2013). Applying a stage and grade to a patient's cancer is a method of assessing prognosis and appropriate treatment type. Stage and grade cannot usually be confirmed prior to surgery and so this component of diagnosis is often combined with the first phase of treatment (NHS, 2015b). Common sites of ovarian cancer metastasis include the bowel, bladder, peritoneum and lymph nodes (Rose et al., 1989; CRUK, 2014a).

#### **1.1.4 Ovarian Cancer Survival**

Ovarian cancer survival rates are comparatively very low and ovarian cancer is the most common cause of death by gynaecological cancer in the UK (CRUK, 2015g).

The five and ten year survival rates are 46.2 and 34.5% respectively (Figure 1.5). This compares unfavourably to the five year survival rate of breast cancer (86.6%), prostate cancer (84.8%), bowel cancer (59.2%), cervical cancer (67.4%) and uterine cancer (79%) (CRUK, 2015c; CRUK, 2015i; CRUK, 2015b; CRUK, 2015d; CRUK, 2015k).

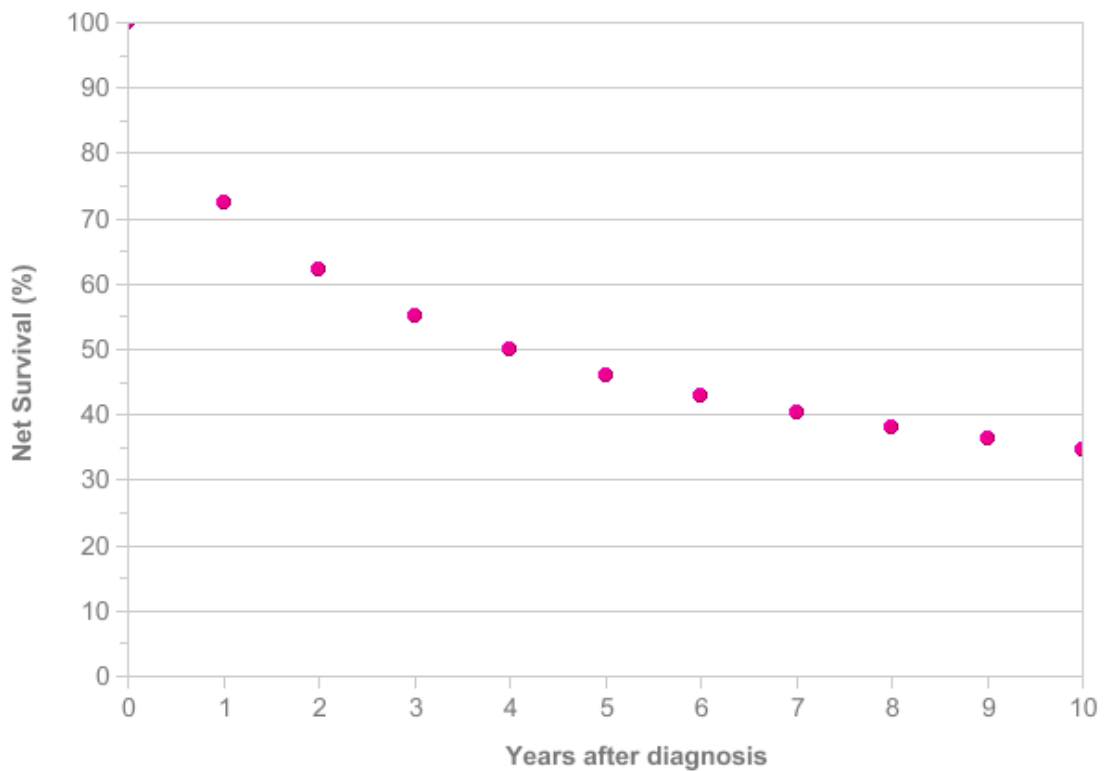


**Figure 1.5** - The net survival (years after diagnosis) of patients with ovarian cancer in the UK. One, five and ten year survival rates for ovarian cancer are 72.4, 46.2 and 34.5% respectively in the UK (CRUK, 2015h)

Ovarian cancer survival depends greatly upon the stage at which it is diagnosed. Survival for cancers diagnosed in stage I is 90% but only 4% for stage IV cancers in the UK (Figure 1.6) (CRUK, 2015h). Due to lack of overt symptoms, the majority of ovarian cancers (up to 78%) are diagnosed at stage III or IV (Buys *et al.*, 2011).

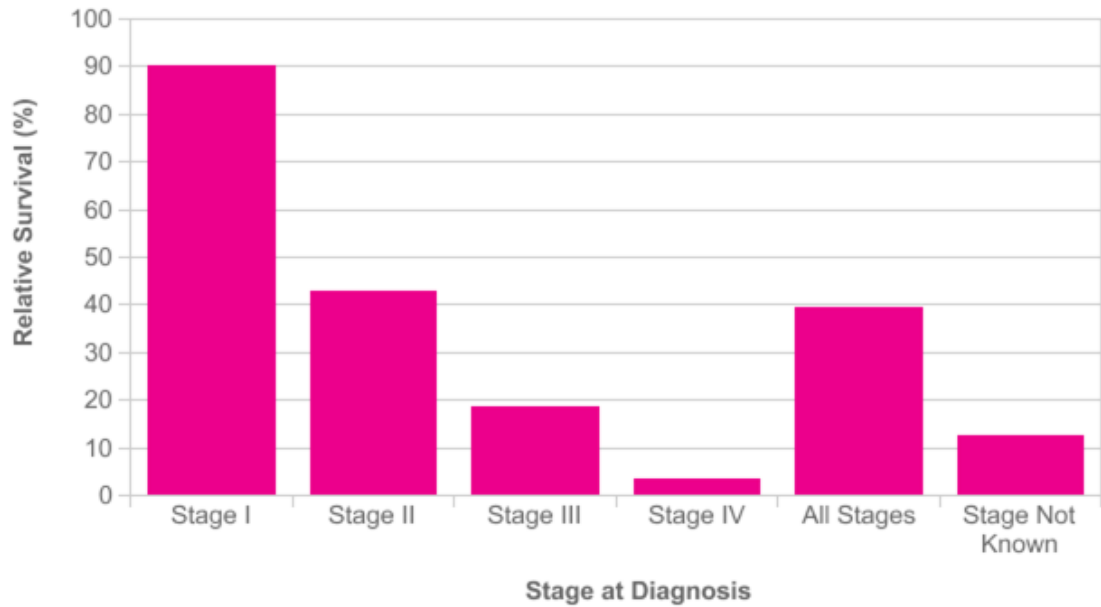


**Figure 1.6** - The ovarian cancer survival rates depending on the stage of disease at diagnosis. Survival is greatly reduced in patients diagnosed in later stages of disease (CRUK, 2015h).

#### 1.1.5 Ovarian Cancer Subtypes

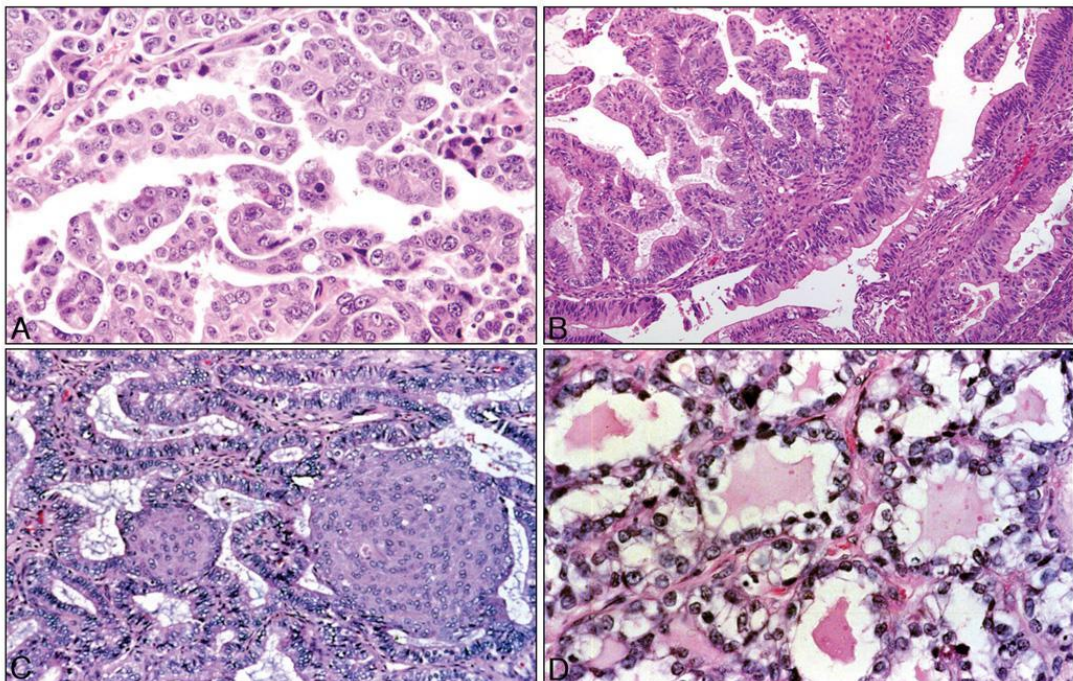


**Figure 1.7** - Histological preparations of haematoxylin and eosin stained ovarian cancer subtypes (A) serous carcinoma (B) mucinous carcinoma (C) endometrioid carcinoma (D) clear cell carcinoma (Cho, 2009, with permission).

Ovarian cancer is a highly heterogeneous disease originating from either epithelial, germ or stromal cells. Epithelial ovarian cancers account for up to 90% of all ovarian cancers (Weiss *et al.*, 1977; Rose *et al.*, 1989) and are subcategorised into four main types: serous, endometrioid, clear cell and mucinous (Figure 1.7, Table 1.3) (Lalwani *et al.*, 2011). The incidence of epithelial ovarian cancers increases with age; however, the same effect is not seen in non-epithelial ovarian cancers (Weiss *et al.*, 1977). Serous types are the most common among epithelial cancers, accounting for around 53-78% of cases and the majority of *BRCA* (breast cancer (1/2), early onset) gene related tumours are serous (Seidman *et al.*, 2004; Callahan *et al.*, 2007). Serous tumours are further categorised as high or low grade based on appearance of nuclei (nuclear atypia) and proliferative rate with high grade serous carcinomas (HGSCs) being more common than low grade serous carcinomas (LGSCs) (Malpica *et al.*, 2004; Plaxe, 2008). Serous ovarian cancer cells resemble surface epithelium of the fallopian tube and there is evidence that this category of tumour arises from the implantation of fallopian tube cells to the ovary (Vang *et al.*, 2009; Reade *et al.*, 2014; Malcolm Coppelson and C. Paul Morrow, 1992). HGSCs often involve tumour protein 53 (*TP53*) mutations that are not seen in LGSCs and LGSCs show a better survival than HGSCs (average 99 months and 57 months respectively) which is not related to stage of disease or metastasis (Salani *et al.*, 2008; Plaxe, 2008). LGSCs are more likely to show mitogen-activated protein (MAP) kinase pathway activation, commonly show mutation in Kirsten rat sarcoma viral oncogene homologue (*KRAS*) and B-Raf proto-oncogene, serine threonine kinase (*BRAF*) genes (Hsu *et al.*, 2004) and are less responsive to platinum based chemotherapies than HGSCs (Schmeler *et al.*, 2008; Santillan *et al.*, 2007).

Endometrioid and clear cell carcinomas (CCCs) are associated with endometriosis with up to 29-50% and 23-49% arising from endometriosis respectively (Machado-Linde *et al.*, 2015; Orezzaoli *et al.*, 2008; Acién *et al.*, 2015). Endometrioid carcinoma tissue resembles that of the endometrium (Malcolm Coppelson and C. Paul Morrow, 1992). *TP53*, AT rich interactive domain 1A (*ARID1A*), phosphatidylinositol-4,5-bisphosphate 3-kinase, catalytic subunit alpha (*PIK3CA*), catenin beta 1 (*CTNNB1*), cyclin D1 (*CCND1*) and phosphatase and tensin

homologue on chromosome ten (*PTEN*) gene deregulations are frequently associated with endometrioid carcinomas (Stewart *et al.*, 2013; McConechy *et al.*, 2014; Forbes *et al.*, 2015; COSMIC, 2015). CCCs account for around 10% of epithelial ovarian cancers and can be further categorised into cystic- and adenofibromata-associated types with cystic CCCs being more frequently associated with endometriosis (91% versus 44%) (Seidman *et al.*, 2004; Veras *et al.*, 2009). CCC tumours contain large, glycogen filled cells and are often present as mixed-cell tumours containing other cell types (Malcolm Coppleson and C. Paul Morrow, 1992). CCCs commonly show mutations in *ARID1A*, *PIK3CA*, telomerase reverse transcriptase (*TERT*), *TP53* and *KRAS* genes (Forbes *et al.*, 2015; COSMIC, 2015). CCC is an aggressive form of ovarian cancer with only a 73% 5 year survival rate for cases presenting at stage I (Kennedy *et al.*, 1999) compared to 90% for all types of ovarian cancer (CRUK, 2015h). Five year survival differs between cystic- and adenofibromata-associated CCCs (77% and 37% respectively) (Veras *et al.*, 2009). However, although endometriosis patients are more likely to develop CCC, endometriosis associated CCCs present 10 years earlier, are more likely to present at an earlier stage and show a better overall prognosis than *de novo* CCCs (Orezzoli *et al.*, 2008).

Mucinous carcinomas account for 10-15% of all epithelial ovarian cancers (Seidman *et al.*, 2004) and are characterised by *TP53*, *KRAS*, ring finger protein 43 (*RNF43*), cyclin-dependent kinase inhibitor 2A (*CDKN2A*) and *BRAF* gene mutations and may also show gastrointestinal markers (Forbes *et al.*, 2015; COSMIC, 2015; Tenti *et al.*, 1992). Cells of mucinous tumours resemble those of the endocervix but may also contain goblet cells similar to those found in the gastrointestinal tract (Malcolm Coppleson and C. Paul Morrow, 1992).

Cell of Origin	Type	Subtype	Associated Genes	Endometriosis Associated?	Age at presentation (years)	Response to platinum based therapies	Five year survival
Epithelial (90-95%)	Serous (40-60%)	High grade (90%)	<i>BRCA1, BRCA2, TP53</i>	No	56	Good	71%
		Low grade (10%)	<i>BRCA1, BRCA2, KRAS, BRAF</i>	No	45-63	Bad	
	Endometrioid (10-20%)	-	<i>TP53, ARID1A, PIK3CA, CTNNB1, CCND1, PTEN</i>	Yes	40-60	Good	62%
	Clear Cell (4-10%)	Cystic	<i>ARID1A, PIK3CA, TERT, TP53,</i>	Yes	58	Bad	77%
		Adenofibroma	<i>KRAS</i>	No			37%
Mucinous (10-15%)	-	<i>TP53, KRAS, RNF43, CDKN2A, BRAF</i>	No	40-50	Bad		
Germ (2.6%)	-	-	<i>KIT, KRAS, CDKN2A</i>	Not available	15-19	Not available	84%
Stromal (1.2%)	-	-	<i>FOXL2, DICER1, TP53</i>	Not available	30-59	Not available	88%

**Table 1.3** - Clinical details of the subtypes of ovarian cancer (Table adapted from Forbes *et al.*, 2015; COSMIC, 2015; Zwart *et al.*, 1998; Lalwani *et al.*, 2011; Guseh *et al.*, 2014; Plaxe, 2008; Schmeler *et al.*, 2008; Santillan *et al.*, 2007; Kennedy *et al.*, 1999; Seidman *et al.*, 2004; Hsu *et al.*, 2004; Machado-Linde *et al.*, 2015; Orezzaoli *et al.*, 2008; Acién *et al.*, 2015; Nakayama *et al.*, 2008; Quirk and Natarajan, 2005; Smith *et al.*, 2006; Sarwar *et al.*, 2014; Alexandre *et al.*, 2010).



### 1.1.6 Diagnosis of Ovarian Cancer

Ovarian cancer often presents with mild and ambiguous symptoms. NICE guidelines advise primary care providers to consider abdominal mass, distension or pain, ascites, early satiety or loss of appetite, urinary urgency or increased urinary frequency, change in bowel habits including apparent onset of irritable bowel syndrome, weight loss and fatigue as potential indications of ovarian cancer (NICE, 2011). Ovarian cancer can readily be mistaken for other, less serious conditions such irritable bowel syndrome. It is for this reason that ovarian cancer is often not diagnosed until it has reached stage III or IV, resulting in a poor prognosis (Buys *et al.*, 2011). The mortality rate has remained almost unchanged in the past 40 years with ovarian cancer deaths decreasing by only 2.4 persons per 100,000 in comparison to 10.1, 13.4 and 11.4 persons in breast, colon and prostate cancer respectively in the USA (Figure 1.8) (SEER, 2015c; SEER, 2015d; SEER, 2015b; SEER, 2015a). Despite this, there is currently no ovarian cancer screening programme available on the NHS.

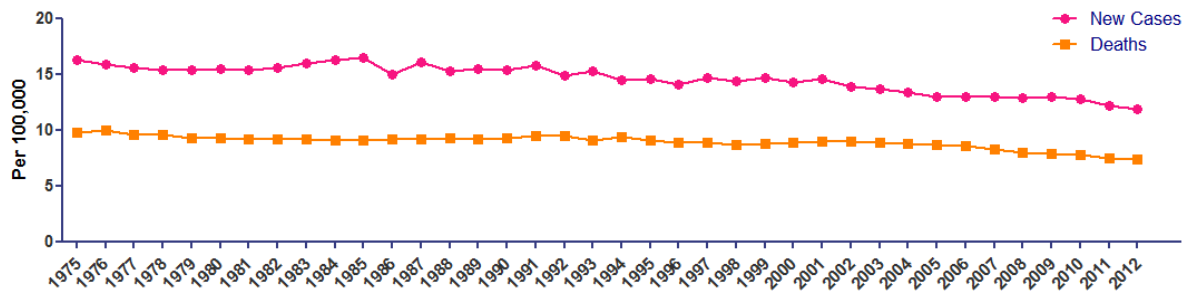


**Figure 1.8** - Graph plotted from SEER data (SEER, 2015c) of new cases and deaths per 100,000 persons associated with ovarian cancer from the SEER 9 registry (Atlanta, Connecticut, Detroit, Hawaii, Iowa, New Mexico, San Francisco-Oakland, Seattle-Puget Sound and Utah in the United States of America). Ovarian cancer 5 year survival has improved by 2.4 persons per 100,000 since 1975.

The lack of an ovarian cancer screening programme in the UK is, in part, due to an absence of known, reliable biomarkers for the disease. Cancer Antigen 125 (CA125), a membrane associated glycoprotein involved in cell adhesion, migration and metastasis, is commonly used to monitor disease progression in patients being treated for ovarian cancer and has been proposed as a good candidate for a

screening assay (Menon *et al.*, 2015; Giannakouros *et al.*, 2014; Reinartz *et al.*, 2012; Rump *et al.*, 2004; Gaetje *et al.*, 1999; Gaetje *et al.*, 2002). The efficacy of CA125, however, is a subject of debate as the propensity for false positives is high. Other conditions, such as heart failure, endometriosis and breast cancer, and demographic and lifestyle factors such as ethnicity, obesity and tobacco use, also raise CA125 levels (Folga *et al.*, 2012; Mol *et al.*, 1998; Johnson *et al.*, 2008). Greater than or equal to 35 units per mL of CA125 is considered to be abnormally high but Johnson *et al.*, found this to be the case in 1.6% of non-cancer individuals (Johnson *et al.*, 2008). An investigation into the benefits of ovarian cancer screening involving 68,557 patients showed that annual screening by CA125 and transvaginal ultrasound caused no reduction in mortality from ovarian cancer but substantially increased screening related harm (for example, 1080 patients underwent surgery based on false positive results) (Buys *et al.*, 2011). Recently, the development of a risk algorithm to determine abnormal CA125 levels in individual patients after annual measurement has been shown to double ovarian cancer detection, indicating that a universal CA125 threshold is not useful as an ovarian cancer screen (Menon *et al.*, 2015). Despite this, CA125 measurement is still recommended as the first-line diagnostic test for ovarian cancer with a universal threshold of 35U/mL by NICE (NICE, 2011).

In addition to CA125 measurement, NICE guidelines also recommend pelvic ultrasound for assessment of ovarian abnormalities. If CA125 measurement suggests pathology but ultrasound does not or *vice versa*, medics are advised to recommend the patient returns if symptoms persist or worsen (NICE, 2011). The use of non-specific testing with a high threshold for further investigation may contribute to the late diagnosis and low survival of ovarian cancer in the UK.

### **1.1.7 Ovarian Cancer Risk Factors**

As previously discussed, the risk of ovarian cancer increases with age (Figure 1.2). Ovarian cancer has a familial aspect and risk is increased when first degree relatives have been diagnosed with ovarian, breast or prostate cancer (Jervis *et al.*, 2014;

Hemminki *et al.*, 2011). Inherited mutations in the *BRCA1* and *BRCA2* genes have been shown to confer a 17-50 fold increased risk of ovarian cancer (Ingham *et al.*, 2013; Mavaddat *et al.*, 2013). Endometriosis is also an important risk factor for ovarian cancer, discussed in section 1.3. In addition to this, a number of lifestyle related factors are also known to increase or decrease the likelihood of developing ovarian cancer (Figure 1.9).

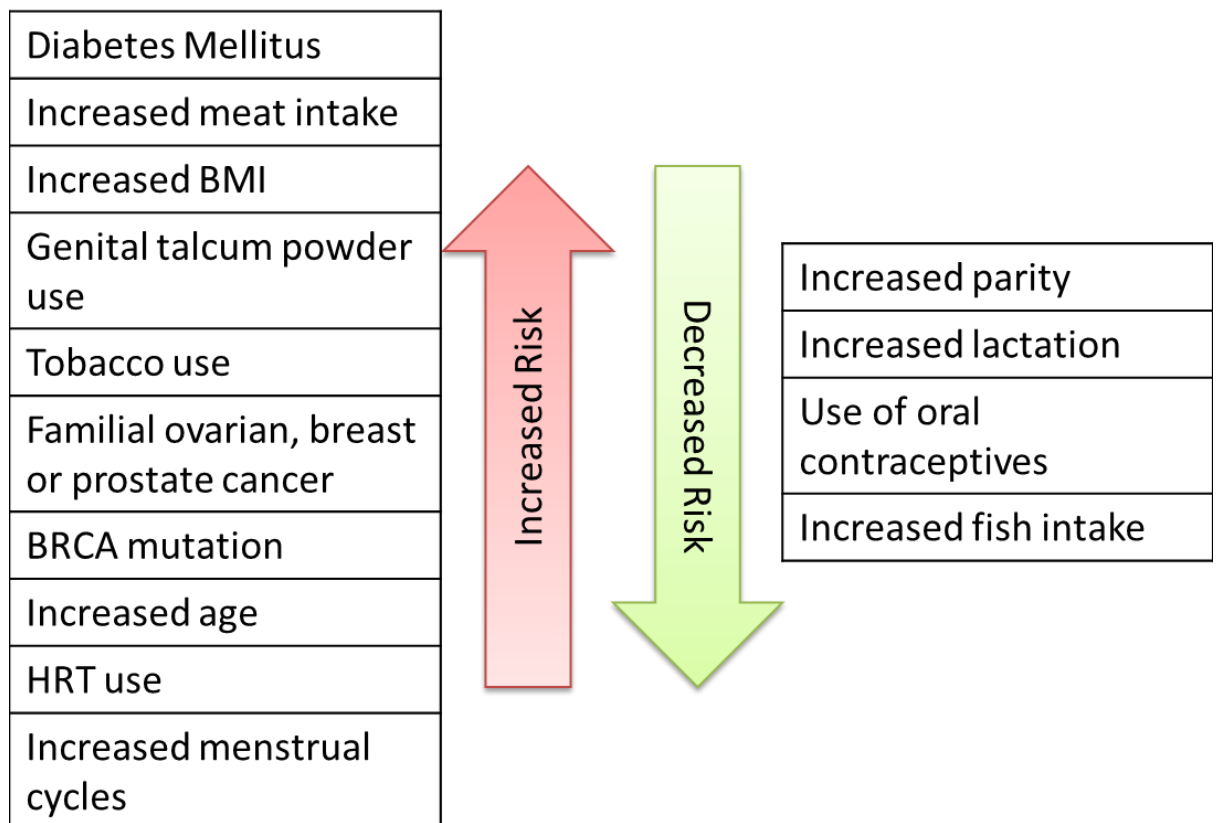


**Figure 1.9** - The lifestyle and health related factors which can increase or decrease ovarian cancer risk (CRUK, 2015f; Beral *et al.*, 2007; Collaborative Group on Epidemiological Studies of Ovarian Cancer, 2012; Terry *et al.*, 2013; Faber *et al.*, 2013; Starup-Linde *et al.*, 2013; CRUK, 2012; Ingham *et al.*, 2013; Mavaddat *et al.*, 2013; Jervis *et al.*, 2014; Hemminki *et al.*, 2011; Risch *et al.*, 1996; Tung *et al.*, 2003; Kurian *et al.*, 2005; Chiaffarino *et al.*, 2007; Beral *et al.*, 2007).

Some risk factors for ovarian cancer are subtype specific. For example, genital talcum powder use is more related to serous, clear cell and endometrioid types (Terry *et al.*, 2013), current and former tobacco use are related more to mucinous and serous subtypes (Faber *et al.*, 2013; Kurian *et al.*, 2005), the risk of serous ovarian cancer is greater than any other subtype with HRT (Beral *et al.*, 2007), and

pregnancy, use of oral contraceptives, increased breastfeeding and decreased menstrual cycles reduce the risk of all types of epithelial ovarian cancer except mucinous (Risch *et al.*, 1996; Tung *et al.*, 2003; Chiaffarino *et al.*, 2007).

### **1.1.8 Treating Ovarian Cancer**

In the UK, ovarian cancer is treated with a combination of surgery, chemotherapy and radiotherapy depending on the type and stage of cancer at diagnosis. Most patients will undergo primary debulking surgery to remove malignant tissue before further treatment (NHS, 2015b). As stage often cannot be determined without surgery, staging and debulking may be performed in the same operation (NHS, 2015b). Debulking surgery may include lateral or bilateral salpingo-oophorectomy (removal of one or both ovaries and fallopian tubes), total abdominal hysterectomy (removal of the uterus and cervix), omentectomy (removal of the fatty layer that lines the peritoneal cavity) and removal of the retroperitoneal lymph nodes (NHS, 2015b; NHS Choices, 2013). Early stage cancers may be treated with surgery only or surgery and adjuvant chemotherapy (Trimbos *et al.*, 2003; NICE, 2011). Late stage ovarian cancers may be treated with a combination of neoadjuvant chemotherapy, debulking surgery, adjuvant chemotherapy and interval debulking surgery (where debulking surgery is performed during a course of chemotherapy) (CRUK, 2015j; NHS, 2015b). If the ovarian cancer is too advanced or the patient is unable to undergo surgery due to extraneous risk factors, radiotherapy may be used as a form of palliative care (CRUK, 2015j).

#### **1.1.8.1 Chemotherapy**

Chemotherapy is used in the treatment of almost all ovarian cancers. Platinum based chemotherapeutic drugs are most commonly used including Carboplatin, a platinum containing analogue of Cisplatin (Figure 1.10, A) (CRUK, 2015e) which induces DNA damage and causes apoptosis through the formation of adducts between DNA bases (Reed *et al.*, 1987; Unger *et al.*, 2009; Hamada *et al.*, 1998; Siemer *et al.*, 1999). In addition to Carboplatin, Paclitaxel is also used as a

combination chemotherapy (Figure 1.10, B) (CRUK, 2015e). Paclitaxel is the active compound in Taxol, an extract of the bark of the Pacific Yew tree, *Taxus brevifolia*. Paclitaxel promotes the assembly and inhibits the depolymerisation of microtubules in the cell (De Brabander *et al.*, 1981; Schiff and Horwitz, 1980; Parness and Horwitz, 1981; Kumar, 1981). Treatment with Paclitaxel results in cell cycle arrest at G<sub>2</sub>/M phase and ultimately apoptosis (Schiff and Horwitz, 1980; Havrilesky *et al.*, 1995; Ireland and Pittman, 1995). Paclitaxel was first approved for use by the European Medicines Agency (EMA) in 1999 under the brand name Paxene and now marketed as Abraxane (European Medicines Agency, 2015a).

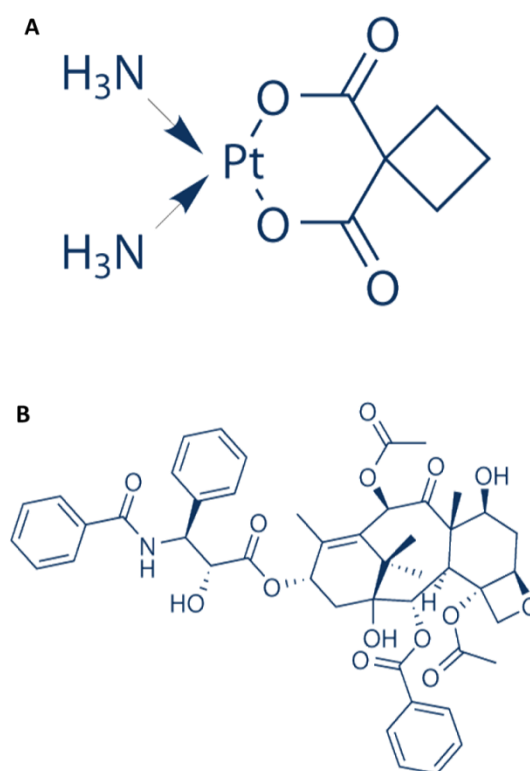


**Figure 1.10** - Chemical structures of Carboplatin (A) and Paclitaxel (B). Images adapted with permission from selleckchem.com.

Bevacizumab (Avastin) may be used as a combination treatment for ovarian cancer (CRUK, 2015e; CRUK, 2015j). Bevacizumab is a monoclonal antibody vascular endothelial growth factor (VEGF) inhibitor which is administered intravenously in three weekly cycles (CRUK, 2015a). VEGF is a growth factor responsible for the

initiation of angiogenesis, an important feature of tumour development, via VEGF receptors (Claffey and Robinson, 1996; Pecorino, 2008). Inhibiting VEGF suppresses tumour growth by blocking cell survival, endothelial permeability and cellular migration (Presta *et al.*, 1997; Wang *et al.*, 2004). Bevacizumab has shown moderate improvement in progression free survival (the cessation of disease progression brought about by treatment) in ovarian cancer patients (Petrillo *et al.*, 2015) and NICE (National Institute for Health and Care Excellence) currently recommends the use of bevacizumab in the treatment of early stage ovarian cancer (NICE, 2013).

## **1.2 Endometriosis**

The endometrium is the lining of the uterus which proliferates during the menstrual cycle in anticipation of zygote implantation and pregnancy. Endometrium consists of a basal layer (*stratum basalis*) which gives rise to a new functional layer (*stratum functionalis*) which proliferates in response to oestrogens and progesterone with each menstrual cycle. If fertilisation does not occur, oestrogen and progesterone return to basal levels due to the degeneration of the corpus luteum, stimulating the release of prostaglandins and causing a reduction in blood supply to the *stratum functionalis*. This results in endometrial cell death and the *stratum functionalis* of the endometrium is discharged via the vagina (Figure 1.11) (Tortora and Derrickson, 2005).

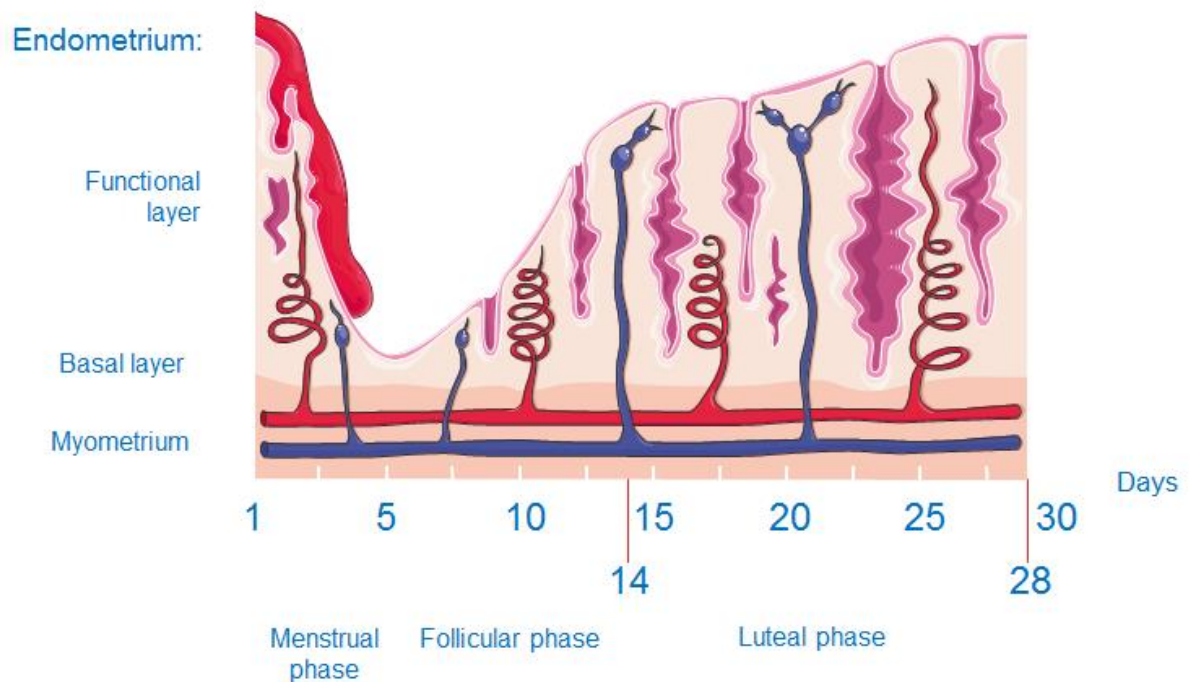


**Figure 1.11** - The stages of endometrium development throughout the menstrual cycle. The menstrual cycle begins with the menstrual phase, during which the stratum functionalis is shed and discharged via the vagina. The preovulatory (follicular) phase follows menstruation during which oestrogen stimulates proliferation of the stratum basalis to form a new stratum functionalis including endometrial glands and arterioles. Ovulation occurs at approximately 14 days and signifies movement into the postovulatory (Luteal) phase. At this time, the endometrium further proliferates and vascularises in preparation of ovum implantation. If fertilisation has not occurred, the menstrual phase begins once again (Tortora and Derrickson, 2005) (image adapted from Servier Medical Art, with permission) (Servier, 2014).

Endometriosis is a non-malignant condition characterised by the ectopic implantation and growth of endometrial tissue in locations within the abdominal cavity such as the fallopian tubes, ovaries, peritoneum, vagina, bladder, bowel and rectum (Figure 1.12). Ectopic endometrium responds to hormonal changes in the same way as eutopic endometrium, by proliferating and shedding with the menstrual cycle causing pain and inflammation in the affected areas. Symptoms of endometriosis include dysmenorrhea (pain during menstruation), dyspareunia (pain during sexual intercourse), dysuria (pain during urination), dyschezia (pain during defecation), infertility and chronic pelvic pain as well as an increased risk of

allergies, asthma, fibromyalgia, autoimmune disease, hypothyroidism, multiple sclerosis and chronic fatigue syndrome (Sinai *et al.*, 2002). Endometriosis is estimated to affect around 2 million people in the UK (NHS Choices, 2015).

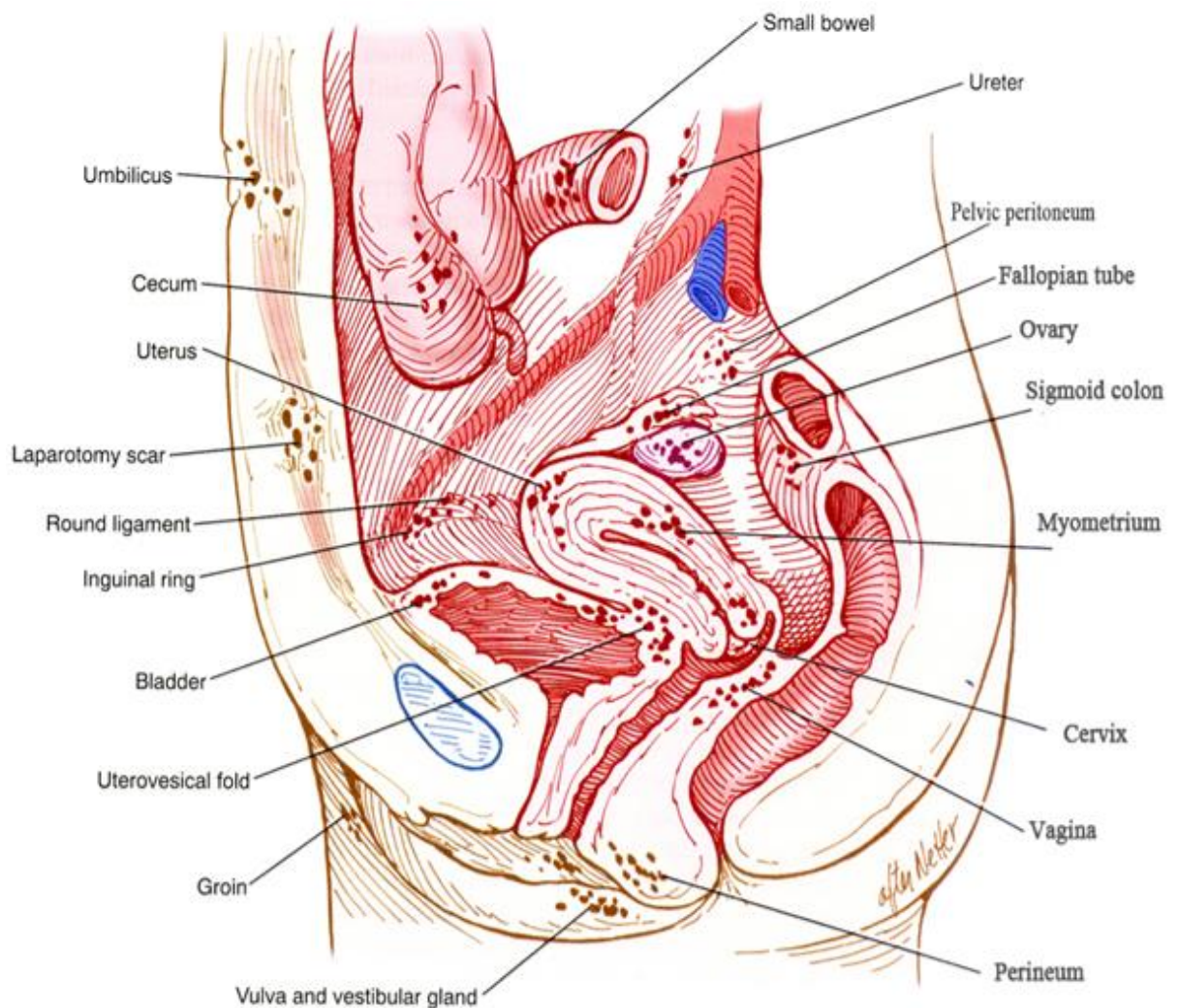


**Figure 1.12** - The common sites of ectopic endometrium implantation in cases of endometriosis (Berek, 2007, with permission).

### 1.2.1 Diagnosing Endometriosis

Diagnosis of endometriosis can only be confirmed surgically by laparoscopy. Endometriosis is currently assessed and classified into one of four stages using guidelines set out by the American Society for Reproductive Medicine (American Society for Reproductive Medicine, 1997) as follows (Table 1.4):



Stage	Description
I (1-5 points)	Minimal: superficial lesions of less than 1cm in the ovary or 1-3cm in the peritoneum.
II (6-15 points)	Mild: deeper implantation and lesions of greater than 3cm.
III (16-40 points)	Moderate: implication of the larger pelvic area.
IV (>40 points)	Severe: deep, dense and infiltrating lesions.

**Table 1.4** - Endometriosis staging parameters as defined by ASRM (American Society for Reproductive Medicine, 1997). Stage is given according to a points based system which relate to the location and infiltration of adhesions.

### 1.2.2 Pathogenesis of Endometriosis

Many theories have been proposed as the cause of endometriosis. The most accepted theory on the mechanism of development, proposed in 1927 by Sampson, is retrograde menstruation where shed endometrium travels into the pelvic cavity via the fallopian tubes and implants on neighbouring organs and structures (Figure 1.13) (Sampson, 1927). The endometriotic lesions can then amplify the symptoms by releasing additional endometrium into the pelvic cavity which can then create further lesions (Burney and Lathi, 2009). This theory is supported by the viable proliferative capacity noted in shed endometrium (Koks *et al.*, 1999; Koks *et al.*, 1997; Groothuis *et al.*, 1999) and the observation that patients with obstructive anomalies of the reproductive tract which do not allow for effective discharge of the endometrium are more likely to develop endometriosis (D'Hooghe and Debrock, 2002). However, it is not clear if retrograde menstruation happens more frequently in patients with endometriosis or if there are other factors which predispose to a higher likelihood of ectopic endometrium implantation (D'Hooghe and Debrock, 2002).

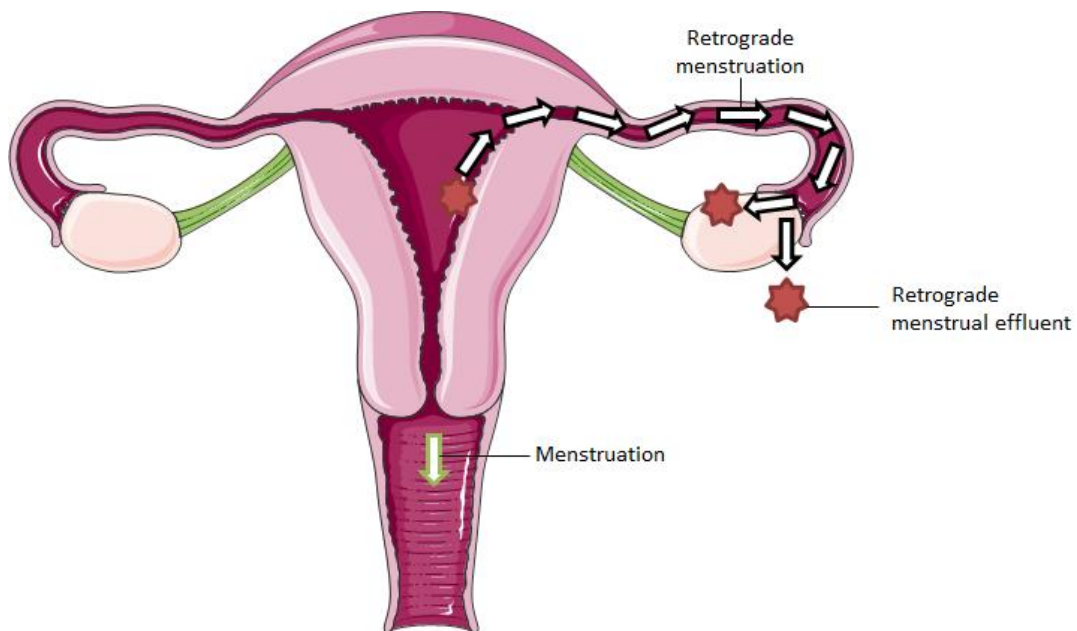


**Figure 1.13** - Retrograde menstruation is the most accepted theory of the pathogenesis of endometriosis. Typical menstruation occurs when the stratum functionalis of the endometrium is discharged via the vagina. Retrograde menstruation involves menstrual effluent travelling into the pelvic cavity via the fallopian tubes and implanting on nearby organs such as the ovaries (image adapted from Servier Medical Art, with permission) (Servier, 2014).

The peritoneum is the lining of the abdominal cavity and often the site of endometrial implantation in endometriosis. It consists of a basement support of areolar connective tissue covered by a single layer of squamous epithelial cells known as the mesothelium (Tortora and Derrickson, 2005). It has been shown that endometrium adheres to the peritoneum only in places where there is damage (i.e. absence of the mesothelial layer) (Koks *et al.*, 1999; Groothuis *et al.*, 1999) indicating that the endometrium cannot adhere to epithelial cells and this layer may provide protection from retrograde menstrual effluent. In support of this, it has also been shown that conditioned media from menstrual effluent changes the morphology of mesothelial cells in culture from a confluent polygonal monolayer to spindle-like cells which do not necessarily adhere to one another and expose the culture flask underneath (Demir Weusten *et al.*, 2000). This suggests an interesting relationship between retrograde menstrual effluent and site of implantation whereby endometrial cells are able to create damage in order to adhere and proliferate.

The genetic profile that characterises endometriosis is poorly understood; there is a familial element with up to a 6 fold increase in risk for first degree relatives of endometriosis patients but inheritance patterns are complex and it is likely that environmental factors also play a role (Dun *et al.*, 2010). Whole exome sequencing of the eutopic and ectopic endometrium of 16 cases of ovarian endometriosis could identify no significant mutations in either sample set (Li *et al.*, 2014). However, gene expression studies in baboons have found significant alterations in the EGF (epidermal growth factor), PI3 kinase/Akt, and MAP kinase pathways in eutopic endometrium upon the onset of endometriosis (Afshar *et al.*, 2013). Dinulescu *et al.*, found that inducing K-Ras activation in the ovarian surface epithelial cells of mice induced an endometriosis-like condition which was benign and never fatal (Dinulescu *et al.*, 2005). K-Ras is an oncogenic protein which is upstream of mTOR and part of the MAP kinase pathway.

### **1.2.3 Treating Endometriosis**

Treatment of endometriosis centres around management of pain and treatment of infertility as there is no cure. Suppression of oestrogen, which induces proliferation of the endometrium, is a common first-line treatment as it can be easily achieved through the oral contraceptive which suppresses ovulation (Morotti *et al.*, 2014; Zito *et al.*, 2014). In addition, gonadotrophin releasing hormone (GnRH) analogues may be used for a short period of time to alleviate symptoms by imitating menopause (NHS Choices, 2015; Ferrero *et al.*, 2015). Analgesics such as paracetamol or non-steroidal anti-inflammatory drugs (NSAIDs) such as ibuprofen may be used to relieve pain and discomfort (NHS Choices, 2014; Zito *et al.*, 2014). Laparoscopic excision of endometriotic lesions or endometriomas (endometriosis related cysts) is a common second-line treatment for the reduction of pain if non-surgical interventions are not effective (NHS Choices, 2014; Kodaman, 2015). In rare cases, hysterectomy (removal of the uterus) may be used to relieve symptoms (NHS Choices, 2014; Magrina *et al.*, 2015); however, this doesn't necessarily result in the dissipation of symptoms (Rizk *et al.*, 2014).

### **1.3 Endometriosis and Ovarian Cancer: The Connection**

Endometriosis is now becoming a well documented risk factor for ovarian cancer with endometriosis occurring in up to 28% of patients with ovarian cancer (Sainz de la Cuesta *et al.*, 1996; Stewart *et al.*, 2013; Pearce *et al.*, 2012; Wu *et al.*, 2009; Merritt *et al.*, 2008; Melin *et al.*, 2006; Borgfeldt and Andolf, 2004; Brinton *et al.*, 1997; Brinton *et al.*, 2004; Rossing *et al.*, 2008; Brinton *et al.*, 2005). A 20 year study by Stewart *et al.*, of more than 21,000 patients seeking fertility treatment in Western Australia has shown that endometriosis is particularly associated with an increased rate of ovarian cancer in patients who remained childless after fertility treatment (Stewart *et al.*, 2013). The study did not classify invasive epithelial ovarian cancer any further however, a similarly large pooled analysis of 13 ovarian cancer risk factor studies looked at the relationship between endometriosis and the four major subtypes of epithelial ovarian cancer: clear cell, endometrioid, mucinous and serous (high and low grade). They found that the association between endometriosis and ovarian cancer differed between subtypes. Patients with low grade serous (9.2%), endometrioid (13.9%) and clear cell (20.2%) subtypes were more likely to have endometriosis (compared to 6.2% of control cases). Mucinous epithelial ovarian cancer was not at all associated with endometriosis (Pearce *et al.*, 2012). In these studies no increased risk of ovarian cancer has been found in patients with pelvic inflammatory disorder, ovarian cysts, fibroids, breastfeeding, weight, height, body-mass index and tubal ligation highlighting the unique relationship between endometriosis and ovarian cancer (Stewart *et al.*, 2013; Pearce *et al.*, 2012; Borgfeldt and Andolf, 2004).

### **1.4 The mTOR Pathway**

The mTOR signalling pathway is an integral mediator of growth and proliferation in the cell; evolving to regulate anabolic and catabolic cellular processes based on the resources available. The mTOR pathway is able to sense external energy and oxygen status, nutrients and growth factors, amino acids and stress signals and modulate protein and lipid synthesis, proliferation, growth, autophagy and

apoptosis accordingly (Laplante and Sabatini, 2012). In recent research, components of the pathway have been implicated in a vast range of diseases and conditions from Epilepsy (Russo *et al.*, 2012) to intellectual disability (Troca-Marín *et al.*, 2012) to a range of malignancies and predispositions to them (Peterson *et al.*, 2009; Lu *et al.*, 2015; Philp *et al.*, 2001; Levine *et al.*, 2005; Wataya-Kaneda, 2015).

#### **1.4.1 mTOR Complexes**

Activities of the mTOR pathway are mediated via two large complexes: mTOR Complex 1 (mTORC1) and mTOR Complex 2 (mTORC2). mTORC1 and mTORC2 have distinct functions, sensitivities and associated proteins that differentiate them from one another and regulate their function under different contexts within the cell. mTORC1 contains mTOR, raptor, DEPTOR, GβL and PRAS40. mTORC2 contains mTOR, rictor, DEPTOR, GβL, mSIN1 and protor. mTORC1 modulates autophagy, angiogenesis and protein and lipid synthesis in response to growth factors, amino acids, genotoxicity, energy stress and hypoxia (Laplante and Sabatini, 2012). mTORC2 is less well understood but it is known to regulate the actin cytoskeleton, cell survival and apoptosis (Figure 1.14) (Jacinto *et al.*, 2004; Dudek *et al.*, 1997; Peterson *et al.*, 2009; García-Martínez and Alessi, 2008; Sarbassov *et al.*, 2004; Masri *et al.*, 2007). mTORC1 is nutrient and Rapamycin sensitive whereas mTORC2 is not nutrient sensitive and is only secondarily sensitive to Rapamycin due to Rapamycin's binding to mTOR and removing it as an available component for mTORC2 assembly (Jacinto *et al.*, 2004; Jacinto *et al.*, 2006; Kim *et al.*, 2003; Kim *et al.*, 2002; Sarbassov *et al.*, 2006). Below is a summary of the components of each mTOR complex.

##### **1.4.1.1 mTOR**

mTOR (also known as FRAP), a 289kDa highly conserved serine/threonine kinase, is the central catalytic component of mTORC1 and mTORC2. mTOR was first identified in 1994 as the target of its inhibitor, Rapamycin (Sabers *et al.*, 1995;

Brown *et al.*, 1994) and in relation to the yeast homologues, DRR1 and DRR2 (Cafferkey *et al.*, 1993) and is a member of the PIK-related kinase family.

#### **1.4.1.2 DEPTOR**

DEPTOR (also known as DEPDC6) is a 48kDa component of the mTOR pathway which inhibits the activities of both mTORC1 and mTORC2 via direct interaction with mTOR. Knockdown of DEPTOR causes an increase in phosphorylation of downstream targets p70S6 kinase, 4EBP1 and Akt; in addition DEPTOR protein expression is increased in response to serum starvation (Peterson *et al.*, 2009). Despite DEPTOR being an inhibitor of both mTORC1 and mTORC2, overexpression of DEPTOR causes a decrease in mTORC1 signalling but an increase in mTORC2 signalling. This is because inhibition of mTORC1 relieves the feedback loop directed at PI3 kinase, an upstream positive regulator of the mTORCs. PI3 kinase signalling is then able to overcome DEPTOR inhibition of mTORC2, shown by Akt phosphorylation at threonine 308 (PI3 kinase associated) and serine 473 (mTORC2 associated) (Peterson *et al.*, 2009).

#### **1.4.1.3 GβL**

GβL (g protein beta subunit-like, also known as mLST8) is a 37kDa component of both mTORC1 and mTORC2. GβL binds directly to the kinase domain of mTOR and stabilises the mTOR-Raptor interaction; however, Raptor is not required for mTOR-GβL interaction. It is a necessary component of mTORC1 and mTORC2 and knockdown of GβL decreases the phosphorylation of downstream effectors p70S6 kinase and Akt and the nutrient sensitivity of mTORC1 (Kim *et al.*, 2003; Guertin *et al.*, 2006). GβL is also necessary for the inhibition of mTORC1 by Rapamycin (Kim *et al.*, 2003).

#### **1.4.1.4 Raptor**

Raptor (regulatory associated protein of TOR, also known as KIAA1303) is a 150kDa protein component of mTORC1 only (Hara *et al.*, 2002). Raptor binds to mTOR directly and at multiple contact points and is responsible for controlling mTOR's kinase activity, phosphorylation of downstream effectors p70S6 kinase and 4EBP1 and cell size (Kim *et al.*, 2002; Hara *et al.*, 2002). The mTOR-Raptor interaction is sensitive to Rapamycin which interacts with FKBP12 to inhibit mTOR kinase activity (Kim *et al.*, 2002; Sedrani *et al.*, 1998; Brown *et al.*, 1995).

#### **1.4.1.5 PRAS40**

PRAS40 (proline rich Akt substrate of 40kDa) is a 40kDa raptor interacting, mTORC1 only component. PRAS40 inhibits mTOR kinase activity in an insulin sensitive manner via phosphorylation by Akt at threonine 246 and decreases cell size when overexpressed in HEK293 cells (Kovacina *et al.*, 2003; Sancak *et al.*, 2007; Thedieck *et al.*, 2007). Insulin stimulation causes PRAS40 phosphorylation and a decrease in the amount bound to mTORC1 (Sancak *et al.*, 2007). PRAS40 also appears to protect from apoptosis in an mTORC1 independent fashion (Thedieck *et al.*, 2007).

#### **1.4.1.6 Rictor**

Rictor (Rapamycin insensitive companion of mTOR) is a 192kDa mTORC2 only component whose interaction with mTOR is not rapamycin sensitive (Sarbasov *et al.*, 2004). Rictor is an essential mTORC2 component for the phosphorylation of PKC $\alpha$ , a downstream target of mTORC2, and for maintaining cell morphology (Sarbasov *et al.*, 2004).

#### **1.4.1.7 mSIN1**

mSIN1 (mammalian stress-activated MAP kinase-interacting protein 1, also known as MAPKAP1) is a 78kDa mTORC2 protein component which mediates the mTORC2

specific Akt phosphorylation at serine 473 (Jacinto *et al.*, 2006). mSIN1 and rictor stabilise one another; knockdown of mSIN1 decreases rictor and *vice versa* (Jacinto *et al.*, 2006; Thedieck *et al.*, 2007) (Pearce *et al.*, 2007). mSIN1 interacts directly with mTORC2 downstream target Akt (Jacinto *et al.*, 2006).

#### **1.4.1.8 Protor**

Protor (protein observed with rictor, also known as PR55L) is an mTORC2 only interacting protein via mSIN1 and/or rictor but is not required for mTORC2 complex stability or kinase activity. Rictor knockout decreases protor expression suggesting that rictor regulates protor (Pearce *et al.*, 2007). Knockdown of protor causes an increase in apoptosis in HeLa cells and cells with protor released from mTORC2 show increased apoptosis indicating that protor functions as a pro-apoptotic protein when not bound to mTORC2 (Thedieck *et al.*, 2007). This is further supported by evidence that the pro-apoptotic function of protor is not diminished when mTORC2 assembly is disrupted (Thedieck *et al.*, 2007).



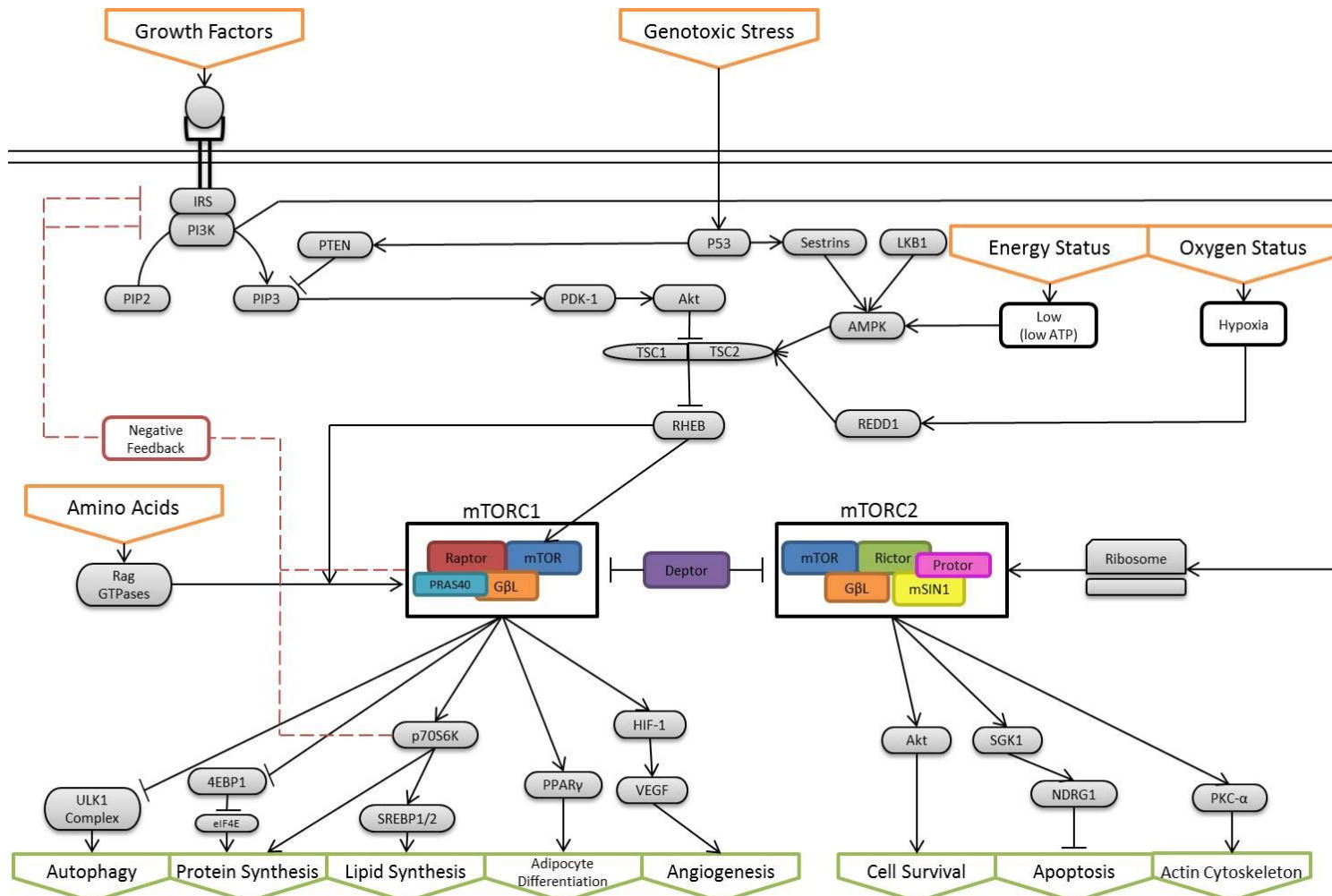


**Figure 1.14** - Diagram of the main components of the mTOR pathway including upstream inputs and downstream effects. Image created based on the research of (Laplane and Sabatini, 2012; Jacinto *et al.*, 2004; Dudek *et al.*, 1997; Peterson *et al.*, 2009; García-Martínez and Alessi, 2008;

Sarbasov *et al.*, 2004; Sarbasov *et al.*, 2005; Sarbasov *et al.*, 2006; Masri *et al.*, 2007; Jacinto *et al.*, 2006; Kim *et al.*, 2002; Kim *et al.*, 2003; Sabers *et al.*, 1995; Brown *et al.*, 1995; Brown *et al.*, 1994; Guertin *et al.*, 2006; Hara *et al.*, 2002; Sedrani *et al.*, 1998; Kovacina *et al.*, 2003; Sancak *et al.*, 2007; Thedieck *et al.*, 2007; Pearce *et al.*, 2007; Ma and Blenis, 2009; Isotani *et al.*, 1999; Burnett *et al.*, 1998; Holz *et al.*, 2005; Fingar *et al.*, 2004; Gebauer and Hentze, 2004; A Pause *et al.*, 1994; Dowling *et al.*, 2010; Wang *et al.*, 2004; Wang *et al.*, 1995; Zhong *et al.*, 2000; Phillips *et al.*, 2005; Hudson *et al.*, 2002; Presta *et al.*, 1997; Li *et al.*, 2011; Peterson *et al.*, 2011; Li *et al.*, 2010; Porstmann *et al.*, 2008; Zhang *et al.*, 2005; Kim and Chen, 2004; Liang *et al.*, 1999; Yue *et al.*, 2003; Qu *et al.*, 2003; Hosokawa *et al.*, 2009; Ganley *et al.*, 2009; Jung *et al.*, 2009; Baskin and Sayeski, 2012; Amato *et al.*, 2007; Aoyama *et al.*, 2005; Lunhua Liu *et al.*, 2010; Prevot *et al.*, 2015; Jianquan Chen *et al.*, 2015; Potter *et al.*, 2002; Misra and Pizzo, 2014; Stokoe *et al.*, 1997; Hsu *et al.*, 2011; Tzatsos and Kandror, 2006; Carracedo *et al.*, 2008; Um *et al.*, 2004; Harrington *et al.*, 2004; Young and Povey, 1998; Carpenter *et al.*, 1990; Thorpe *et al.*, 2015; Franke *et al.*, 1995; Datta *et al.*, 1996; Alessi *et al.*, 1997; Stambolic *et al.*, 2001; Weng *et al.*, 1999; Leslie *et al.*, 2000; Sun *et al.*, 1999; Manning *et al.*, 2002; Inoki *et al.*, 2002; Inoki *et al.*, 2003; Gwinn *et al.*, 2008; Tee *et al.*, 2003; Kenerson *et al.*, 2002; Kastan *et al.*, 1991; Sablina *et al.*, 2005; Feng *et al.*, 2005; Shaw *et al.*, 2004; Maxwell *et al.*, 1997; Yoon *et al.*, 2006; Sudhagar *et al.*, 2011; Treins *et al.*, 2002; Brugarolas *et al.*, 2004; DeYoung *et al.*, 2008; Blommaart *et al.*, 1995; Fox *et al.*, 1998; Hara *et al.*, 1998; Sancak *et al.*, 2010; Kim *et al.*, 2008; Zinzalla *et al.*, 2011; Smith *et al.*, 2005)

## 1.4.2 Downstream of mTOR Complexes

mTOR is known to induce or inhibit many cellular processes including protein synthesis, angiogenesis, cell cycle progression, cell growth, lipid synthesis, autophagy, cytoskeletal organisation, apoptosis and cell survival. The majority of mTOR signalling occurs via mTORC1 and is involved in the initiation of translation through the activation of translation machinery (Ma and Blenis, 2009).

### 1.4.2.1 mTORC1

mTORC1 acts via five main downstream effectors: p70S6 kinase, 4EBP1 (4E binding protein 1, also known as EIF-4EBP1), HIF-1 (hypoxia inducible factor 1), PPAR $\gamma$  (peroxisome proliferator-activated receptor gamma) and the ULK1 complex. mTORC1 phosphorylates and activates p70S6 kinase at threonines 389 and 412 (Isotani *et al.*, 1999; Burnett *et al.*, 1998). p70S6 kinase stimulates cell cycle progression and protein synthesis (Holz *et al.*, 2005; Fingar *et al.*, 2004). mTORC1 also directly phosphorylates 4EBP1 to initiate translation. Translation initiation is the first stage of protein synthesis which involves the binding of the 40S ribosomal subunit to the 5' end of mRNA and 'scanning' until it reaches the start codon (AUG) followed by the recruitment of the 60S ribosomal subunit to make a complete ribosome (Gebauer and Hentze, 2004). When hypophosphorylated, 4EBP1 binds to the 5' mRNA cap binding protein eIF-4E (eukaryotic translation initiation factor 4E) and removes it as an available component in the binding of the ribosome to mRNA and therefore cap dependent translation (A Pause *et al.*, 1994; Gebauer and Hentze, 2004). mTORC1 phosphorylates 4EBP1 at threonines 36 and 45 which prevents its association with eIF-4E and allows eIF-4E to act within the translation initiation complex (Burnett *et al.*, 1998). This results in protein synthesis which promotes proliferation and cell cycle progression (Dowling *et al.*, 2010).

The HIF-1 transcription factor and VEGF pathway are known to control angiogenesis via mTORC1. The HIF-1 $\alpha$  subunit of HIF-1 accumulates under hypoxic conditions allowing for its association with HIF-1 $\beta$  (Wang *et al.*, 1995). HIF-1 $\alpha$  expression is

controlled by mTORC1 signalling (Zhong *et al.*, 2000; Phillips *et al.*, 2005; Hudson *et al.*, 2002) and HIF-1 induces the VEGF pathway which increases endothelial permeability and cellular migration (Presta *et al.*, 1997; Wang *et al.*, 2004). In support of its role in inducing proliferation, mTOR signalling is also able to initiate lipid synthesis for cellular membranes and cell growth. mTORC1 induces lipid synthesis via the transcription factor SREBP (sterol regulatory element-binding protein) which is regulated by p70S6 kinase (Li *et al.*, 2011; Peterson *et al.*, 2011; Li *et al.*, 2010; Porstmann *et al.*, 2008). mTORC1 also plays a role in adipocyte differentiation via the transcription factor PPAR $\gamma$  (Zhang *et al.*, 2005; Kim and Chen, 2004).

Autophagy is the lysosomal degradation and recycling of damaged or unneeded cellular components and is a tumour suppressor function as it rids cells of damaged organelles and decreases proliferation and tumourigenesis (Liang *et al.*, 1999; Yue *et al.*, 2003; Qu *et al.*, 2003). mTORC1 signalling suppresses autophagy via the ULK1 complex. The ULK1 complex is comprised of ULK1 (unc-51 like autophagy activating kinase 1), Atg13 (autophagy related 13) and FIP200 (FAK family kinase-interacting protein of 200 kDa) (Hosokawa *et al.*, 2009; Ganley *et al.*, 2009). mTORC1 phosphorylates ULK1 and Atg13 which inhibits the ULK1 complex and therefore autophagy (Ganley *et al.*, 2009; Jung *et al.*, 2009).

#### **1.4.2.2 mTORC2**

mTORC2 acts independently of p70S6 kinase and the TSC1/TSC2 complex and is not involved in some of the mTORC1 downstream effects such as regulation of cell size (Sarbasov *et al.*, 2004; Guertin *et al.*, 2006). The Rictor-mTOR complex is responsible for the phosphorylation of PKC $\alpha$  (protein kinase C alpha) which is in turn, at least partially, responsible for organisation of the actin cytoskeleton and maintenance of cell morphology (Sarbasov *et al.*, 2004; Masri *et al.*, 2007). mTORC2 but not mTORC1 is responsible for control of apoptosis via SGK1 (serum and glucocorticoid-inducible kinase 1) (Dudek *et al.*, 1997; García-Martínez and Alessi, 2008; Peterson *et al.*, 2009). SGK1 is inhibitory of apoptosis via its target

NDRG1 (N-myc downstream regulated 1) (García-Martínez and Alessi, 2008; Baskin and Sayeski, 2012; Amato *et al.*, 2007; Aoyama *et al.*, 2005). mTORC2 has also been shown to play a role in anchorage dependent growth and motility, development of immune cells, neutrophil chemotaxis and skeletal development (Masri *et al.*, 2007; Lunhua Liu *et al.*, 2010; Prevot *et al.*, 2015; Jianquan Chen *et al.*, 2015).

Akt is both upstream of mTORC1 and downstream of mTORC2 and is differentially phosphorylated with a dual role in mTOR pathway signalling. Akt is phosphorylated on threonine 308 by PDK-1 after activation by PIP<sub>3</sub> and is involved in disrupting the TSC1/TSC2 complex upstream of mTORC1, affecting p70S6 kinase and 4EBP1 phosphorylation (Jacinto *et al.*, 2006; Potter *et al.*, 2002; Misra and Pizzo, 2014; Stokoe *et al.*, 1997). mTORC2 phosphorylates Akt on serine 473 which affects only mTORC2 related functions such as phosphorylation of the FOXO1 and FOXO3a transcription factors (Sarbasov *et al.*, 2005; Jacinto *et al.*, 2006). Phosphorylation of Akt at serine 473 promotes cell survival and dephosphorylation at this site can induce apoptosis (Jacinto *et al.*, 2006).

The mTOR pathway is stabilised by a number of negative feedback loops. mTOR mediates inhibition of PI3 kinase via adapter protein Grb10 (growth factor receptor-bound protein 10), insulin receptor substrate (IRS) via raptor and the MAP kinase pathway (Hsu *et al.*, 2011; Tzatsos and Kandror, 2006; Carracedo *et al.*, 2008). Downstream of mTORC1, there is also evidence of IRS inhibition by p70S6 kinase (Um *et al.*, 2004; Harrington *et al.*, 2004).

### **1.4.3 Upstream of mTOR Complexes**

#### **1.4.3.1 mTORC1**

##### **1.4.3.1.1 TSC1/TSC2**

The TSC1 (tuberous sclerosis complex 1, also known as hamartin) and TSC2 (tuberous sclerosis complex 2, also known as tuberin) heterodimeric complex is responsible for mediating the majority of upstream signals to mTORC1 (Laplante and Sabatini, 2012). The components of the TSC complex are named for their involvement in the condition tuberous sclerosis which is characterised by benign growths affecting the whole body (Young and Povey, 1998).

##### **1.4.3.1.2 The PI3 Kinase/Akt/mTOR Axis**

The majority of mTOR signalling to TSC1/TSC2 is via the multifunctional PI3 kinase/Akt axis. PI3 kinase is a heterodimeric signalling protein composed of an 85kDa regulatory subunit and a 110kDa catalytic subunit of the class IA family of PI3 kinases (Carpenter *et al.*, 1990; Thorpe *et al.*, 2015). The kinase activity of PI3 kinase is inhibited by its regulatory subunit until receptor activation after which it is able to phosphorylate phosphatidylinositide (PtdIns) 4,5-bisphosphate (PIP<sub>2</sub>) to PtdIns 3,4,5-bisphosphate (PIP<sub>3</sub>) (Thorpe *et al.*, 2015). Activation of PI3 kinase signalling activates Akt via PIP<sub>3</sub> dependent protein kinase 1 (PDK1) (Misra and Pizzo, 2014; Franke *et al.*, 1995; Datta *et al.*, 1996; Stokoe *et al.*, 1997; Alessi *et al.*, 1997). The tumour suppressor PTEN (phosphatase and tensin homologue on chromosome ten) acts to downregulate PI3 kinase signalling by dephosphorylating PIP<sub>3</sub> to PIP<sub>2</sub> and is controlled by p53 (Stambolic *et al.*, 2001; Weng *et al.*, 1999; Leslie *et al.*, 2000; Sun *et al.*, 1999).

Activated Akt by phosphorylation of threonine 308 prevents the colocalisation of TSC1 with TSC2 and therefore the formation of the TSC1/TSC2 complex by phosphorylating TSC2 at serines 939, 1086 and 1088 and threonines 1462 and 1422

(Misra and Pizzo, 2014; Potter *et al.*, 2002; Manning *et al.*, 2002; Inoki *et al.*, 2002). The TSC1/TSC2 complex is differentially regulated by alternative phosphorylation sites. Phosphorylation of threonine 1227 and serine 1345 can cause inhibition of downstream mTOR signalling (Inoki *et al.*, 2003; Gwinn *et al.*, 2008). When in complex with TSC1, TSC2 shows GAP (GTPase activating protein) activity toward Rheb (rat homologue enriched in brain), converting Rheb-GTP to Rheb-GDP and preventing its phosphorylation of mTOR at serine 2448 and therefore the phosphorylation of downstream effectors of the mTOR pathway p70S6 kinase, S6, 4EBP1 and EIF-4G (eukaryotic translation initiation factor 4G) (Inoki *et al.*, 2003; Inoki *et al.*, 2002; Tee *et al.*, 2003; Kenerson *et al.*, 2002).

#### **1.4.3.1.3 The Ras/MAP Kinase pathway**

In addition to PI3 kinase and Akt, TSC1/TSC2 is also downstream of the Ras/MAP kinase pathway. MAP kinase (Erk) acts in a similar way to Akt on the TSC1/TSC2 complex by phosphorylating TSC2 and inducing its dissociation from TSC1; thereby inactivating its inhibitory effect on mTOR. However, MAPK phosphorylates serine 664 on TSC2, which is different to the two phosphorylation sites targeted by Akt (Ma and Blenis, 2009).

#### **1.4.3.1.4 Stress Signals: Energy, Hypoxia and DNA Damage**

It is critical that the cell is able to sense stress signals and respond accordingly, by downregulating the positive growth effects of the mTOR pathway. Most stress-mediated inhibition of mTOR signalling acts via the TSC1/TSC2 complex and mTORC1. Many cellular indicators of stress cause mTOR pathway downregulation (Figure 1.15) by the activation of tumour suppressor gene p53. p53 is activated in cases of DNA damage and oxidative stress (Kastan *et al.*, 1991; Sablina *et al.*, 2005) and acts via both the PI3 kinase/Akt pathway and in a PI3 kinase independent manner. p53 causes the upregulation of PTEN protein expression by directly binding to the PTEN gene promoter (Stambolic *et al.*, 2001). PTEN dephosphorylates PIP<sub>3</sub> to form PIP<sub>2</sub> in order to inhibit PI3 kinase signalling and is

therefore a tumour suppressor gene (Weng *et al.*, 1999; Leslie *et al.*, 2000; Sun *et al.*, 1999; Thorpe *et al.*, 2015). DNA damage, therefore, is able to inhibit the mTOR pathway to halt growth in the case of aberrant genetic mutation by inducing PTEN expression (Feng *et al.*, 2005). p53 also acts by upregulating the expression of Sestrin1 and Sestrin2 which act via AMP-responsive protein kinase (AMPK) to inhibit mTORC1 pathway signalling by alternative phosphorylation of TSC2 (Budanov and Karin, 2008). AMPK is also activated by LKB1 (liver kinase B1) by activating phosphorylation at threonine 172 (Shaw *et al.*, 2004). In contrast to the TSC1/TSC2 complex dissociating phosphorylation described above, AMPK phosphorylation at threonine 1227 and serine 1345 does not activate mTOR pathway signalling but inhibits it through an as yet unknown mechanism (Inoki *et al.*, 2003; Gwinn *et al.*, 2008). In addition to involvement in the response to DNA damage, AMPK is also important in sensing and responding to cellular energy levels. Cellular energy is measured by ATP (adenosine triphosphate), the phosphate group donor molecule used in signal transduction pathways which is critical in cell signalling. Protein synthesis is a high energy consuming process and the cell must be able to respond to ATP levels accordingly. AMPK also phosphorylates raptor to inhibit mTORC1 signalling (Gwinn *et al.*, 2008).

Hypoxia, the state of having lower than optimal levels of available oxygen, is a major indicator of cellular stress. Oxygen is used in cellular respiration to create energy and is critical in normal cellular metabolism. The expression of hypoxia inducible factor 1 alpha (HIF-1 $\alpha$ ), a subunit of the HIF-1 transcription factor which induces the upregulation of genes involved in angiogenesis and erythropoiesis (Maxwell *et al.*, 1997; Yoon *et al.*, 2006) is mediated via the mTOR signalling pathway (Sudhagar *et al.*, 2011; Treins *et al.*, 2002). Hypoxia also upregulates REDD1 which induces mTOR inhibition via the TSC1/TSC2 complex (Brugarolas *et al.*, 2004; DeYoung *et al.*, 2008).



#### 1.4.3.1.5 Growth Signals: Nutrients and Amino Acids

Amino acids are a major cellular cue for the induction of protein synthesis and inhibition of autophagy (Blommaert *et al.*, 1995). Amino acids, particularly leucine, phenylalanine and tyrosine, stimulate the mTOR pathway and cause the phosphorylation of p70S6 kinase and 4EBP1 but do not act via the PI3 kinase or MAP kinase pathways (Fox *et al.*, 1998; Hara *et al.*, 1998; Blommaert *et al.*, 1995). Instead amino acids directly activate Rag GTPases and promote the interaction of Rag GTPases with mTORC1. This alters the cellular localisation of mTOR to Rheb containing cellular compartments (Sancak *et al.*, 2010; Kim *et al.*, 2008; Smith *et al.*, 2005). Active Rheb induces mTORC1 signalling by phosphorylating mTOR at serine 2448 (Tee *et al.*, 2003; Tee and Blenis, 2005; Inoki *et al.*, 2003). In addition, glucose starvation in cells activates p53 which in turn upregulates PTEN protein expression and therefore downregulates the mTOR pathway (Feng *et al.*, 2005) and insulin stimulation disrupts TSC1/TSC2 complex formation via activated Akt (Potter *et al.*, 2002).

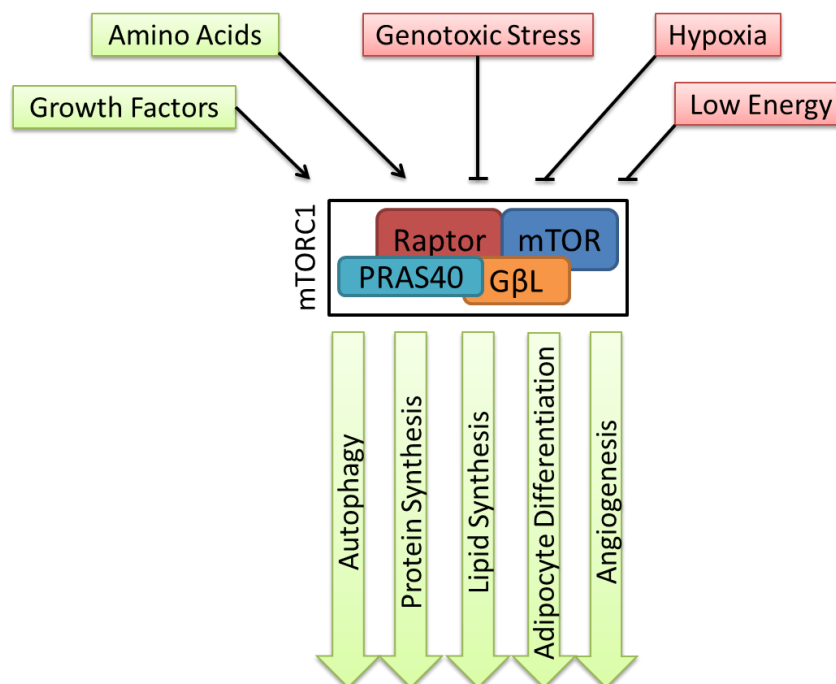


**Figure 1.15** - The cellular and extracellular cues that activate and inhibit mTORC1 signalling and the resulting downstream effects of mTORC1 activation (Ma and Blenis, 2009; Isotani *et al.*, 1999; Burnett *et al.*, 1998; Holz *et al.*, 2005; Fingar *et al.*, 2004; Gebauer and Hentze, 2004; A Pause *et al.*, 1994; A. Pause *et al.*, 1994;

Dowling *et al.*, 2010; Wang *et al.*, 1995; Zhong *et al.*, 2000; Phillips *et al.*, 2005; Presta *et al.*, 1997; Wang *et al.*, 2004; Li *et al.*, 2011; Peterson *et al.*, 2011; Li *et al.*, 2010; Porstmann *et al.*, 2008; Zhang *et al.*, 2005; Kim and Chen, 2004; Liang *et al.*, 1999; Yue *et al.*, 2003; Qu *et al.*, 2003; Hosokawa *et al.*, 2009; Ganley *et al.*, 2009; Jung *et al.*, 2009; Sarbassov *et al.*, 2004; Guertin *et al.*, 2006; Sarbassov *et al.*, 2004; Masri *et al.*, 2007; Dudek *et al.*, 1997; García-Martínez and Alessi, 2008; Baskin and Sayeski, 2012; Amato *et al.*, 2007; Aoyama *et al.*, 2005; Lunhua Liu *et al.*, 2010; Prevot *et al.*, 2015; Jianquan Chen *et al.*, 2015; Jacinto *et al.*, 2006; Potter *et al.*, 2002; Misra and Pizzo, 2014; Stokoe *et al.*, 1997; Sarbassov *et al.*, 2005; Hsu *et al.*, 2011; Tzatsos and Kandror, 2006; Carracedo *et al.*, 2008; Um *et al.*, 2004; Harrington *et al.*, 2004; Laplante and Sabatini, 2012; Young and Povey, 1998; Carpenter *et al.*, 1990; Thorpe *et al.*, 2015; Franke *et al.*, 1995; Datta *et al.*, 1996; Stokoe *et al.*, 1997; Alessi *et al.*, 1997; Stambolic *et al.*, 2001; Weng *et al.*, 1999; Leslie *et al.*, 2000; Sun *et al.*, 1999; Potter *et al.*, 2002; Manning *et al.*, 2002; Inoki *et al.*, 2002; Inoki *et al.*, 2003; Gwinn *et al.*, 2008; Tee *et al.*, 2003; Kenerson *et al.*, 2002; Kastan *et al.*, 1991; Sablina *et al.*, 2005; Stambolic *et al.*, 2001; Feng *et al.*, 2005; Budanov and Karin, 2008; Shaw *et al.*, 2004; Maxwell *et al.*, 1997; Yoon *et al.*, 2006; Sudhagar *et al.*, 2011; Treins *et al.*, 2002; Brugarolas *et al.*, 2004; DeYoung *et al.*, 2008; Blommaert *et al.*, 1995; Fox *et al.*, 1998; Hara *et al.*, 1998; Sancak *et al.*, 2010; Kim *et al.*, 2008; Smith *et al.*, 2005; Tee and Blenis, 2005; Tee *et al.*, 2003; Feng *et al.*, 2005).

#### **1.4.3.2 mTORC2**

Less is understood of the upstream effectors of mTORC2 signalling. Zinzalla *et al.*, demonstrated that the ribosome is required for mTORC2 signalling and that active mTORC2 interacts with the ribosome directly, an association which is promoted by PI3 kinase signalling. Although mTORC2 signalling requires the ribosome, it is independent of protein synthesis (Zinzalla *et al.*, 2011).

#### **1.5 Ovarian Cancer, Endometriosis and the mTOR pathway**

Due to its involvement in growth factor and energy sensing and its effects on protein synthesis and cell cycle progression, the mTOR pathway is highly relevant in disorders involving loss of growth restriction such as cancer. The mTOR pathway has been shown to be implicated in a range of malignancies (Figure 1.16).

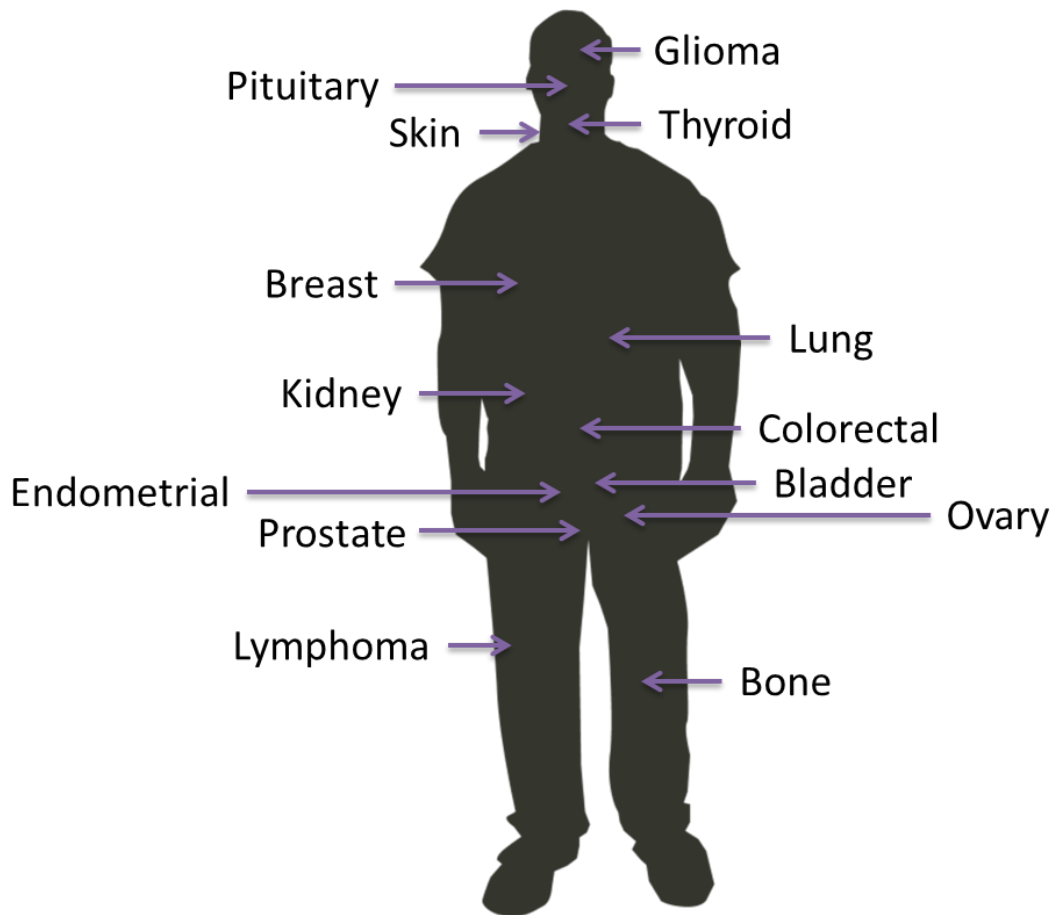


**Figure 1.16** - The mTOR pathway has been shown to be implicated in breast cancer, colorectal cancer, prostate cancer, glioma, lung cancer, melanoma, osteosarcoma, renal cell carcinoma, lymphomas, thyroid cancers, endometrial cancer, pituitary cancer and bladder cancer (Karthik *et al.*, 2015; Lu *et al.*, 2015; Majumder *et al.*, 2004; Masri *et al.*, 2007; Guertin *et al.*, 2009; Jiang *et al.*, 2009; Jiang *et al.*, 2015; Shin *et al.*, 2015; Shao *et al.*, 2015; Song *et al.*, 2015; Kawada *et al.*, 2014; Moraitis *et al.*, 2014; Schrauwen *et al.*, 2015; Lee *et al.*, 2015; Shu *et al.*, 2015; Arumugam *et al.*, 2012; Campbell *et al.*, 2004; Campbell *et al.*, 2008).

The mTOR pathway has been implicated in ovarian cancer in a number of ways. Phosphorylated 4EBP1 and p70S6 kinase show high expression in comparison to non-malignant tissues (Castellvi *et al.*, 2006) and phosphorylated 4EBP1 specifically shows correlation with advanced stage and grade, greater chemoresistance and shorter disease free survival (No *et al.*, 2011). In addition to this, Akt, PTEN, the catalytic and regulatory subunits of PI3 kinase, PPAR $\gamma$  and VEGF have also been shown to be mutated or upregulated in ovarian cancer (Zhang *et al.*, 2005; Masoumi-Moghaddam *et al.*, 2015; De Marco *et al.*, 2013; Philp *et al.*, 2001; Levine *et al.*, 2005; Carpten *et al.*, 2007; Yang *et al.*, 2006; Obata *et al.*, 1998).

Upregulation of the mTOR pathway in ovarian cancer has also been associated *in vitro* with increased invasion and migration including upregulation of matrix metalloproteinase (MMP) 9, epithelial-mesenchymal transition (EMT), angiogenesis, metastasis, increased proliferation and chemoresistance (Zhou and Wong, 2006; Meng *et al.*, 2006; Pon *et al.*, 2008; Bian *et al.*, 2010; Ip *et al.*, 2014; Im-aram *et al.*, 2013; Foster *et al.*, 2010). However, little is known about the actual expression of mTORC components in ovarian cancer. Preliminary studies have shown that both mTORC1 and mTORC2 via raptor and rictor are important for ovarian cancer proliferation (Montero *et al.*, 2012) and that mTORC2 is more frequently active in clear cell carcinoma than serous adenocarcinoma (Hisamatsu *et al.*, 2013).

The genetic changes that characterise endometriosis are poorly understood; however, the mTOR pathway has been implicated in a number of ways. Leconte *et al.*, found that protein expression of both Akt and p70S6K was increased in both the eutopic endometrium and endometriotic lesions of patients with deep infiltrating endometriosis (DIE) in comparison to control endometrium. Interestingly, there was minimal or no difference in expression between eutopic and lesion endometrium in patients with DIE (Leconte *et al.*, 2011). Afshar *et al.*, showed changes in 23 PI3 kinase/Akt pathway related genes and 26 MAP kinase pathway related genes in the eutopic endometrium of baboons with endometriosis (Afshar *et al.*, 2013). Both the PI3 kinase and MAP kinase pathways can inactivate the TSC1/TSC2 complex causing a release of its inhibitory effect on mTOR kinase activity (Potter *et al.*, 2002; Manning *et al.*, 2002; Ma and Blenis, 2009). Guo *et al.*, noted higher phosphorylated mTOR in ectopic endometrium than in eutopic or control endometrium (Guo *et al.*, 2015).

An interesting study by Dinulescu *et al.*, found that inducing K-ras activation caused an endometriosis-like condition in mice that was benign. The addition of deletion of PTEN, a tumour suppressor gene upstream of mTOR and involved in the PI3 kinase/Akt/mTOR axis, in mice induced ovarian endometrioid adenocarcinoma. PTEN deletion alone did not induce pathology in the same time-span. In addition,

the study found that the combination of K-ras phosphorylation and PTEN deletion induced the phosphorylation of Akt, mTOR and p70S6 kinase indicating that the mTOR pathway, either by PI3 kinase/Akt or Ras/MAP kinase activation is implicated in the transformation of endometriosis to ovarian cancer (Dinulescu *et al.*, 2005). This is further supported by the frequent downregulation of PTEN found in ovarian cancers (Laudański *et al.*, 2011; De Marco *et al.*, 2013) and increased K-ras activation in endometriosis (Shahrabi-Farahani *et al.*, 2014; Amemiya *et al.*, 2004).

## **1.6 mTOR Pathway Inhibitors**

### **1.6.1 Rapamycin and the Rapalogues**

Rapamycin (also known as Sirolimus), the first known inhibitor of mTOR kinase, was first described in 1975 in two papers by Vezina *et al.*, and Sehgal *et al.*. Isolated from the bacteria *Streptomyces hygroscopicus* found in a soil sample from Chilean Easter Island and named for the Polynesian name for the island, Rapa Nui, Rapamycin is a potent inhibitor of yeast and filamentous fungi but not bacteria (Vézina *et al.*, 1975; Sehgal *et al.*, 1975). In 1991 the first target of Rapamycin, the yeast equivalent of the kinase we now call mechanistic target of rapamycin (mTOR), was identified by Heitman *et al.*, (Heitman *et al.*, 1991). The mammalian TOR was discovered in 1994 and 1995 by Brown *et al.*, and Sabers *et al.*, respectively (Brown *et al.*, 1994; Sabers *et al.*, 1995). Rapamycin's anti-fungal properties were quickly overshadowed when it was found to be a potent immunosuppressant and a useful compound in preventing the rejection of transplanted organs by inhibiting the proliferation and activation of T- and B-lymphocytes (Kay *et al.*, 1991; Dumont *et al.*, 1990; Morelon *et al.*, 2001). Rapamycin, under the brand name Rapamune (Pfizer), was licenced for use in renal transplantation in the EU in 2001 (European Medicines Agency, 2015c).

Since the discovery of Rapamycin, a host of semi-synthetic Rapamycin-related mTOR inhibitors, known as Rapalogues, have been developed by modifying the C40 hydroxyl group to improve the aqueous solubility and pharmacokinetics of

Rapamycin. These include Everolimus (Novartis), Deforolimus (Merck/ARIAD Pharmaceuticals) and Temsirolimus (Pfizer), among others. Everolimus (also known as RAD001) was developed by chemical modification of Rapamycin to introduce a 2-hydroxyethyl group to the hydroxyl in position 40 (Sedrani *et al.*, 1998). The resulting derivative has improved pharmacokinetics for oral administration without loss of immunosuppressive properties (Sedrani *et al.*, 1998; Benjamin *et al.*, 2011) and Everolimus was approved for the treatment of renal cell carcinoma and pancreatic and breast neoplasms by the EMA in 2009. Deforolimus (also known as Ridaforolimus, AP23573 and MK-8669) is a non-Rapamycin prodrug derivative of Rapamycin where the second alcohol moiety of carbon 43 has been replaced with a phosphate group to improve solubility for oral administration (Benjamin *et al.*, 2011). Although Deforolimus is considered a non-Rapamycin prodrug, its mechanism of action is the same as Rapamycin and the other rapalogues. Deforolimus is not yet approved for use by the EMA but is currently being evaluated in clinical trials for patients with advanced solid tumours (Di Cosimo *et al.*, 2015; Brana *et al.*, 2014; Tsoref *et al.*, 2014). Temsirolimus (also known as CCI-779) is an ester derivative of Rapamycin. Temsirolimus was licenced in 2007 by the EMA for treatment of renal cell carcinoma and mantle cell lymphoma (Table 1.5).

#### **1.6.1.1 Rapamycin: Mechanism of Action**

Rapamycin and the rapalogues are primarily mTORC1 inhibitors due to their effect on raptor. They act by binding the intracellular protein FK-506 binding protein 12 (FKBP12) (Sedrani *et al.*, 1998; Brown *et al.*, 1994) and acting in complex to inhibit mTOR activity by causing the dissociation of mTOR and raptor (Figure 1.17) (Beuvink *et al.*, 2005; Kim *et al.*, 2002; Yip *et al.*, 2010). The Rapamycin/FKBP12 complex binds to a domain within mTOR known as the FRB (FKBP12 Rapamycin binding) domain and identified as amino acids 2025-2114 (Chen *et al.*, 1995). Rapamycin and rapalogues have been shown to have a wide range of effects both *in vitro* and *in vivo* including G<sub>1</sub> cell cycle arrest, inhibition of proliferation, tumour growth, angiogenesis and ascites production, improved survival, enhancement of cytotoxic agents, suppression of T-cell proliferation and T- and B-cell activation

(Brown *et al.*, 1994; Beuvink *et al.*, 2005; Treeck *et al.*, 2006; Hahn *et al.*, 2005; Dumont *et al.*, 1990; Kay *et al.*, 1991; Mabuchi, Deborah A Altomare, *et al.*, 2007; Mabuchi, Deborah A. Altomare, *et al.*, 2007; Fagone *et al.*, 2013).

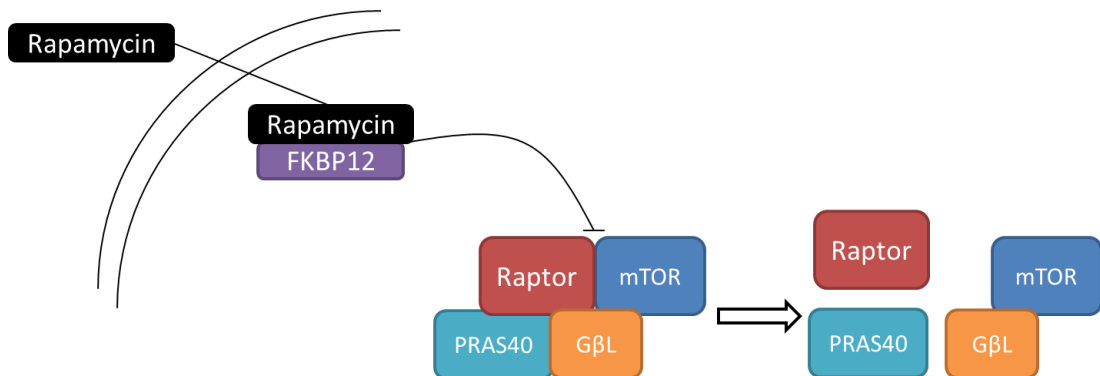


**Figure 1.17** - The mechanism of action of Rapamycin and the rapalogues.

Rapamycin complexes with FKBP12 and disrupts the interaction of mTOR and raptor via the FRB domain of mTOR (Sedrani *et al.*, 1998; Brown *et al.*, 1994; Beuvink *et al.*, 2005; Kim *et al.*, 2002; Yip *et al.*, 2010; Chen *et al.*, 1995).

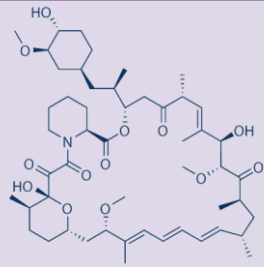
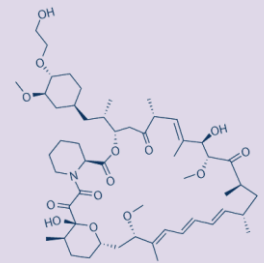
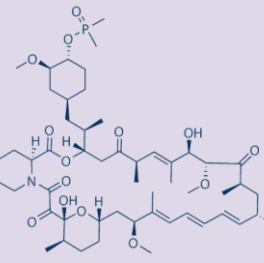
It has recently been suggested that Rapamycin may have a secondary inhibitory effect on mTORC2. Although Rapamycin doesn't target mTORC2 directly, it does bind to free mTOR (Brown *et al.*, 1994; Sabers *et al.*, 1995) which removes it as an available complex component and thereupon disrupts mTORC2 assembly (Sarbasov *et al.*, 2006). Although the effect of Rapamycin on mTORC1 is potent and immediate (30 minutes) the effect on mTORC2 is less so (24 hours) (Sarbasov *et al.*, 2006). However, this phenomenon has only been detected in HeLa and PC3 cell lines. This may be a cell type specific response and further studies are required to determine if this effect can be detected in other cells.

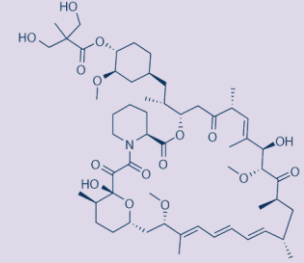
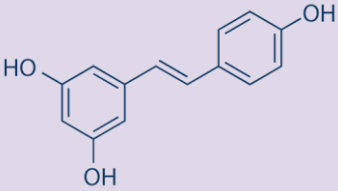
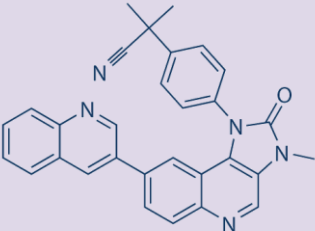
### 1.6.2 Dual mTOR and PI3 Kinase Inhibitors

Rapalogues are not the only method of mTOR pathway inhibition and recent interests have turned to single compounds with dual inhibitory properties. Targeting both mTOR and PI3 kinase is advantageous as mTOR inhibition can relieve negative feedback loops directed at the PI3 kinase and MAP kinase pathways which in turn activate mTORC2 signalling (Zitzmann *et al.*, 2010; Carracedo *et al.*, 2008).

Resveratrol is a natural polyphenol found in some fruits, most notably in the skin of grapes, which is a dual mTOR and PI3 kinase inhibitor. Resveratrol inhibits mTOR by enhancing its interaction with native inhibitor DEPTOR (Meilian Liu *et al.*, 2010) and PI3 kinase directly via its ATP binding site (Fröjdö *et al.*, 2007). Resveratrol is not currently licenced for use in any conditions but has been the subject of a number of clinical trials focussing on nonalcoholic fatty liver disease, metabolic syndrome and insulin sensitivity with mixed outcomes (Faghihzadeh *et al.*, 2014; Kjaer *et al.*, 2015; Liu *et al.*, 2014). NVP BEZ-235 (Novartis) is a synthetic dual mTOR and PI3 kinase inhibitor which acts by binding to the ATP binding sites of both proteins (Maira *et al.*, 2008). NVP BEZ-235 inhibits the mTOR pathway and lessens the negative feedback induced upregulation of mTORC2 signalling by mTORC1 inhibition by also targeting PI3 kinase (Serra *et al.*, 2008; Brünner-Kubath *et al.*, 2011). NVP BEZ-235 has shown more potent antiproliferative effects than rapalogues and suppresses tumour growth in mice (Serra *et al.*, 2008).



Inhibitor	Mechanism of Action	Molecular Structure	Chemical Formula	Licensed Uses
<b>Rapamycin (Sirolimus)</b>	Forms a complex with FKBP12 to allosterically inhibit mTOR		$C_{51}H_{79}NO_{13}$	<b>Pfizer</b> Rapamune: prophylaxis for organ rejection
<b>Everolimus (RAD001)</b>	Prodrug form of Rapamycin		$C_{53}H_{83}NO_{14}$	<b>Novartis</b> Afinitor/Zortress: Advanced kidney cancer, post-menopausal breast cancer, neuroendocrine pancreatic cancer
<b>Deforolimus (Ridaforolimus, AP23573, MK-8669)</b>	Non-Rapamycin prodrug		$C_{53}H_{84}NO_{14}P$	<b>Merck/ARIAD Pharmaceuticals</b> None

<b>Temsirolimus (CCI-779)</b>	Prodrug form of Rapamycin		$C_{56}H_{87}NO_{16}$	<b>Pfizer</b> Torisel: Renal cell carcinoma
<b>Resveratrol</b>	Inhibits mTOR by promoting interaction with native inhibitor DEPTOR. Binds directly to ATP binding site of PI3 kinase.		$C_{14}H_{12}O_3$	None
<b>NVP BEZ-235 (Dactolisib)</b>	Binds to ATP binding sites of both mTOR and PI3 kinase.		$C_{30}H_{23}N_5O$	None

**Table 1.5** - Molecular structures, chemical formulas and licenced uses of six mTOR or mTOR/PI3 kinase inhibitors. Table made using the following sources (Vézina *et al.*, 1975; Sehgal *et al.*, 1975; Heitman *et al.*, 1991; Brown *et al.*, 1994; Sabers *et al.*, 1995; Kay *et al.*, 1991; Dumont *et al.*, 1990; Morelon *et al.*, 2001; Sedrani *et al.*, 1998; Benjamin *et al.*, 2011; Di Cosimo *et al.*, 2015; Brana *et al.*, 2014; Tsoref *et al.*, 2014;

Beuvink *et al.*, 2005; Kim *et al.*, 2002; Yip *et al.*, 2010, p.2010; Chen *et al.*, 1995; Treeck *et al.*, 2006; Hahn *et al.*, 2005; Dumont *et al.*, 1990; Kay *et al.*, 1991; Mabuchi, Deborah A Altomare, *et al.*, 2007; Mabuchi, Deborah A. Altomare, *et al.*, 2007; Fagone *et al.*, 2013; Zitzmann *et al.*, 2010; Carracedo *et al.*, 2008; Fröjdö *et al.*, 2007; Maira *et al.*, 2008; Serra *et al.*, 2008; Brünner-Kubath *et al.*, 2011). *Molecular structure diagrams adapted from selleckchem.com with permission*

## 1.7 Point of Care Diagnostics

PoCT is becoming the gold standard of diagnostics in medical fields. PoCT allows a test to be carried out and results obtained in a single visit to a primary or secondary care health provider, dramatically reducing the wait time between doctor consultation and diagnosis. This allows for immediate commencement of treatment, increasing the likelihood of a favourable patient outcome, reducing the chance of transmission in the case of communicable conditions, eliminating the rate of specimen loss in transit and increasing the potential for personalised medicine. In developing countries and low-resource settings, PoCT is perhaps even more effective; the need for expensive central laboratories, highly trained technicians and a reliable method of data storage can all be removed with the implementation of a well-designed multifunctional PoCT system. Bringing the test into the clinic in areas of high displacement reduces the likelihood of losing patient contact before the condition has been effectively treated. With over 15,000 NHS patients waiting longer than 6 weeks for the implementation of a diagnostic test in England in May 2015 (NHS, 2015a), PoC diagnostics is not yet a reality in the UK and is even less so in the developing world.

### 1.7.1 qPCR

qPCR, the method by which a nucleotide sequence can be exponentially amplified and quantitatively measured in real-time, is now a mainstay in research and medical laboratories alike. The polymerase chain reaction (PCR) was first described by Har Gobind Khorana and Kjell Kleppe in the early 1960s but was not fully appreciated until development by Kary Mullis in 1983, for which he won a Nobel Prize. The method uses cycling temperatures and short nucleotide primers to induce the amplification of deoxyribonucleic acid (DNA) with a DNA polymerase. Significant improvements have now been made to the technique, including the development of thermally stable DNA polymerases from the thermophilic bacteria *Thermus aquaticus* (*Taq*) which was originally found in the hot springs of Yellowstone National Park (Brock and Freeze, 1969). PCR was able to become

quantitative with the addition of SYBR® Green, a fluorophore which selectively binds to double stranded DNA (Zipper *et al.*, 2004) and allows amplification to be measured in real-time by fluorescence measurement.

Full details of the development and mechanism of qPCR can be found in Appendix 1.

### **1.7.2 Thermal Cyclers**

The three stages of the qPCR process, dissociation, primer annealing and extension, are temperature dependent. qPCR assays are carried out on thermal cyclers; instruments which serve to incubate the sample at appropriate temperatures and measure fluorescence change over time. The PCR process cycles samples through a temperature profile; typically 95°C, 60°C, and 72°C, forty times or more. The time taken to increase or decrease the temperature between these levels, known as the ramp rate, varies from instrument to instrument and can lengthen a qPCR experiment to a greater or lesser degree beyond the incubation times. A typical qPCR experiment can take more than 2 hours to complete; a time which is not compatible with PoCT and limits the potential benefits of qPCR diagnostics.

Thermal uniformity in qPCR is the degree to which there is a temperature gradient over the sample area and is in opposition with test speed. The absence of thermal uniformity can cause divergence in the cycling conditions experienced by different samples in the same assay. qPCR instruments typically connect a heat source to sample tray via a conductive metal block. The nature of the block allows heat to distribute evenly, after a period of equilibration. It is the time taken to even out the applied temperature that can constrain the speed at which thermal cycling can proceed. In addition to this, the so called 'edge effect' by which heat loss is greater at the edges of the block means that thermal uniformity is difficult to maintain without active control over the sample area. A fast qPCR instrument is only useful if experimental integrity can be maintained (Tania Nolan, 2013).

### 1.7.3 Point of Care Testing

The use of qPCR as a diagnostic method is not new but, in recent years, efforts to improve the technique have increased and qPCR diagnostics is an ever rapidly developing field. As the process has evolved, the applications for it have increased, and now range from infectious diseases to paternity identification and from forensic analysis to food processing.

qPCR diagnostic tests have been developed for many infectious conditions; Cepheid, who specialise in clinical diagnostic testing, have cartridge based diagnostic tests for a range of clinically relevant conditions such as MRSA and Norovirus to accompany their GeneXpert system (Cepheid, 2015). In the cases of infectious diseases, qPCR can be carried out for nucleic acid sequences specific to the pathogen, for example the Zaire Ebola virus nucleoprotein gene in Ebola haemorrhagic fever (Liu *et al.*, 2015). However, the diagnosis of cancer by qPCR can be challenging as it requires a comparison of 'self with self' and not 'self with other' as with infectious diseases. In the case of cancer, there is rarely a gene expressed solely in disease states that is not also expressed to some degree in normal tissue and so research must be used to assess the threshold for increase or decrease in expression which can be reliably correlated with malignancy. This would require large, multifactorial studies into cancer expression profiles which take into account all variables which may affect gene expression including cancer type, severity, age, race, gender, diet and lifestyle (Wu *et al.*, 2015; Samaan *et al.*, 2015; Knappskog *et al.*, 2014; Saeed *et al.*, 2015; Liedtke *et al.*, 2015). Due to this, the potential for false positives or false negatives in cancer diagnosis by gene expression is high. Some genetic biomarkers of cancer have been established, and proof of principle cancer diagnostics by qPCR have been demonstrated. For example Dong *et al.*, identified the *ST13* (suppression of tumorigenicity 13) gene as being expressed in lesser quantities in colorectal mucosal carcinoma tissue in comparison to normal adjacent intestinal mucosa in 50 patients (Dong *et al.*, 2005). Zhou *et al.*, showed by qPCR that the microRNAs (miRNAs) miR-652 and miR-660 were upregulated in non-small cell lung cancer (NSCLC) in 300 patients (Zhou *et al.*, 2015). Jia *et al.*, also showed

the predictive value of miRNAs, specifically miR-21, miR-29a, miR-200a, miR-25 and miR-486-5p, in 371 cervical cancer patients (Jia *et al.*, 2015). Fan *et al.*, showed that the engulfment and cell motility 3 (*ELMO3*) gene is significantly upregulated in 125 non-small cell lung carcinoma (NSCLC) patients in comparison to unaffected adjacent tissue and 89 control patients (Fan *et al.*, 2015). However, none of these studies is sufficiently extensive to be able to conclude that these changes could be applied to general populations and therefore form the basis of a robust diagnostic test.

Although a number of cancer biomarkers have been determined, limitations to their use in PoCT exist. Consideration must be given to the source of sample for testing by qPCR. Less invasive techniques such as blood extraction are preferable; however, this requires that the biomarker is present in high enough quantity for detection, if present at all, in the blood. In addition to this, haem compounds found in blood inhibit the PCR reaction (Akane *et al.*, 1994) which can contribute to false negative results and eliminates whole blood from being a suitable candidate for qPCR before processing. More invasive methods of sample collection, such as tissue biopsy, preclude true PoCT as they require surgery.

In addition to diagnostic uses, qPCR testing can be used to assess clinically relevant biomarkers for determining appropriate treatment approaches. Response to certain therapeutic approaches can be highly diverse even within one cancer type (Lalwani *et al.*, 2011). Assessing a patient prior to treatment to establish the most effective therapeutic path is an example of personalised medicine and would represent a significant improvement to current methods. For example, melanoma patients with Raf-1 proto-oncogene, serine/threonine kinase (*RAF1*), *KRAS* and *CCND1* gene copy number increases show an improved response to the addition of Sorafenib therapy to Carboplatin and Paclitaxel treatment and low grade serous ovarian cancer patients do not respond as well to conventional chemotherapies (Carboplatin and Paclitaxel) as they do to alternative therapies such as Etoposide, Doxorubicin and Topotecan (Wilson *et al.*, 2015; Santillan *et al.*, 2007).

# ***Chapter 2***

## ***Methodology***

### **2.1 Tissue Culture**

#### **2.1.1 Cell Lines**

SKOV3 and MDAH-2774 cell lines were used as models for epithelial ovarian cancer. SKOV3 human ovarian clear cell adenocarcinoma cells were purchased from ATCC and were derived in 1973 from the ascites of a Caucasian female patient aged 64 years. MDAH-2774 cells were purchased from ATCC and are human ovarian endometrioid adenocarcinoma derived. They were isolated from the ascites of an untreated female patient in 1972. MDAH-2774 cells show a trend towards triploidy, particularly trisomy of chromosomes 1, 2, 3, 6, 11, 12, 16 and X and monosomy of chromosomes 17 and 21; the modal number of chromosomes being 66-68 (Freedman *et al.*, 1978). Characteristics of both cell lines are summarised in Table 2.1.

SKOV3 and MDAH-2774 cells were grown in DMEM (Dulbecco's Modified Eagle's Medium, Gibco) supplemented with 10% FBS (fetal bovine serum, Gibco), 1% penicillin/streptomycin (Gibco) and 1% L-glutamine (Gibco). Both cell lines were cultured at 37°C/5% carbon dioxide (CO<sub>2</sub>) and subcultured when approaching 80% confluency, approximately three times a week.



Cell Line	Origin	Grade	Key Gene Mutations	Chemotherapeutic Sensitivities
<b>SKOV3</b>	Ascites	1/2	<i>TP53</i> <i>PIK3CA</i>	Docetaxel Paclitaxel Carboplatin Doxorubicin
<b>MDAH-2774</b>	Ascites	2	<i>TP53</i> <i>PIK3CA</i> <i>KRAS</i> <i>BRCA1</i> (silent) <i>BRCA2</i> (silent)	Docetaxel Paclitaxel Oxaliplatin Fluorouracil Doxorubicin

**Table 2.1** - Characteristics of two epithelial ovarian cancer cell lines, SKOV3 and MDAH-2774. Table adapted from Beaufort et al., (Beaufort et al., 2014).

### 2.1.2 Tissue Culture Practice

An aseptic environment was maintained with the use of a HERAsafe laminar flow cabinet (Heraeus), and generous and repeated applications of TriGene Advance (Medimark Scientific) and 70% industrial methylated spirits (IMS) in dH<sub>2</sub>O to all surfaces and equipment used. Where possible, commercial pre-packed and pre-sterilised items were used. Plasticware was sterilised by autoclave.

### 2.1.3 Thawing Cryopreserved Cells

When growing cells up from stocks frozen in liquid nitrogen, 20mL of media was first stored in a T-75 cell culture flask in the incubator for at least one hour to allow the media to equilibrate to the temperature and CO<sub>2</sub> conditions. After this period, the cells were moved with speed from liquid nitrogen, defrosted in a water bath at 37°C and immediately transferred to the pre-warmed media which was then left undisturbed in the incubator for 12 hours. At 12 hours the media was replaced with fresh media that had been warmed to 37°C, removing the high concentration of DMSO remaining from the freezing medium and replenishing the nutrients.

#### **2.1.4 Subculturing Cells**

Cells were subcultured at around 80% confluency by aspirating the media, incubating with 2.5ml TrypLE™ Express (Invitrogen) per  $\sim 75\text{cm}^2$  growth surface area and manually disturbing the flask to detach adherent cells. The detached cells were then suspended in 17.5mL of their appropriate media and 5mL transferred to each of four new T-75 cell culture flasks already containing 15mL of media. All media used in the subculturing process was first warmed to 37°C. MDAH-2774 and SKOV3 cell lines required a 1 in 4 split approximately three times per week.

#### **2.1.5 Cryopreserving Cells**

When no longer needed, stocks of each cell line were stored in liquid nitrogen. This was achieved by aspirating the media and detaching the cells by incubating them for two minutes with 2.5mL TrypLE™ Express (Invitrogen) per  $\sim 75\text{cm}^2$  surface area and manually disturbing the flask to detach adherent cells. The cells were resuspended in 4mL of media, the suspension moved to a 50mL centrifuge tube and centrifuged for five minutes at 12,000 RPM to form a cell pellet. The supernatant was removed and 0.5mL of FBS and 0.4mL of media was used to resuspend the cells. The cell suspension with 100 $\mu\text{l}$  DMSO was added to a cryovial and cooled slowly, first to -80°C in a Mr. Frosty freezing container (Nalgene) and then in liquid nitrogen 24 hours later.

### **2.2 Cell treatments**

#### **2.2.1 Seeding Cells**

Cells were seeded in 6-well plates ( $\sim 10\text{cm}^2$  surface area per well) at a specific seeding density (100,000 cells per well except for wound healing assays where cells were cultured to a confluent monolayer) with 2mL of appropriate media. Cell counts to determine seeding requirements were performed with a Countess®

Automated Cell Counter (Invitrogen) using an equal volume of Trypan Blue (0.4%) stain to cell suspension for cell viability. Seeding volume was calculated as follows:

*Total number of cells*

$$= \text{Viable cells per mL} \times \text{Volume (in mL) of suspension}$$

*Number of cells per  $\mu\text{L}$*

$$= \text{Total number of cells} / \text{Volume (in } \mu\text{L) of suspension}$$

*Volume of suspension to add to well*

$$= \text{Seeding density required} / \text{Number of cells per } \mu\text{L}$$

Cells were allowed to proliferate for 24 hours before processing.

### 2.2.2 Treating Cells

Compound	Concentrations
Rapamycin	20nM
	100nM
Everolimus	20nM
	100nM
Deforolimus	100nM
	1000nM
Temsirolimus	10nM
	100nM
Resveratrol	25 $\mu\text{M}$
	50 $\mu\text{M}$
NVP BEZ-235	10nM
	100nM

**Table 2.2** - Details of treatment compounds and concentrations used in cell treatments.

Cells treatment compounds were dissolved in a dimethyl sulfoxide (DMSO) carrier. As DMSO can be cytotoxic, dilutions were calculated such that equal amounts (0.5%) of carrier were exposed to each well despite the concentration of the treatment. Cells treated with only carrier were used as a control. Treatment compounds were stored at -20°C. Cell treatments used are detailed in Table 2.2.

Treatments were first mixed into prewarmed media before being applied to the cells to ensure full homogenisation and avoid cells experiencing toxically high concentrations of carrier or inhibitor.

### **2.3 Proliferation Assay**

Proliferation, death and viability of the cells were assessed after treatment using a Countess® Automated Cell Counter (Invitrogen) and trypan blue stain. Media was aspirated from the cells which were then incubated with 200µL of TrypLE™ Express (Life Technologies) per well and manually agitated to detach the cells. The cells were resuspended in 800µL of appropriate media to make 1mL of cell suspension in total. An equal volume of cell suspension was mixed thoroughly with trypan blue stain (0.4%, trypan blue is selectively absorbed by dead cells) and applied to a Countess® cell counting chamber slide (Invitrogen). Three readings were taken per sample and an average value calculated.

### **2.4 Wound Healing Assay**

Cells were assessed for their ability to close a created gap in cell growth area. One confluent T-75 cell culture flask was seeded per three 6-well plates with 2mL appropriate media per well and grown until there was a confluent monolayer. A 20µL pipette tip was used create a 'scratch' in growth area perpendicular to a line drawn on the underside of the well in marker pen. The media was then aspirated and replaced with treated media. The scratch was then monitored and an image taken after 0, 6, 12 and 18 hours. The perpendicular line of marker was used as a landmark to ensure that an image of the same area was taken at each time point.

## 2.5 Clinical Samples

### 2.5.1 Fresh Ovarian Tissues

Ovarian clinical tissue samples from patients with ovarian cancer, endometrial cancer, endometriosis and fibroids as well as unaffected controls were obtained from the University of Thessanoliiki, Greece (ethical approval obtained by the local hospital authority and by Brunel University ethics committee, Table 2.3). Samples were shipped on dry ice in RNAlater® (Life Technologies) to preserve RNA integrity.

Pathology	Total	Age ≤30	Age >30	Unknown Age
Control	34	12	9	13
Endometriosis	Total	Grade score <50	Grade Score >50	Unknown grade score
	24	12	9	3
		Age ≤30	Age >30	Unknown age
	12	9	3	
Ovarian Cancer	13			
Fibroids	4			
Endometrial Cancer	4			

**Table 2.3** - Table detailing clinical sample details including pathology and, where available, stage and grade of disease and age of patient at time of surgery.

### 2.5.2 Paraffin Embedded Ovarian Tissues

Clinical tissue arrays containing paraffin embedded ovarian samples from 20 or 70 malignancies were purchased from US Biomax (Tables 2.4 and 2.5 respectively).

Position	Age	Diagnosis	Grade
A1	40	Endometrioid adenocarcinoma	II
A2	40	Necrosis tissue	-
A3	57	Serous papillary cystadenocarcinoma	II
A4	57	Serous papillary cystadenocarcinoma	II
A5	48	Clear cell carcinoma	-
A6	48	Clear cell carcinoma	-
B1	57	Serous papillary cystadenocarcinoma	II
B2	57	Serous papillary cystadenocarcinoma	II
B3	46	Fibrofatty tissue	-
B4	46	Serous papillary cystadenocarcinoma	III
B5	42	Endometrioid adenocarcinoma	I
B6	42	Endometrioid adenocarcinoma	I
C1	66	Serous papillary cystadenocarcinoma	III
C2	66	Serous papillary cystadenocarcinoma	III
C3	53	Serous papillary cystadenocarcinoma	III
C4	53	Serous papillary cystadenocarcinoma	III
C5	35	Serous papillary cystadenocarcinoma	II
C6	35	Serous papillary cystadenocarcinoma	II
D1	52	Serous papillary cystadenocarcinoma	III
D2	52	Serous papillary cystadenocarcinoma	III

**Table 2.4** - Details of paraffin embedded tissue on 20 sample slide.

Position	Age	Diagnosis	Grade	Stage
A1	40	Clear cell carcinoma	-	I
A2	57	Serous papillary carcinoma	II	Ic
A3	48	Clear cell carcinoma	-	II
A4	57	Serous papillary carcinoma	II	IIIc
A5	43	Serous papillary carcinoma	III	IIIc
A6	54	Serous papillary carcinoma	I	Ic

<b>A7</b>	63	Serous papillary carcinoma	III	IV
<b>A8</b>	46	Serous papillary carcinoma	III	IIIc
<b>A9</b>	54	Serous papillary carcinoma	III	IIIc
<b>A10</b>	56	Hyperplastic fibrous tissue	–	–
<b>B1</b>	44	Granular cell tumor	–	–
<b>B2</b>	49	Serous papillary carcinoma	III	II
<b>B3</b>	18	Immature teratoma	–	–
<b>B4</b>	15	Endodermal sinus carcinoma	–	IIa
<b>B5</b>	38	Metastatic adenocarcinoma	III	–
<b>B6</b>	39	Serous papillary carcinoma	III	IV
<b>B7</b>	24	Endodermal sinus carcinoma	–	II
<b>B8</b>	42	Serous papillary carcinoma	III	II
<b>B9</b>	50	Serous papillary carcinoma	III	I
<b>B10</b>	49	Serous papillary carcinoma	III	IIIc
<b>C1</b>	62	Serous papillary carcinoma	III	II
<b>C2</b>	53	Mucinous papillary carcinoma	I	IV
<b>C3</b>	38	Metastatic adenocarcinoma	III	–
<b>C4</b>	43	Clear cell carcinoma	–	Ia
<b>C5</b>	26	Serous papillary carcinoma	I	Ic
<b>C6</b>	47	Serous papillary carcinoma	I	I
<b>C7</b>	62	Squamous cell carcinoma	III	I
<b>C8</b>	35	Dysgerminoma	–	Ia
<b>C9</b>	41	Dysgerminoma	–	I
<b>C10</b>	47	Serous papillary carcinoma	III	I
<b>D1</b>	42	Clear cell carcinoma	–	Ic
<b>D2</b>	39	Metastatic adenocarcinoma	I	–
<b>D3</b>	66	Metastatic adenocarcinoma	III	–
<b>D4</b>	48	Malignant follicular theca cytoma	–	III
<b>D5</b>	51	Serous papillary carcinoma	I	IIIc
<b>D6</b>	33	Metastatic signet-ring cell carcinoma	–	

<b>D7</b>	18	Mixed germ cell tumor	–	Ib
<b>D8</b>	40	Metastatic signet-ring cell carcinoma	–	–
<b>D9</b>	43	Granular cell tumor	–	–
<b>D10</b>	55	Serous papillary carcinoma	III	II
<b>E1</b>	46	Serous papillary carcinoma	III	IIIc
<b>E2</b>	57	Serous papillary carcinoma	III	IIIc
<b>E3</b>	75	Serous papillary carcinoma	III	IIIc
<b>E4</b>	69	Serous papillary carcinoma (sparse)	III	Ia
<b>E5</b>	30	Serous papillary carcinoma	III	I
<b>E6</b>	42	Serous papillary carcinoma	II	IIIc
<b>E7</b>	48	Clear cell carcinoma	–	I
<b>E8</b>	22	Serous papillary carcinoma	I	IIb
<b>E9</b>	50	Clear cell carcinoma	–	I
<b>E10</b>	32	Serous papillary carcinoma	II	I
<b>F1</b>	48	Serous papillary carcinoma	II	I
<b>F2</b>	50	Serous papillary carcinoma	II	II
<b>F3</b>	65	Serous papillary carcinoma	III	IIIc
<b>F4</b>	38	Serous papillary carcinoma	III	IIIc
<b>F5</b>	31	Metastatic adenocarcinoma	III	–
<b>F6</b>	55	Metastatic adenocarcinoma	III	–
<b>F7</b>	51	Serous papillary carcinoma	III	II
<b>F8</b>	65	Serous papillary carcinoma	II	I
<b>F9</b>	26	Serous papillary carcinoma	II	IIIc
<b>F10</b>	55	Serous papillary carcinoma	II	I
<b>G1</b>	49	Serous papillary carcinoma	III	II
<b>G2</b>	48	Metastatic signet-ring cell carcinoma	–	–
<b>G3</b>	46	Serous papillary carcinoma	III	IIIc
<b>G4</b>	63	Serous papillary carcinoma	III	II
<b>G5</b>	37	Serous papillary carcinoma	II	IV
<b>G6</b>	35	Malignant tumor (sparse)	–	IIIc



<b>G7</b>	12	Dysgerminoma	–	Ib
<b>G8</b>	55	Serous papillary carcinoma	II	I
<b>G9</b>	20	Malignant tumor cell (sparse)	–	I
<b>G10</b>	55	Serous papillary carcinoma	II	I

**Table 2.5** - Details of paraffin embedded tissue on 70 sample slide.

### 2.5.3 Whole Blood

Whole blood from 7 ovarian cancer patients and 6 unaffected controls were obtained from the Department of Obstetrics and Gynaecology at University Hospital, University of Crete, Greece (ethical approval obtained by the local hospital authority and by Brunel University ethics committee). Samples were extracted into EDTA vacuum tubes and shipped on dry ice.

## 2.6 RNA Extraction

mRNA was extracted from cells to examine gene expression transcripts. All surfaces and equipment were cleaned thoroughly with 70% IMS before and throughout any RNA work. RNA was stored at -80°C when not in use and kept on ice at all other times to prevent degradation.

### 2.6.1 From Cultured Cells

#### 2.6.1.1 GenElute™ (Sigma Aldrich)

GenElute™ Mammalian Total RNA MiniPrep Kit is a commercially available silica membrane, spin column based RNA extraction system. Media was removed from the cells, collected in pre-labelled sample tubes and stored at -80°C for later use. The cells were briefly washed in phosphate buffered saline (PBS, Gibco) and 250µL of lysis buffer per 10cm<sup>2</sup> cell growth area containing 1% β-mercaptoethanol per well was applied directly to the cells to lyse cell membranes and inactivate RNases.

The plate was then gently rocked to ensure all cells were covered and incubated at room temperature for 60 seconds to ensure complete cell lysis. The bottom of each well was scraped with a pipette tip and the lysate was transferred into a blue filtration column contained within a collection tube and centrifuged for 2 minutes at 12,000 x g to remove cellular debris and shear DNA. The filtered lysate was then mixed with 250µL of 70% ethanol to enhance binding of nucleic acids to the silica membrane and loaded into a red silica column contained within a collection tube. \*The column was centrifuged for 15 seconds at 12,000 x g; the flow-through was discarded as the RNA was now bound to the membrane. The RNA was washed three times, once with Wash Solution I and twice with Wash Solution II (supplied in kit) by centrifuging for 15 seconds at 12,000 x g to remove impurities including proteins, cellular debris and salts. A final centrifugation of 12,000 x g for 2 minutes was carried out to ensure that the ethanol was completely removed from the membrane. RNA was eluted by placing the membrane column in a fresh collection tube, applying 50µL of pure water (elution solution) to the membrane and centrifuging at 12,000 x g for 60 seconds. RNA was stored at -80°C until further use.

#### **2.6.1.2 NucleoSpin® (Macherey-Nagel)**

NucleoSpin® RNA/Protein is a commercially available silica membrane, spin column based dual RNA and protein extraction system. Media was removed from the cells, collected in pre-labelled sample tubes and stored at -80°C for later use. The cells were briefly washed in PBS (Gibco) and lysis buffer (350µl per 10cm<sup>2</sup> of cells) was added directly to the adherent cells to lyse cell membranes and inactivate RNases. The bottom of each well was scraped with a pipette tip and the lysates were collected in sample tubes and stored on ice before processing. Each tube was vortexed for at least ten seconds to ensure complete lysis of the cells. Each lysate was passed through a clearing membrane to reduce viscosity and remove cellular debris. 350µl of 70% ethanol was added to each of the lysates to enhance the RNA binding efficiency to the silica membrane. The lysates were then passed through a silica membrane by centrifugation for 30 seconds at 11,000 x g. The protein, now

contained within the flow through, was stored at +4°C for later processing. Salt was removed from the membrane and bound RNA with 350µl Membrane Desalting Buffer (centrifuged for one minute at 11,000 x g) to enhance the subsequent rDNase digest where 95µl of rDNase reaction mixture was incubated on the silica membrane for 15 minutes at room temperature to remove any DNA. The rDNase was inactivated and residual protein, salts and contaminants removed by one wash with 200µl of Buffer RA2 (centrifuged for 30 seconds at 11,000 x g), one wash with 600µl of Buffer RA3 (centrifuge for 30 seconds at 11,000 x g) and one wash with 250µl of Buffer RA3 (centrifuge for 2 minutes at 11,000 x g). The membrane bound RNA was rehydrated and eluted with 60µl of RNase-free water and stored at -80°C until further use.

### **2.6.2 From Tissue Samples (from GenElute™ kit by Sigma Aldrich, above)**

Tissue samples were removed from RNA<sup>later</sup>® (Life Technologies) and 40mg of tissue was placed in a sterile 2mL sample tube with 500µL of lysis buffer containing 1% β-Mercaptoethanol and a 2mm ball bearing. The tissue was then homogenised, membranes lysed and RNases inactivated with a TissueLyser II (Qiagen) tissue lyser for 2 minutes. The homogenised tissue was transferred into a blue filtration column contained within a collection tube and centrifuged for 2 minutes at 12,000 x g to remove cellular debris and shear DNA. The filtered lysate was then mixed with 500µL of 70% ethanol to enhance binding of nucleic acids to the silica membrane and loaded into a red silica column contained within a collection tube. GenElute™ protocol was then continued as above from \*.

### **2.6.3 From Whole Blood**

RNA was extracted from whole blood using the QIAamp® RNA Blood Mini Kit (Qiagen). 1mL of whole blood was mixed with 1mL of Buffer EL and incubated on ice for 15 minutes to lyse erythrocytes. Samples were centrifuged for 10 minutes at 400 x g to form a cell pellet and the supernatant was discarded. 2mL of Buffer EL

was vortexed with the pellet which was centrifuged for a further 10 minutes at 400 x g to ensure complete removal of erythrocytes and supernatant was discarded. 600µL of Buffer RLT was added to the pellet and vortexed to remove clumps. The cell mixture was then transferred to a QIAshredder spin column and centrifuged for 2 minutes at 13,000 x g to lyse cells and remove debris. 600µL of 70% ethanol was mixed into the lysate to enhance RNA binding efficiency and was then transferred into a QIAamp® spin column. The QIAamp® spin column was centrifuged for 15 seconds at 8000 x g to bind RNA to the silica membrane. Flow through was discarded and the spin column was transferred to a fresh collection tube. The membrane was washed in 700µL Buffer RW1 followed by 500µL of Buffer RPE by centrifuging for 15 seconds at 8000 x g. A further wash in 500µL of Buffer RPE was followed by centrifugation for 3 minutes at 20,000 x g to dry the membrane before RNA elution. The QIAamp® spin column was transferred to a fresh collection tube and 30µL of RNase-free water was applied directly to the membrane. Samples were centrifuged for 1 minute at 8000 x g and eluted RNA was stored at -80°C until further processing.

#### **2.6.4 RNA Quantification**

1µL of extracted RNA per sample was analysed spectrophotometrically for concentration and purity using a NanoDrop 2000C (Thermo Fisher Scientific). Concentration was calculated from absorbance at 280nm and purity was calculated by  $A_{260}/A_{280}$  ratio with an acceptable range of 1.7-2.0.

#### **2.7 cDNA Synthesis**

Complementary DNA (cDNA) was synthesised from extracted RNA for use in qPCR experiments. All surfaces and equipment were cleaned thoroughly with 70% IMS before and throughout cDNA synthesis work. Random primers were chosen over oligo-dT in order to avoid 3' poly-A tail weighting. RNA volume input was calculated by the following:

RNA input

=desired cDNA concentration/RNA concentration (ng/ $\mu$ L)

### 2.7.1 SuperScript® II (Life Technologies)

RNA input was calculated and the appropriate amount, made up to 10 $\mu$ L with pure H<sub>2</sub>O, was mixed in one 0.6mL, thin walled sample tube for each sample. 2 $\mu$ L of primer/dNTP mix (Table 2.6) was added each tube which was then heated to 65°C for 5 minutes in a heat block to denature RNA secondary structure. Samples were cooled on ice immediately after incubation to stop the reaction.

Reagent	Volume per sample
Random Hexamer Primers (3 $\mu$ g/ $\mu$ L)	1 $\mu$ L
dNTPs (10mM)	1 $\mu$ L

**Table 2.6** - Reagent volumes for primer/dNTP mix for one sample for use in the SuperScript® II Reverse Transcriptase cDNA synthesis kit (Life Technologies)

Each tube was briefly centrifuged to collect contents. 7 $\mu$ L of First Strand Buffer mix (Table 2.7) was added to each sample to maintain appropriate pH and incubated at room temperature for 2 minutes before 1 $\mu$ L Superscript® II enzyme was added. The samples were then incubated at room temperature for 10 minutes to anneal the primers, 42°C for 50 minutes to extend the synthesis and 70°C for 10 minutes to inactivate the enzyme. cDNA was stored at -20°C until further processing.

Reagent	Volume per sample
First Strand Buffer	4 $\mu$ L
0.1M DTT	2 $\mu$ L
Pure H <sub>2</sub> O	1 $\mu$ L

**Table 2.7** - Reagent volumes for First Strand Buffer mix for one sample for use in the SuperScript® II Reverse Transcriptase cDNA synthesis kit (Life Technologies).

### 2.7.2 nanoScript™ 2 (Primerdesign)

RNA input was calculated and the appropriate amount, made up to 9µL with pure H<sub>2</sub>O, was mixed in one 0.6mL, thin walled sample tube for each sample. 1µL of random nonamer primers were added to each sample which were then incubated at 65°C for 5 minutes to denature RNA secondary structure. The samples were cooled on ice and 10µL of extension buffer (Table 2.8) was added to each sample.

Reagent	Volume per sample
nanoScript™ 2 4X Buffer	5µL
dNTP mix (10nM)	1µL
Pure H <sub>2</sub> O	3µL
nanoScript™ 2 enzyme	1µL

**Table 2.8** - Reagent volumes for extension buffer for one sample for use in the nanoScript™ 2 Reverse Transcription kit (Primerdesign).

Tubes were vortexed and briefly centrifuged to collect reagents. The samples were incubated at room temperature for five minutes to allow primer annealing, 42°C for 20 minutes to extend the reaction and 75°C for 10 minutes to inactivate the reaction. cDNA was stored at -20°C until further processing.

## 2.8 Protein Extraction

Protein was extracted from cultured cells in 6-well plates in order to examine expression patterns of phosphorylated p70S6 kinase, caspase 3 and caspase 9.

### 2.8.1 Laemmli Buffer

Media was aspirated and cells were washed briefly in PBS (Gibco). 100µL of Laemmli buffer (Table 2.9) was added per 10cm<sup>2</sup> cell growth area and the plate gently rocked to cover all cells. Cells were scraped with a pipette tip and lysate was

transferred into a sterile 1.5mL sample tube. Lysates were denatured by boiling for 10 minutes at 95°C in a heat block before storage at -20°C until further use.

Reagent	Volume
Tris (pH 6.8)	1mL
10% SDS	4mL
Glycerol	2mL
β-mercaptoethanol	0.5mL
dH <sub>2</sub> O	2.5mL
Bromophenol blue	Small amount to achieve desired colour to aid visualisation

**Table 2.9** – Volume of components of 10mL Laemmli buffer.

## 2.9 Reference Gene Assessment

Gene Name	Gene
<b>ACTB*</b>	Actin, beta (mRNA)
<b>GAPDH*</b>	Glyceraldehyde-3-phosphate dehydrogenase (mRNA)
<b>UBC*</b>	Ubiquitin C (mRNA)
<b>B2M*</b>	Beta-2-microglobulin (mRNA)
<b>YWHAZ*</b>	Phospholipase A2 (mRNA)
<b>RPL13A*</b>	Ribosomal protein L13A (mRNA)
<b>18S</b>	18S RNA (rRNA)
<b>CYC1</b>	Cytochrome C-1 (mRNA)
<b>EIF4A2</b>	Eukaryotic translation initiation factor 4A isoform 2 (mRNA)
<b>SDHA</b>	Succinate dehydrogenase complex (mRNA)
<b>TOP1</b>	Topoisomerase (DNA) 1 (mRNA)
<b>ATP5B</b>	ATP synthase subunit (mRNA)

**Table 2.10** – Clinical samples were assessed for the most stably expressed reference gene using the geNorm™ human 12 gene kit from Primerdesign. The above table details the 12 genes included in the kit. Genes included in the 6 gene kit are denoted with an asterisk.

According to MIQE guidelines (minimum information for the publication of qPCR experiments), an assessment of the most appropriate reference genes specific to the samples used must be carried out prior to any qPCR experiment. In light of this, a selection of samples representing the whole cohort in each experiment were assessed using either the geNorm™ human 12 gene kit or geNorm™ human 6 gene kit (Primerdesign). The genes assessed are detailed in Table 2.10.

### **2.9.1 geNorm™ with PrecisionPLUS™ Mastermix (Primerdesign)**

geNorm™ experiments were prepared in a qPCR exclusive area and all equipment used was sterilised using TriGene Advance (Medimark Scientific) and 70% IMS (industrial methylated spirits) initially and repeatedly throughout the preparation. All reagents were defrosted and stored on ice when in use to preserve their integrity and SYBR® Green containing reagents were kept in a light proof bag whenever possible. geNorm™ experiments were carried out on a 7900HT Fast thermal cycler (Life Technologies). PrecisionPLUS™ Mastermix by Primerdesign was used for geNorm™ experiments as per manufacturer's instructions. PrecisionPlus™ Mastermix is pre-prepared master mix containing a hot start *Taq* polymerase enzyme, SYBR® Green I dye and deoxynucleoside triphosphates (dNTPs). Primers in the geNorm™ kit were supplied lyophilised and so tubes were briefly centrifuged to collect dry components at the bottom of the tubes which were then rehydrated with 220µL of pure H<sub>2</sub>O. Forward and reverse primers were contained within the same tube. Samples were run in duplicate and so small mixes were made up for each primer for (n x 2)+1 containing the following (Table 2.11):



Reagent	Volume ( $\mu\text{L}$ ) for $n=1$
Primer Mixture	1
PrecisionPLUS™ Mastermix	10
Pure H <sub>2</sub> O	4
cDNA (5ng/ $\mu\text{L}$ )	5
<b>Total</b>	<b>20</b>

**Table 2.11** - Volume of components for primer mixes in geNorm™ experiment.

cDNAs for representative samples were diluted to be 5ng/ $\mu\text{L}$ . 15 $\mu\text{L}$  of the primer mix was pipetted into each well (two reactions for each sample) of a MicroAmp® Fast Optical 96-Well Reaction Plate (Life Technologies) followed by 5 $\mu\text{L}$  of appropriate cDNA. The wells were sealed hermetically with a transparent, contact adhesive sealing film and the plate centrifuged to ensure all the reagents had collected. The reagents were then subject to the following thermal protocol (Table 2.12):

Temperature	Time	Cycles
95°C	2 minutes	1
95°C	15 seconds	40
60°C	60 seconds	
Fluorescence Measurement	-	
Dissociation Curve	60-95°C	1

**Table 2.12** - The thermal protocol of a geNorm™ experiment on a 7900HT Fast thermal cycler (Life Technologies).

Following the amplification protocol, the dissociation temperature of the PCR products generated were assessed by a dissociation protocol. In this protocol the temperature was increased by 1°C from 60-95°C and a fluorescence measurement taken at each increase. The differential fluorescence was plotted against the temperature (°C) to determine the temperature at which the product strands dissociated.

## 2.9.2 geNorm™ Analysis

geNorm™ was analysed using qBase+ software (Biogazelle). qPCR data was uploaded and qBase+ calculated an M and V value for expressional stability and optimum number of reference genes to use respectively.

## 2.10 qPCR

qPCR (quantitative polymerase chain reaction) was used to assess relative gene expression in a number of different experiments. qPCR experiments were prepared in an exclusive area and all equipment used was sterilised using TriGene Advance (Medimark Scientific) and 70% IMS (industrial methylated spirits) initially and repeatedly throughout the preparation. All reagents were defrosted and stored on ice when in use to preserve their integrity and SYBR® Green containing reagents were kept in a light proof bag whenever possible.

### 2.10.1 Primers

The primer sequences for mTOR, DEPTOR, rictor, raptor and 18S RNA were taken from Foster *et al.*, (Foster *et al.*, 2010). Primer Design does not disclose the sequence of the primers used in their geNorm™ kit. As it is a MIQE requirement to publish primer sequences, alternative primers were designed for the selected reference genes, *YWHAZ* and *RPL13A*, using the OligoPerfect™ Designer (Life Technologies), keeping the  $T_m$  and product size (base pairs, bp) as similar as possible to the Primer Design primers. Below is a summary of the primers (Table 2.13):

Name	Amplicon Size (bps)	Strand	Size (bases)	Sequence (5'-3')
<b>mTOR</b>	135	Forward	20	t g c c a a c t a c c t t c g g a a c c
		Reverse	20	g c t c g c t t c a c c t c a a a t t c
<b>DEPTOR</b>	202	Forward	20	c a c c a t g t g t g t g a t g a g c a
		Reverse	20	t g a a g g t g c g c t c a t a c t t g
<b>Rictor</b>	117	Forward	20	g g a a g c c t g t t g a t g g t g a t
		Reverse	20	g g c a g c c t g t t t t a t g g t g t
<b>Raptor</b>	170	Forward	20	a c t g a t g g a g t c c g a a a t g c
		Reverse	20	t c a t c c g a t c c t t c a t c c t c
<b>YWHAZ</b>	127	Forward	20	a g a c g g a a g g t g c t g a g a a a
		Reverse	20	g a a g c a t t g g g g a t c a a g a a
<b>RPL13A</b>	144	Forward	20	c c t g g t c t g a g c c c a a t a a a
		Reverse	20	c t t g c t c c c a g c t t c c t a t g
<b>18S RNA</b>	155	Forward	20	a a a c g g c t a c c a c a t c c a a g
		Reverse	20	c c t c c a a t g g a t c c t c g t t a

**Table 2.13** - The primer sequences for the *mTOR*, *Deptor*, *Rictor* and *Raptor*, *YWHAZ* and *RPL13A* genes. *mTOR*, *DEPTOR*, *rictor*, *raptor* and *18S RNA* were taken from Foster et al., (Foster et al., 2010). *YWHAZ* and *RPL13A* primers were designed by Oligo Perfect Designer (Invitrogen). All primers were synthesised by Sigma-Aldrich. None of the primers used showed evidence of primer dimer formation.

Primers were supplied lyophilised and so were briefly centrifuged to collect dry components at the bottom of the tubes. Primers were then rehydrated according to manufacturer's direction.

### 2.10.2 Gel Electrophoresis

Primers were validated by running PCR products on a 2% agarose gel. 2g of agarose (Fisher Scientific) was added to 100mL of 1 X tris borate EDTA (TBE, 89mM Tris-borate, 2mM EDTA, pH 8.3) buffer and microwaved for 2 minutes or until the agarose has dissolved and the mixture was clear. The mixture was cooled to

approximately 50°C and 5µL ethidium bromide was added and mixed well. The gel was poured into a prepared casting tray on a level surface and a 20 well comb inserted at one end. The gel was left to set for approximately 25 minutes and transferred into a tank containing 1 X TBE buffer. 2µL of DNA loading buffer was added to 20µL qPCR product and mixed well to aid loading and visualisation of migration through the gel. 15µL of this mixture was added to each well. In a separate well 5µL of 1kb Plus DNA Ladder™ (Life Technologies) was added as a measure of product size. The gel was run at 100V and 400mA for approximately 45 minutes until the product had migrated a satisfactory distance. The gel was visualised using a Gel Doc™ XR+ Imaging System (Bio-Rad) and analysed visually for consistency of product size to predicted product size and the presence of extra products which may represent contamination or primer dimers.

### 2.10.3 Power SYBR® Master Mix (Life Technologies)

Power SYBR® Master Mix (Life Technologies) was used with a 7900HT Fast thermal cycler (Life Technologies). Power SYBR® Master Mix is pre-prepared master mix containing AmpliTaq Gold DNA Polymerase, SYBR® Green I dye and dNTPs (with a blend of dUTP and dTTP). Reactions were formulated as follows (Table 2.14):

Reagent	Volume (µL) for n=1
Power SYBR® Master Mix (2x)	10
Pure H <sub>2</sub> O	7
Forward Primer (10µM)	1
Reverse Primer (10µM)	1
cDNA (100ng/µL)	1
<b>Total</b>	<b>20</b>

**Table 2.14** - Volume of components for primer mixes in qPCR experiment with Power SYBR® Master Mix (Life Technologies).

A different mix was prepared for each primer set. 19µL of the appropriate mix and 1µL of cDNA was dispensed into a MicroAmp® Fast Optical 96-Well Reaction Plate (Life Technologies) according to a pre-designed well plan. NTCs (non-template controls), where water was substituted for cDNA, were included for each of the primer mixes as a negative control. According to MIQE guidelines and geNorm™ analysis completed previously, 2 reference genes, *RPL13A* and *YWHAZ*, were expressionally stable and thus were included as an endogenous controls. The wells were sealed hermetically with a transparent, contact adhesive sealing film and the plate centrifuged to ensure all the reagents had collected. The sample plate was subjected to a temperature protocol consisting of the following (Table 2.15):

Step	Temperature	Time	Cycles
Hot Start	95°C	10 minutes	1
Amplification	95°C	15 seconds	40
	60°C	60 seconds	
Fluorescence Measurement	60°C	-	
Dissociation Curve	60-95°C	1	1

**Table 2.15** - The thermal protocol of a qPCR experiment using Power SYBR® Master Mix on a 7900HT Fast thermal cycler (both Life Technologies).

Following the amplification protocol, the dissociation temperature of the PCR products generated were assessed by a dissociation protocol as described above.

#### 2.10.4 Kapa SYBR® Fast Universal Master Mix (Kapa Biosystems)

Kapa SYBR® Fast Universal Master Mix (Kapa Biosystems) was used with an xpress® thermal cycler (BJS Biotechnologies). Kapa SYBR® Fast Universal Master Mix is pre-prepared master mix containing a DNA Polymerase, SYBR® Green I dye and dNTPs. Reactions were formulated as follows (Table 2.16):

Reagent	Volume ( $\mu\text{L}$ ) for $n=1$
Kapa SYBR <sup>®</sup> Fast Universal Master Mix (2x)	2
Forward Primer (2.5 $\mu\text{M}$ )	1
Reverse Primer (2.5 $\mu\text{M}$ )	1
cDNA (25ng/ $\mu\text{L}$ )	1
<b>Total</b>	<b>5</b>

**Table 2.16** - Volume of components for primer mixes in qPCR experiment with Kapa SYBR<sup>®</sup> Fast Master Mix (Kapa Biosystems).

A different mix was prepared for each primer and cDNA set. 5 $\mu\text{L}$  of the appropriate mix was dispensed into a 96-Well xplate<sup>™</sup> (BJS Biotechnologies) according to a pre-designed well plan. NTCs (non-template controls), where water was substituted for cDNA, were included for each of the primer mixes as a negative control. The wells were sealed hermetically with a transparent, heat adhesive sealing film using an xsealer (BJS Biotechnologies). The sample plate was subjected to a temperature protocol consisting of the following (Table 2.17):

Step	Temperature	Time	Cycles
Hot Start	95°C	3 minutes	1
Amplification	95°C	15 seconds	40
	60°C	60 seconds	
Fluorescence Measurement	60°C	-	
Dissociation Curve	50-95°C	-	1

**Table 2.17** - The thermal protocol of a qPCR experiment using Kapa SYBR<sup>®</sup> Master Mix (Kapa Biosystems) on an xpress<sup>®</sup> thermal cycler (BJS Biotechnologies).

Following the amplification protocol, the dissociation temperature of the PCR products generated were assessed by a dissociation protocol as shown in Table 2.17.

### 2.10.5 qPCR Analysis

Amplicon load can be measured in two ways, by absolute or relative quantification. Absolute quantification measures amplification in relation to a known standard to provide an absolute copy number. Relative quantification measures amplification in relation to a reference gene or genes which are stably expressed under the conditions of the experiment (for example after treatment of cultured cells with a drug compound). The most common way to analyse relative quantification qPCR data is the  $\Delta$  or  $\Delta\Delta C_q$  method detailed below:

$$\Delta C_q$$

$$= C_q (\text{gene of interest}) - C_q (\text{reference gene})$$

(Normalises GOI expression to the reference gene)

$$\Delta\Delta C_q$$

$$= \Delta C_q (\text{sample}) - \Delta C_q (\text{calibrator})$$

(Normalises GOI expression in a sample to that of a calibrator, for example untreated cells)

$$\text{For } \Delta C_q \text{ method: } RQ = 2^{-\Delta C_q}$$

$$\text{For } \Delta\Delta C_q \text{ method: } RQ = 2^{-\Delta\Delta C_q}$$

(Inverts value to show change whilst assuming 100% efficiency)

The  $\Delta\Delta C_q$  method demonstrates fold change in expression in comparison to a calibrator and is only appropriate when a valid calibrator is available; for example in the case of cultured cells treated with a drug compound the calibrator would be the same cells under basal conditions. In the case of gene expression in clinical samples, unless each sample is matched to non-affected adjacent tissue and the assumption is made that the tissue is 'normal', it is not acceptable to match the  $\Delta C_q$  value from one patient to that of a different patient as natural individual differences will mean that gene expression will differ from person to person. If this

is the case, the  $\Delta C_q$  method can be used to provide a comparison between samples and calibrators.

## 2.11 Western Blotting

Protein expression of caspases 3 and 9 and phosphorylated p70S6 kinase in cell lysates was analysed by western blot. Proteins were separated by mass by SDS-PAGE (sodium dodecyl sulphate polyacrylamide gel electrophoresis). A 12% resolving and 5% stacking gel were used and were prepared as follows (Table 2.18):

Reagent	Resolving Gel (mL)	Stacking Gel (mL)
dH <sub>2</sub> O	1.6	3.4
30% Acrylamide/Bisacrylamide (Sigma-Aldrich)	2	0.83
1.5M Tris (pH 8.8)	1.3	N/A
1M Tris (pH 6.8)	N/A	0.63
10% SDS (sodium dodecyl sulphate)	0.05	0.05
10% Ammonium Persulphate (APS) in dH <sub>2</sub> O	0.05	0.05
TEMED (tetramethylethylenediamine)	0.002	0.005
Total	5	5

**Table 2.18** - Formulations of resolving and stacking gels.

The gels were poured at a thickness of 1mm between glass plates according to the recipes in Table 2.18. Resolving gel was topped with 100% methanol to level and allowed to set for 20-30 minutes at room temperature. Once the resolving gel had set the methanol was poured away, the gel was washed with distilled H<sub>2</sub>O and excess water removed with filter paper. The stacking gel was poured on top of the resolving gel at an approximate height of 2cm, and a comb placed between the glass plates to form wells. The stacking gel was left to set for a further 20-30 minutes at room temperature.



Cell lysates were incubated at 95-100°C for at least 10 minutes to linearise the protein, break down disulphide bonds and remove tertiary structure. SDS in the protein buffer and gel serves to coat the protein in a consistent negative charge to avoid the varying charges on amino acids to affect migration of the protein through the gel. 10µl of each sample was loaded into each well according to a predesigned well plan. 5µl of PageRuler™ Prestained Protein Ladder (Life Technologies) was used as a reference of mass. The gels were run in 1X Running Buffer (Table 2.19) at 100V and 40mA per gel until the visible blue band of Laemmli buffer was close to the bottom of the gel and the ladder was fully separated out. When the samples move through the stacking gel they are concentrated between a chloride and glycine front and so enter the resolving gel simultaneously. The proteins are then able to separate based on their mass by their differential rate of movement through the resolving gel.

Reagent	Quantity
Tris Base	30g
Glycine	44g
10% SDS	100mL
dH <sub>2</sub> O	Up to 1L

**Table 2.19** - Formulation of 10X Running Buffer.

The separated proteins were then electrophoretically transferred onto a nitrocellulose membrane (Thermo Scientific) in Wet-Transfer Buffer (Table 2.20). The transfer apparatus were assembled while immersed in Wet-Transfer Buffer to avoid the gel and membrane drying out. The membrane and gel were sandwiched between sponges and filter paper and placed in a cassette before being placed in a tank of Wet-Transfer buffer and run at 100V and 300mA for 2 hours.

Reagent	Quantity
Tris Base	2.41g
Glycine	11.25g
dH <sub>2</sub> O	Up to 800mL
Methanol	200mL

**Table 2.20** - Formulation of 1X Wet-Transfer Buffer.

After successful transfer the protein ladder was visible on the nitrocellulose membrane. The membrane was then rinsed briefly in 1X TBS Tween (Tables 2.21 and 2.22) and incubated in 50mL of 5% cow's milk (Marvel milk powder in TBS Tween) for one hour at room temperature on a shaker.

Reagent	Quantity
Tris Base	24.2g
NaCl	80g
dH <sub>2</sub> O	Up to 1L

**Table 2.21** - Formulation of 10X TBS.

Reagent	Quantity
10X TBS	100mL
dH <sub>2</sub> O	899mL
Tween 20	1mL

**Table 2.22** - Formulation of 1X TBS Tween.

After blocking, the membrane was washed four times for ten minutes each in TBS Tween to remove any unbound milk proteins. A primary antibody (Table 2.23) diluted in 5% bovine serum albumin/TBS Tween was applied to the membrane and incubated overnight at 4°C on a shaker. The membrane was then washed a further four times for ten minutes each in TBS Tween to remove any unbound primary antibody. The secondary antibody (Table 2.23) was diluted in 5% bovine serum

albumin/TBS Tween and incubated with the membrane for one hour at room temperature.

After a further four ten minute washes in TBS Tween to remove any unbound secondary antibody, the membrane was stored in TBS Tween while reagents are prepared for visualisation of the proteins by enhanced chemiluminescence (ECL). Development of the membranes was carried out in a dark room so as not to spoil the light-sensitive x-ray films. Solution A and B were prepared (Table 2.24) beforehand, mixed and applied to the drained membranes in the dark room. The membranes were incubated for five minutes, blotted on filter paper and exposed to x-ray film within a light impermeable cassette for a range of times (usually 30 seconds to 5 minutes). The films were developed on a Curix60 (AGFA) automatic developing machine.

Primary Antibody	Dilution	Species	Molecular Weight (kDa)	Supplier	Secondary Antibody	Dilution	Supplier
Anti-Caspase 3 (full length and large cleaved fragment)	1:1000	Rabbit	17, 19 & 35	Cell Signaling	Anti-rabbit, HRP-conjugated	1:2000	Sigma
Anti-Caspase 9 (full length and large cleaved fragment)	1:1000	Rabbit	35, 37 & 47	Cell Signaling	Anti-rabbit, HRP-conjugated	1:2000	Sigma
Phosphorylated p70S6 kinase (Thr <sup>389</sup> )	1:750	Rabbit	70	Cell Signaling	Anti-rabbit, HRP-conjugated	1:2000	Sigma
GAPDH	1:1000	Rabbit	37	Cell Signaling	Anti-rabbit, HRP-conjugated	1:2000	Sigma

**Table 2.23** - Details of antibodies used in western blotting experiments

Solution A		Solution B	
Reagent	Quantity	Reagent	Quantity
100mM TRIS (pH 8)	5mL	100mM TRIS (pH 8)	5mL
Luminol	50μL	Hydrogen Peroxide (30%)	3μL
Coumaric Acid	22μL		

**Table 2.24** - Formulation of solutions A and B for enhanced chemiluminescence.

### **2.11.1 Western Blot Analysis**

Western blots for caspase 9 were analysed densitometrically using ImageJ software (National Institutes of Health). Optical density (OD) of the bands representing total and cleaved fragment caspase 9 was measured and a ratio calculated by dividing the cleaved fragment OD by the total OD.

### **2.12 ImageStream**

Protein expression and localisation was investigated using ImageStream (Amnis) high resolution flow cytometry. Expression and cellular location of mTOR, DEPTOR, rictor and raptor was assessed using ImageStream™ (Amnis) imaging flow cytometry.

#### **2.12.1 Fixing Cells**

Cells were cultured in T-75 tissue culture flasks until 80-90% confluent. Media was aspirated and the cells were washed briefly in PBS (Gibco). The cells were incubated with 2.5mL of TrypLE™ Express (Invitrogen) per  $\sim 75\text{cm}^2$  growth surface area and the flask was manually disturbed to detach adherent cells which were resuspended in 2.5mL of prewarmed PBS (Gibco). Cell suspension was transferred into a 50mL centrifuge tube and centrifuged for 5 minutes at 1200 RPM to form a pellet. Supernatant was removed and cells were resuspended in 5mL of prewarmed PBS (Gibco) a further two times to remove debris. The pellet was then resuspended in 1mL of prewarmed PBS (Gibco), transferred to a 1.5mL microcentrifuge tube and centrifuged for 5 minutes at 1200 RPM. The supernatant was removed and the cells were resuspended and incubated in 4% paraformaldehyde (PFA, Sigma) for 7 minutes to crosslink proteins in the cells. The cell suspension was centrifuged for 2 minutes at 3600 RPM and the PFA removed. The cells were washed in prewarmed PBS a further three times, centrifuging for 2 minutes at 3600 RPM between each wash. The cells were then resuspended in ice-cold methanol-acetone (1:1) and stored at  $-20^\circ\text{C}$  until further use.

### 2.12.2 Staining Cells

The cells were incubated in blocking buffer (5% bovine serum in PBS) for 30 minutes with gentle agitation. Cells were centrifuged for 3 minutes at 2000 RPM and the blocking buffer was removed. The cells were then incubated in the appropriate primary antibody (Table 2.25) diluted in blocking buffer overnight at 4°C with gentle agitation. Following primary antibody incubation, cells were centrifuged for 3 minutes at 2000 RPM and the antibody removed. The cells were resuspended in PBS (Gibco) to remove any remaining antibody and centrifuged again for 3 minutes at 2000 RPM. From this step onwards the cell were protected from light as the fluorophore conjugated to the secondary antibody is light sensitive. The PBS was removed and the cells incubated in secondary antibody (Table 2.25) diluted in blocking buffer for 30 minutes with gentle agitation. After secondary antibody incubation the cells were centrifuged for 3 minutes at 2000 RPM and the secondary antibody removed. The cells were resuspended in PBS (Gibco) to remove any remaining antibody and and centrifuged for 3 minutes at 2000 RPM. PBS was removed and the cells were resuspended in 100µL Accumax (Innovative Cell Technologies) to dissociate any cellular aggregates. 1µL of Draq5 nuclear stain was added before visualisation on ImageStream.

<b>Primary Antibody</b>	<b>Dilution</b>	<b>Species</b>	<b>Supplier</b>	<b>Secondary Antibody</b>	<b>Dilution</b>	<b>Supplier</b>
Anti-mTOR	1:200	Rabbit	Cell Signaling	Anti-rabbit, alexafluor conjugated	1:1000	Molecular Probes
Anti-DEPTOR	1:200	Rabbit	Cell Signaling	Anti-rabbit, alexafluor conjugated	1:1000	Molecular Probes
Anti-Rictor	1:200	Mouse	AbCam	Anti-mouse, alexafluor conjugated	1:1000	Molecular Probes
Anti-Raptor	1:200	Rabbit	Cell Signaling	Anti-rabbit, alexafluor conjugated	1:1000	Molecular Probes

**Table 2.25** - Details of antibodies used in ImageStream experiments.

### 2.13 Immunohistochemistry

Immunohistochemistry and DAB (3,3'-Diaminobenzidine) staining was used to visualise mTOR, DEPTOR, rictor, raptor and phosphorylated p70S6 kinase protein expression in paraffin embedded ovarian cancer tissue samples. Tissue was deparaffinised and rehydrated by incubation in Histo-Clear (National Diagnostics) and decreasing concentrations of ethanol as follows (Table 2.26):

Solution	Time
Histoclear	3 x 5 minutes
Histoclear:ethanol (1:1)	3 minutes
100% ethanol	3 minutes
95% ethanol	3 minutes
70% ethanol	3 minutes
50% ethanol	3 minutes
Running tap water	3 minutes

**Table 2.26** - Incubations to deparaffinise and rehydrate paraffin embedded tissue samples.

Antigen retrieval was achieved by boiling slides in sodium citrate (pH6, Table 2.27) for 20 minutes. Additional sodium citrate was added every 5 minutes to avoid the slides boiling dry.

Reagent	Volume
Sodium citrate	2.94g
dH <sub>2</sub> O	1L
Tween 20	500µL

**Table 2.27** - Formulation of antigen retrieval solution.

The slides were then washed in running tap water for 10 minutes and TBS 0.025% Triton X 2 times for 5 minutes to remove sodium citrate. Endogenous hydrogen



peroxidase activity was blocked by incubation with 0.3% hydrogen peroxide for 30 minutes. The slides were then washed in TBS 0.025% Triton X 3 times for 5 minutes each on a shaker. A humidity chamber was created by placing dH<sub>2</sub>O soaked tissue in a tray and covering with cling film; slides were placed in the humidity chamber for subsequent incubations to avoid evaporation. The tissue was blocked in 1% donkey serum in TBS for 1 hour at room temperature by dispensing 200µL onto the tissue area of the slide and using a small square of parafilm to ensure the blocking buffer spreads over the tissue. Blocking buffer was carefully removed from the slides with tissue and the primary antibody (diluted blocking buffer) was applied to tissue in the same way as the blocking buffer and incubated over two nights at 4°C. After primary antibody incubation, the slides were washed 3 times for 5 minutes each time in TBS 0.025% Triton X on a shaker to remove any unbound primary antibody. The tissue was then incubated in horseradish peroxidase (HRP) conjugated secondary antibody (diluted in blocking buffer) at room temperature for 1 hour in the same way as blocking buffer. The slides were then washed 3 times for 5 minutes in TBS 0.025% Triton X on a shaker to remove any unbound secondary antibody. DAB solution (VectorLabs) was prepared in 5mL dH<sub>2</sub>O as follows: 2 drops of buffer stock solution, 4 drops of DAB stock solution, 2 drops of hydrogen peroxide solution. 200µL of DAB solution was applied to the tissue and incubated at room temperature for 2-10 minutes until a brown colour develops. DAB solution was washed off the slide by incubation in dH<sub>2</sub>O for 5 minutes on a shaker. Haematoxylin (Fisher Scientific) was used to stain nuclei blue to provide contrast to the brown DAB staining. The tissue was incubated in haematoxylin for 1 minute and rinsed off with running tap water followed by incubation in 0.1% sodium bicarbonate for 1 minute and a second wash in running tap water. Tissue was dehydrated prior to coverslip mounting as follows (Table 2.28):

Solution	Time
50% ethanol	3 minutes
70% ethanol	3 minutes
95% ethanol	3 minutes
100% ethanol	3 minutes
Histoclear:ethanol (1:1)	3 minutes
Histoclear	3 minutes

**Table 2.28** - Incubations to dehydrate stained tissue samples.

Coverslips were mounted with di-N-butyl phthalate in xylene (DPX) to protect the tissue. DPX was dried overnight at 4°C before observation.

#### 2.14 Statistical Analysis

Changes observed in experiments were assessed for statistical significance using the Student's *t*-test. An assessment for homoscedasticity of data from each category was made using the F-test. If homoscedasticity was proven, an unpaired, two-tailed Student's *t*-test was performed to assess significance in all cases as no matched pairs of samples were used. If data were not homoscedastic, an unpaired, two-tailed Student's *t*-test with Welch's correction was performed to account for variance. All statistical tests were performed using GraphPad Prism® Software (GraphPad Software). *p* values were denoted on graphs as follows (Table 2.29):

<i>p</i> value	Denotation
0.01-0.05	*
0.001-0.009	**
<0.0009	***

**Table 2.29** - The asterisk denotations of *p* values on graphs.

## **Chapter 3**

### ***mTOR, DEPTOR, rictor and raptor expression in ovarian cancer models and in response to mTOR pathway inhibition***

#### **3.1 Introduction**

SKOV3 (clear cell adenocarcinoma) and MDAH-2774 (endometrioid adenocarcinoma) human adherent epithelial cell lines were used as *in vitro* models of human ovarian cancer. SKOV3 cells were obtained from the ascites of a 64 year old caucasian female patient in 1973 and are hypodiploid, containing a number of chromosome derivatives and deletions (ATCC, 2014). They are designated as grade 1-2 for well to moderately differentiated cells (CRUK, 2014a; Beaufort *et al.*, 2014). SKOV3 cells are p53 null and show mutation in the *PIK3CA* gene for the catalytic subunit of PI3 kinase but are wildtype for *PTEN*, *BRCA1*, *BRCA2* and *KRAS* and sensitive to Docetaxel, Paclitaxel, Carboplatin and Doxorubicin (Mabuchi, Deborah A. Altomare, *et al.*, 2007; Beaufort *et al.*, 2014). MDAH-2774 cells were obtained from the ascites of a female patient of unknown age in 1972 and shows triploidy of many chromosomes and monosomy of chromosomes 17 and 21 (AddexBio, 2015; Beaufort *et al.*, 2014). They are designated as grade 2 for moderately differentiated cells. MDAH-2774 cells show mutations in *TP53*, *PIK3CA*, *KRAS* and silent mutations in *BRCA1* and *BRCA2*. They are sensitive to the effects of Docetaxel, Paclitaxel, Oxaliplatin, Fluorouracil and Doxorubicin (Beaufort *et al.*, 2014).

Rapamycin (Rap, C<sub>51</sub>H<sub>79</sub>NO<sub>13</sub>) was first discovered in 1975 from a soil sample taken from Rapa Nui (Easter Island) and was originally shown to be an anti-fungal agent produced by *streptomyces hygroscopicus* (Vézina *et al.*, 1975; Sehgal *et al.*, 1975). It was not until 1994 that interacting partners of Rap were found. Rapamycin and FK-506 Binding Protein 12 (FKBP12) were found to interact with one another and,

as a complex, with mechanistic (formerly mammalian) target of rapamycin (mTOR) to inhibit cell growth (Sabers *et al.*, 1995; Brown *et al.*, 1994). The mTOR pathway is now known to control proliferation, cell growth, protein and lipid synthesis, metabolism, survival, autophagy and apoptosis in response to stress, growth factors, amino acids, energy and oxygen status (Laplante and Sabatini, 2012).

Rap is now accompanied by a range of semi synthetic analogues known as rapalogues: Everolimus (Eve,  $C_{53}H_{83}NO_{14}$ ), Deforolimus (Def,  $C_{53}H_{84}NO_{14}P$ ) and Temsirolimus (Tem,  $C_{56}H_{87}NO_{16}$ ), like Rap, are allosteric mTORC1 inhibitors (Benjamin *et al.*, 2011). mTORC2 was previously thought to be entirely unaffected by Rap and is Rap insensitive in the short-term (Jacinto *et al.*, 2004; Sarbassov *et al.*, 2006) but long term treatment (100nM for 24 hours) may prevent mTORC2 assembly by removing mTOR as an available component (Sarbassov *et al.*, 2006). The rapalogues possess the same basic structure as Rap with small functional group modifications. Eve and Tem are prodrug forms of Rap and Def a non-Rap prodrug designed to improve aqueous solubility and oral pharmacokinetics (Benjamin *et al.*, 2011; Grunt and Mariani, 2013; Neuhaus *et al.*, 2001). Resveratrol (Res,  $C_{14}H_{12}O_3$ ) and NVP BEZ-235 (BEZ,  $C_{30}H_{23}N_5O$ ) differ from the rapalogues as they are dual mTOR and phosphoinositide-3-kinase (PI3 kinase) inhibitors. PI3 kinase is an upstream activator of Akt and, in turn, mTOR. Res is a natural phenol produced in the skin of red grapes among other fruits. Res inhibits both PI3 kinase, by direct ATP-binding site interaction (Fröjdö *et al.*, 2007) and mTOR indirectly, by promoting its association with inhibitor DEPTOR (Meilian Liu *et al.*, 2010). NVP BEZ-235 ( $C_{30}H_{23}N_5O$ ) is a synthetically developed inhibitor by Novartis which directly targets the ATP binding sites of both PI3 kinase and mTOR (Maira *et al.*, 2008).

### 3.2 Objectives

-To validate the gene and protein expression of four main mTOR complex components, mTOR, DEPTOR, rictor and raptor in SKOV3 and MDAH-2774 cell lines.

-To map the gene expression of mTOR signalling components mTOR, DEPTOR, rictor and raptor in cell treated with mTOR pathway inhibitors and untreated controls.

### **3.3 Results**

#### **3.3.1 Confirmation of mTOR pathway component expression in SKOV3 and MDAH-2774 ovarian cancer cell lines**

We first sought to confirm the expression of four main mTOR pathway components at gene and protein level in two ovarian cancer cell lines. qPCR experiments were carried out to assess gene expression of mTOR, DEPTOR, rictor and raptor in SKOV3 and MDAH-2774 cells grown under basal conditions. Cells were seeded in 6-well plates at a density of 100,000 per well (~10cm<sup>2</sup> growth area). RNA was purified at 48 and 72 hours with the NucleoSpin® RNA/Protein extraction kit and cDNA synthesised using the nanoScript™ 2 Reverse Transcription kit (Primerdesign) as previously described (Sections 2.6.1.2 and 2.7.2). qPCR on cDNA was performed as previously described on an xxpress® (BJS Biotechnologies) thermal cycler using Kapa SYBR® Fast Master Mix (Kapa Biosystems) (Section 2.10.4) using primers for mTOR, Deptor, Rictor, Raptor and reference gene YWHAZ. Biological and technical triplicates were performed for each condition.

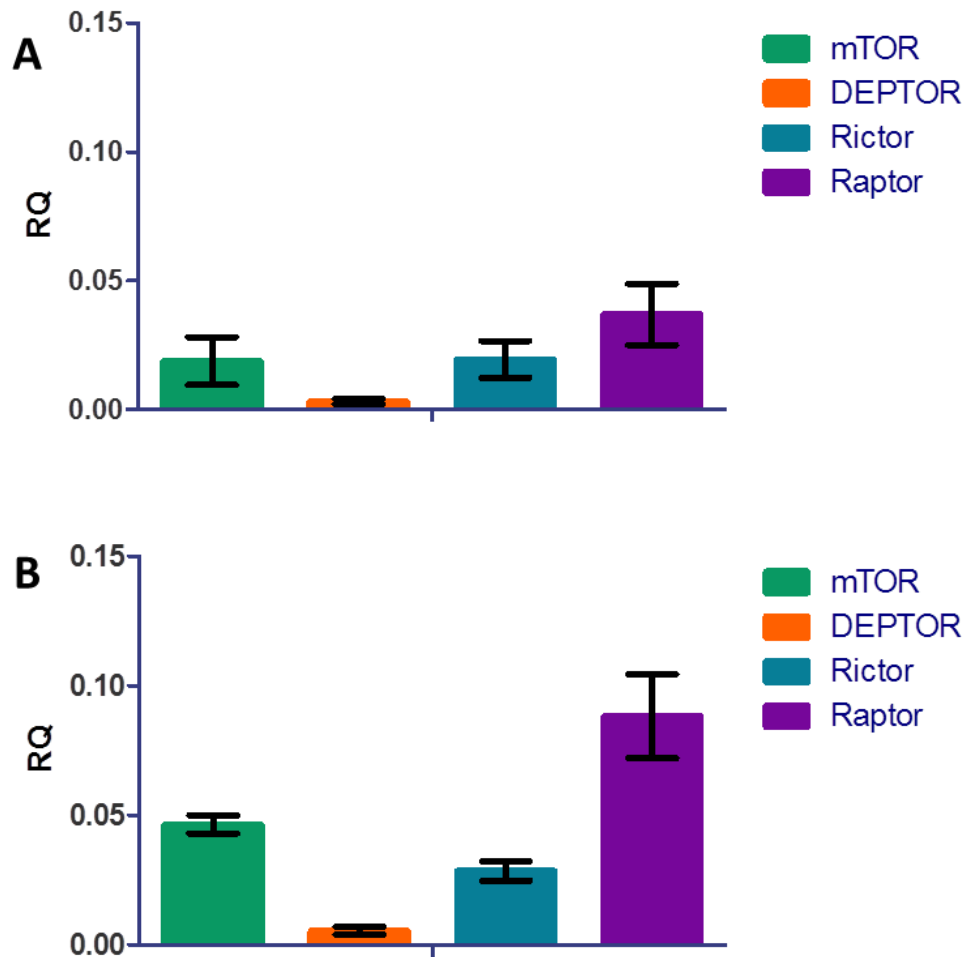


**Figure 3.1** - Relative mTOR, DEPTOR, rictor and raptor expression was measured by qPCR in SKOV3 (A) and MDAH (B) cells under basal conditions. cDNA was synthesised from extracted RNA from 3 biological replicates for each condition. Three technical replicates were performed per biological replicate. Data were analysed using the  $\Delta C_q$  method and an RQ value calculated by  $2^{-\Delta C_q}$ . Error bars depict standard deviation. Expression of mTOR, DEPTOR, rictor and raptor can be detected in both SKOV3 and MDAH-2774 cells. Significantly more expression of mTOR and raptor was detected in MDAH-2774 cells than in SKOV3 cells ( $p=0.0085$  and  $0.0116$  respectively).

Expression of mTOR, DEPTOR, rictor and raptor was detected in both SKOV3 (A) and MDAH-2774 (B) cell lines cultured under basal conditions. Both cell lines show a similar pattern of expression, with raptor being more highly expressed than rictor. DEPTOR shows relatively low levels of expression in comparison to other

components. The MDAH-2774 cell line showed higher relative expression of mTOR and raptor than the SKOV3 cell line ( $p=0.0085$  and  $0.0116$  respectively).

ImageStream flow cytometry was used to confirm protein expression of mTOR, DEPTOR, rictor and raptor in SKOV3 and MDAH-2774 cell lines. Cells were grown under basal conditions and fixed with 4% PFA before being stained with primary antibodies for mTOR, DEPTOR, rictor or raptor and a secondary alexafluor 488 conjugated antibody. Nuclei were stained using Draq5 (described in 2.12).

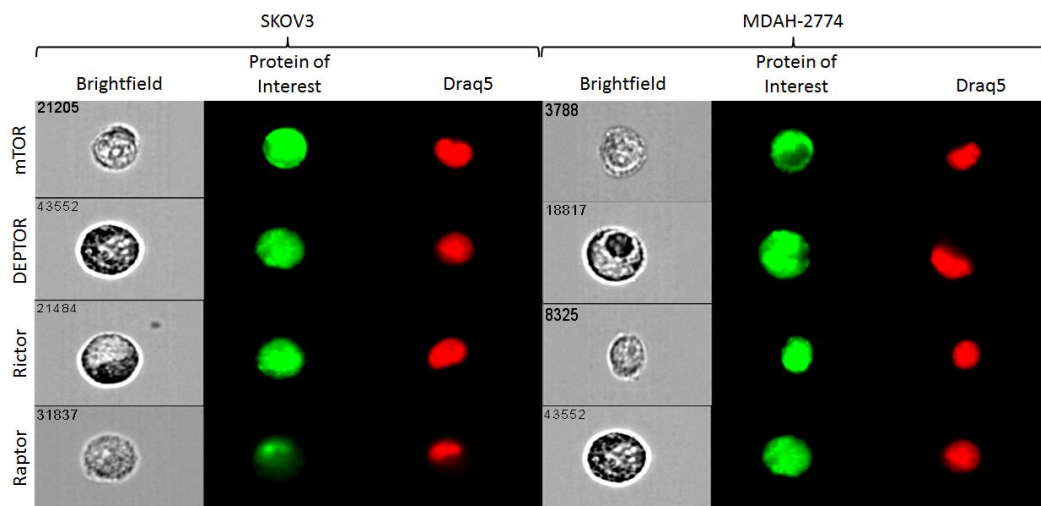


**Figure 3.2** - Images of individual SKOV3 and MDAH-2774 cells after mTOR, DEPTOR, rictor and raptor in brightfield, with alexafluor (protein of interest) and Draq5 (nuclei) staining. Images show that mTOR, DEPTOR, rictor and raptor are present in the cytoplasm of SKOV3 and MDAH-2774 cells.

Staining for mTOR, DEPTOR, rictor and raptor was detected in both SKOV3 and MDAH-2774 cells confirming that protein expression of these components is present at basal levels in both cell lines (Figure 3.2).

### 3.3.2 Gene Expression of mTOR pathway components and mTOR pathway inhibition

We next sought to investigate the effects of mTOR pathway inhibition on the gene expression of mTOR, DEPTOR, rictor and raptor in SKOV3 and MDAH-2774 cells. The effect of mTOR pathway inhibition was investigated using 6 different inhibitory

agents: Rap, Eve, Def, Tem, Res and BEZ. mTOR inhibitors were applied in concentrations and for times proven to be effective in the literature (Table 3.1). Böhm *et al.*, showed a decrease in cell viability of primary acute myeloid leukaemia cells after treatment with 20 and 100nM Rap, Eve and Tem (Böhm *et al.*, 2009). Squillace *et al.*, treated a range of metastatic sarcoma and endometrial carcinoma cell lines with up to 1000nM Def and demonstrated decreased proliferation as a result (Squillace *et al.*, 2011). Resveratrol treatment was shown to be effective at inhibiting proliferation in medullary thyroid cancer cell lines at 50µM by Truong *et al.*, (Truong *et al.*, 2011). To the best of our knowledge, no *in vitro* experiments using BEZ were published at the time this study was devised and so we chose 10 and 100nM as initial exploratory concentrations.

Inhibitor	MoA	Concentrations		Times (hours)	
Rap	Allosteric mTOR inhibitor.	20nM	100nM	48	72
Eve		20nM	100nM		
Def		100nM	1000nM		
Tem		10nM	100nM		
Res	Dual mTOR (via DEPTOR) & PI3 kinase (via ATP binding site) inhibitor.	25µM	50µM		
BEZ	Dual mTOR and PI3 kinase inhibitor via ATP binding sites of both.	10nM	100nM		

**Table 3.1** - Details of the mTOR pathway inhibitory agent used in this study. Inhibitor concentrations were chosen to reflect the range of which other studies had found effective. Treatments were conducted for 48 and 72 hours.

qPCR experiments were performed in order to map the gene expression of mTOR, DEPTOR, rictor and raptor in treated and control SKOV3 and MDAH-2774 cells. Cells were seeded in 6-well plates at a density of 100,000 per well (~10cm<sup>2</sup> growth area) and allowed to proliferate for 24 hours before treatment with Rap (20 and 100nM), Eve (20 and 100nM), Def (100 and 1000nM), Tem (10 and 100nM), Res (25



and 50), BEZ (10 and 100nM) or carrier (DMSO) (Section 2.2). RNA was purified at 48 and 72 hours after treatment with the NucleoSpin® RNA/Protein extraction kit and cDNA synthesised using the nanoScript™ 2 Reverse Transcription kit (Primerdesign) as previously described (Sections 2.6.1.2 and 2.7.2). qPCR on cDNA from treated and control cells was performed as previously described on an xpress® (BJS Biotechnologies) thermal cycler using Kapa SYBR® Fast Master Mix (Kapa Biosystems) (Section 2.10.4). Primers for mTOR, Deptor, rictor, raptor and reference gene YWHAZ were used. Biological and technical triplicates were performed for each condition. Analysis was performed using the  $\Delta C_q$  method as described previously (Section 2.10.5).

### 3.3.2.1 mTOR Expression in SKOV3 Cells

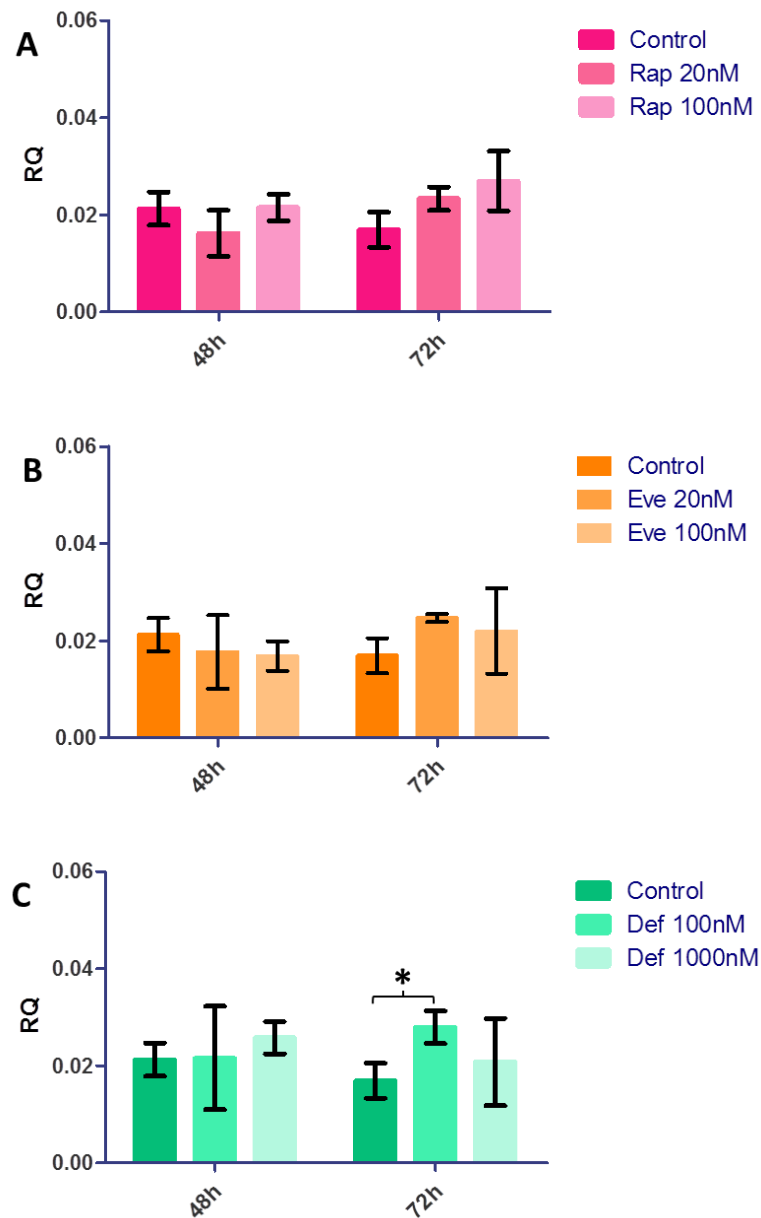


**Figure 3.3** - Relative mTOR expression was measured by qPCR in SKOV3 cells treated with Rap (20 and 100nM), Eve (20 and 100nM), Def (100 and 1000nM) and carrier (DMSO) only control for 48 and 72 hours. cDNA was synthesised from extracted RNA from 3 biological replicates for each condition. Three technical replicates were performed per biological replicate. Data were analysed using the  $\Delta C_q$  method and an RQ value calculated by  $2^{-\Delta C_q}$ . An F-test was performed to assess variance between groups and two-tailed, unpaired Student's t-tests with Welch's correction for unequal variance were performed to assess significance. Error bars depict standard deviation and asterisks denote significance. Results show no change in expression resulting from Rap or Eve treatment (**A** and **B** respectively). An increase was detected after 72 hours treatment with 100nM Def (**C**,  $p=0.0301$ ).

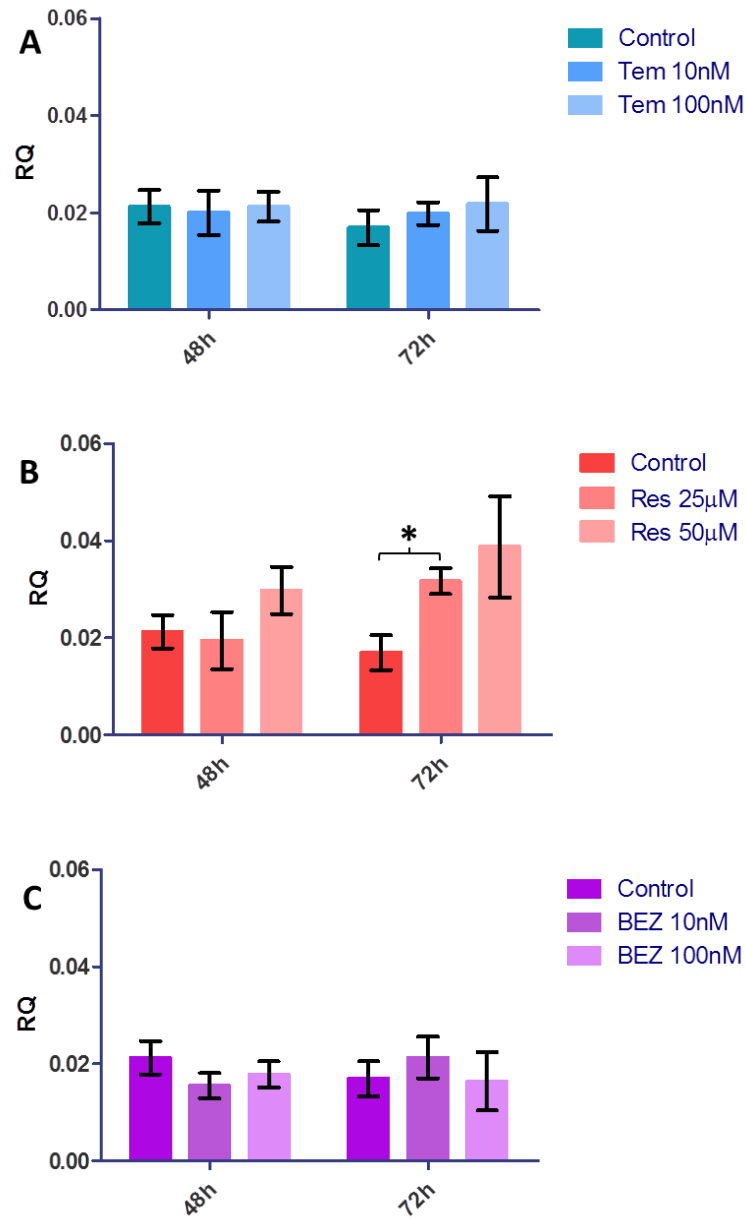


**Figure 3.4** - Relative mTOR expression was measured by qPCR in SKOV3 cells treated with Tem (10nM and 100nM), Res (25 and 50µM), BEZ (10 and 100nM) and carrier (DMSO) only control for 48 and 72 hours. cDNA was synthesised from extracted RNA from 3 biological replicates for each condition. Three technical replicates were performed per biological replicate. Data were analysed using the  $\Delta C_q$  method and an RQ value calculated by  $2^{-\Delta C_q}$ . An F-test was performed to assess variance between groups and two-tailed, unpaired Student's t-tests with Welch's correction for unequal variance were performed to assess significance. Error bars depict standard deviation and asterisks denote significance. Results show no change in expression resulting from Tem or BEZ treatment (A and C respectively). An increase was detected after 72 hours treatment with 25µM Res (B,  $p=0.0107$ ).

### 3.3.2.2 mTOR Expression in MDAH-2774 Cells

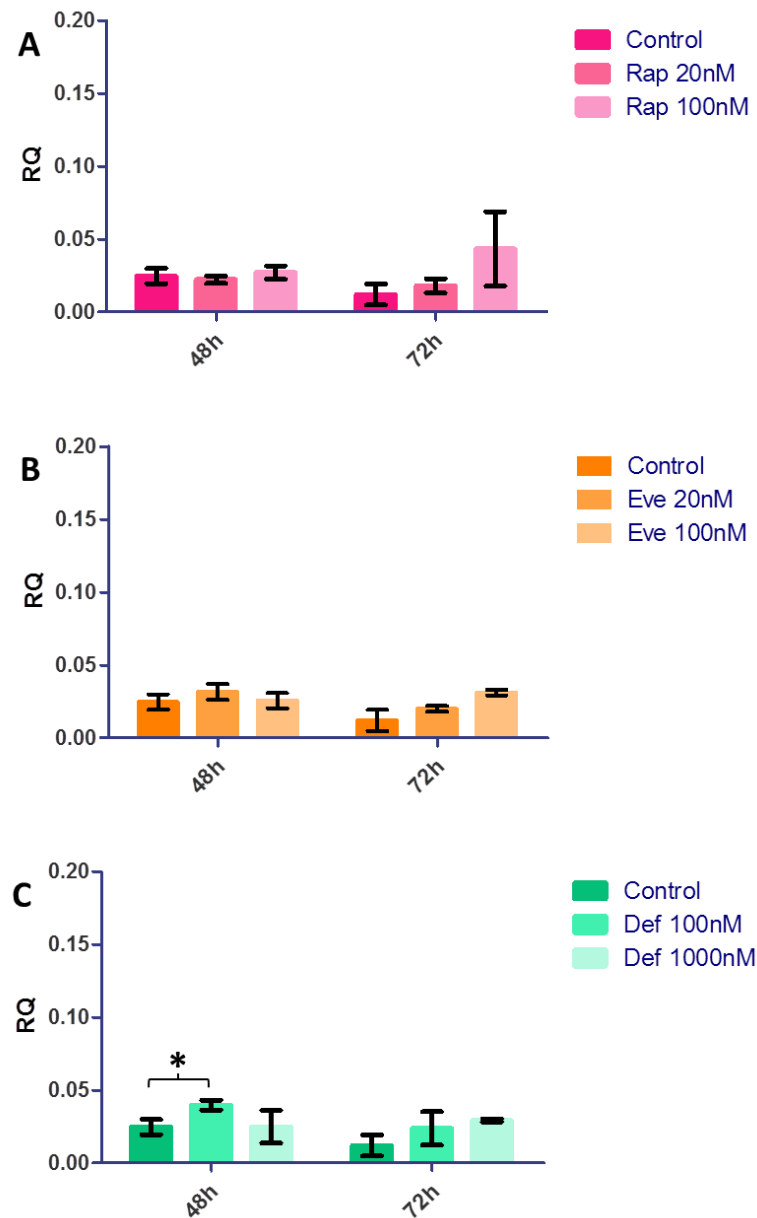


**Figure 3.5** - Relative mTOR expression was measured by qPCR in MDAH-2774 cells treated with Rap (20 and 100nM), Eve (20 and 100nM), Def (100 and 1000nM) and carrier (DMSO) only control for 48 and 72 hours. cDNA was synthesised from extracted RNA from 3 biological replicates for each condition. Three technical replicates were performed per biological replicate. Data were analysed using the  $\Delta C_q$  method and an RQ value calculated by  $2^{-\Delta C_q}$ . An F-test was performed to assess variance between groups and two-tailed, unpaired Student's t-tests with Welch's correction for unequal variance were performed to assess significance. Error bars depict standard deviation and asterisks denote significance. Results show no change in expression resulting from Rap or Eve (**A** and **B** respectively). 100nM treatment with Def induced an increase after 48 hours (**C**,  $p=0.0251$ ).

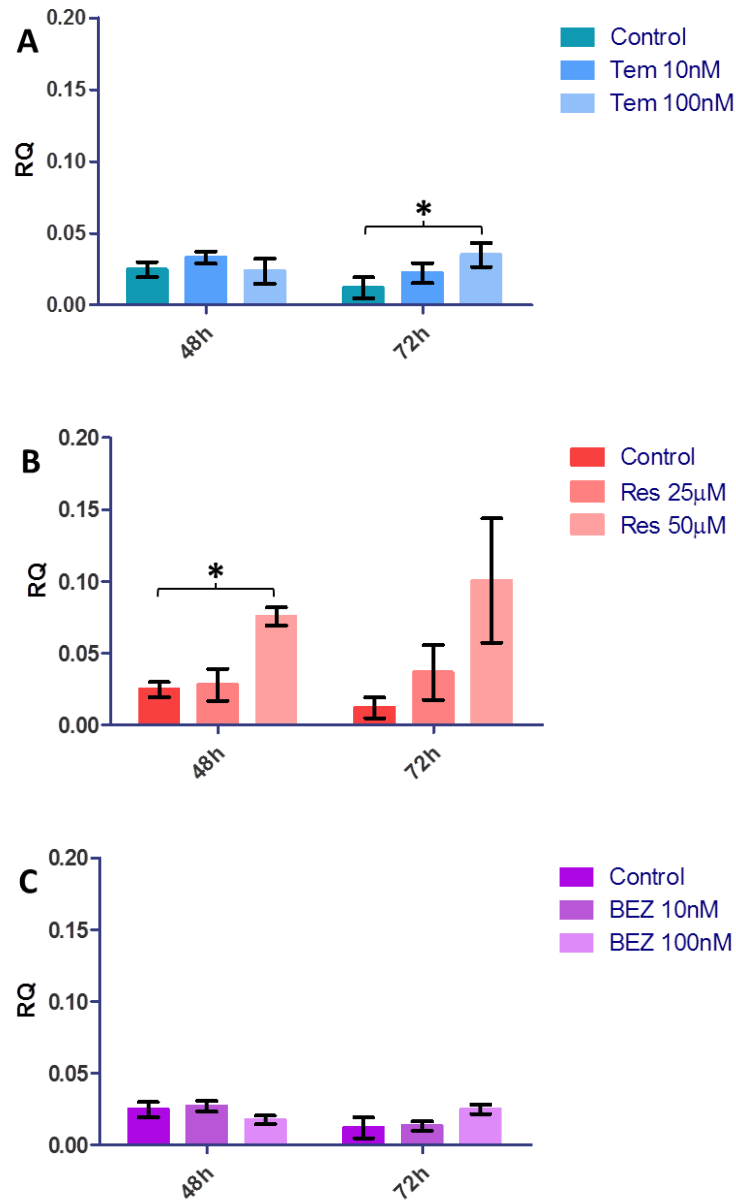


**Figure 3.6** - Relative mTOR expression was measured by qPCR in MDAH-2774 cells treated with Tem (10nM and 100nM), Res (25 and 50µM), BEZ (10 and 100nM) and carrier (DMSO) only control for 48 and 72 hours. cDNA was synthesised from extracted RNA from 3 biological replicates for each condition. Three technical replicates were performed per biological replicate. Data were analysed using the  $\Delta C_q$  method and an RQ value calculated by  $2^{-\Delta C_q}$ . An F-test was performed to assess variance between groups and two-tailed, unpaired Student's t-tests with Welch's correction for unequal variance were performed to assess significance. Error bars depict standard deviation and asterisks denote significance. Results show no change in expression resulting from BEZ treatment (C). 100nM Tem treatment induced an increase in mTOR expression after 72 hours (A,  $p=0.0366$ ). 50µM Res treatment showed an increase after 48 hours (B,  $p=0.0017$ ).

mTOR expression was generally unchanged in SKOV3 and MDAH-2774 cells. There was no change in SKOV3 cells at 48 or 72 hours induced by Rap, Eve, Tem, or BEZ at low or high concentrations (Figure 3.3, A and B, Figure 3.4 A and C). A significant increase was detected after treatment with 100nM Def after 72 hours (Figure 3.3, C,  $p=0.0301$ ) and 72 hours after 25 $\mu$ M Res treatments in comparison to controls (Figure 3.4, B,  $p=0.0107$ ). MDAH-2774 cells showed no change in mTOR expression at 48 and 72 hours after treatment with Rap, Eve or BEZ at high or low concentration (Figure 3.5, A and B, Figure 3.6, C). A significant increase was detected in mTOR expression in MDAH-2774 cells after 100nM Def treatment at 48 hours in comparison to controls (Figure 3.5, C,  $p=0.0251$ ). A significant increase in mTOR expression was detected after 100nM Tem treatment at 72 hours (Figure 3.6, A,  $p=0.0366$ ) and after 50 $\mu$ M Res treatment at 48 hours (Figure 3.6, B,  $p=0.0017$ ) in comparison to controls.

### 3.3.2.3 DEPTOR Expression in SKOV3 Cells

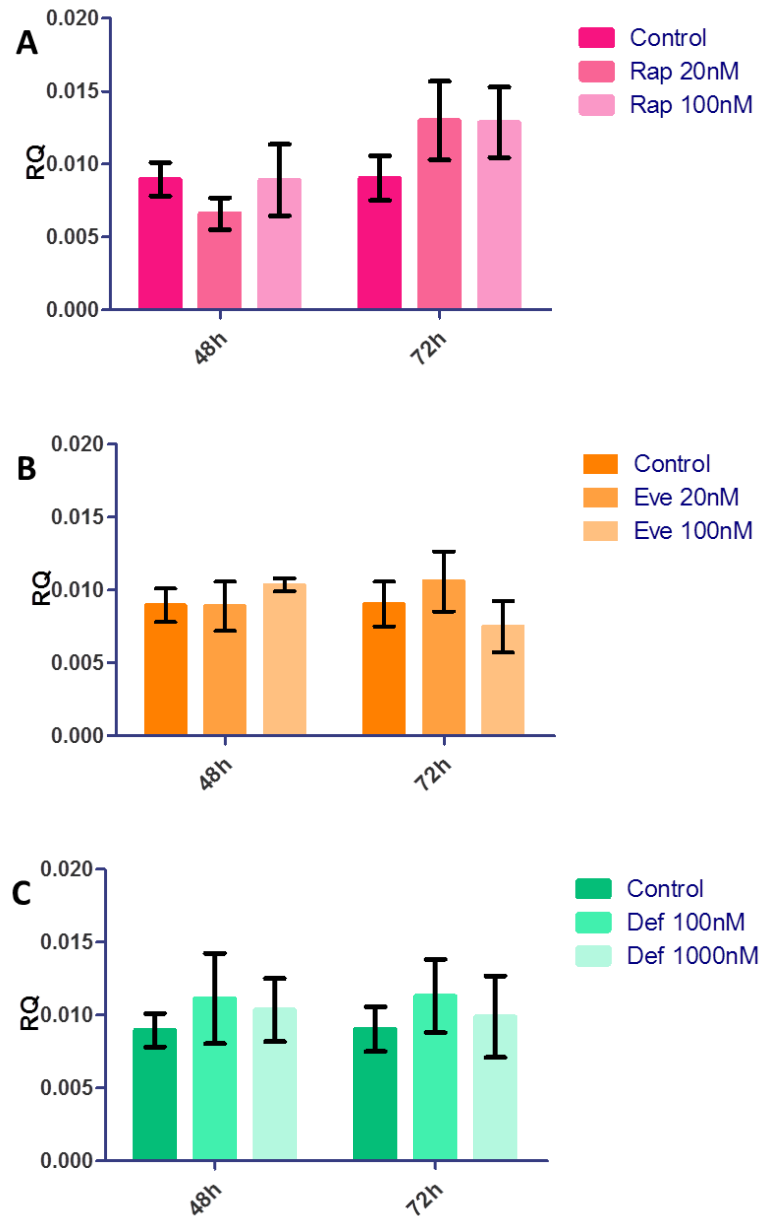


**Figure 3.7** - Relative DEPTOR expression was measured by qPCR in SKOV3 cells treated with Rap (20 and 100nM), Eve (20 and 100nM), Def (100 and 1000nM) and carrier (DMSO) only control for 48 and 72 hours. cDNA was synthesised from extracted RNA from 3 biological replicates for each condition. Three technical replicates were performed per biological replicate. Data were analysed using the  $\Delta C_q$  method and an RQ value calculated by  $2^{-\Delta C_q}$ . An F-test was performed to assess variance between groups and two-tailed, unpaired Student's t-tests with Welch's correction for unequal variance were performed to assess significance. Error bars depict standard deviation and asterisks denote significance. No change in expression was detected as a result of Rap, Eve or Def treatment (**A**, **B** and **C** respectively).

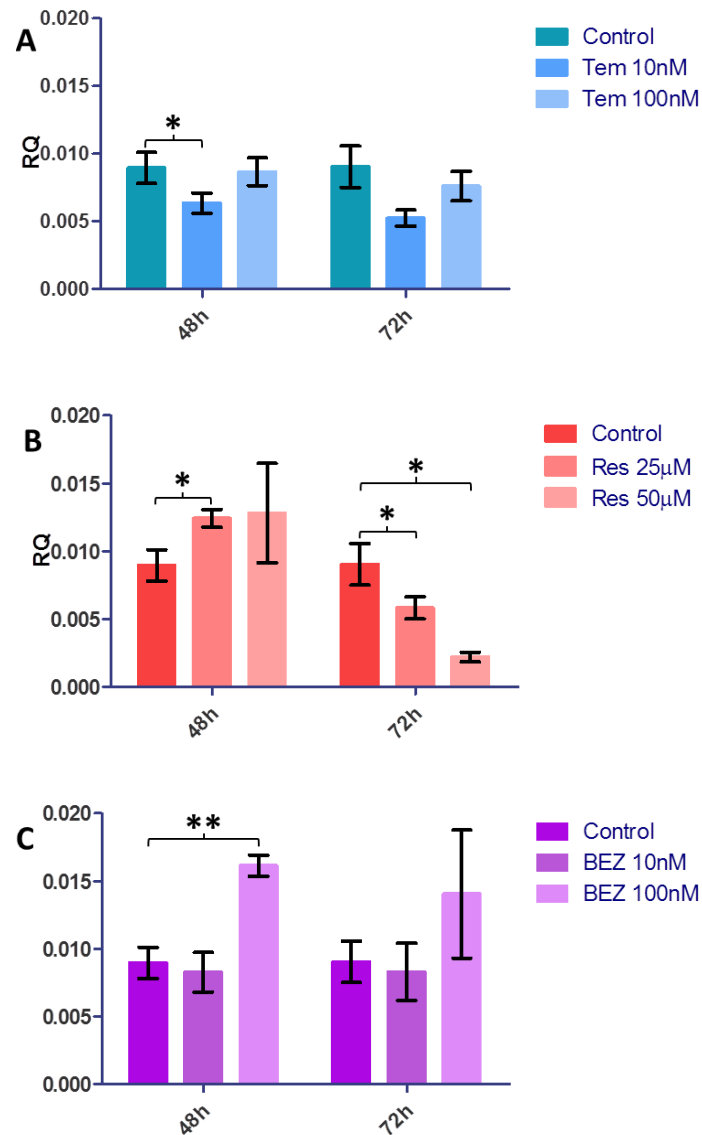


**Figure 3.8** - Relative DEPTOR expression was measured by qPCR in SKOV3 cells treated with Tem (10nM and 100nM), Res (25 and 50µM), BEZ (10 and 100nM) and carrier (DMSO) only control for 48 and 72 hours. cDNA was synthesised from extracted RNA from 3 biological replicates for each condition. Three technical replicates were performed per biological replicate. Data were analysed using the  $\Delta C_q$  method and an RQ value calculated by  $2^{-\Delta C_q}$ . An F-test was performed to assess variance between groups and two-tailed, unpaired Student's t-tests with Welch's correction for unequal variance were performed to assess significance. Error bars depict standard deviation and asterisks denote significance. A decrease was detected in DEPTOR expression after 48 hour 10nM Tem treatment (**A**,  $p=0.0463$ ). 25µM Res treatment induced an increase in DEPTOR expression at 48 hours but a decrease in DEPTOR expression at 72 hours (**B**,  $p=0.0203$  and  $0.0493$  respectively). 50µM Res treatment induced a decrease in DEPTOR expression at 72 hours (**B**,  $p=0.0173$ ). An increase in DEPTOR expression was detected after 48 hour treatment with 100nM BEZ (**C**,  $p=0.003$ ).



### 3.3.2.4 DEPTOR Expression in MDAH-2774 Cells

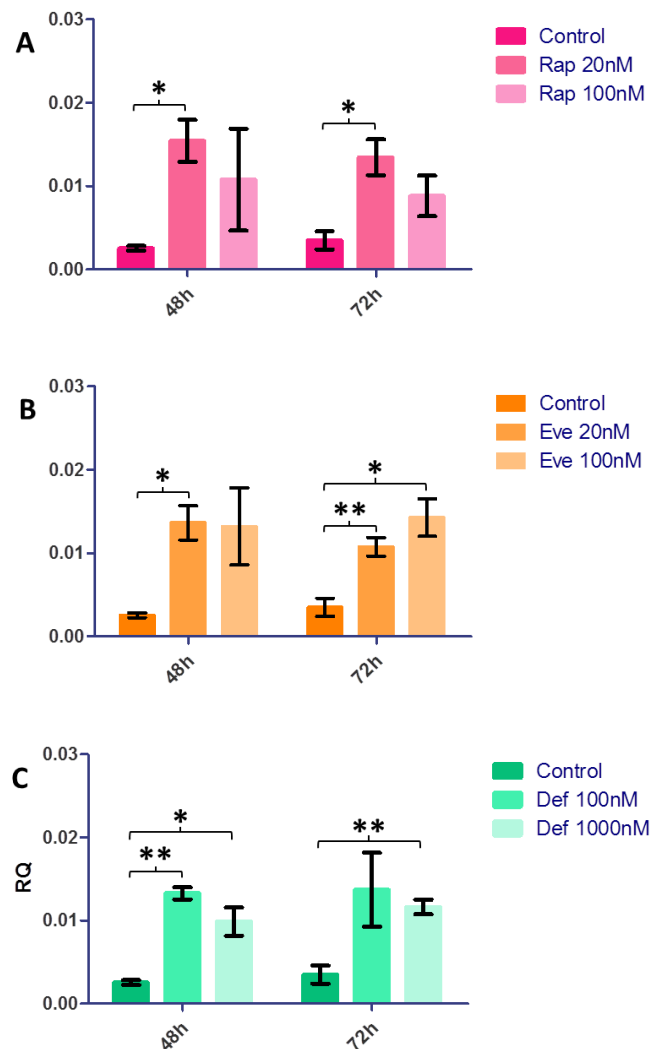


**Figure 3.9** - Relative DEPTOR expression was measured by qPCR in MDAH-2774 cells treated with Rap (20 and 100nM), Eve (20 and 100nM), Def (100 and 1000nM) and carrier (DMSO) only control for 48 and 72 hours. cDNA was synthesised from extracted RNA from 3 biological replicates for each condition. Three technical replicates were performed per biological replicate. Data were analysed using the  $\Delta C_q$  method and an RQ value calculated by  $2^{-\Delta C_q}$ . An F-test was performed to assess variance between groups and two-tailed, unpaired Student's t-tests with Welch's correction for unequal variance were performed to assess significance. Error bars depict standard deviation and asterisks denote significance. An increase in DEPTOR expression was detected after 48 and 72 hour treatment with 20nM Rap (**A**,  $p=0.0125$  and  $0.0189$  respectively). 100nM Eve treatment induced an increase in DEPTOR expression after 48 hours (**B**,  $p=0.0175$ ) and 20nM Eve treatment induced an increase in DEPTOR expression after 48 and 72 hours (**B**,  $p=0.0114$  and  $0.004$  respectively). 1000nM Def treatment resulted in an increase in DEPTOR at 48 and 72 hours (**C**,  $p=0.0184$  and  $0.0021$  respectively). 100nM treatment with Def also induced a DEPTOR increase after 48 hours (**C**,  $p=0.0018$ ).

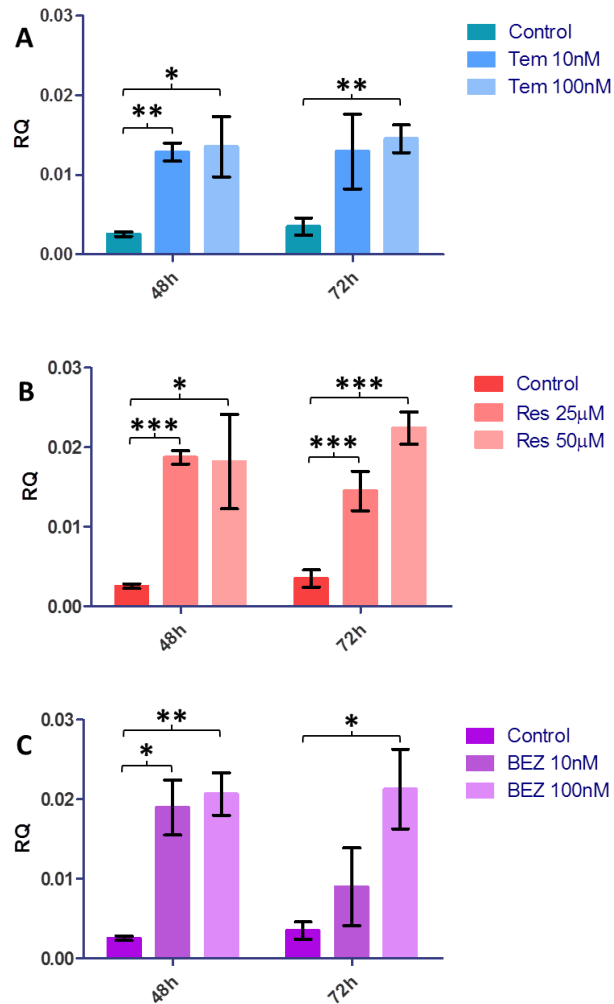


**Figure 3.10** - Relative DEPTOR expression was measured by qPCR in MDAH-2774 cells treated with Tem (10nM and 100nM), Res (25 and 50µM), BEZ (10 and 100nM) and carrier (DMSO) only control for 48 and 72 hours. cDNA was synthesised from extracted RNA from 3 biological replicates for each condition. Three technical replicates were performed per biological replicate. Data were analysed using the  $\Delta C_q$  method and an RQ value calculated by  $2^{-\Delta C_q}$ . An F-test was performed to assess variance between groups and two-tailed, unpaired Student's t-tests with Welch's correction for unequal variance were performed to assess significance. Error bars depict standard deviation and asterisks denote significance. 100nM Tem treatment induced an increase in DEPTOR expression after 48 and 72 hours (A,  $p=0.0377$  and  $0.0026$  respectively). 10nM Tem treatment induced an increase in DEPTOR after 48 hours (A,  $p=0.0043$ ). 25µM treatment with Res induced an increase in DEPTOR expression at 48 and 72 hours (B,  $p=0.0001$  and  $0.0007$  respectively) and 50µM treatment with Res induced an increase in DEPTOR expression after 48 and 72 hours (B,  $p=0.0449$  and  $0.0007$  respectively). 100nM BEZ treatment resulted in an increase in DEPTOR expression after 48 and 72 hours (C,  $p=0.0072$  and  $0.0266$  respectively) and 10nM BEZ treatment also induced an increase at 48 hours (C,  $p=0.0146$ ).

DEPTOR was generally increased in response to mTOR pathway inhibition particularly in MDAH-2774 cells. SKOV3 cells showed no change in DEPTOR expression at 48 and 72 hours after Rap, Eve and Def treatment at high or low concentrations (Figure 3.7, A, B and C). A significant decrease was detected in SKOV3 cells at 48 hours after 10nM Tem treatment in comparison to controls but no other change was detected as a result of Tem treatment (Figure 3.8, A,  $p=0.0463$ ). A significant increase in DEPTOR expression was detected in SKOV3 cells at 48 hours after 25 $\mu$ M Res treatment in comparison to controls (Figure 3.8, B,  $p=0.0203$ ). At 72 hours after treatment, Res induced a dose dependent decrease in DEPTOR expression in comparison to controls (Figure 3.8, B,  $p=0.0493$  [25 $\mu$ M] and  $p=0.0173$  [50 $\mu$ M]). BEZ treatment induced an increase in DEPTOR expression at 48 hours after 100nM BEZ treatment (Figure 3.8, C,  $p=0.0030$ ) in comparison to controls. MDAH-2774 cells showed an increase in DEPTOR expression induced by all inhibitors in comparison to controls. 20nM Rap treatment induced a significant increase in DEPTOR expression after 48 and 72 hours (Figure 3.9, A,  $p=0.0125$  and 0.0189 respectively). 20nM Eve treatment induced an increase in DEPTOR after 48 and 72 hours in comparison to controls (Figure 3.9, B,  $p=0.0114$  and 0.004 respectively). 100nM Eve treatment induced an increase in DEPTOR after 72 hours in comparison to controls (Figure 3.9, B,  $p=0.0175$ ). Def treatment induced an increase in DEPTOR expression after 48 hours treatment at 100nM (Figure 3.9, C,  $p=0.0018$ ) and after 48 and 72 hours treatment at 1000nM (Figure 3.9, C,  $p=0.0184$  and 0.0021 respectively). 10nM Tem treatment induced an increase in DEPTOR expression after 48 hours in comparison to controls (Figure 3.10, A,  $p=0.0043$ ). 100nM Tem treatment induced an increase in DEPTOR expression after 48 and 72 hours in comparison to controls (Figure 3.10, A,  $p=0.0377$  and 0.0026 respectively). 25 $\mu$ M Res treatment induced an increase in DEPTOR expression after 48 and 72 hours in comparison to controls (Figure 3.9, B,  $p=0.0001$  and 0.0194 respectively). 50 $\mu$ M Res treatment induced an increase in DEPTOR expression after 48 and 72 hours in comparison to controls (Figure 3.9, B,  $p=0.0449$ , 0.0007 respectively). An increase in DEPTOR expression was detected in comparison to controls after 10nM BEZ treatment for 48 hours (Figure 3.9, C,  $p=0.0146$ ) and after 100nM BEZ treatment for 48 and 72 hours (Figure 3.9, C,  $p=0.0072$  and 0.0266 respectively).

### 3.3.2.5 Rictor Expression in SKOV3 Cells

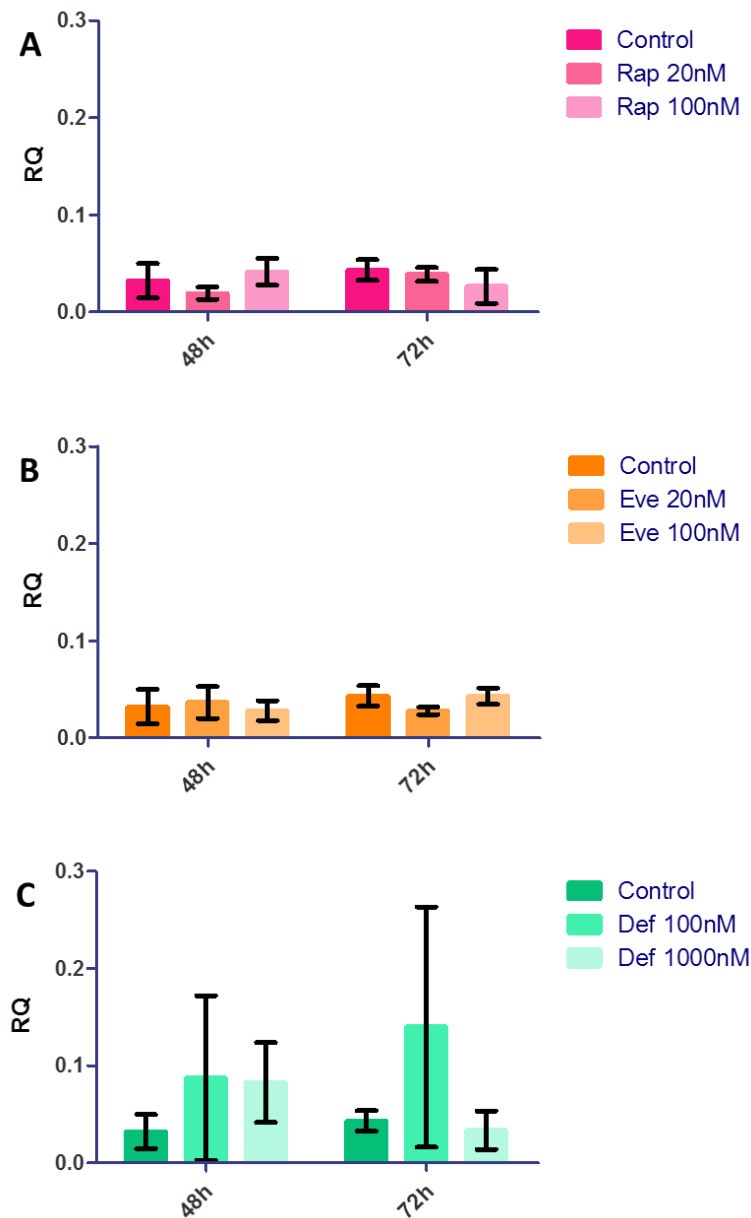


**Figure 3.11** - Relative rictor expression was measured by qPCR in SKOV3 cells treated with Rap (20 and 100nM), Eve (20 and 100nM), Def (100 and 1000nM) and carrier (DMSO) only control for 48 and 72 hours. cDNA was synthesised from extracted RNA from 3 biological replicates for each condition. Three technical replicates were performed per biological replicate. Data were analysed using the  $\Delta C_q$  method and an RQ value calculated by  $2^{-\Delta C_q}$ . An F-test was performed to assess variance between groups and two-tailed, unpaired Student's t-tests with Welch's correction for unequal variance were performed to assess significance. Error bars depict standard deviation and asterisks denote significance. No change in rictor expression was detected as a result of treatment with Rap, Eve or Def (**A**, **B** and **C** respectively).

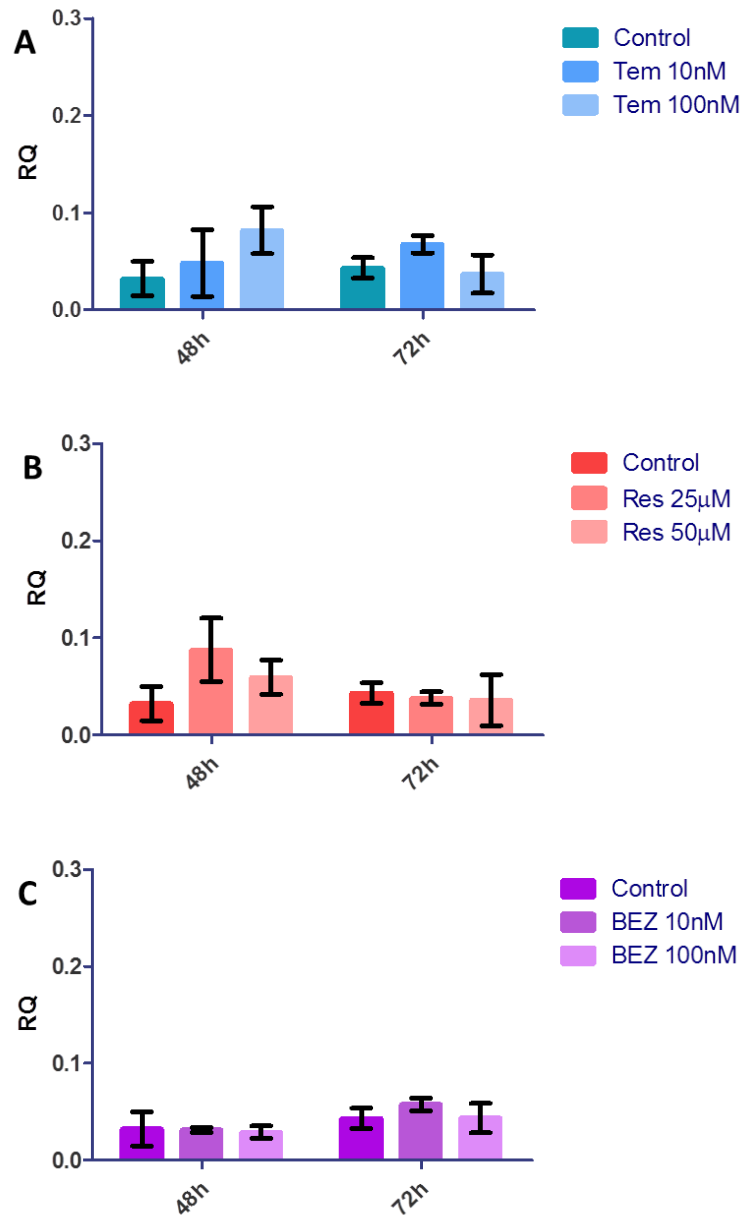


**Figure 3.12** - Relative rictor expression was measured by qPCR in SKOV3 cells treated with Tem (10nM and 100nM), Res (25 and 50µM), BEZ (10 and 100nM) and carrier (DMSO) only control for 48 and 72 hours. cDNA was synthesised from extracted RNA from 3 biological replicates for each condition. Three technical replicates were performed per biological replicate. Data were analysed using the  $\Delta C_q$  method and an RQ value calculated by  $2^{-\Delta C_q}$ . An F-test was performed to assess variance between groups and two-tailed, unpaired Student's t-tests with Welch's correction for unequal variance were performed to assess significance. Error bars depict standard deviation and asterisks denote significance. No change in rictor expression was detected as a result of treatment with Tem, Res or BEZ (A, B and C respectively).

### 3.3.2.6 Rictor Expression in MDAH-2774 Cells

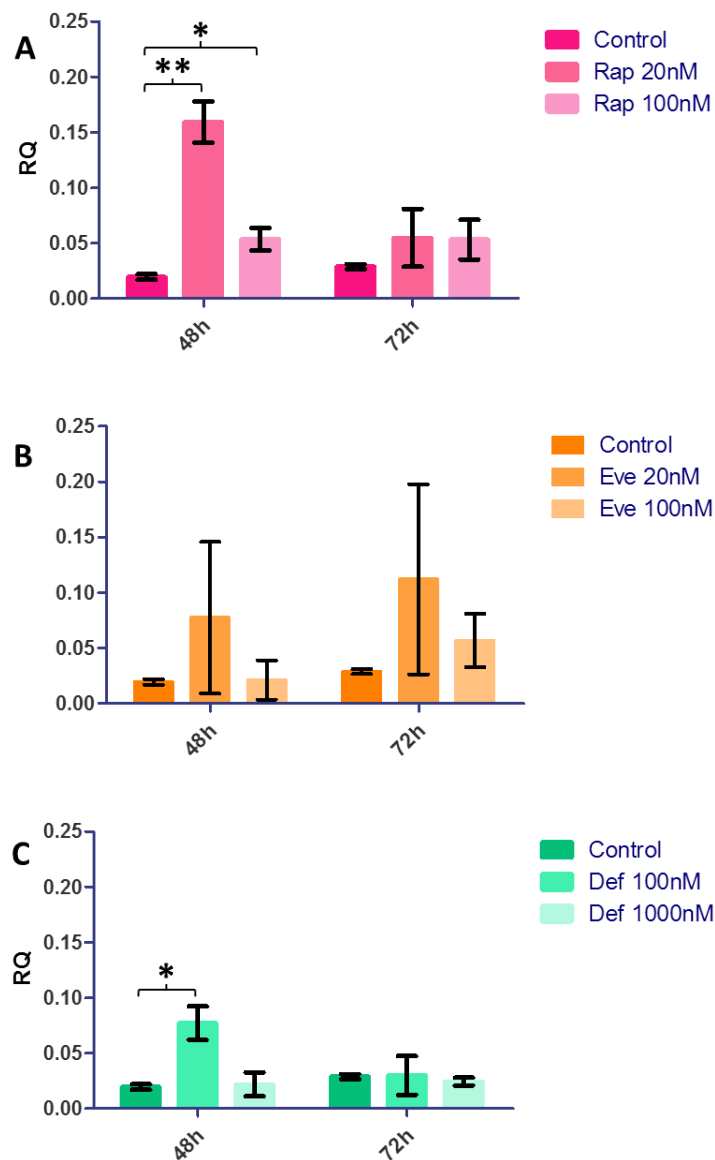


**Figure 3.13** - Relative rictor expression was measured by qPCR in MDAH-2774 cells treated with Rap (20 and 100nM), Eve (20 and 100nM), Def (100 and 1000nM) and carrier (DMSO) only control for 48 and 72 hours. cDNA was synthesised from extracted RNA from 3 biological replicates for each condition. Three technical replicates were performed per biological replicate. Data were analysed using the  $\Delta C_q$  method and an RQ value calculated by  $2^{-\Delta C_q}$ . An F-test was performed to assess variance between groups and two-tailed, unpaired Student's t-tests with Welch's correction for unequal variance were performed to assess significance. No change in rictor expression was detected in response to Eve treatment (B). 20nM Rap treatment induced an increase in rictor expression after 48 hours treatment (A,  $p=0.006$ ). 100nM Rap treatment also induced an increase in rictor expression after 48 hours (A,  $p=0.0302$ ). An increase was detected in rictor expression after 48 hours of 100nM Def treatment (C,  $p=0.0227$ ).

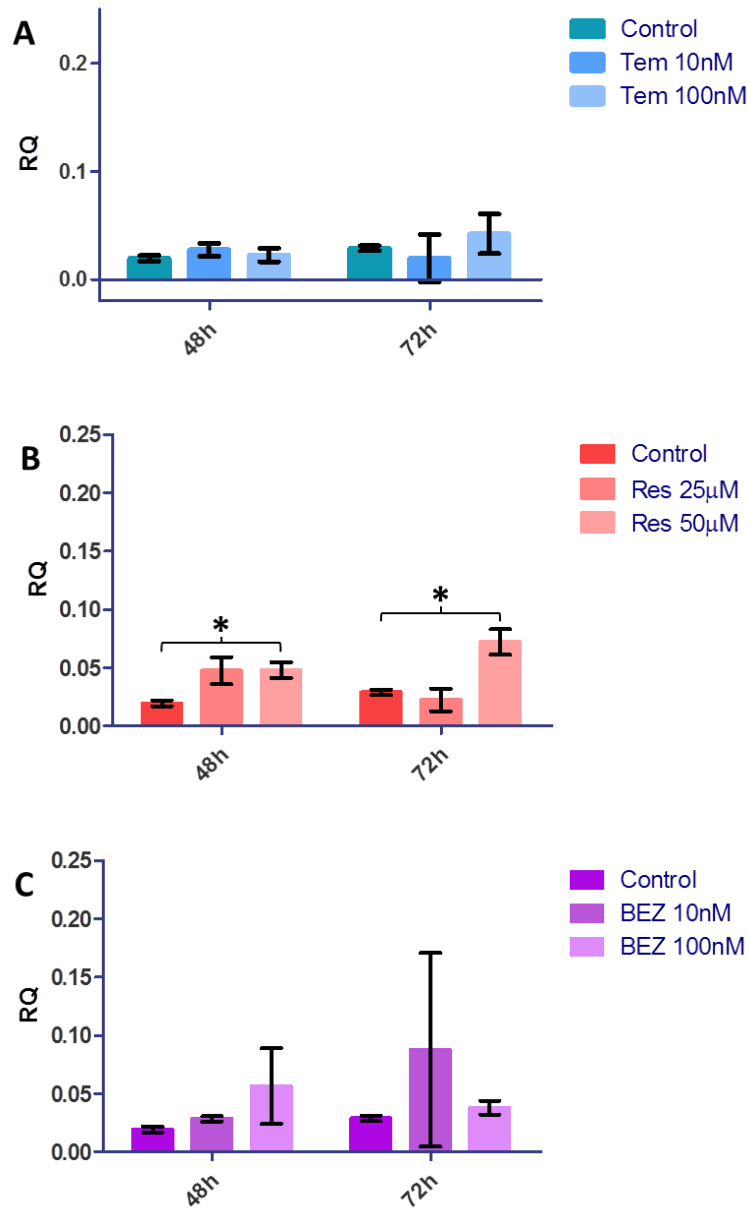


**Figure 3.14** - Relative rictor expression was measured by qPCR in MDAH-2774 cells treated with Tem (10nM and 100nM), Res (25 and 50µM), BEZ (10 and 100nM) and carrier (DMSO) only control for 48 and 72 hours. cDNA was synthesised from extracted RNA from 3 biological replicates for each condition. Three technical replicates were performed per biological replicate. Data were analysed using the  $\Delta C_q$  method and an RQ value calculated by  $2^{-\Delta C_q}$ . An F-test was performed to assess variance between groups and two-tailed, unpaired Student's t-tests with Welch's correction for unequal variance were performed to assess significance. No change in rictor expression was detected in response to Tem or BEZ treatment (**A** and **C** respectively). 50µM Res treatment induced a significant increase in rictor expression after 48 and 72 hours (**B**,  $p=0.0210$  and  $0.0213$  respectively).

No change was detected in rictor expression in SKOV3 cells in response to mTOR pathway inhibition (Figures 3.11 and 3.12). 20nM Rap treatment induced a significant increase in rictor expression after 48 hours in MDAH-2774 cells in comparison to controls (Figure 3.13, A,  $p=0.006$ ). 100nM Rap treatment induced an increase in rictor expression after 48 hours (Figure 3.13, A,  $p=0.0302$ ). An increase in rictor expression was detected at 48 hours after 100nM Def treatment in comparison to controls (Figure 3.13, C,  $p=0.0227$ ). Res treatment at 50 $\mu$ M induced an increase in rictor expression after 48 and 72 hours in comparison to controls (Figure 3.13, B,  $p=0.021$  and 0.0213 respectively). No significant change was detected in rictor expression in response to Tem or BEZ treatment at high or low concentration in MDAH-2774 cells at any time point (Figure 3.14, A and C).



### 3.3.2.7 Raptor Expression in SKOV3 Cells

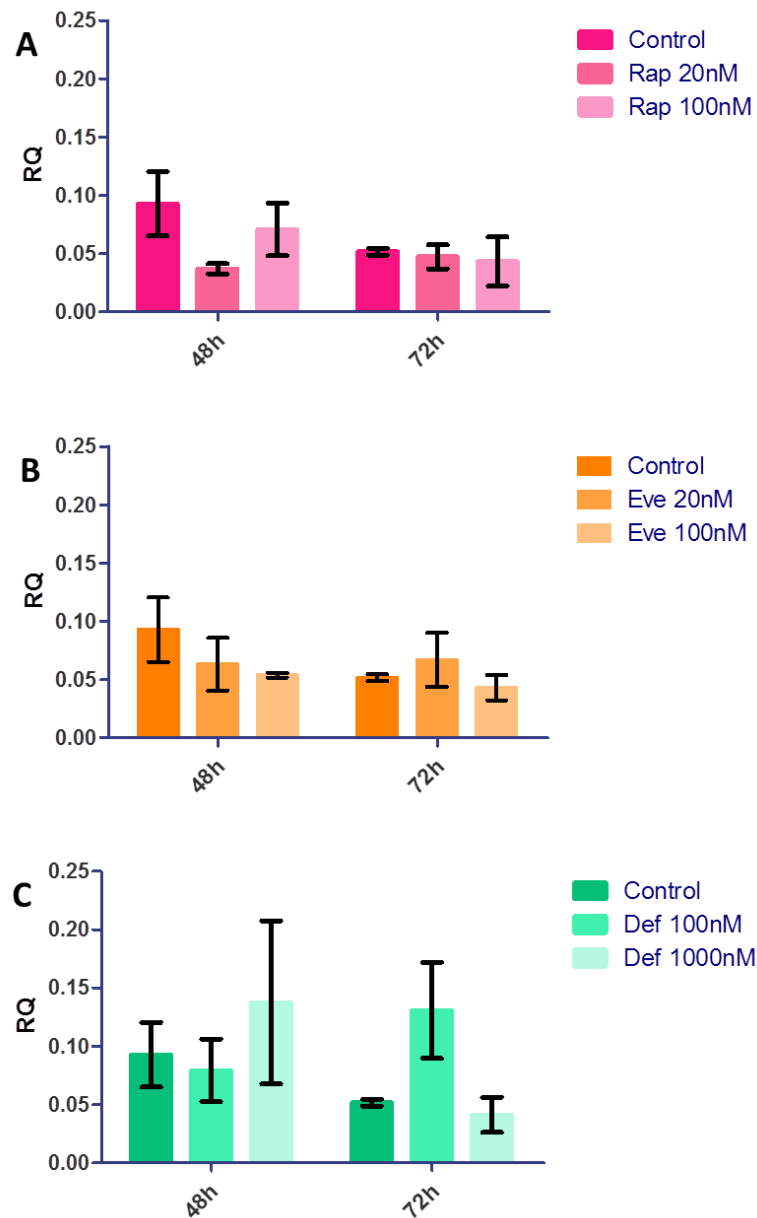


**Figure 3.15** - Relative raptor expression was measured by qPCR in SKOV3 cells treated with Rap (20 and 100nM), Eve (20 and 100nM), Def (100 and 1000nM) and carrier (DMSO) only control for 48 and 72 hours. cDNA was synthesised from extracted RNA from 3 biological replicates for each condition. Three technical replicates were performed per biological replicate. Data were analysed using the  $\Delta C_q$  method and an RQ value calculated by  $2^{-\Delta C_q}$ . An F-test was performed to assess variance between groups and two-tailed, unpaired Student's t-tests with Welch's correction for unequal variance were performed to assess significance. No change in raptor expression was detected after treatment with Rap, Eve or Def (A, B and C respectively).

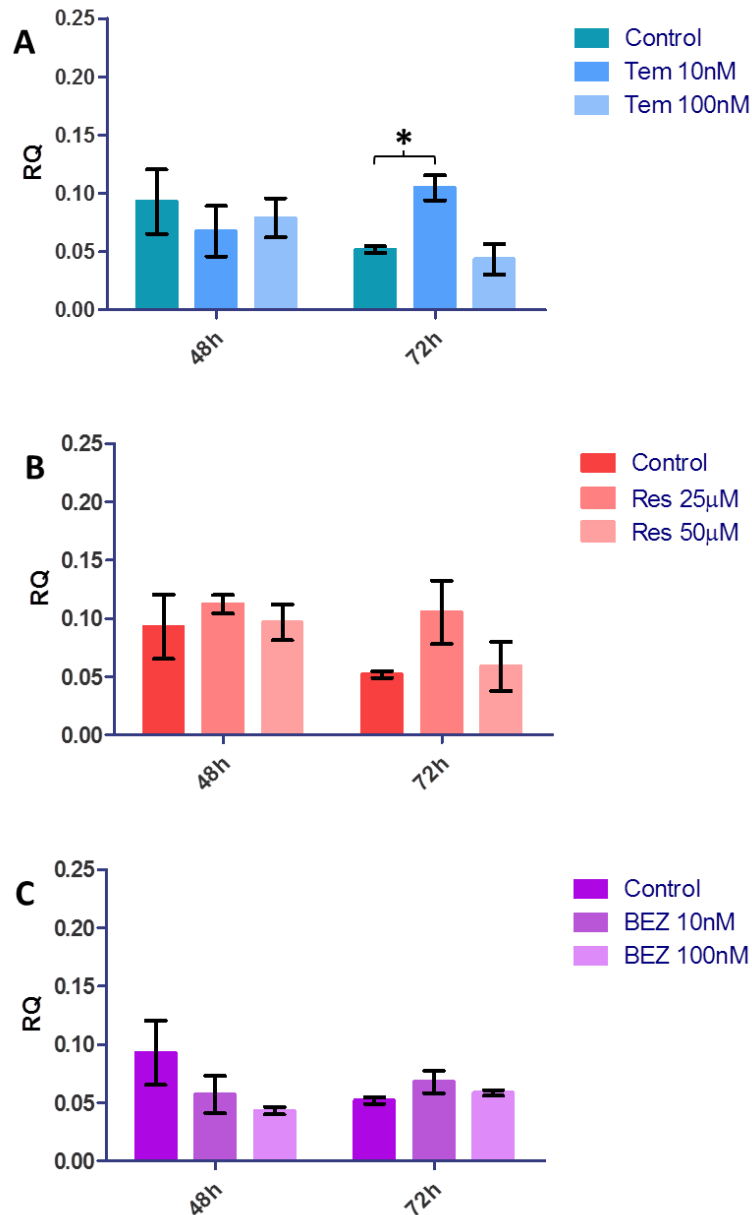


**Figure 3.16** - Relative raptor expression was measured by qPCR in SKOV3 cells treated with Tem (10nM and 100nM), Res (25 and 50µM), BEZ (10 and 100nM) and carrier (DMSO) only control for 48 and 72 hours. cDNA was synthesised from extracted RNA from 3 biological replicates for each condition. Three technical replicates were performed per biological replicate. Data were analysed using the  $\Delta C_q$  method and an RQ value calculated by  $2^{-\Delta C_q}$ . An F-test was performed to assess variance between groups and two-tailed, unpaired Student's t-tests with Welch's correction for unequal variance were performed to assess significance. No change in raptor expression was detected after treatment with Res or BEZ (B and C respectively). 10nM Tem treatment induced an increase in raptor expression after 72 hours (A,  $p=0.0144$ ).

### 3.3.2.8 Raptor Expression in MDAH-2774 Cells

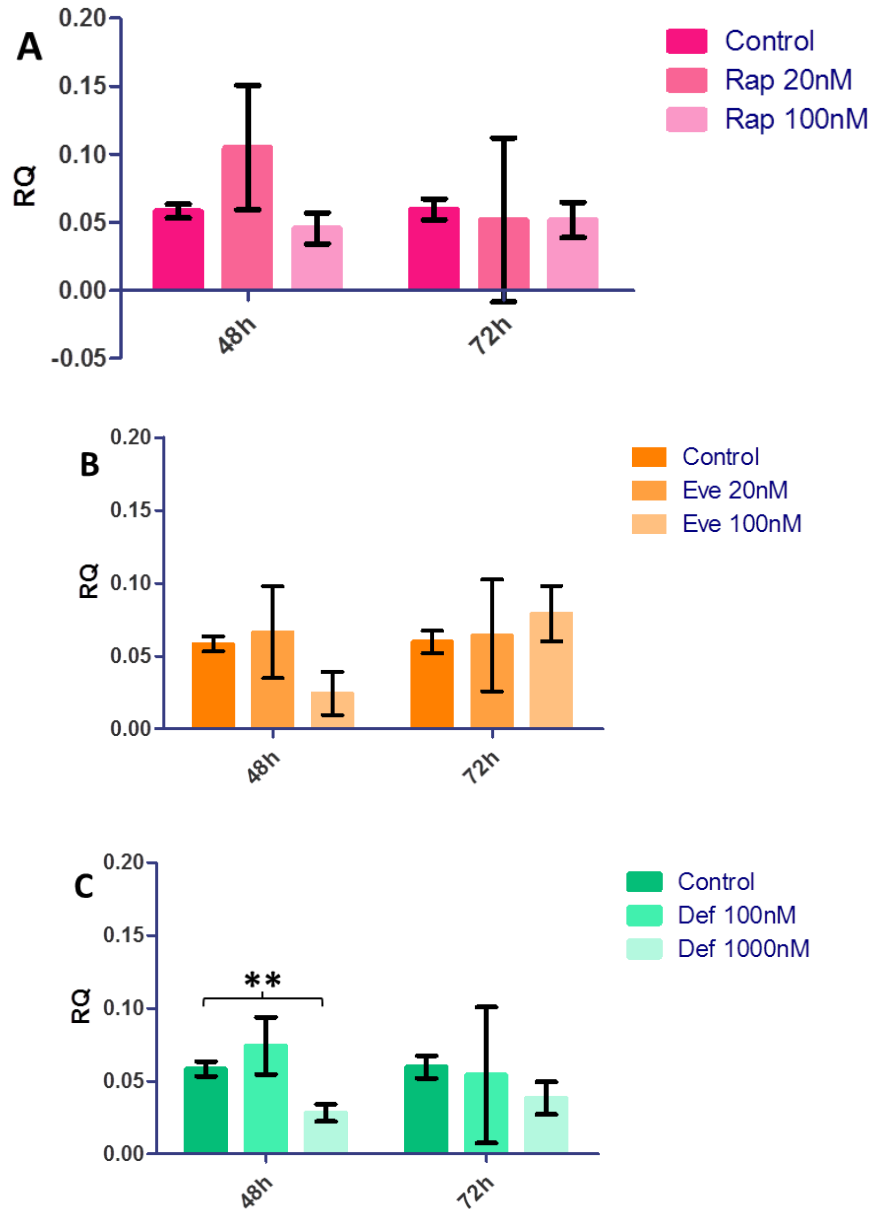


**Figure 3.17** - Relative raptor expression was measured by qPCR in MDAH-2774 cells treated with Rap (20 and 100nM), Eve (20 and 100nM), Def (100 and 1000nM) and carrier (DMSO) only control for 48 and 72 hours. cDNA was synthesised from extracted RNA from 3 biological replicates for each condition. Three technical replicates were performed per biological replicate. Data were analysed using the  $\Delta C_q$  method and an RQ value calculated by  $2^{-\Delta C_q}$ . An F-test was performed to assess variance between groups and two-tailed, unpaired Student's t-tests with Welch's correction for unequal variance were performed to assess significance. No change in expression was detected as a result of Rap or Eve treatment (**A** and **B** respectively). 1000nM Def treatment induced a decrease in raptor expression after 48 hours (**C**,  $p=0.0067$ ).

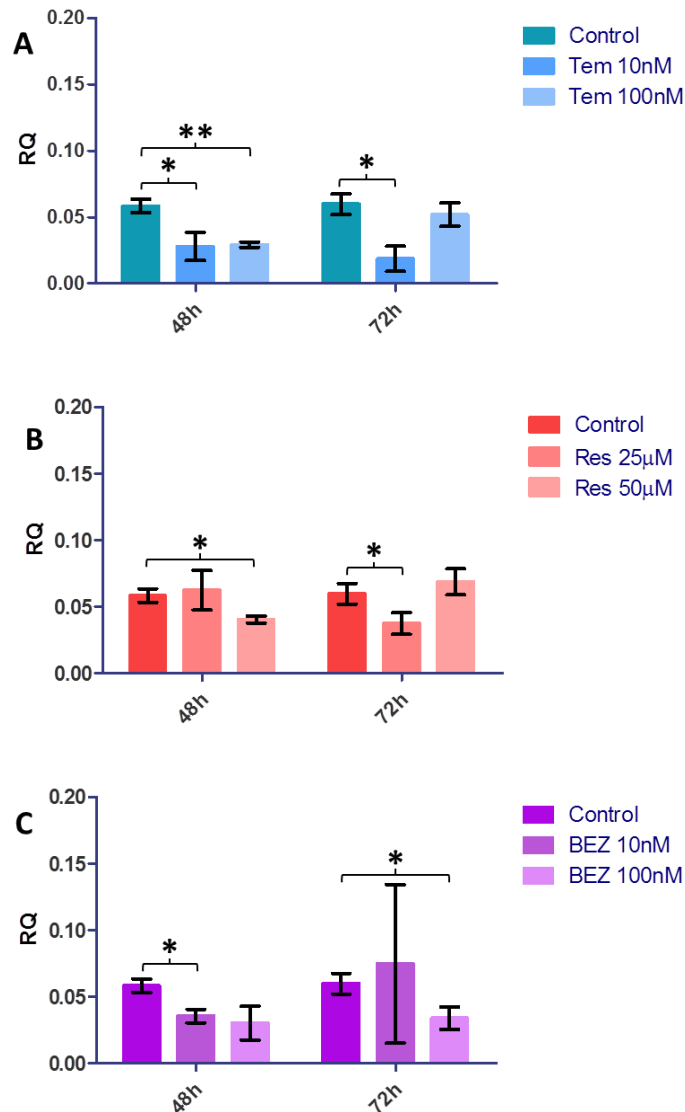


**Figure 3.18** - Relative raptor expression was measured by qPCR in MDAH-2774 cells treated with Tem (10nM and 100nM), Res (25 and 50µM), BEZ (10 and 100nM) and carrier (DMSO) only control for 48 and 72 hours. cDNA was synthesised from extracted RNA from 3 biological replicates for each condition. Three technical replicates were performed per biological replicate. Data were analysed using the  $\Delta C_q$  method and an RQ value calculated by  $2^{-\Delta C_q}$ . An F-test was performed to assess variance between groups and two-tailed, unpaired Student's t-tests with Welch's correction for unequal variance were performed to assess significance. 10nM Tem treatment showed a decrease in raptor expression after 48 and 72 hours (A,  $p=0.0457$  and  $0.0101$  respectively). 100nM Tem treatment also decreased raptor expression at 48 hours (A,  $p=0.0115$ ). 25µM Res treatment caused a decrease in raptor expression after 72 hours (B,  $p=0.0412$ ) and 50µM Res treatment showed a decrease after 48 hours (B,  $p=0.0318$ ). BEZ treatment induced a decrease in raptor expression after 48 hour 10nM treatment (C,  $p=0.0120$ ) and after 72 hour 100nM treatment (C,  $p=0.0298$ ).

Little change in raptor expression was detected in SKOV3 cells. No change was detected in raptor expression in comparison to controls in response to Rap, Eve, Def, Res or BEZ treatment at high or low concentrations and at any time point (Figure 3.15, A, B and C, Figure 3.16 B and C). An increase in raptor expression was detected after 72 hours of 10nM Tem treatment (Figure 3.16, A,  $p=0.0144$ ). MDAH-2774 cells showed an overall trend towards decreasing raptor expression in response to mTOR pathway inhibition. Rap and Eve treatment induced no change in expression at any time point or in response to high or low concentrations in MDAH-2774 cells (Figure 3.17, A and B respectively). 1000nM Def treatment induced a decrease in raptor expression after 48 hours of treatment in comparison to controls (Figure 3.17, C,  $p=0.0067$ ). 10nM Tem treatment induced a decrease in raptor expression after 48 and 72 hours of treatment in MDAH-2774 cells in comparison to controls (Figure 3.18, A,  $p=0.0457$  and  $0.0101$  respectively). In addition, 100nM Tem treatment also induced a decrease in raptor expression after 48 hours of treatment (Figure 3.18, A,  $p=0.0115$ ). 25 $\mu$ M Res treatment resulted in decreased raptor expression after 72 hours in comparison to controls and 50 $\mu$ M Res treatment had the same effect after 48 hours treatment (Figure 3.18, B,  $p=0.0412$  and  $0.0318$  respectively). 10nM BEZ treatment induced a decrease in raptor expression after 48 hours of treatment and 100nM BEZ treatment resulted in decreased raptor expression after 72 hours in comparison to controls (Figure 3.18, C,  $p=0.012$  and  $0.0298$  respectively).

### 3.3.3 Summary

Component	Cell Line	
	SKOV3	MDAH-2774
	Expressional Change	
mTOR	X	X
DEPTOR	X	Increase
Rictor	X	X
Raptor	X	Decrease

**Table 3.2** - Summary of gene expression changes of mTOR components in SKOV2 and MDAH-2774 cells following treatment with mTOR pathway inhibitors. Expressional change was included when observed in greater than five instances.

### 3.4 Discussion

This study validated the expression of four core mTOR complex components, mTOR, DEPTOR, rictor and raptor in two *in vitro* models of ovarian cancer. Both gene and protein expression of mTOR, DEPTOR, rictor and raptor was confirmed. In agreement with previous studies, we showed that these components are primarily located in the cytoplasm (Roos *et al.*, 2007; Foster *et al.*, 2010; Zhang *et al.*, 2002). We detected a significant increase in mTOR and raptor gene expression in MDAH-2774 cells in comparison to SKOV3 cells. Raptor is an mTORC1 component (Hara *et al.*, 2002) and the detected upregulation may suggest increased mTORC1 assembly and signalling in this cell line. We also examined the gene expression changes that occurred in mTOR, DEPTOR, rictor and raptor in SKOV3 and MDAH-2774 ovarian cancer cell lines after treatment with single mTOR and dual mTOR and PI3 kinase inhibitors. There are few reports on the effect of mTOR pathway inhibition on expression of mTOR pathway components. Differential effects were detected in response to mTOR pathway inhibition in SKOV3 and MDAH-2774 cells. In agreement with previous data, mTOR showed little change in expression in SKOV3 or MDAH-2774 cells after treatment with rapalogues, Res or BEZ. No consistent change in DEPTOR expression was detected with rapalogue treatment in SKOV3

cells. In contrast to SKOV3 cells DEPTOR expression was increased in response to all treatments in MDAH-2774 cells.

SKOV3 and MDAH-2774 cells also showed a differential effect in rictor and raptor expression in response to mTOR pathway inhibition. Rictor and raptor expression was unaffected by Rap, rapalogues, Res and BEZ in SKOV3 cells; however, MDAH cells showed a general increase in rictor expression and a general decrease in raptor expression. mTOR pathway inhibitors have been shown to increase mTORC2 signalling through the inactivation of a negative feedback loop to PI3 kinase as a result of mTOR inhibition (Peterson *et al.*, 2009). Rictor is an mTORC2 component (Sarbasov *et al.*, 2004) and an increase may suggest increased mTORC2 assembly and signalling. SKOV3 and MDAH-2774 cells differ in their origins; SKOV3 cells were derived from a clear cell adenocarcinoma and MDAH-2774 cells were derived from an endometrioid adenocarcinoma. As discussed previously, these cell lines differ substantially in the types of genetic aberrations they carry (Beaufort *et al.*, 2014) and this may contribute to the differential effects on DEPTOR, rictor and raptor expression detected after mTOR pathway inhibition.

Res treatment of SKOV3 cells showed an increase in expression after 48 hours and a decrease after 72 hours, suggesting that the effects of Res treatment on DEPTOR expression are biphasic. Res inhibits mTOR by enhancing its interaction with DEPTOR (Meilian Liu *et al.*, 2010) and in this cell type, DEPTOR expression at RNA level may be regulated by the amount of unbound DEPTOR protein. There is limited research into the transcriptional and translational control of DEPTOR but recent research has shown that mTOR activation is able to induce the degradation of DEPTOR protein (Gao *et al.*, 2011). DEPTOR expression at both RNA and protein level is decreased in response to TGF $\beta$  (Das *et al.*, 2013) which activates mTORC1 signalling (Lamouille *et al.*, 2012; Rozen-Zvi *et al.*, 2013). Collectively, these data show that mTOR component expression at gene level are differentially regulated dependent on cell type and that phenotypic responses to mTOR pathway inhibition may vary.

## ***Chapter 4***

### ***The effects of mTOR pathway inhibition in in vitro models of ovarian cancer***

#### **4.1 Introduction**

The mTOR pathway is a key regulator of growth and proliferation and responds to stimuli such as growth factors, amino acids, DNA damage, energy and oxygen status to mediate proliferation, cell growth and autophagy among other processes. mTOR, DEPTOR, rictor and raptor are four main components of mTORC1 and mTORC2, the central complexes of the mTOR pathway, and it is evident that a majority of the pathway's actions are mediated by mTORC1 (Laplante and Sabatini, 2012).

mTOR inhibitor Rap was first approved for clinical use throughout the European Union (EU) in 2001 under the brand name Rapamune in patients who had undergone kidney transplantation to prevent rejection due to Rap's potent immuno-inhibitory effects (European Medicines Agency, 2015c; Kay *et al.*, 1991; Dumont *et al.*, 1990; Morelon *et al.*, 2001). Since this time, Everolimus (Afinitor, Novartis) and Temsirolumab (Torisel, Pfizer) have also been approved for renal cell carcinoma, pancreatic and breast cancers and mantle cell lymphomas (European Medicines Agency, 2015b; European Medicines Agency, 2015d; Benjamin *et al.*, 2011). Multiple clinical trials are currently underway involving the rapalogues, Everolimus and BEZ235 for the treatment of autoimmune disease, epilepsy, organ transplant rejection and a range of cancers (clinicaltrials.gov). Although mTOR inhibitors are a much studied source of cancer treatment, the effects of mTOR inhibition have not yet been fully realised. mTOR inhibition is likely to be most effective in subsets of malignancies with mTOR aberrations and more work must be done to define the conditions in which these inhibitors are likely to be most effective. We sought to elucidate the



effect that mTOR pathway inhibition has on cell growth, proliferation, apoptosis and mTOR pathway activation in SKOV3 and MDAH-2774 cell lines.

## **4.2 Objectives**

-To elucidate the effect that mTOR pathway inhibition has on migration and proliferation of SKOV3 and MDAH-2774 cells.

-To assess the proliferative capacity of SKOV3 and MDAH-2774 cells after mTOR inhibition.

-To investigate the effects that mTOR pathway inhibition has on mTOR pathway activation (phosphorylation of p70S6 kinase) and cell death (cleavage of caspases 3 and 9).

## **4.3 Results**

mTOR pathway inhibitors were used according to section 3.3.2.

### **4.3.1 Proliferation and migration of SKOV3 and MDAH-2774 cells in a wound healing scenario**

We initially investigated the proliferative and migratory capacity of SKOV3 and MDAH-2774 cells after treatment with mTOR pathway inhibitors. As this was a preliminary investigation, we used Rap to represent rapalogues, Res and BEZ. Wound healing assays can give a visual indication of cells' proliferative and migratory capacity spatially *in vitro*. Wound healing assays were completed as described previously (Section 2.4). Briefly, cells were seeded in 6-well plates (~10cm<sup>2</sup> growth area) and grown into a confluent monolayer. Three 'wounds' were created in the cells with a p200 pipette tip immediately before treatment with Rap (20 and 100nM), Res (25 and 50µM) and BEZ (10nM and 100nM) and images taken

at 0, 6, 12 and 18 hours after treatment. Three biological replicates were performed per condition.

#### 4.3.1.1 SKOV3

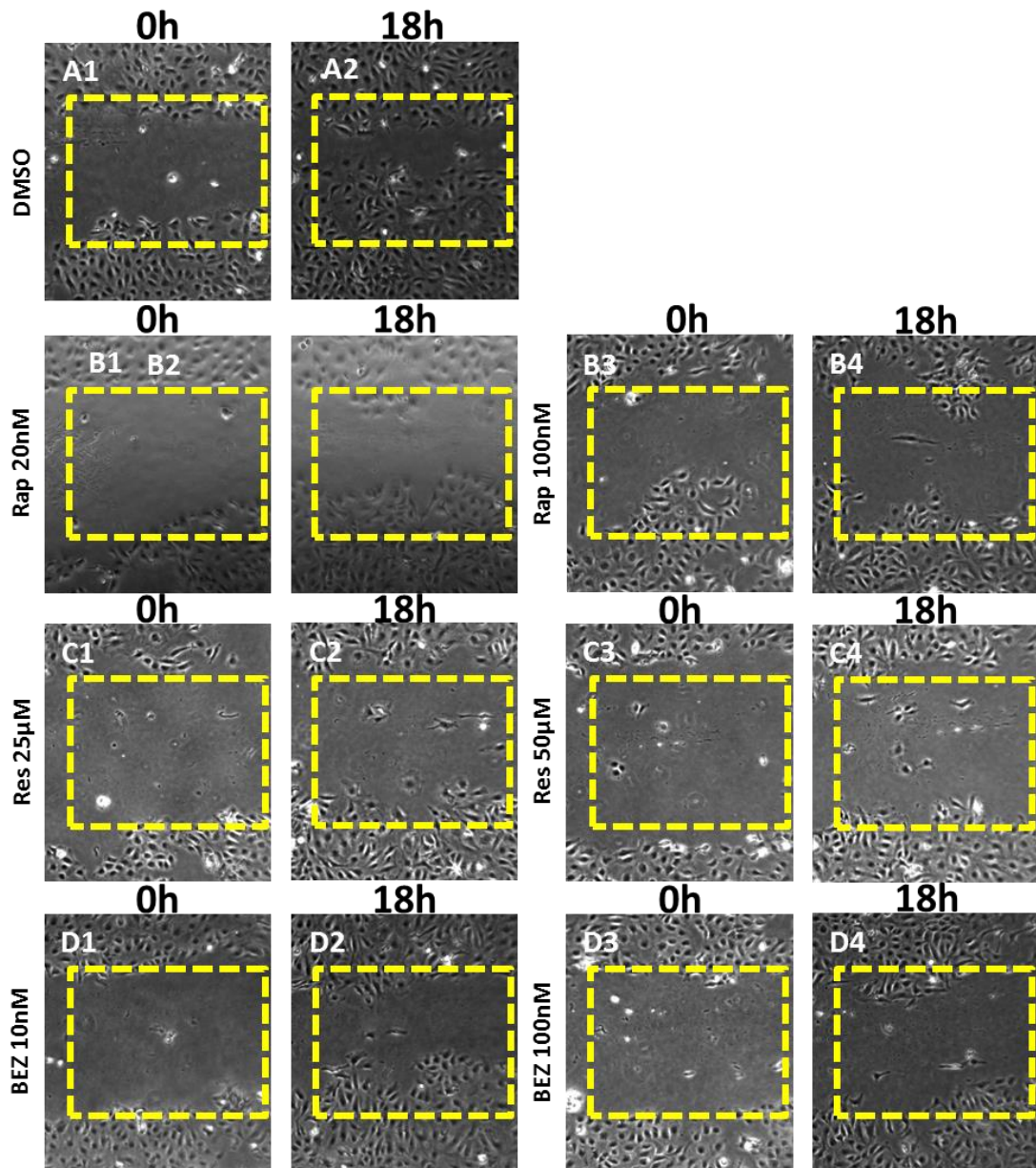


**Figure 4.1** - A 'wound' was created in a confluent monolayer of SKOV3 cells which were then treated with Rap (20 and 100nM), Res (25 and 50μM) and BEZ (10 and 100nM). Images were taken up to 18 hours after treatment. Figure shows cells at 0 and 18 hours after treatment.

#### 4.3.1.2 MDAH-2774

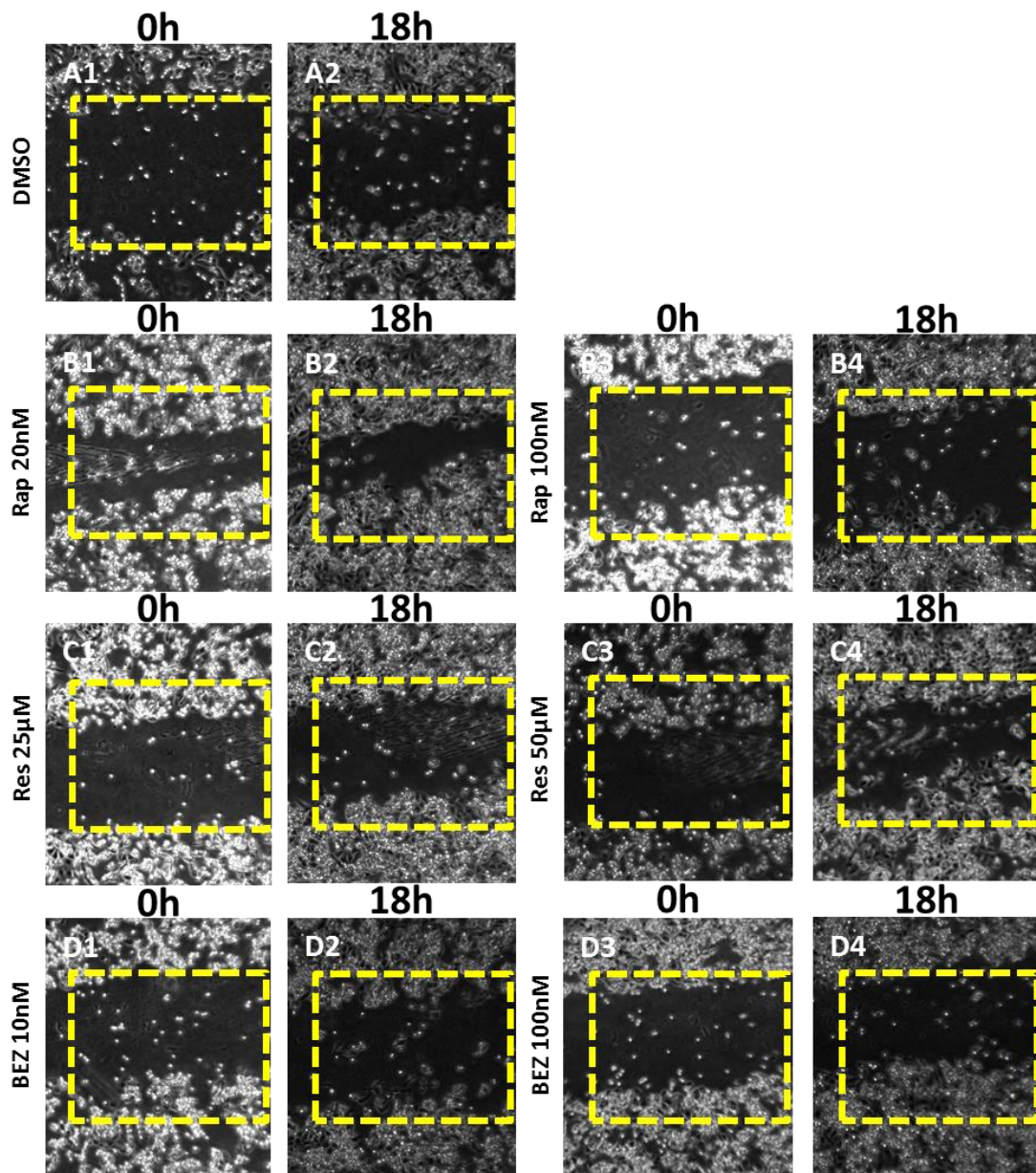


**Figure 4.2** - A 'wound' was created in a confluent monolayer of MDAH-2774 cells which were then treated with Rap (20 and 100nM), Res (25 and 50 µM) and BEZ (10 and 100nM). Images were taken up to 18 hours after treatment. Figure shows cells at 0 and 18 hours after treatment.

Untreated SKOV3 cells showed a marked growth into the wound (Figure 4.1, A1 and A2) which was not shared by any of the inhibitor treated cells. Rap and Res treated cells showed little growth at both concentrations (Figure 4.1, B1-4 and C1-4) 10nM BEZ treatment showed a moderate change which was not shared by 100nM treatment (Figure 4.1, D1-4). MDAH-2774 showed little proliferation under all

conditions; limited differences between control and treated cells were detected (Figure 4.2). No decrease in cell number was visually detected, indicating that these inhibitory treatments do not exert a cytotoxic effect.

#### **4.3.2 Proliferative capacity of SKOV3 and MDAH-2774 cells after mTOR pathway inhibition**

To expand the investigation of the effects of mTOR pathway inhibition on cell viability, a proliferation assay was performed using trypan blue staining to make an assessment of the proliferative capacity of the SKOV3 and MDAH-2774 cells up to 72 hours after treatment with mTOR pathway inhibitors including the rapalogues Eve, Def and Tem. Proliferation assays were performed as described previously (Section 2.3). Briefly, cells were seeded in 6-well plates at a density of 100,000 cells per well ( $\sim 10\text{cm}^2$  growth area) and allowed to proliferate for 24 hours before treatment with Rap (20 and 100nM), Eve (20 and 100nM), Def (100 and 1000nM), Tem (10 and 100nM), Res (25 and 50), BEZ (10 and 100nM) or carrier (DMSO). Cells were detached from the wells at 24, 48 and 72 hours by TrypLe™ Express (Life Technologies) and resuspended in media. An equal volume of cell suspension was mixed thoroughly with trypan blue stain (0.4%, Invitrogen) and viable and dead cells were counted using a Countess® Automated Cell Counter (Life Technologies). Biological and technical triplicates were performed for each condition.

#### 4.3.2.1 SKOV3

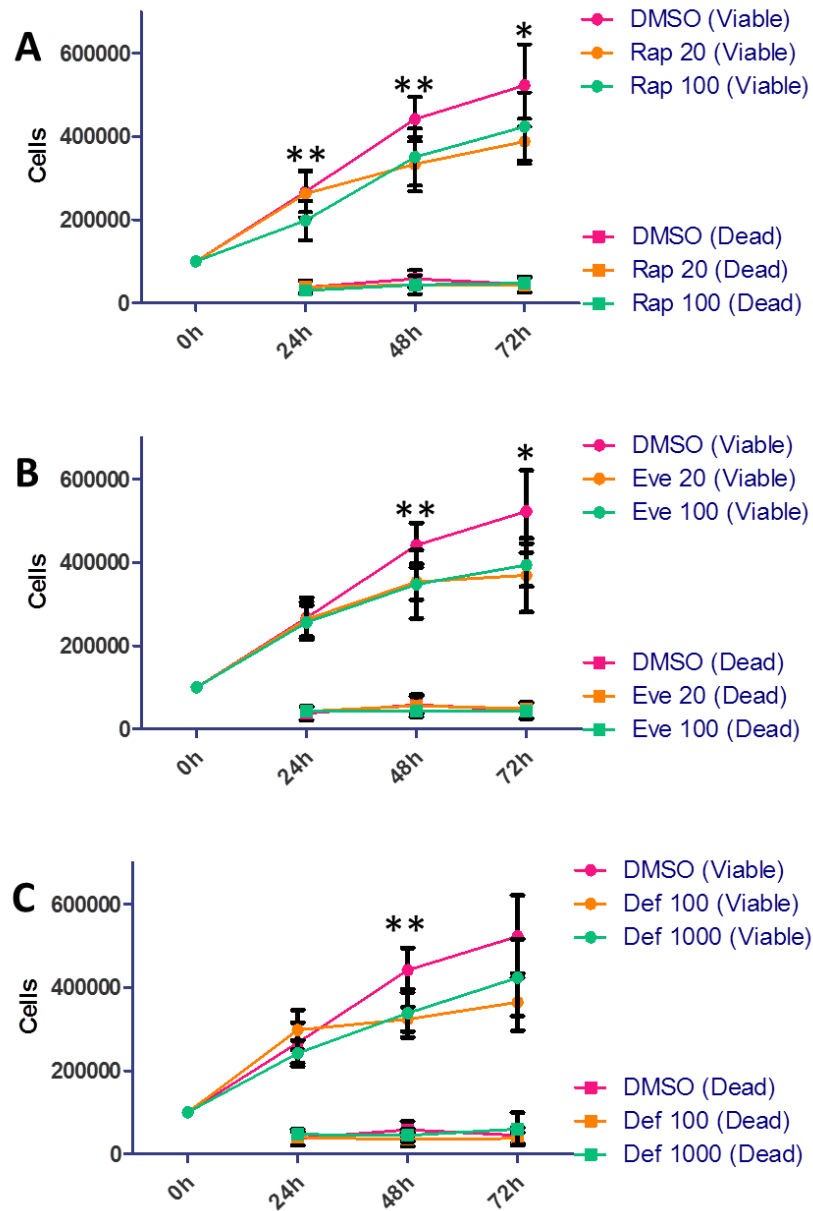


**Figure 4.3** - SKOV3 cells were treated with mTOR pathway inhibitors and carrier (DMSO). Cell counts were performed 24, 48 and 72 hours after treatment. An F-Test was performed to assess variance and two-tailed, unpaired Student's t-tests were performed with Welch's correction for unequal variance to assess significance.

Error bars depict standard deviation and asterisks denote significant changes between control and higher concentration treatments. Rap treatment induced a non-dose dependent decrease in viable cells after 24, 48 and 72 hours (**A**,  $p=0.0081$ ,  $0.0067$  and  $0.0355$  respectively). Eve treatment induced a non-dose dependent decrease in viable cells after 48 and 72 hours (**B**,  $p=0.012$  and  $0.0047$  respectively). Def treatment induced a non-dose dependent decrease in viable cells after 48 hours (**C**,  $p=0.005$ ).

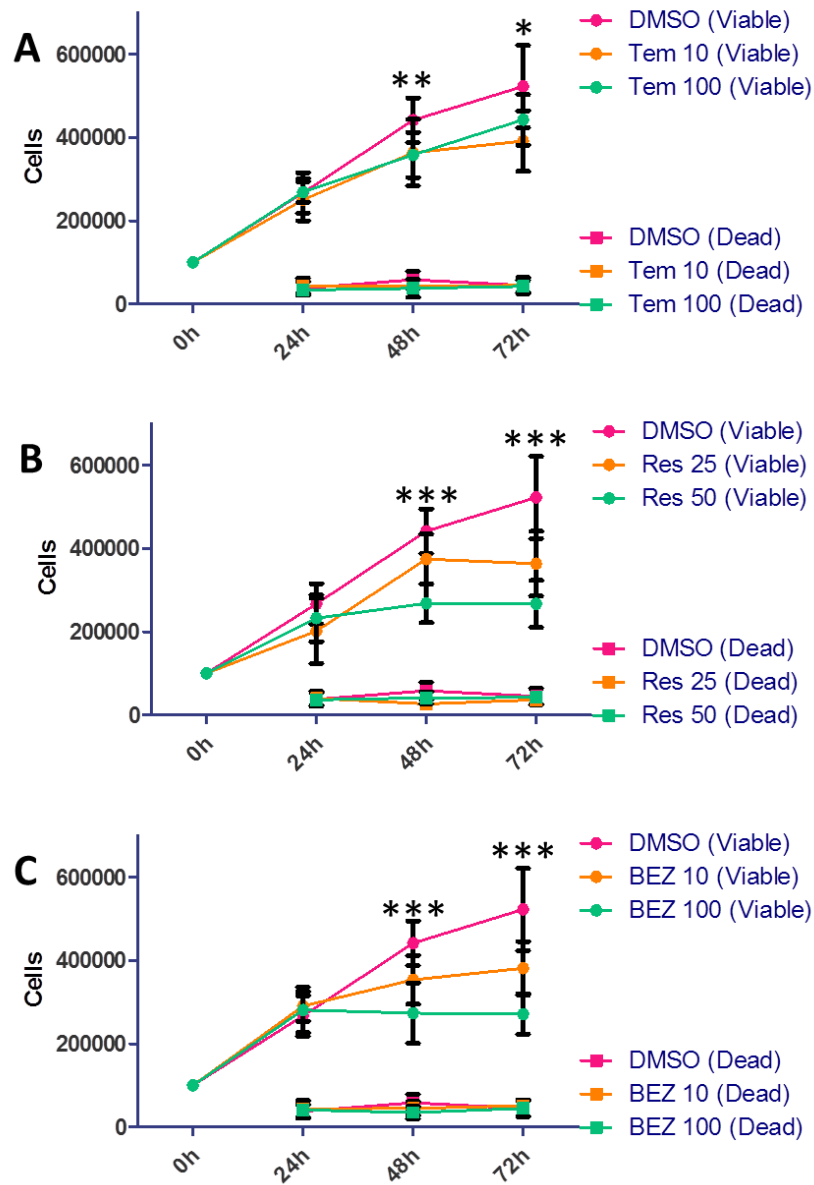


**Figure 4.4** - SKOV3 cells were treated with mTOR pathway inhibitors and carrier (DMSO). Cell counts were performed 24, 48 and 72 hours after treatment. An F-Test was performed to assess variance and two-tailed, unpaired Student's t-tests were performed with Welch's correction for unequal variance to assess significance. Error bars depict standard deviation and asterisks denote significant changes between control and higher concentration treatments. Tem showed a non-dose dependent decrease in viable cells after 48 and 72 hours (A,  $p=0.0013$  and  $0.0446$  respectively) whereas the decrease in Res and BEZ treated cells was dose dependent and significant at 48 and 72 hours (B & C,  $p<0.0001$  in all cases).

#### 4.3.2.2 MDAH-2774

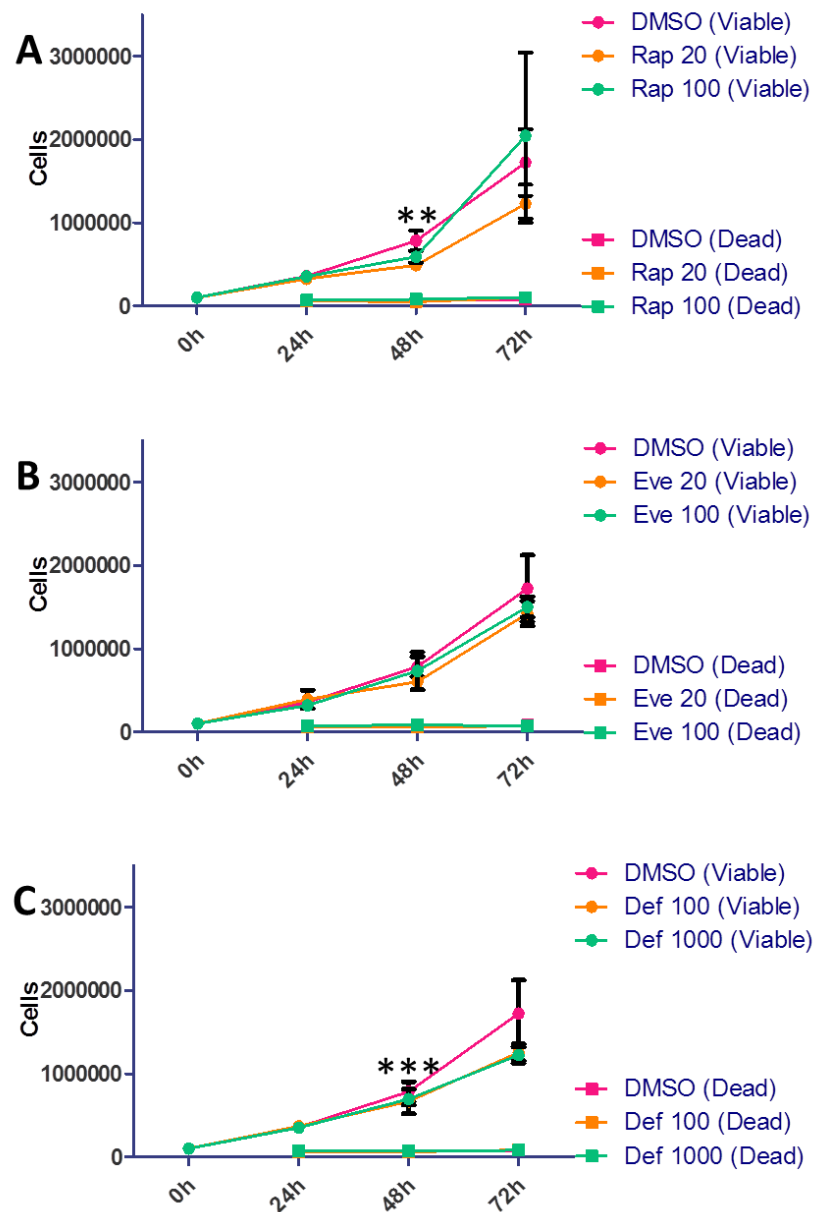


**Figure 4.5** - MDAH-2774 cells were treated with mTOR pathway inhibitors and carrier (DMSO). Cell counts were performed 24, 48 and 72 hours after treatment. An F-Test was performed to assess variance and two-tailed, unpaired Student's t-tests were performed with Welch's correction for unequal variance to assess significance. Error bars depict standard deviation and asterisks denote significant changes between control and higher concentration treatments. Rap and Def showed a significant decrease in viable cells after 48 hours (A & C,  $p=0.0013$  and  $0.0004$  respectively). No effect on viable cells was detected after Eve treatment (B).

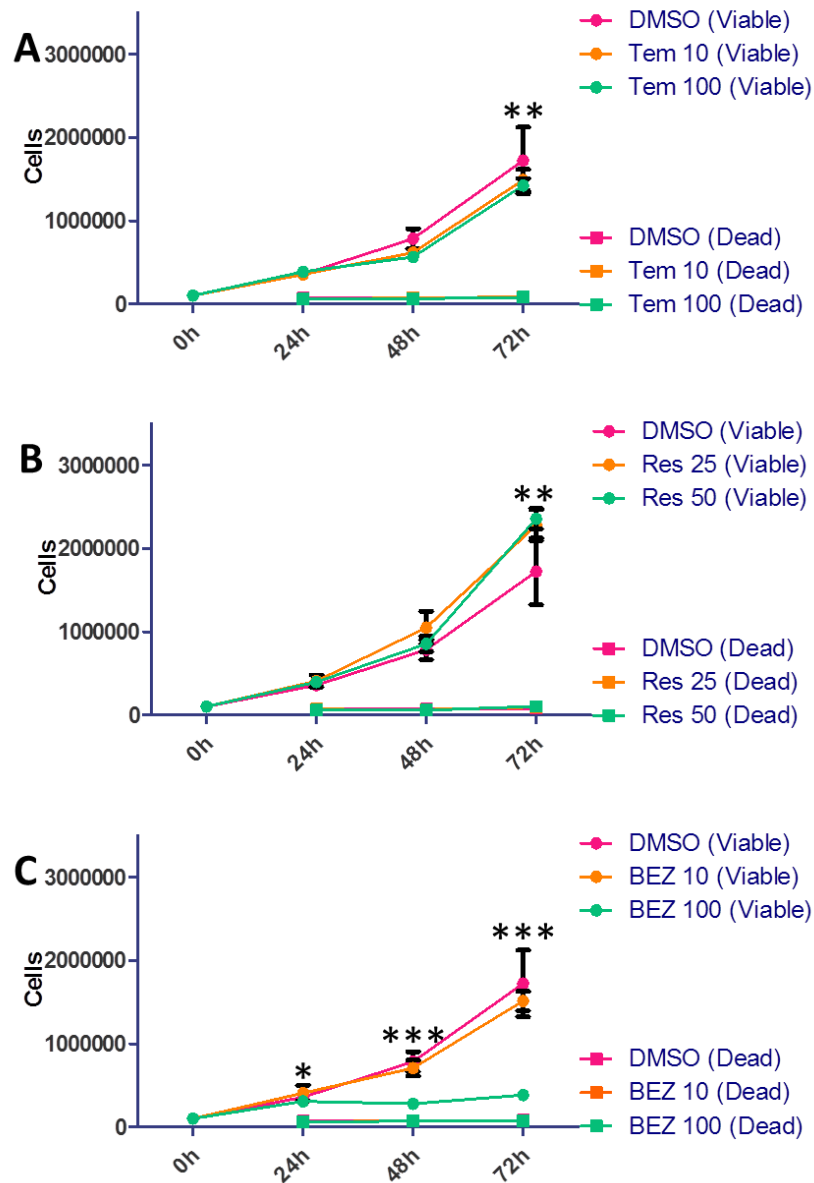


**Figure 4.6** - MDAH-2774 cells were treated with mTOR pathway inhibitors and carrier (DMSO). Cell counts were performed 24, 48 and 72 hours after treatment. An F-Test was performed to assess variance and two-tailed, unpaired Student's *t*-tests were performed with Welch's correction for unequal variance to assess significance. Error bars depict standard deviation and asterisks denote significant changes between control and higher concentration treatments. Tem treatment induced a non-dose dependent decrease in viable cells after 72 hours (**A**,  $p=0.0065$ ). BEZ treatment at 10nM showed no effect; however, 100nM treatment completely halted proliferation (**C**,  $p<0.0001$  at both 48 and 72 hours).



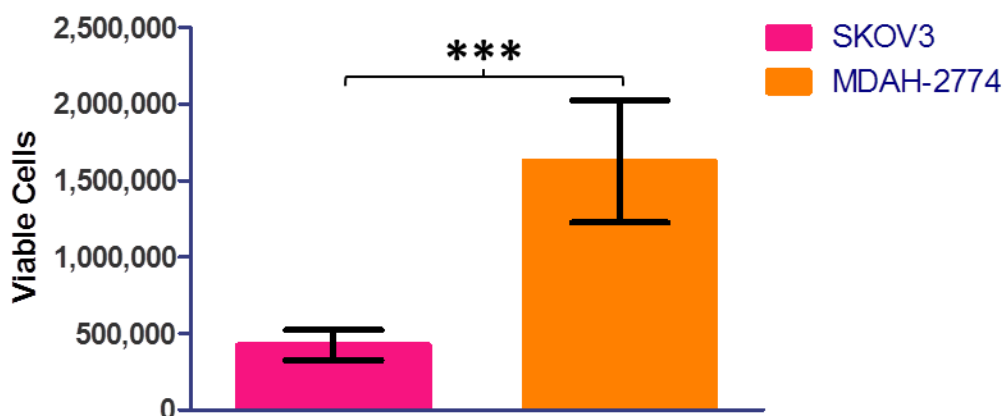


**Figure 4.7** - SKOV3 and MDAH-2774 cells were seeded at 100,000 cells per well and treated with 5% DMSO for 72 hours. An F-Test was performed to assess variance and an unpaired, two-tailed Student's t-test with Welch's correction for unequal variance performed to assess significance. Error bars depict standard deviation and asterisks denote significance. The average increase in control cell number was significantly greater for MDAH-2774 cells than SKOV3 cells ( $p < 0.0001$ ).

MDAH-2774 cells have a greater proliferative capacity than SKOV3 cells, showing an average increase in viable cells of 1,600,000 in comparison to 400,000 (Figure 4.7,  $p < 0.0001$ ). Treatment of the SKOV3 cell line with Rap and the rapalogues showed a non dose-dependent decrease in viable cells (Figure 4.3 A, B and C, Figure 4.4, A, Rap 100nM:  $p = 0.0355$  at 72 hours, Eve 100nM:  $p = 0.0047$  at 72 hours, Tem 100nM:  $p = 0.0446$  at 72 hours, Def 1000nM did not reach statistical significance:  $p = 0.0597$ ). The decrease in viable cells shown by Res and BEZ was dose dependent (Figure 4.4, B and C, Res 50 $\mu$ M:  $p < 0.0001$  at 72 hours, BEZ 100nM:  $p < 0.0001$  at 72 hours). Viable cell count in MDAH-2774 cells was little affected by Rap, rapalogue or Res treatment (Figure 4.5 A, B and C, Figure 4.6, A and B, Rap 100nM:  $p = 0.0013$  at 48 hours, Def 1000nM:  $p = 0.0004$  at 48 hours, Tem 100nM:  $p = 0.0065$  at 72 hours). BEZ treatment at 10nM concentration also did not have an effect on viable cell count but at 100nM, proliferation was almost entirely eliminated (Figure 4.6 C,  $p < 0.0001$  at 48 and 72 hours). Number of dead cells counted over the course of the experiment did not change significantly (Figures 4.3, 4.4, 4.5 and 4.6), further indicating that mTOR pathway inhibition induces a cytostatic and not cytotoxic response.

### 4.3.3 Activity of mTOR and caspase pathways after mTOR pathway inhibition

To further elucidate the cytostatic effects that mTOR pathway inhibition has on SKOV3 and MDAH-2774 cells, we investigated the activity of the mTOR and caspase pathways. p70S6 kinase is a terminal kinase in the mTOR pathway responsible for promoting protein synthesis (Laplante and Sabatini, 2012). It is active when phosphorylated and can be used as evidence of an active mTOR pathway via the mTORC1 complex (Isotani *et al.*, 1999; Burnett *et al.*, 1998). Caspases (cysteine-dependent aspartate-directed proteases) are cysteine proteases involved in apoptosis (programmed cell death). Caspase 9 is an initiator caspase whereas caspase 3 is an effector caspase. Initiator caspases activate effector caspases by cleaving their inactive (pro) form (Hao Chen *et al.*, 2015).

Western Blot experiments were performed in order to assess the activation status of the mTOR and caspase pathways after treatment with mTOR pathway inhibitors. Western blots were performed in triplicate as previously described (Section 2.11) on proteins extracted from treated and control cells (SKOV3 and MDAH-2774) using antibodies for endogenous full length (35kDa) and cleaved large fragment (17/19kDa) caspase 3, endogenous full length (47kDa) and cleaved large fragment (35/37kDa) caspase 9 and phosphorylated (Thr<sup>389</sup>) p70S6 kinase. Analysis was performed densitometrically using ImageJ software (National Institutes of Health) as described previously (Section 2.11.1).

#### 4.3.3.1 Caspase 9

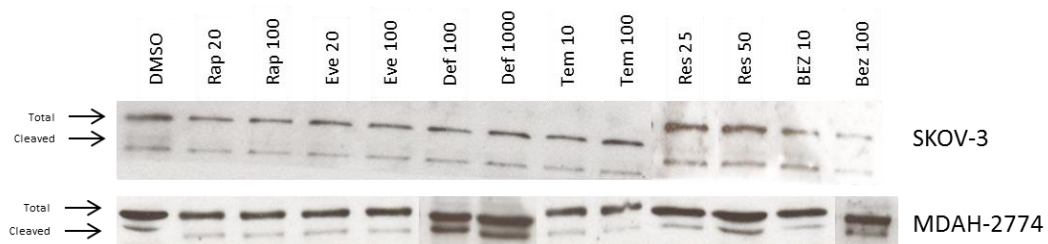


**Figure 4.8** - Western blots were performed on proteins extracted from SKOV3 and MDAH-2774 cells treated with mTOR pathway inhibitors for 24, 48 and 72 hours. Caspase 9 cleavage can be detected in all cases. Representative image shows extractions after 72 hours.

#### 4.3.3.1.1 SKOV3

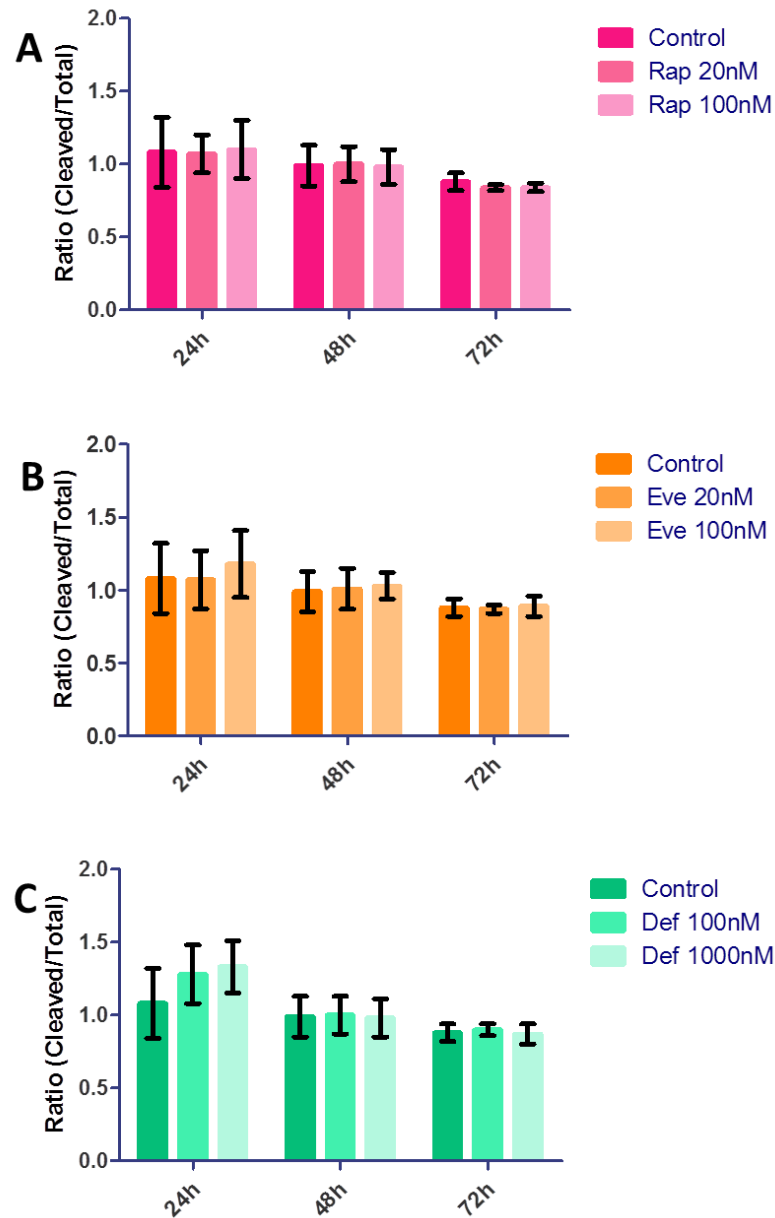


**Figure 4.9** - Western blots were performed on proteins extracted from SKOV3 cells treated with Rap (A, 20nM and 100nM), Eve (B, 20nM and 100nM) and Def (C, 100nM and 1000nM) for 24, 48 and 72 hours. Graphs show ratio of endogenous full length and cleaved large fragment caspase 9 when analysed densitometrically using ImageJ software. The F-Test was performed to assess variance and two-tailed, unpaired Student's t-tests were performed with Welch's correction for unequal variance to assess significance. Error bars depict standard deviation. No significant change in caspase 9 cleavage was detected in SKOV3 cells.

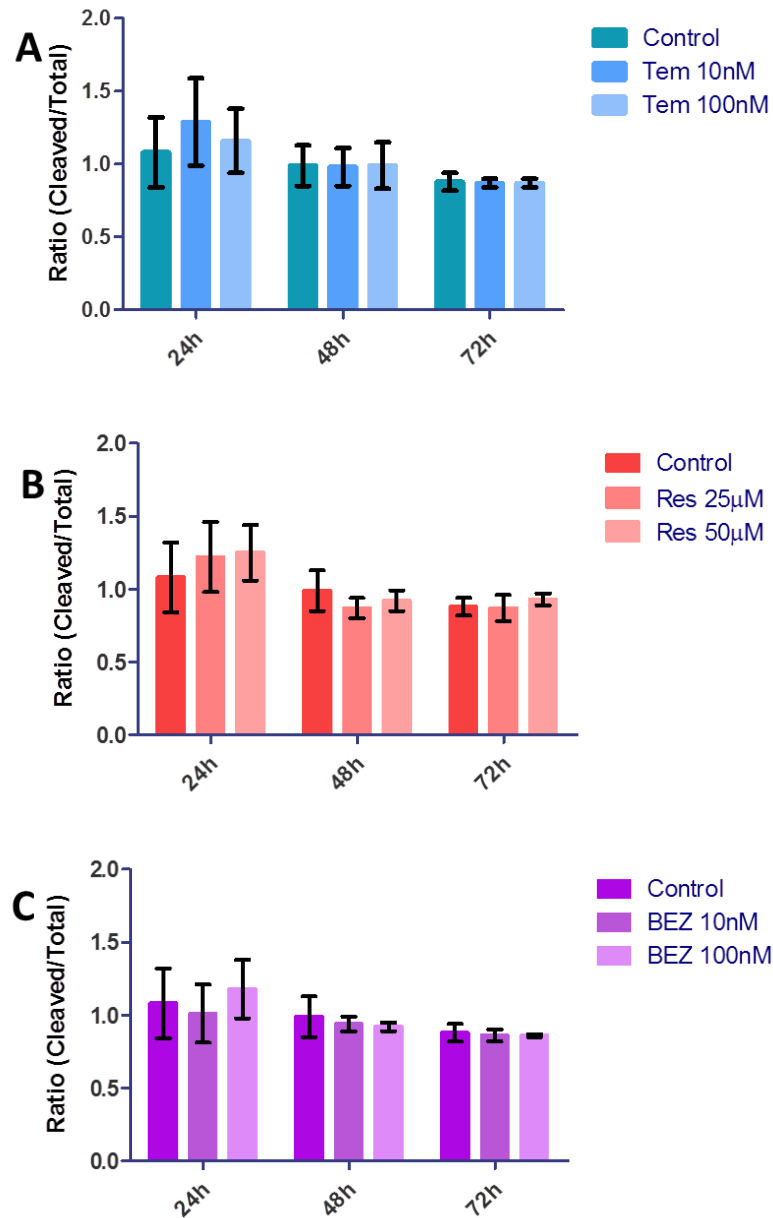


**Figure 4.10** - Western blots were performed on proteins extracted from SKOV3 cells treated with Tem (**A**, 10nM and 100nM), Res (**B**, 25µM and 50µM) and BEZ (**C**, 10nM and 100nM) for 24, 48 and 72 hours. Graphs show ratio of endogenous full length and cleaved large fragment caspase 9 when analysed densitometrically using ImageJ software. The F-Test was performed to assess variance and two-tailed, unpaired Student's t-tests were performed with Welch's correction for unequal variance to assess significance. Error bars depict standard deviation. No significant change in caspase 9 cleavage was detected in SKOV3 cells.

#### 4.3.3.1.2 MDAH-2774

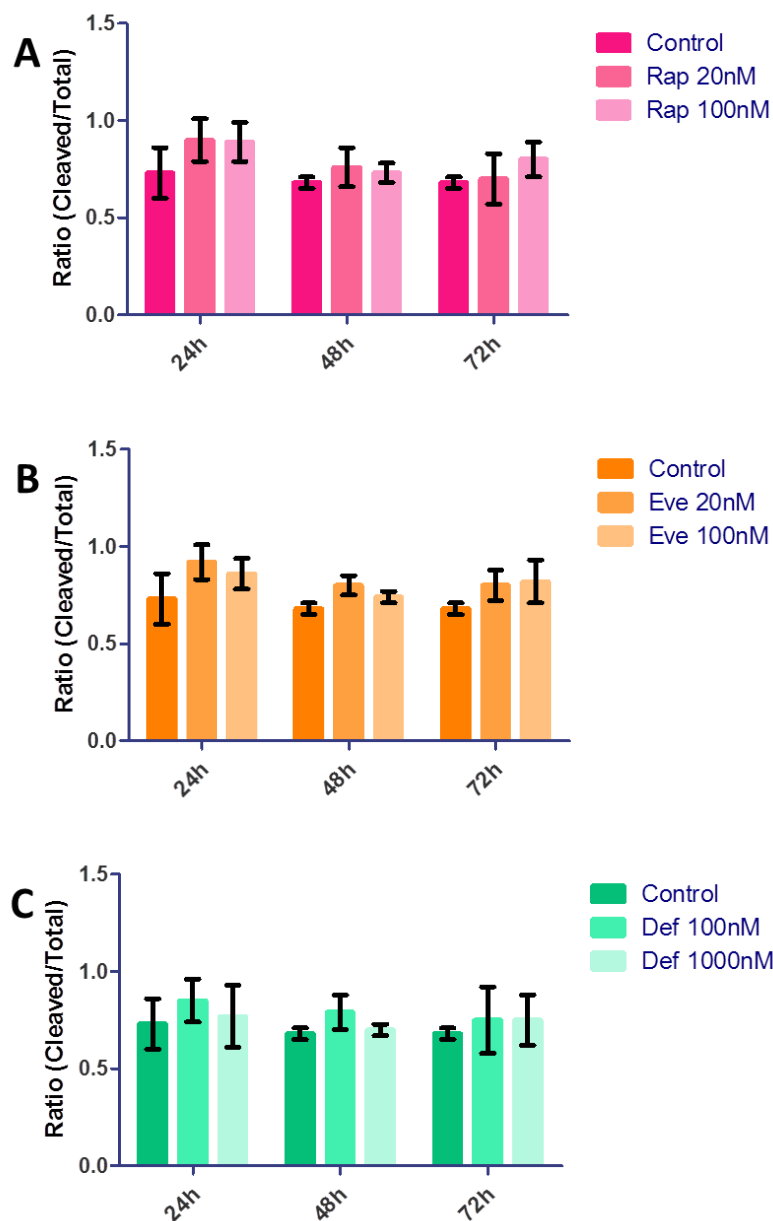


**Figure 4.11** - Western blots were performed on proteins extracted from MDAH-2774 cells treated with Rap (A, 20nM and 100nM), Eve (B, 20nM and 100nM) and Def (C, 100nM and 1000nM) for 24, 48 and 72 hours. Graphs show ratio of endogenous full length and cleaved large fragment caspase 9 when analysed densitometrically using ImageJ software. The F-Test was performed to assess variance and two-tailed, unpaired Student's t-tests were performed with Welch's correction for unequal variance to assess significance. Error bars depict standard deviation. No significant change in caspase 9 cleavage was detected in MDAH-2774 cells.

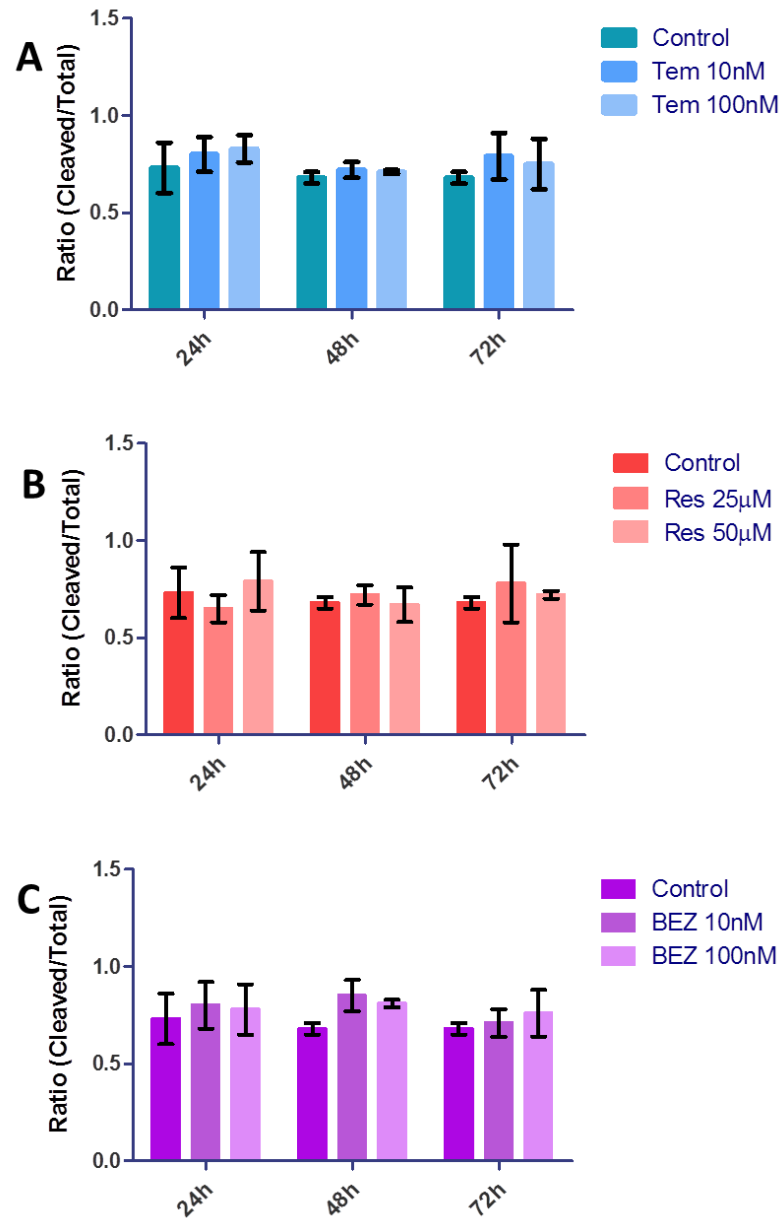


**Figure 4.12** - Western blots were performed on proteins extracted from MDAH-2774 cells treated with Tem (**A**, 10nM and 100nM), Res (**B**, 25 $\mu$ M and 50 $\mu$ M) and BEZ (**C**, 10nM and 100nM) for 24, 48 and 72 hours. Graphs show ratio of endogenous full length and cleaved large fragment caspase 9 when analysed densitometrically using ImageJ software. The F-Test was performed to assess variance and two-tailed, unpaired Student's t-tests were performed with Welch's correction for unequal variance to assess significance. Error bars depict standard deviation. No significant change in caspase 9 cleavage was detected in MDAH-2774 cells.

Cleavage of caspase 9 was detected following all treatments and time points (Figure 4.8). When analysed densitometrically, SKOV3 cells showed a trend of high caspase 9 cleavage at 24 hours, decreasing over time in each case. These changes did not reach statistical significance in comparison to controls; however, significant decreases were detected between time points in Rap 20nM ( $p=0.0069$ , 24h-72h), Rap 100nM ( $p=0.00159$ , 24h-72h), Def 1000nM ( $p=0.0496$ , 24h-48h), Res 25 $\mu$ M ( $p=0.0367$ , 24-48h and  $p=0.0353$ , 24-72h) and Res 50 $\mu$ M ( $p=0.0483$ , 24h-72h) treatments, indicating that cleavage of caspase 9 does decrease significantly over time in these cases.

#### 4.3.3.2 Caspase 3

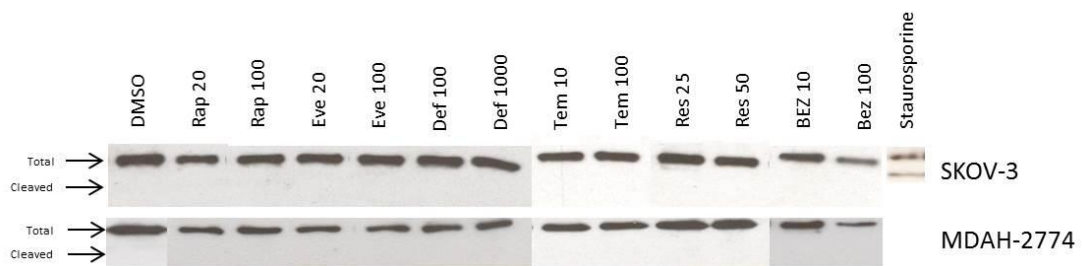


**Figure 4.13** - Western blots were performed on proteins extracted from SKOV3 and MDAH-2774 cells treated with mTOR pathway inhibitors for 24, 48 and 72 hours.

No caspase 3 cleavage was seen under any condition. SKOV3 cells were treated with staurosporine to validate the caspase 3 antibody. Representative image shows extractions after 24 hours.

The antibody recognising both cleaved and full length caspase 3 was validated by staurosporine treatment. The 19kDa cleaved fragment of caspase 3 was not detected under any condition (Figure 4.13) indicating that caspase 3 was not activated in response to mTOR pathway inhibition.

#### 4.3.3.3 p70S6 Kinase

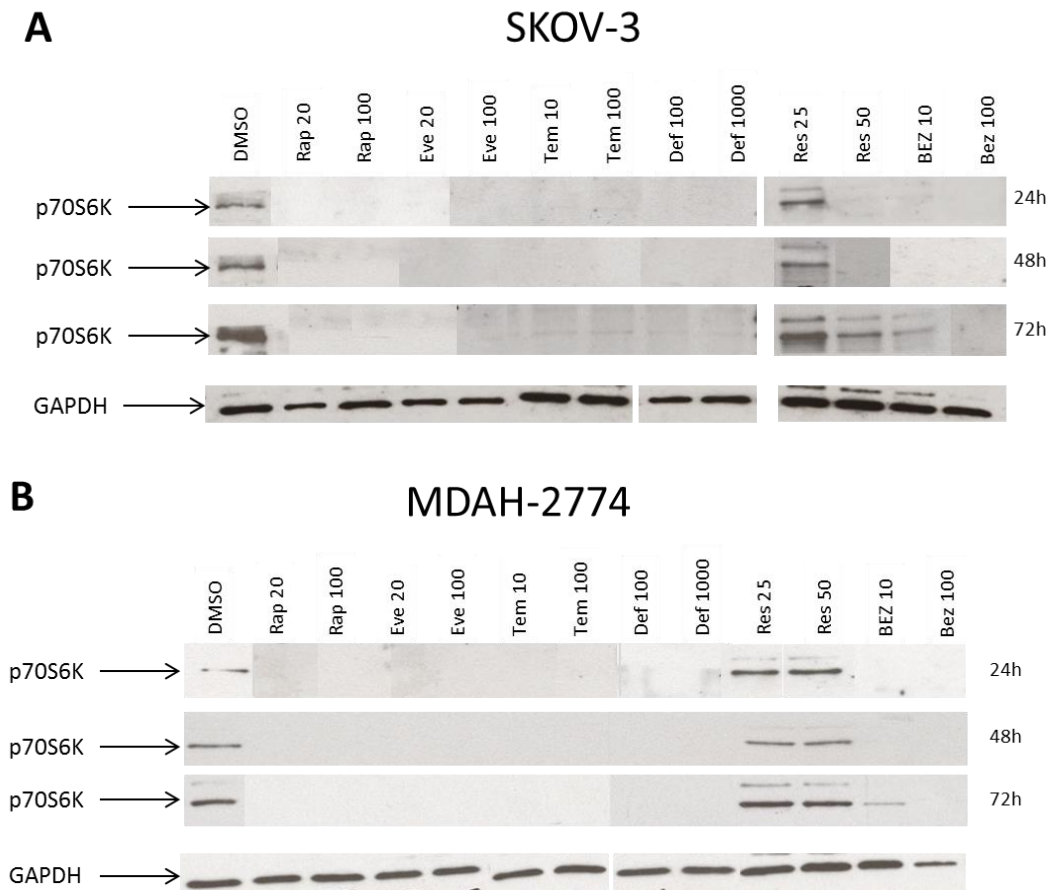


**Figure 4.14** - Western blots were performed on proteins extracted from SKOV3 (A) and MDAH-2774 (B) cells treated with mTOR pathway inhibitors for 24, 48 and 72 hours. Rap and the rapalogues completely eliminated p70S6 kinase phosphorylation in both SKOV3 and MDAH-2774 cells at 24, 48 and 72 hours. In Res treated SKOV3 cells, phosphorylated p70S6 kinase was seen at 25 $\mu$ M at all time points, at 50 $\mu$ M after 72 hours and in 10nM BEZ treated cells after 72 hours but not in 100nM BEZ treated cells. In MDAH-2774 cells, Res treatment at both 25 and 50 $\mu$ M and BEZ treatment at 10nM did not eliminate p70S6 kinase phosphorylation.

Phosphorylation status of p70S6 kinase was examined to better understand the activity of the mTOR pathway after inhibition. At 24, 48 and 72 hours, p70S6 kinase was dephosphorylated in both SKOV3 and MDAH-2774 cells treated with Rap and all of the rapalogues. In SKOV3 cells treated with Res, phosphorylation p70S6 kinase was abolished at 50 $\mu$ M concentration at 24 and 48 hours but phosphorylated p70S6 kinase was detected after 72 hours. 25 or 50 $\mu$ M Res treatment did not dephosphorylate p70S6 kinase in MDAH-2774 cells. In both



SKOV3 and MDAH-2774 cells, 100nM BEZ treatment dephosphorylated p70S6 kinase at all time points. No phosphorylated p70S6 kinase was detected after 24 and 48 hour treatment with 10nM BEZ but was detected after 72 hours in both cases (Figure 4.14).

#### 4.4 Discussion

This study investigated the effects of mTOR pathway inhibition on aspects of cellular activity using two different ovarian cancer cell lines. SKOV3 (clear cell) and MDAH-2774 (endometrioid) are models of the two types of ovarian cancer which are most associated with endometriosis (Pearce *et al.*, 2012; Brinton *et al.*, 2005; Merritt *et al.*, 2008). Using a wound healing assay we were able to show that the effects of mTOR pathway inhibition were cytostatic up to 18 hours.

When we investigated the effects of mTOR pathway inhibition up to 72 hours, we were able to show that MDAH-2774 cells have an increased proliferative capacity in comparison to SKOV3 cells under basal conditions and that mTOR pathway inhibition was less effective in these cells. Previously we have shown that mTOR and raptor are upregulated in MDAH-2774 cells in comparison to SKOV3 cells suggesting higher levels of mTORC1 signalling in this cell line (Section 4.3.2). This suggests that the effects of mTOR pathway inhibition may be diminished in cells that are more readily able to undergo mitosis. Rap and rapalogue treatment induced a non dose dependent decrease in viable cells in the SKOV3 cell line and little to no decrease in the MDAH-2774 cell line. The non dose dependent effect seen in SKOV3 cells is in agreement with previous work on Eve treatment on neuroendocrine tumour cells (Zitzmann *et al.*, 2010) and suggests that the effective concentration range of these agents might be below the concentrations used for this experiment. Res and BEZ treatment of SKOV3 cells showed a moderate dose dependency and inhibitory effects were significantly greater for these dual mTOR/PI3 kinase inhibitors than they were for sole mTOR inhibitors indicating that additionally targeting PI3 kinase increases efficacy in these cells. In the more proliferative MDAH-2774 cell line, Res treatment at 25 or 50µM or BEZ treatment at

10nM had no effect on number of viable cells; however, 100nM BEZ treatment profoundly decreased the number of viable cells to almost basal level. Previous research has shown that BEZ has a cytostatic effect and these data suggest that the concentration at which this occurs in MDAH-2774 cells is above 10nM (Montero *et al.*, 2012). In agreement with the previous chapter, the differences in responses to mTOR inhibition, particularly dual mTOR and PI3 kinase inhibition, in these cell lines highlights how individual differences can play a role in reaction to drug treatments and specifically how effective doses may change from patient to patient.

We further investigated the effects of mTOR pathway inhibition on apoptotic and mTOR pathway activity. Western blot experiments demonstrated cleavage of caspase 9 after 24 hour treatment which decreased by 48 and 72 hours in SKOV3 cells. This indicates that initial response to mTOR inhibitor treatment is to induce apoptosis but this effect is rescued by 48 hours after treatment. No pattern of change was seen in caspase 9 cleavage in MDAH-2774 cells and no caspase 3 cleavage was detected in either cell line. Caspase 9 is an initiator caspase which cleaves the pro form of caspase 3 to induce apoptosis. That caspase 9 was unaffected by treatment and no caspase 3 cleavage was detected indicates that the effect of caspase 9 cleavage was not substantial enough to induce apoptosis in these cells. Our findings are supported by proliferation assays showing no change in dead cell number over 72 hours. These data further confirm that the effects of mTOR pathway inhibition are cytostatic as opposed to cytotoxic. Previous reports which show that Rapamycin and Temsirolimus cause cell cycle arrest at G<sub>0</sub>/G<sub>1</sub> phase (Fagone *et al.*, 2013) and that rapalogue treatment is not able to induce apoptosis, including Eve treatment in SKOV3 cells (Treeck *et al.*, 2006; Avellino *et al.*, 2005; Hahn *et al.*, 2005; Beuvink *et al.*, 2005) confirm this. Evidence shows that apoptosis is inhibited by mTORC2 signalling via SGK1 (Dudek *et al.*, 1997; Peterson *et al.*, 2009; García-Martínez and Alessi, 2008) and the lack of an apoptotic effect induced by the rapalogues may be explained by their ineffective inhibition of mTORC2. It may be useful to study the effects of dual and single mTOR pathway inhibition on SGK1 and NDRG9, downstream effectors of mTORC2 involved in the control of apoptosis (García-Martínez and Alessi, 2008).

p70S6 kinase is a direct kinase target of mTORC1 signalling and modulates cellular processes such as protein and lipid synthesis (Laplane and Sabatini, 2012). Rapalogue treatment induced p70S6 kinase dephosphorylation at 24 hours, the earliest time point measured, in agreement with previous data (Koo *et al.*, 2015; Leung *et al.*, 2015; Xu *et al.*, 2015). Although treatment with Res showed a dose dependent decrease in viable cell count in SKOV3 cells and BEZ treatment inhibited proliferation in both SKOV3 and MDAH-2774 cells, phosphorylated p70S6 kinase was still detected in these cells by western blot. These data suggest that Res and BEZ may not affect the phosphorylation status of p70S6 kinase to the same extent as Rap and rapalogues and the inhibitory effects of these inhibitors may be mediated through alternative pathways.

The non-apoptotic effects of the mTOR pathway inhibitors used in this study may exclude them from being effective single agent therapies in the treatment of malignancy. However, it has been shown that rapalogue treatment is able to potentiate the apoptotic effects of Tamoxifen, Doxorubicin, UCN-01 and Cisplatin treatment *in vitro*, indicating that mTOR pathway inhibitors may be useful in combinatorial therapeutic approaches to cancer treatment (Treeck *et al.*, 2006; Avellino *et al.*, 2005; Hahn *et al.*, 2005; Beuvink *et al.*, 2005). A mechanism by which mTOR pathway inhibition enhances apoptosis whilst not inducing it as a single agent treatment has been described by Beuvink *et al.*. The authors have shown Eve is a potent inhibitor of p21 protein expression, a protein that is activated by p53 and causes cell cycle arrest and DNA damage repair. A reduction in p21 reduces cell cycle arrest and the potential for DNA damage repair therefore initiating apoptosis in response to DNA damage (Beuvink *et al.*, 2005). It would be interesting to further elucidate the effects that mTOR pathway inhibitors have in both p53-null and wild type p53 cell lines to fully understand the mechanisms by which mTOR pathway inhibition enhances apoptosis whilst not inducing it. Interestingly, Beuvink *et al.*, also showed that Eve treatment was able to enhance the effects of Cisplatin when at concentrations that would usually not induce a decrease in cell viability, indicating that using mTOR pathway inhibitors may allow for lower doses of cytotoxic chemotherapeutic agents in cancer treatment and

therefore a reduction in the harmful side-effects brought about by these drugs (Beuvink *et al.*, 2005).

Inhibiting mTOR and PI3 kinase in parallel proved to be more effective at reducing viable cell number in SKOV3 but not MDAH-2774 cells. This may be due to a negative feedback loop directed to PI3 kinase that is relieved on mTORC1 inhibition and can induce PI3 kinase signalling via Akt to cause an upregulation in mTORC2 signalling (Peterson *et al.*, 2009). Dual mTOR and PI3 kinase, or mTORC1 and mTORC2 inhibitors are able to target both mTORC1 signalling and the aftereffect mTORC2 signalling and therefore induce more effective repression of the mTOR pathway (Zitzmann *et al.*, 2010; Hisamatsu *et al.*, 2013). Both SKOV3 and MDAH-2774 cells carry mutation of the *PIK3CA* gene encoding the catalytic subunit of PI3 kinase; however, only MDAH-2774 cells have *KRAS* and *BRAF* mutations (Beaufort *et al.*, 2014; Nakayama *et al.*, 2008). *KRAS* and *BRAF* are part of the MAP kinase signalling pathway which has been shown to regulate the mTOR pathway by inhibiting the TSC1/TSC2 complex (Ma and Blenis, 2009). Everolimus has been shown to activate the MAP kinase pathway in breast and colon cancer and melanoma, and cell lines with *KRAS* and *BRAF* mutation are particularly susceptible to the growth inhibitory effects of MAP kinase inhibition (Carracedo and Pandolfi, 2008; Nakayama *et al.*, 2008). This additional activation of the mTOR pathway in MDAH-2774 cells which would not be affected by PI3 kinase inhibition by Res or BEZ may contribute to the increased proliferative capacity and decreased response to dual inhibitors seen in these cells. In support of this, inhibition of both the MAP kinase and PI3 kinase pathways proved to be more effective than targeting solely PI3 kinase in neuroendocrine tumour cell lines (Zitzmann *et al.*, 2010).

mTORC2 was previously thought to be Rap insensitive but a more recent study has shown that inhibition of mTOR by Rap may remove it as a component of both mTORC1 and mTORC2 and so longer term treatment with Rap interrupts mTORC2 assembly. mTORC2 inhibition was shown with 100nM Rap treatment after 24 hours (Sarbasov *et al.*, 2006). In this study, SKOV3 and MDAH-2774 cells were treated with 20 and 100nM Rap for up to 72 hours. According to previous research, which

showed a partial reduction in the mTOR association with rictor after 24 hour treatment with 100nM Rap, the higher concentration of Rap used in this study would have inhibited mTORC2 activity, at least in part. mTORC2 is known to suppress apoptosis (Dudek *et al.*, 1997; Peterson *et al.*, 2009; García-Martínez and Alessi, 2008); however, no dose dependent apoptotic or proliferative effect was detected following Rap treatment of SKOV3 or MDAH-2774 cells, indicating that, if present, mTORC2 inhibition is not affecting these mechanisms. mTORC2 signalling via Akt is known to play a role in cell survival (Jacinto *et al.*, 2006) and so it would be interesting to further elucidate the effects of all the rapalogues used in this study on mTOR and rictor association and activation of the mTORC2 signalling pathway.

The survival rate for ovarian cancer is uncharacteristically low and advances in ovarian cancer therapeutics have not kept pace with other cancer types. mTOR pathway inhibition presents an as yet unexploited treatment method for ovarian cancer. In agreement with the previous chapter, mTOR pathway inhibition shows differential effects in SKOV3 and MDAH-2774 cells, highlighting the need for tumour specific therapies. Dual mTOR and PI3 kinase inhibition proved to be more effective than mTOR inhibition alone and further inhibition of the MAP kinase pathway in addition to effective mTORC2 downregulation may prove to be the key to effective mTOR pathway inhibition that has thus far remained elusive.

## ***Chapter 5***

### ***Mapping of mTOR, DEPTOR, rictor, raptor and p70S6 kinase at gene and protein level in ovarian cancer clinical samples***

#### **5.1 Introduction**

Ovarian cancer, most often epithelial in origin (CRUK, 2014b), is the fifth most common cancer to affect women in the UK and the most common cause of death by gynaecological cancer, proving fatal for around 4300 women in 2012 (CRUK, 2015g). Ovarian cancer can be difficult to diagnose because symptoms are often mild or ambiguous and it is often not identified until it has progressed into the more advanced stages, at which chemotherapeutic treatment is less effective (Buys *et al.*, 2011). There is currently no reliable biomarker for ovarian cancer and no general population screening programme available on the NHS.

Ovarian cancer has an increased incidence in patients with endometriosis (Stewart *et al.*, 2013; Pearce *et al.*, 2012; Wu *et al.*, 2009; Merritt *et al.*, 2008; Borgfeldt and Andolf, 2004; Brinton *et al.*, 2005; Brinton *et al.*, 2004) that has not been seen in other gynaecological conditions such as pelvic inflammatory disease, borderline ovarian cancers, fibroids and ovarian cysts (Stewart *et al.*, 2013; Pearce *et al.*, 2012; Brinton *et al.*, 2005; Borgfeldt and Andolf, 2004). It is particularly associated with risk of clear cell and endometrioid ovarian cancers (Pearce *et al.*, 2012; Brinton *et al.*, 2005; Merritt *et al.*, 2008; Rossing *et al.*, 2008). Endometriosis is a non-malignant condition characterised by the explantation and growth of extraneous endometrium in areas such as the ovaries, fallopian tubes, vagina, peritoneum and bladder. Endometriosis is estimated to affect around 2 million women in the UK (NHS Choices, 2015) causing dysmenorrhoea, dyspareunia, dysuria, dyschezia, infertility and chronic pelvic pain.

The mTOR pathway, a central regulator of growth and proliferation, has been shown to play a role in both ovarian cancer and endometriosis (Leconte *et al.*, 2011; Mabuchi, Deborah A Altomare, *et al.*, 2007). However, the deregulations of this pathway in both conditions are currently poorly categorised. Due to the unique relationship between endometriosis and ovarian cancer, we hypothesised that mTOR components may be implicated in the pathogenesis of ovarian cancer and endometriosis.

## 5.2 Objectives

-To elucidate the most stable reference gene(s) for use in qPCR for a set of ovarian tissue sample cDNAs using a geNorm™ 12 gene kit (Primerdesign) in order to achieve accurate qPCR normalisation.

-To assess gene expression of mTOR, DEPTOR, rictor and raptor in a range of ovarian tissue samples from patients with ovarian cancer, endometriosis, endometrial cancer, fibroids and control patients with no known gynaecological conditions.

-To compare gene expression of mTOR components and survival using *in silico* analyses of mRNA expression.

-To elucidate the expression of mTOR, DEPTOR, rictor, raptor and phosphorylated p70S6 kinase in different stages, grades and pathologies of ovarian cancer at protein level.

## 5.3 Results

Clinical samples were obtained from the University of Thessaloniki (Table 5.1, detailed in 2.5.1); ethical approval was obtained by the local hospital authority and by Brunel University ethics committee. Tissue samples were homogenised and RNA

extracted using the GenElute™ Mammalian Total RNA MiniPrep Kit (Sigma Aldrich) as previously described in 2.6.1.1. cDNA was synthesised using the SuperScript® II Reverse Transcriptase kit (Life Technologies, described in 2.7.1).

Pathology	Number
Control	34
Endometriosis	24
Ovarian Cancer	13
Fibroids	4
Endometrial Cancer	4

**Table 5.1** - A summary of the pathologies and numbers pertaining to the clinical tissue samples used in this study.

### 5.3.1 Analysis of reference gene stability in ovarian clinical tissue samples using the geNorm™ 12 gene kit

Commonly used reference genes for qPCR experiments can lack the expressional stability that they were once thought to have (Gutierrez *et al.*, 2008). A reference gene's stability is cell type and context dependent; it cannot be taken for granted that interpatient variability will not affect expression. It is becoming more widely accepted that an explorative test should be carried out for each set of samples to determine a suitable reference gene in each case (Bustin *et al.*, 2009; Jacob *et al.*, 2013). According to MIQE (Minimum Information for the Publication of Quantitative Real-Time qPCR) guidelines, reference gene expression should be stably and strongly correlated with total mRNA expression. As ovarian cancer is a highly heterogeneous disease, it is particularly prudent to assess reference gene stability in ovarian tumour tissue samples. geNorm™ (Primerdesign) is a commercially available assessment kit for suitable reference genes within a sample set. The geNorm™ human 12 gene kit assesses twelve different human reference genes for average expression stability and the optimum number of reference genes to use in qPCR experiments for each set of samples.



Eight clinical samples were selected to represent the whole cohort and were tested in triplicate using the geNorm™ 12 gene kit (Primerdesign). An equal number of samples were used from each group to eliminate bias towards any variable. The kit contains primers for *ATB5P*, *SDHA*, *B2M*, *UBC*, *ACTB*, *18S RNA*, *GAPDH*, *TOP1*, *CYC1*, *EIF4A2*, *YWHAZ* and *RPL13A* (detailed in Section 2.9). 2X PrecisionPlus™ qPCR MasterMix (Primerdesign) was used on a 7900HT Fast thermal cycler (Life Technologies, described in Section 2.9). cDNA was used at a concentration of 5ng/μL as per manufacturer’s instruction. qPCR results were analysed using qBase+ software (Biogazelle).

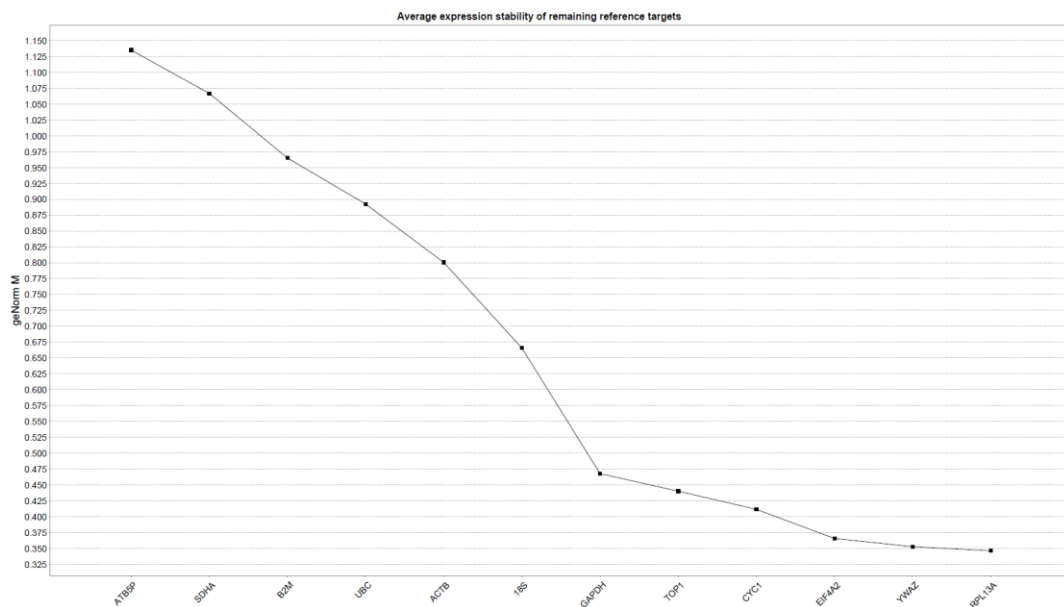


**Figure 5.1** - 12 genes from the geNorm™ 12 gene kit (Primerdesign) were assessed for expressional stability in a selection of cDNAs from clinical samples representing the whole cohort. Data were analysed with qBase+ software (Biogazelle). qBase+ provides a geNorm™ M value representing expressional stability; a low M value indicates greater expressional stability. The graph shows genes in order of least stable to most stable (left to right). The most stable genes were RPL13A and YWHAZ.

geNorm™ M value (Figure 5.1) represents average gene expression stability within the samples tested. A lower M value confers greater stability. The genes are arranged on the graph in order of stability, the least stable being on the left and the most stable on the right.

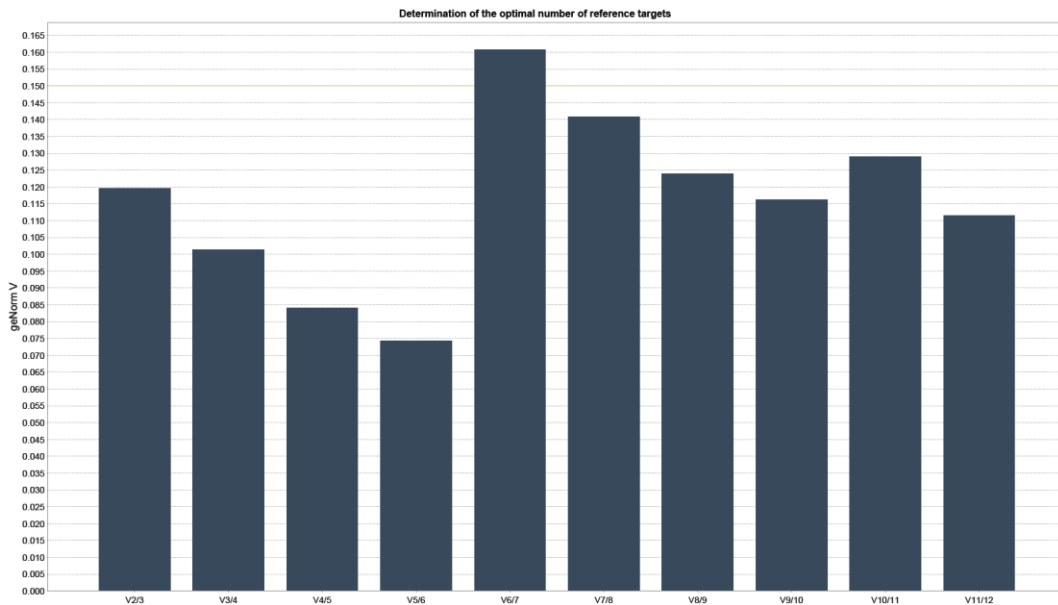


**Figure 5.2** - 12 genes from the geNorm™ 12 gene kit (Primerdesign) were assessed for expressional stability in a selection of cDNAs from clinical samples representing the whole cohort. Data were analysed with qBase+ software (Biogazelle). qBase+ provides a geNorm™ V graph showing cumulative variability of successive genes indicating how many must be used in each qPCR experiment for optimum normalisation. Working from left to right, the first column to achieve a value below 0.15 represents the optimum number of reference genes to use with these samples. In this case, 2-3 reference genes is acceptable.

The geNorm™ V graph (Figure 5.2) shows the optimal number of reference genes to use for the samples tested, measured by the average variation in stability between each successive gene. A V value of less than 0.15 is considered acceptable (Primerdesign, 2014). The first column on the graph shows the V value of the three most stably expressed genes (RPL13A, YWHAZ and EIF4A2). Each additional column to the right shows the V value of the previous column plus the next stable gene. The first column to achieve a value below 0.15 shows the optimum number of reference genes to use. In this case, qBase+ recommends two to three reference genes (MIQE guidelines suggest that *at least* two reference genes are used). In this case, the two most stable genes are *RPL13A* (ribosomal protein L13A; a gene that encodes a component of the 60S ribosomal subunit) and *YWHAZ* (a gene that encodes a 14-3-3 signal transduction protein). Going forward, these reference genes will be used in qPCR experiments involving these clinical samples as they have been proven stable enough to provide robust normalisation.

### 5.3.2 Gene expression analysis of mTOR, DEPTOR, rictor and raptor in ovarian tissue clinical samples from patients with ovarian cancer, endometrial cancer, endometriosis and fibroids

We first sought to assess the gene expression of mTOR pathway components in ovarian tumour tissue samples. qPCR was performed in triplicate on the ovarian cDNAs for mTOR, DEPTOR, rictor and raptor using the reference genes *RPL13A* and *YWHAZ*. Power SYBR® Master Mix (Life Technologies) was used on a 7900HT Fast thermal cycler (Life Technologies, described in 2.10.3).

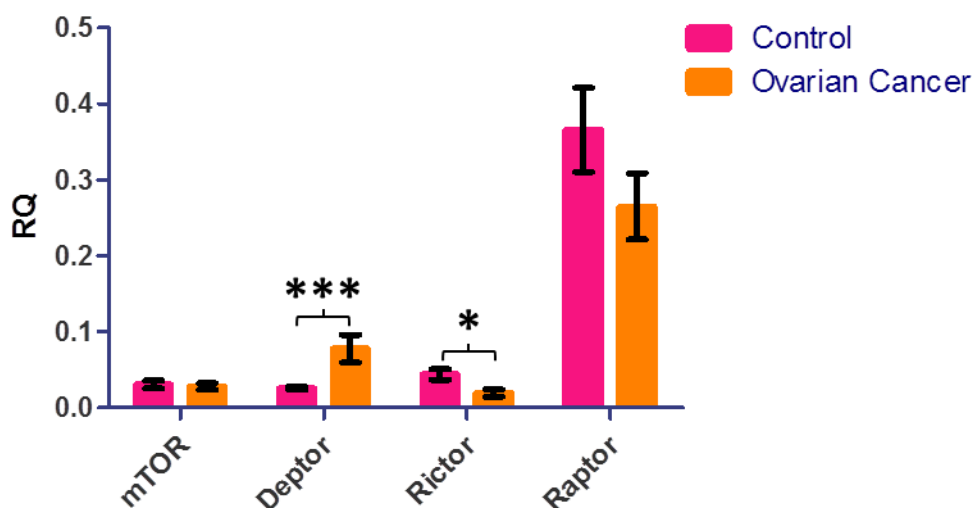


**Figure 5.3** - qPCR for mTOR, DEPTOR, rictor and raptor was carried out using the reference genes *RPL13A* and *YWHAZ* in triplicate on cDNA synthesised from the extracted RNA from ovarian tissue of ovarian cancer patients and non-affected controls. Data were analysed using the  $\Delta C_q$  method and an RQ value calculated by  $2^{-\Delta C_q}$ . An F-test was performed to assess variance between groups and two-tailed, unpaired Student's t-tests were performed to assess significance. Error bars depict standard error and asterisks denote significance. Results show a significant increase in DEPTOR expression ( $p=0.0007$ ) and a significant decrease in rictor expression ( $p=0.0388$ ) in comparison to control.

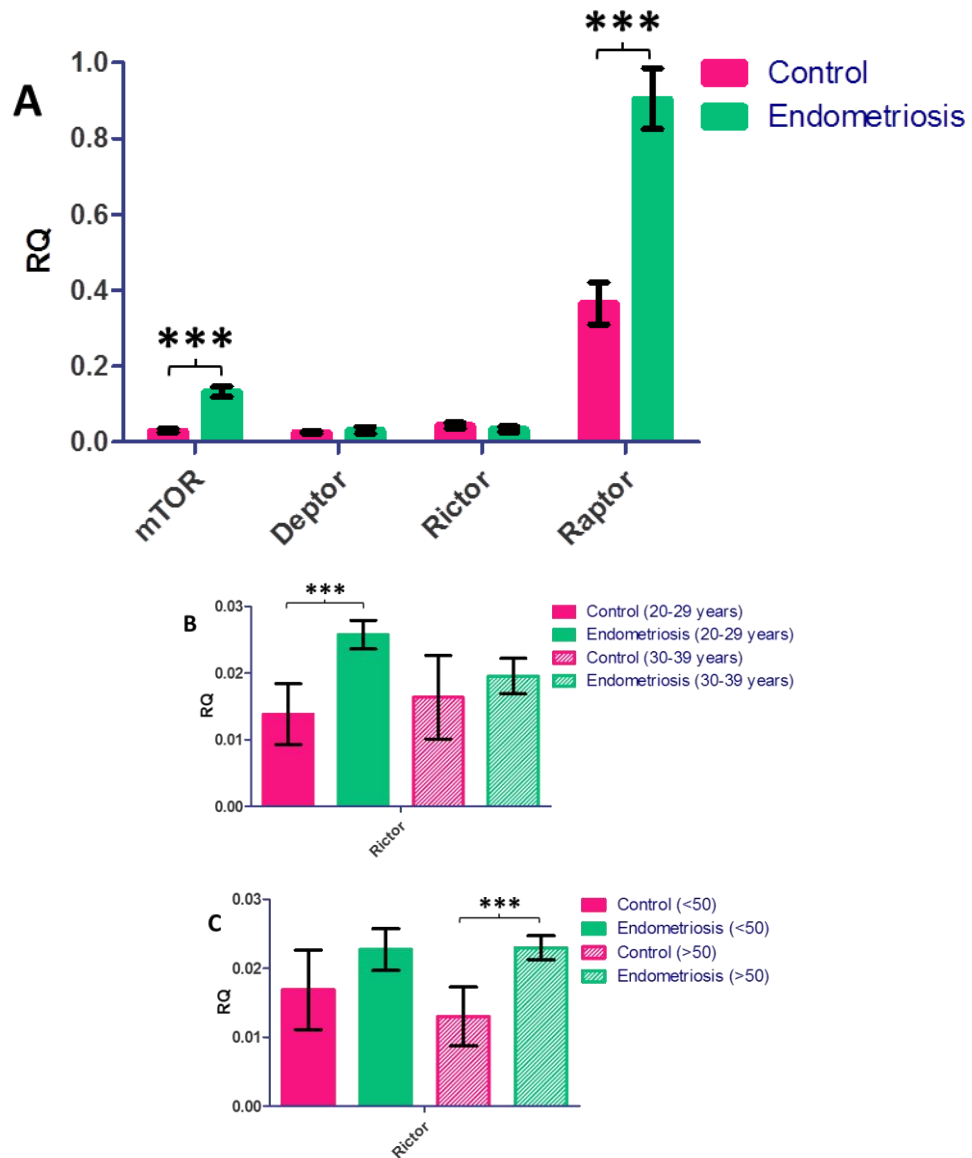


**Figure 5.4** - qPCR for *mTOR*, *DEPTOR*, *rictor* and *raptor* was carried out using the reference genes *RPL13A* and *YWHAZ* in triplicate on cDNA synthesised from the extracted RNA from ovarian tissue of Endometriosis patients and non-affected controls. Data were analysed using the  $\Delta C_q$  method and an RQ value calculated by  $2^{-\Delta C_q}$ . An F-test was performed to assess variance between groups and two-tailed, unpaired Student's t-tests were performed to assess significance. Error bars depict standard error and asterisks denote significance. *mTOR* and *raptor* showed a significant increase in expression (**A**,  $p < 0.0001$  for both groups). *Rictor* showed no significant change over all but when segregated by age of patient (20-29 years and 30-39 years) and grade points (below 50 and above 50) significant changes were seen. *Rictor* showed a significant increase in patients aged 20-29 years ( $p = 0.0004$ ) but not in patients aged 30-39 years (**B**). There was also a significant increase in *rictor* expression in patients with disease grade points above 50 ( $p = 0.0004$ ) but not in those with a disease grade below 50 (**C**).

Differing patterns of expressional change were seen between ovarian cancer and endometriosis. Ovarian cancer showed an increase in DEPTOR expression ( $p=0.0007$ ) and a decrease in rictor expression ( $p=0.0388$ ). Raptor expression was higher than that of mTOR, DEPTOR or rictor but there was no significant change between control and affected patients (Figure 5.3). Endometriosis showed an increase in both mTOR and raptor expression ( $p<0.0001$  in both cases) with raptor again showing greater expression levels than all other components studied (Figure 5.4, A). In the case of endometriosis, no change in rictor was seen over all. However, when patients were separated based on their age or prescribed disease grade, a significant change was seen in younger patients (20-29 years compared to 30-39 years,  $p=0.0004$ , Figure 5.4, B) and patients with a more severe disease ( $>50$  compared to  $<50$ ,  $p=0.0004$ , Figure 5.4, C). Similar comparisons were made of mTOR, DEPTOR and raptor but no change was seen in relation to age and disease grade score.

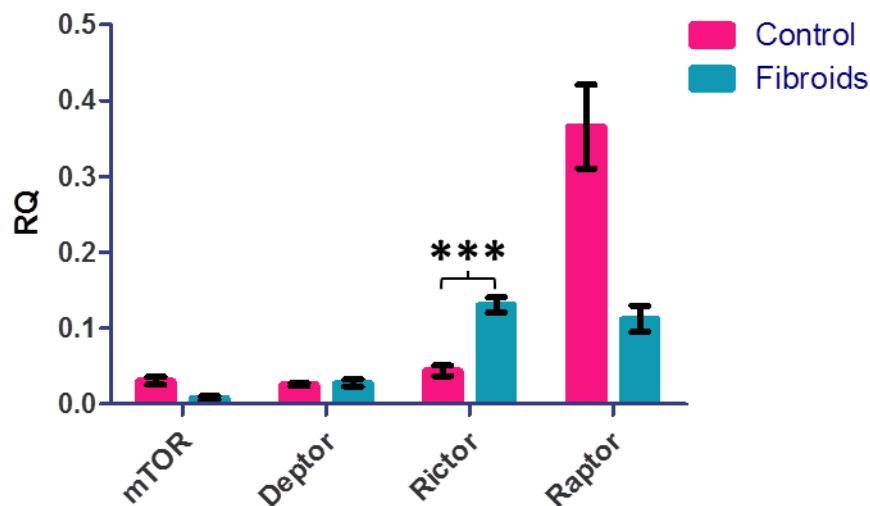


**Figure 5.5** - qPCR for mTOR, DEPTOR, rictor and raptor was carried out using the reference genes RPL13A and YWHAZ in triplicate on cDNA synthesised from the extracted RNA from ovarian tissue of Fibroids patients and non-affected controls. Data were analysed using the  $\Delta C_q$  method and an RQ value calculated by  $2^{-\Delta C_q}$ . An F- test was performed to assess variance between groups and two-tailed, unpaired Student's t-tests were performed to assess significance. Error bars depict standard error and asterisks denote significance. Rictor showed a significant increase in expression in comparison to the control ( $p=0.0002$ ).

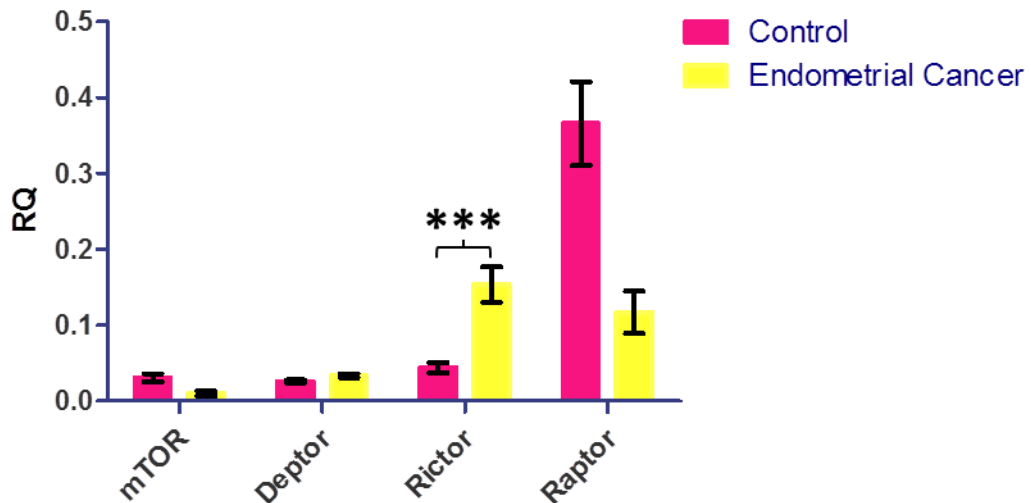


**Figure 5.6** - qPCR for mTOR, DEPTOR, rictor and raptor was carried out using the reference genes RPL13A and YWHAZ in triplicate on cDNA synthesised from the extracted RNA from ovarian tissue of Endometrial Cancer patients and non-affected controls. Data were analysed using the  $\Delta C_q$  method and an RQ value calculated by  $2^{-\Delta C_q}$ . An F-test was performed to assess variance between groups and two-tailed, unpaired Student's t-tests were performed to assess significance. Error bars depict standard error and asterisks denote significance. Rictor showed a significant increase in expression in comparison to the control ( $p < 0.0001$ ).

Fibroids and Endometrial cancer showed very similar expression profiles for mTOR, DEPTOR, rictor and raptor. The only component they both showed a significant change in was an increase in rictor compared to control ( $p = 0.0002$  and  $< 0.0001$  respectively). In both cases, a marked reduction in raptor can be seen but these results did not reach statistical significance (Figures 5.5 and 5.6).

### 5.3.3 *In silico* analysis of mTOR pathway component gene expression levels in normal and ovarian cancer patients

In order to assess mTOR pathway component gene expression in a large cohort of patients, we utilised the *in silico* analysis method Oncomine™. Oncomine™ (oncomine.org) is an online resource combining large DNA microarray datasets (Rhodes *et al.*, 2004). We used Oncomine™ to perform 'Cancer vs. Normal' analysis in datasets with greater than 50 samples. mTOR, DEPTOR and raptor expression was analysed but due to low sample size, rictor data was not suitable for analysis.

### 5.3.3.1 mTOR

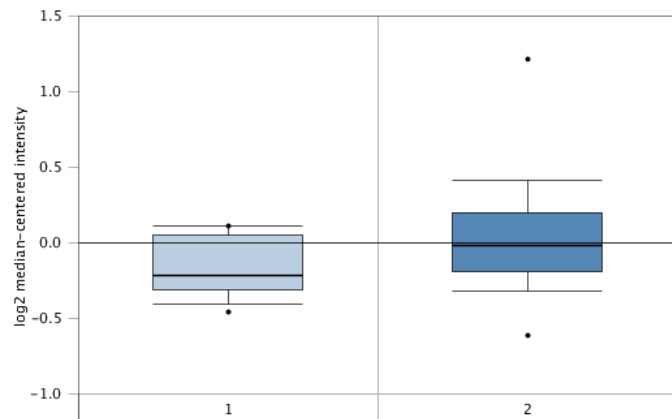


**Figure 5.7** - mTOR gene expression data from the Bonome et al., dataset plotted by Oncomine showing the mean mTOR gene expression in control ovarian surface epithelium (1, n=10) and ovarian carcinoma (2, n=185). Boxes represent the 25th-75th percentile (with median line), bars show the 10th-90th percentile and dots show the complete spread of data. A 1.166 fold increase in mTOR expression was seen ( $p=0.002$ ) (Bonome et al., 2008).

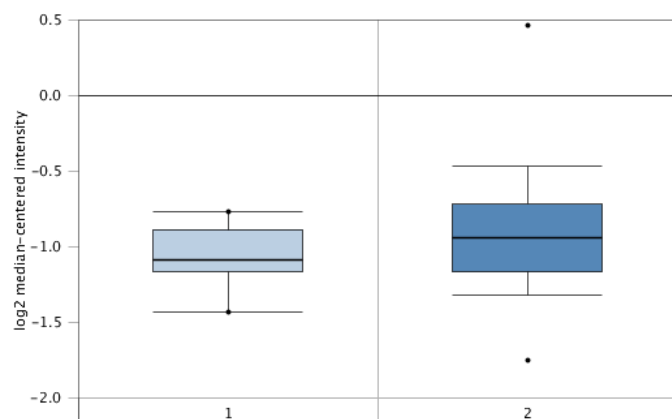


**Figure 5.8** - mTOR gene expression data from the TCGA dataset plotted by Oncomine showing the mean mTOR gene expression in control ovary (1, n=8) and ovarian serous cystadenocarcinoma (2, n=586). Boxes represent the 25th-75th percentile (with median line), bars show the 10th-90th percentile and dots show the complete spread of data. A 1.122 fold increase in mTOR expression was seen ( $p=0.034$ ) (The Cancer Genome Atlas, 2015).

Oncomine analysis supports the mTOR gene expression data in this study. A small increase in mTOR expression was seen in ovarian cancer in comparison to controls (Figure 5.7, 1.166 fold increase,  $p=0.002$  and Figure 5.8, 1.122 fold increase,  $p=0.034$ )

### 5.3.3.2 DEPTOR

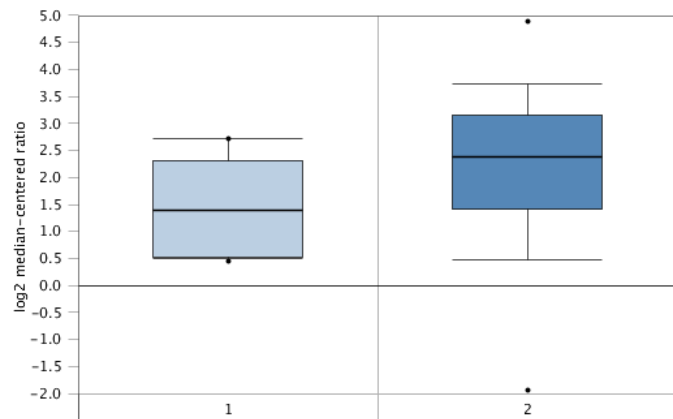


**Figure 5.9** - DEPTOR gene expression data from the Yoshihara et al., dataset plotted by OncoPrint showing the mean DEPTOR gene expression in control peritoneum (1, n=10) and ovarian serous adenocarcinoma (2, n=43). Boxes represent the 25th-75th percentile (with median line), bars show the 10th-90th percentile and dots show the complete spread of data. A 1.683 fold increase in DEPTOR expression was seen ( $p=0.019$ ) (Yoshihara et al., 2009).

OncoPrint analysis supports the DEPTOR gene expression data in this study. A significant increase in DEPTOR expression in comparison to control (Figure 5.9, 1.683 fold increase,  $p=0.019$ ).

### 5.3.3.3 Raptor

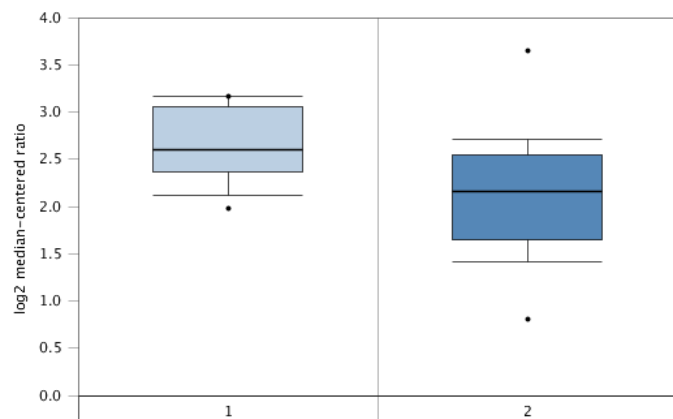


**Figure 5.10** - Raptor gene expression data from the Yoshihara et al., dataset plotted by OncoPrint showing the mean raptor gene expression in control peritoneum (1, n=10) and ovarian serous adenocarcinoma (2, n=43). Boxes represent the 25th-75th percentile (with median line), bars show the 10th-90th percentile and dots show the complete spread of data. A non-significant 1.410 fold decrease in raptor expression was seen ( $p=0.998$ ) (Yoshihara et al., 2009).



In concurrence with the data in this study, a non-significant decrease in raptor expression was seen in ovarian cancer in comparison to control (Figure 5.10, 1.410 fold decrease,  $p=0.998$ ).

#### **5.3.4 Protein expression analysis of mTOR, DEPTOR, rictor, raptor and p70S6 kinase in paraffin embedded ovarian tissue clinical samples from patients with malignant cancer**

We next sought to evaluate protein expression of mTOR pathway components in different stages, grades and types of ovarian cancer. Tissue arrays (detailed in Section 2.5.2) were probed for mTOR, DEPTOR, rictor, raptor and phosphorylated p70S6 kinase by immunohistochemistry using the DAB method as described previously (Section 2.13). Three areas of each tissue sample were selected at random and total cells and total positive cells were counted in each area. An average percentage of positive cells was calculated.

#### 5.3.4.1 mTOR

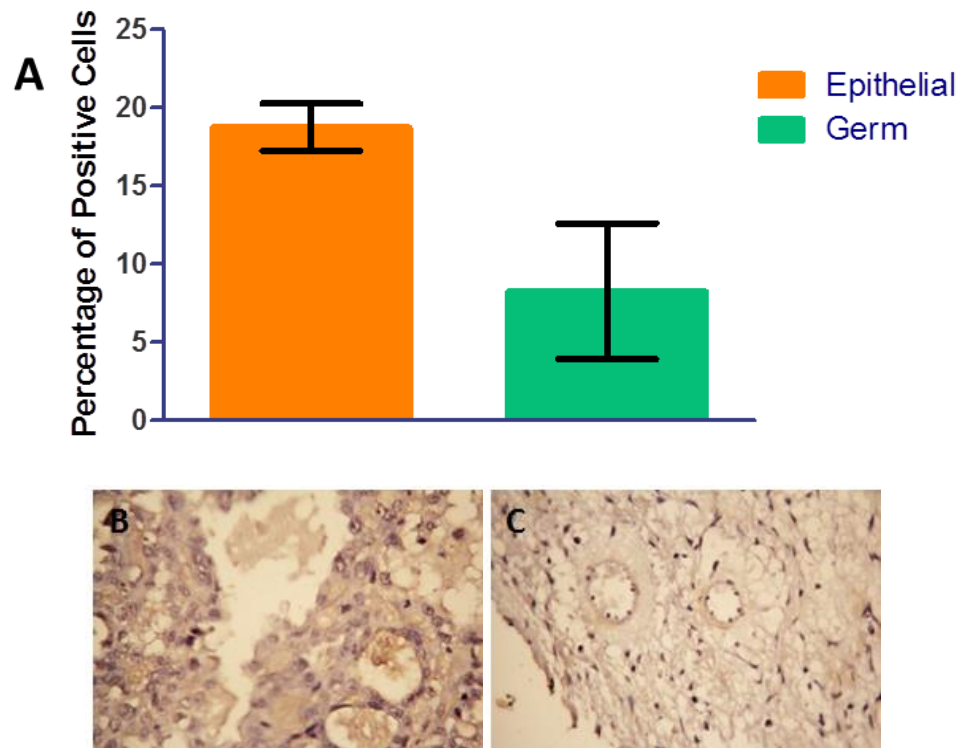


**Figure 5.11** - Immunohistochemistry for mTOR was performed on paraffin embedded ovarian tissue clinical samples from epithelial and germ cell ovarian tumours. F-Tests were performed to assess variance and unpaired, two-tailed Student's t-tests with Welch's correction for unequal variance used to assess significance. Error bars depict standard error. No significant change was detected between epithelial and germ cell tumours (A). B and C show representative images of clear cell carcinoma (epithelial) and dysgerminoma (germ) respectively.

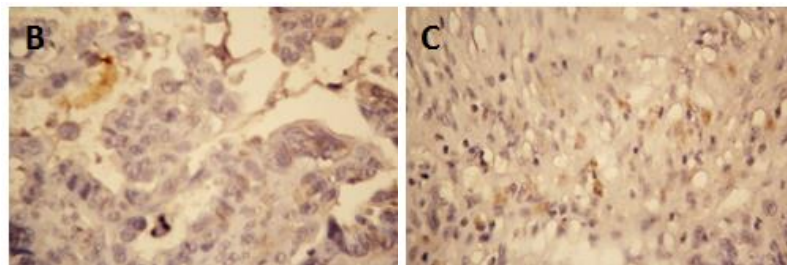
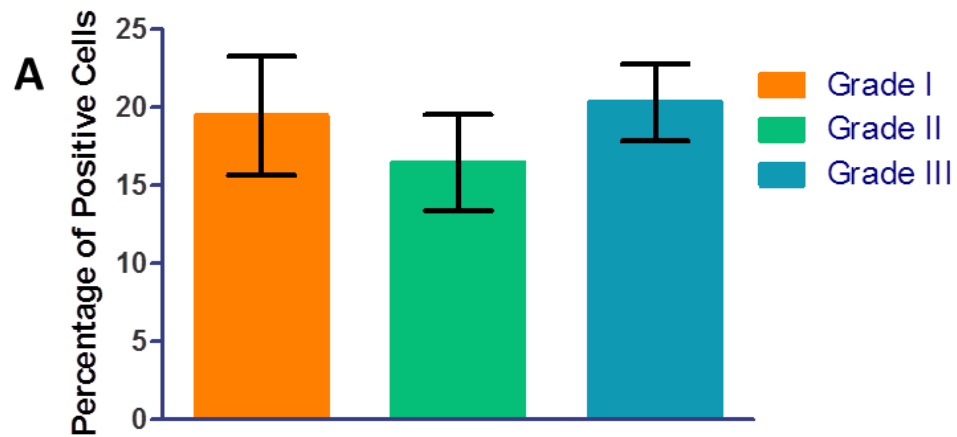


**Figure 5.12** - Immunohistochemistry for mTOR was performed on paraffin embedded ovarian tissue clinical samples from grade I, grade II and grade III ovarian tumours. F-Tests were performed to assess variance and unpaired, two-tailed Student's t-tests with Welch's correction for unequal variance used to assess significance. Error bars depict standard error. No significant change was detected between grade of tumour (A). B and C show representative images of grade II and grade III serous papillary carcinoma respectively.

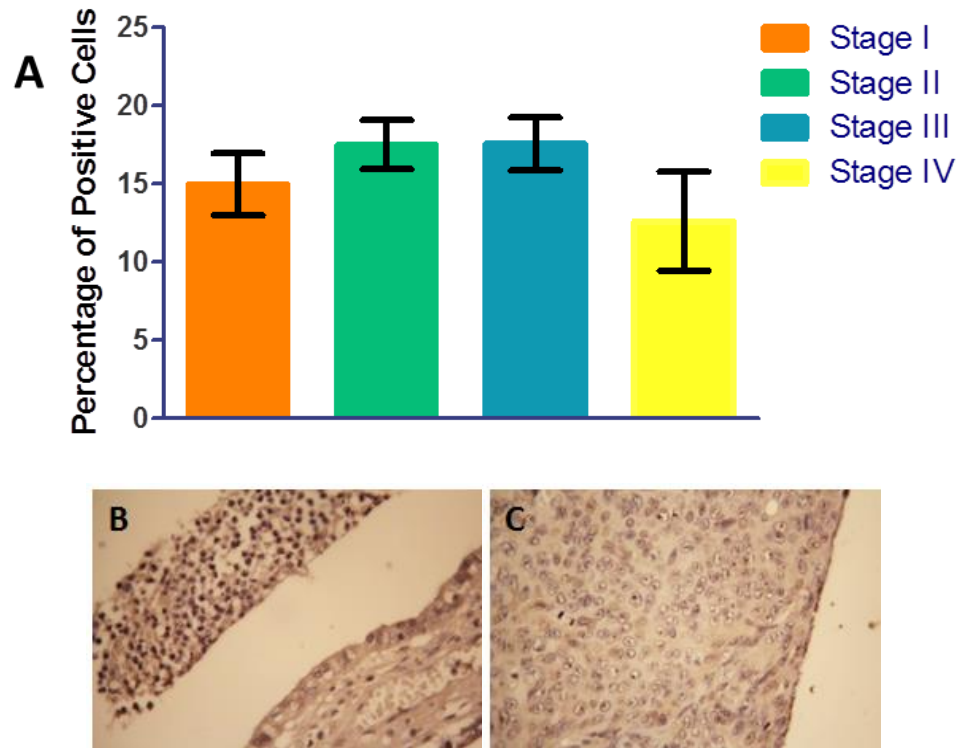


**Figure 5.13** - Immunohistochemistry for mTOR was performed on paraffin embedded ovarian tissue clinical samples from stage I, stage II, stage III and stage IV ovarian tumours. F-Tests were performed to assess variance and unpaired, two-tailed Student's t-tests with Welch's correction for unequal variance used to assess significance. Error bars depict standard error. No significant change was detected between stage of disease (A). B and C show representative images of stage I and stage IV serous papillary carcinoma respectively.

#### 5.3.4.2 DEPTOR

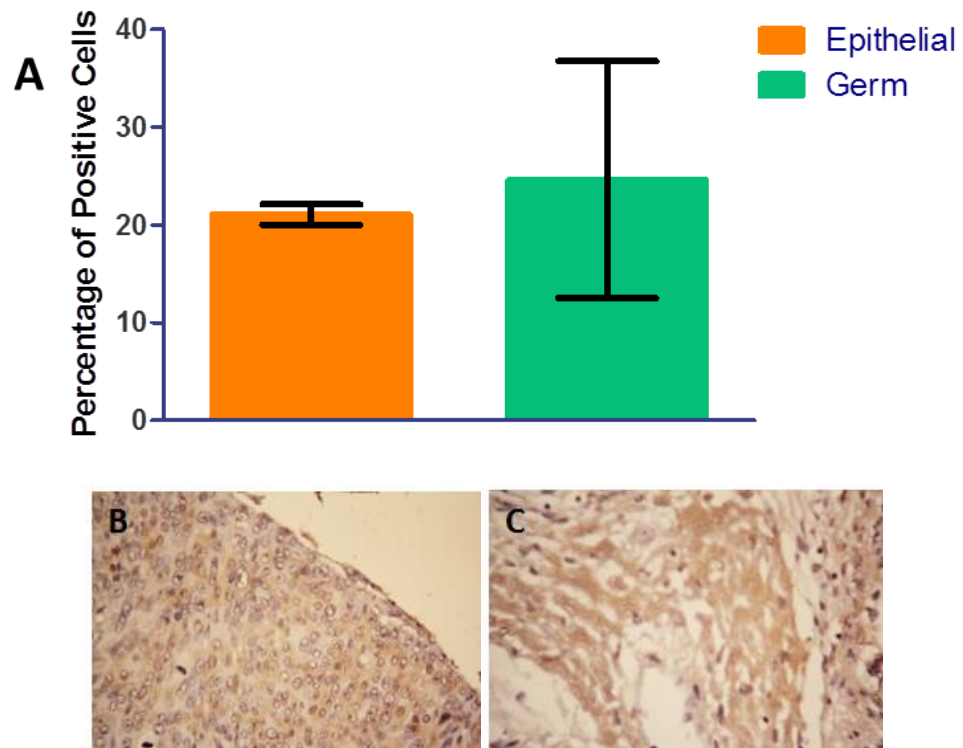


**Figure 5.14** - Immunohistochemistry for DEPTOR was performed on paraffin embedded ovarian tissue clinical samples from epithelial and germ cell ovarian tumours. F-Tests were performed to assess variance and unpaired, two-tailed Student's t-tests with Welch's correction for unequal variance used to assess significance. Error bars depict standard error. No significant change was seen between epithelial and germ cell tumours (A). B and C show representative images of serous papillary carcinoma (epithelial) and teratoma (germ) respectively.

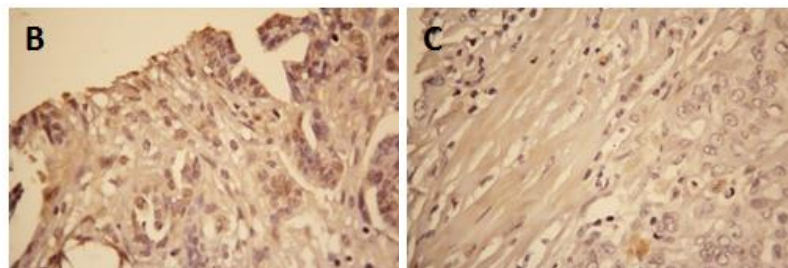
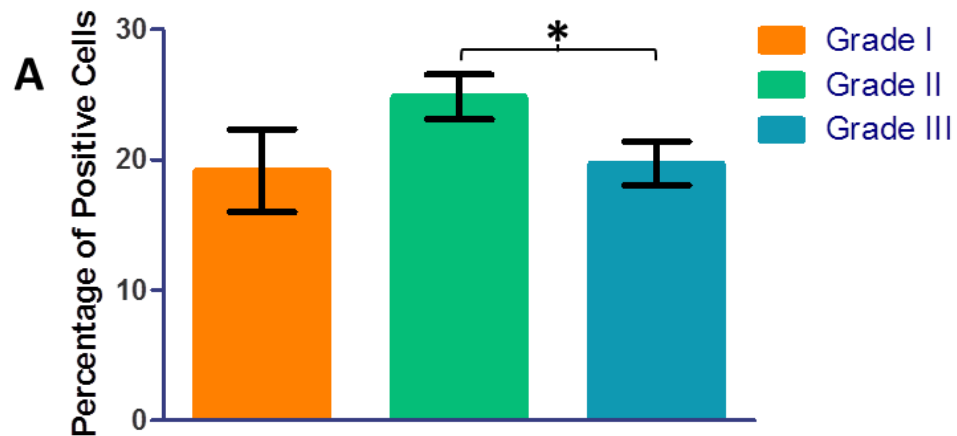


**Figure 5.15** - Immunohistochemistry for DEPTOR was performed on paraffin embedded ovarian tissue clinical samples from grade I, grade II and grade III ovarian tumours. F-Tests were performed to assess variance and unpaired, two-tailed Student's t-tests with Welch's correction for unequal variance used to assess significance. Error bars depict standard error. A significant decrease was seen between grade II and grade III (A). B and C show representative images of grade II and grade III serous papillary carcinoma respectively.

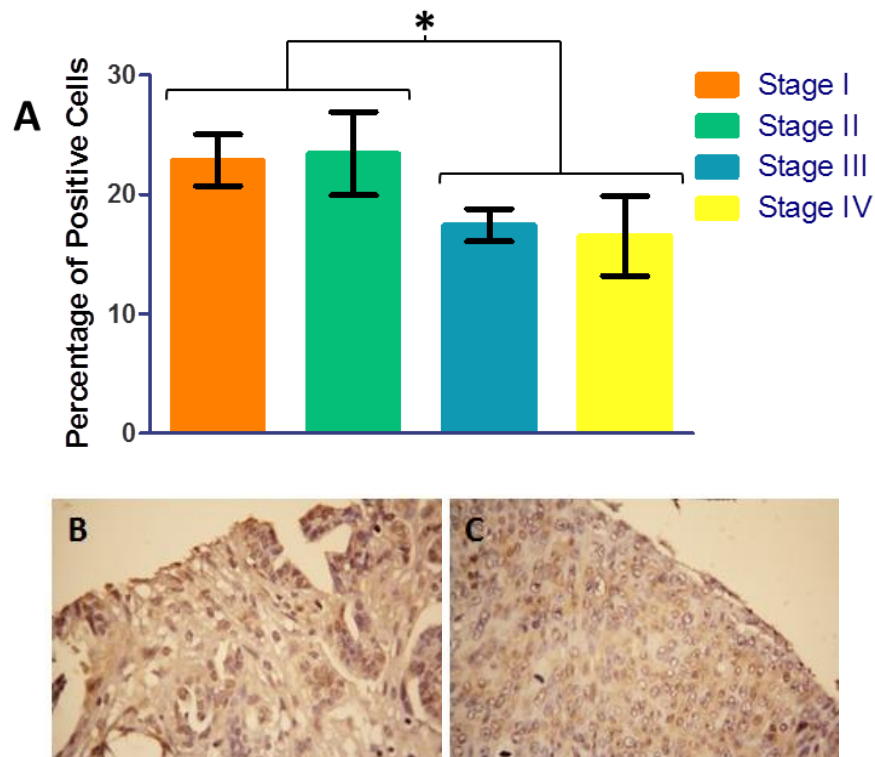


**Figure 5.16** - Immunohistochemistry for DEPTOR was performed on paraffin embedded ovarian tissue clinical samples from stage I, stage II, stage III and stage IV ovarian tumours. F-Tests were performed to assess variance and unpaired, two-tailed Student's t-tests with Welch's correction for unequal variance used to assess significance. Error bars depict standard error. No significant change was seen between individual stage of disease; however a significant difference was detected between early stage and late stage disease ( $p=0.0109$ , **A**). **B** and **C** show representative images of stage I and stage IV serous papillary carcinoma respectively.

#### 5.3.4.3 Rictor

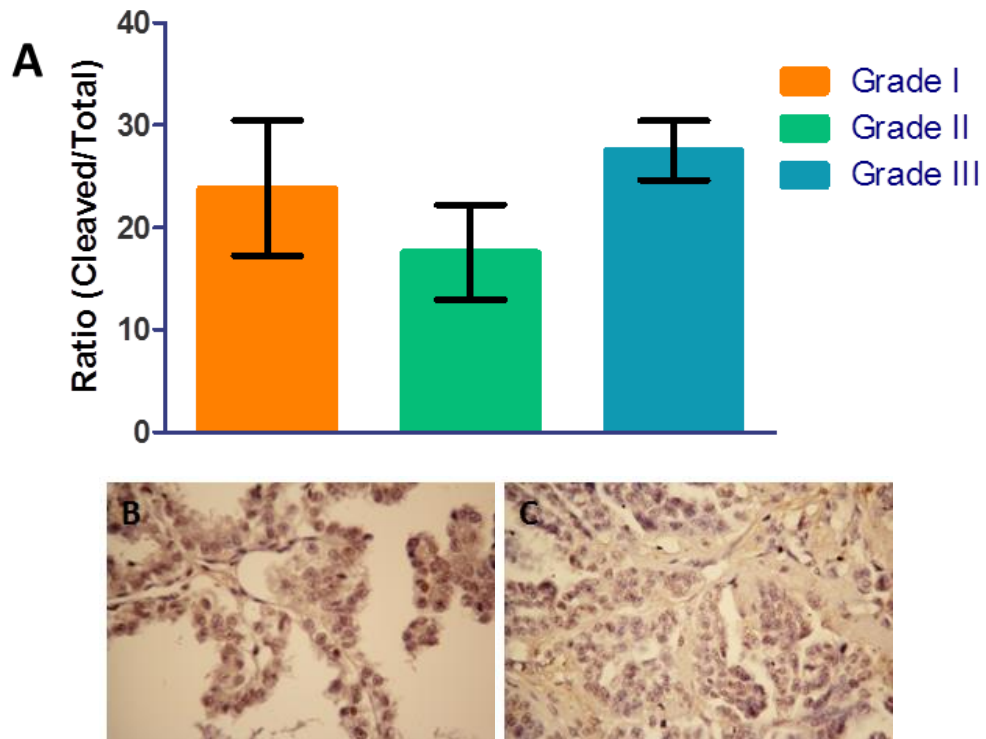


**Figure 5.17** - Immunohistochemistry for rictor was performed on paraffin embedded ovarian tissue clinical samples from grade I, grade II and stage III ovarian tumours. F-Tests were performed to assess variance and unpaired, two-tailed Student's t-tests with Welch's correction for unequal variance used to assess significance. Error bars depict standard error. No significant change was seen between grade of tumour (A). B and C show representative images of grade I and grade III serous papillary carcinoma respectively.



#### 5.3.4.4 Raptor

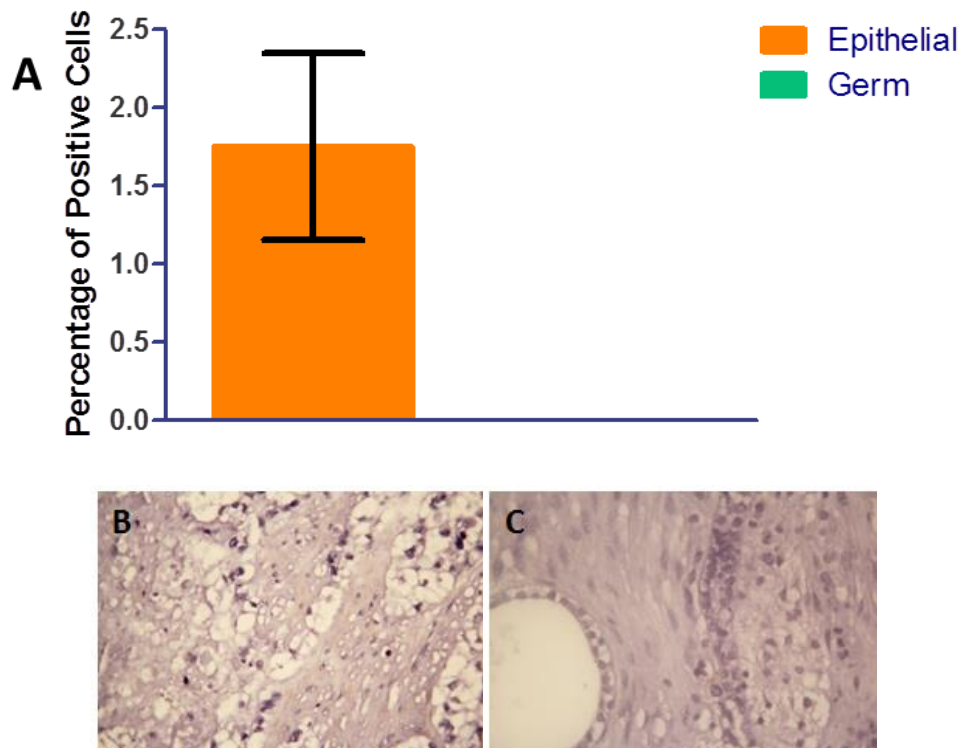


**Figure 5.18** - Immunohistochemistry for raptor was performed on paraffin embedded ovarian tissue clinical samples from epithelial and germ cell ovarian tumours. F-Tests were performed to assess variance and unpaired, two-tailed Student's t-tests with Welch's correction for unequal variance used to assess significance. Error bars depict standard error. No staining was seen in germ cell tumours (A). B and C show representative images of clear cell carcinoma (epithelial) and a germ cell tumour respectively.

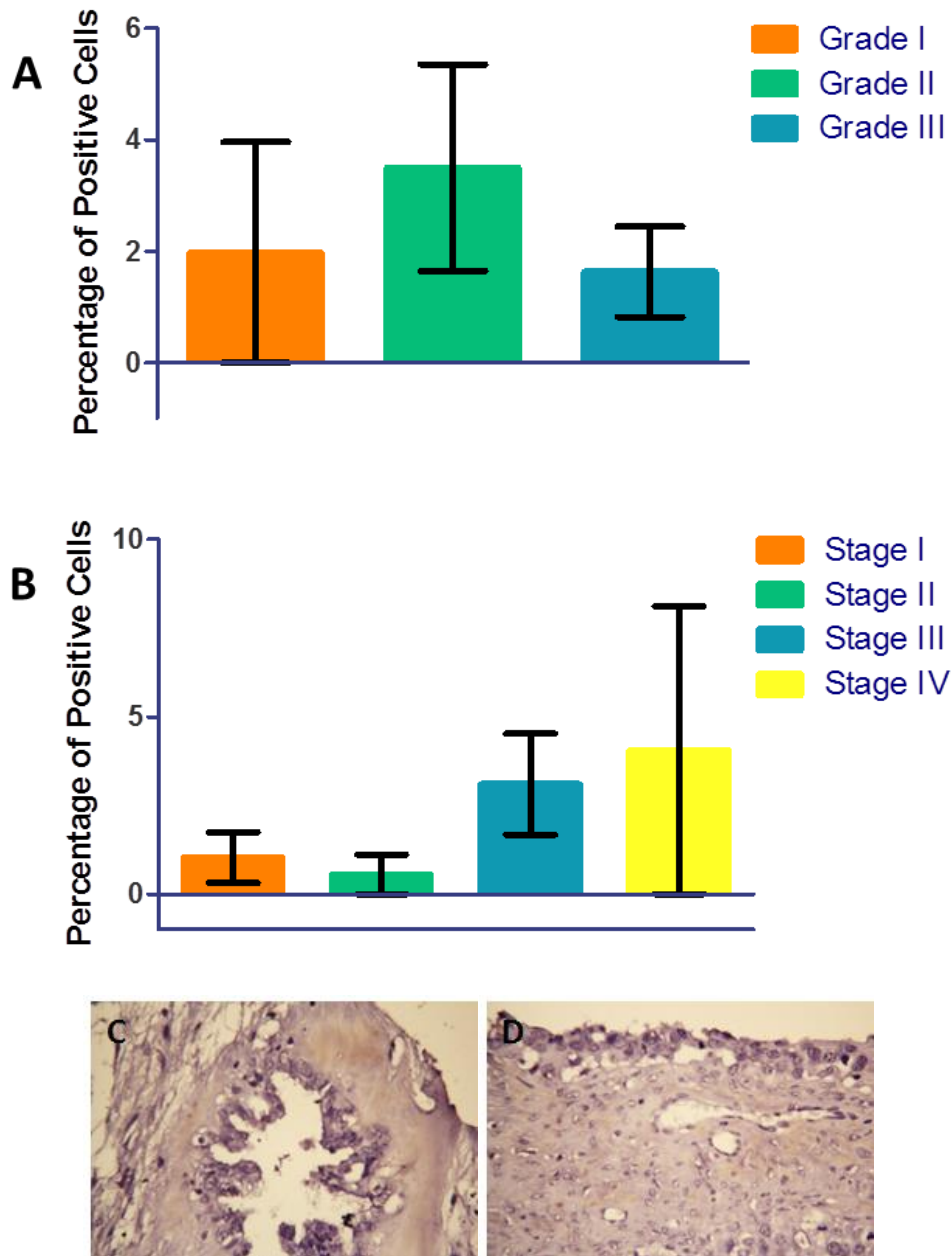


**Figure 5.19** - Immunohistochemistry for raptor was performed on paraffin embedded ovarian tissue clinical samples from grade I, grade II, grade III and stage I, stage II, stage III and stage IV ovarian tumours. F-Tests were performed to assess variance and unpaired, two-tailed Student's t-tests with Welch's correction for unequal variance used to assess significance. Error bars depict standard error. No significant change was seen between grade (A) or stage (B) of tumour. C and D show representative images of grade I/stage I and grade III/stage III serous papillary carcinoma respectively.

#### 5.3.4.5 p70S6 Kinase

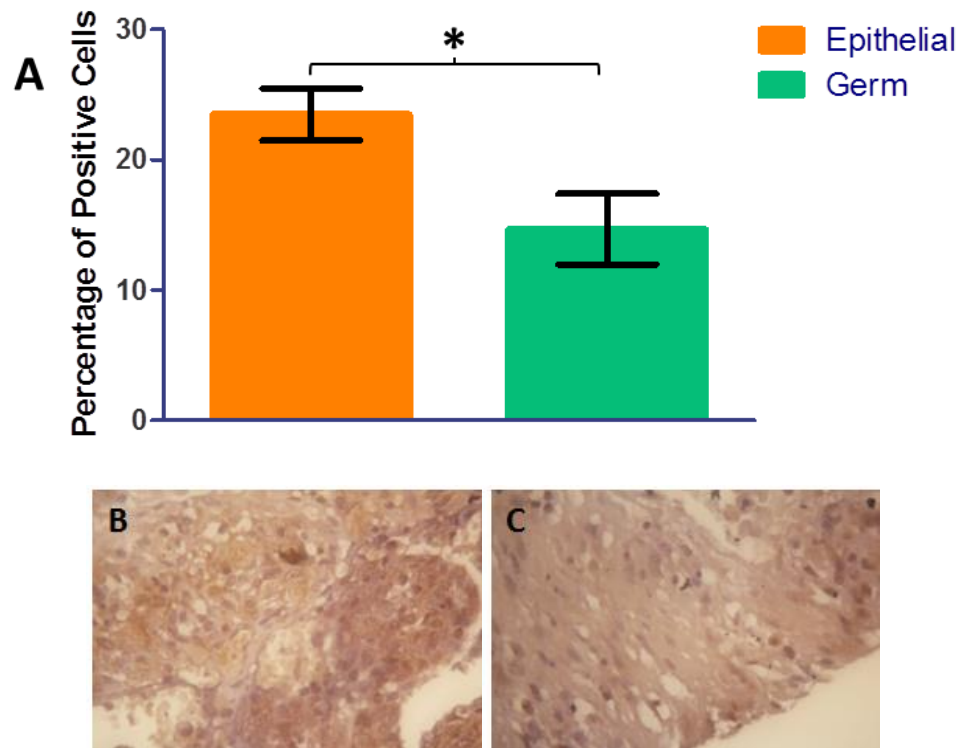


**Figure 5.20** - Immunohistochemistry for p70S6 kinase was performed on paraffin embedded ovarian tissue clinical samples from epithelial and germ cell ovarian tumours. F-Tests were performed to assess variance and unpaired, two-tailed Student's t-tests with Welch's correction for unequal variance used to assess significance. Error bars depict standard error. A significant decrease was seen in germ cell tumours in comparison to epithelial tumours (**A**). **B** and **C** show representative images of serous papillary carcinoma (epithelial) and a germ cell tumour respectively.

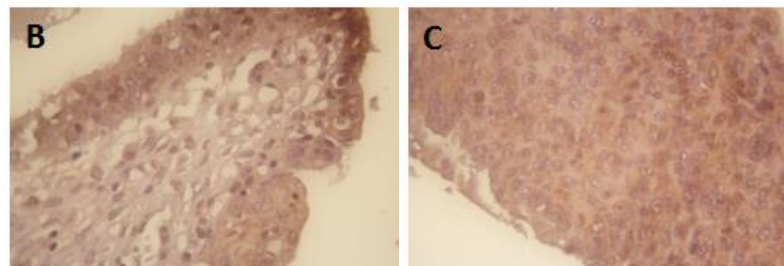
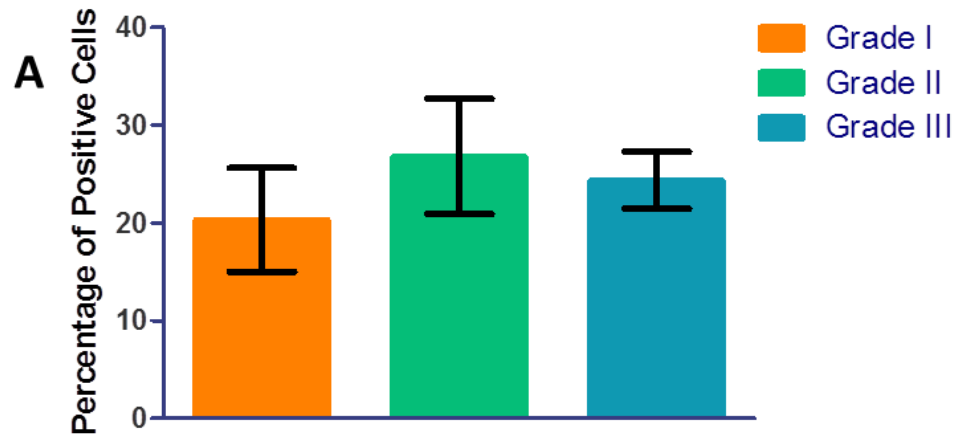


**Figure 5.21** - Immunohistochemistry for p70S6 kinase was performed on paraffin embedded ovarian tissue clinical samples from grade I, grade II and grade III ovarian tumours. F-Tests were performed to assess variance and unpaired, two-tailed Student's t-tests with Welch's correction for unequal variance used to assess significance. Error bars depict standard error. No significant change was seen between grade of tumour (A). B and C show representative images of grade I and grade III serous papillary carcinoma respectively.

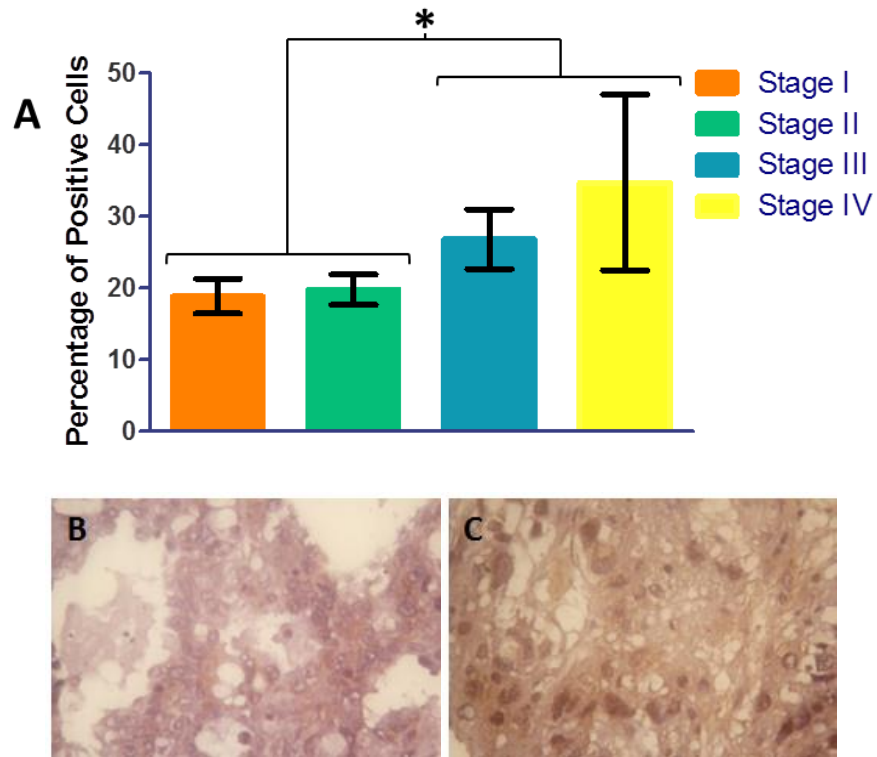


**Figure 5.22** - Immunohistochemistry for p70S6 kinase was performed on paraffin embedded ovarian tissue clinical samples from stage I, stage II, stage III and stage IV ovarian tumours. F-Tests were performed to assess variance and unpaired, two-tailed Student's t-tests with Welch's correction for unequal variance used to assess significance. Error bars depict standard error. No significant change was seen between individual stage of disease; however a significant difference was detected between early and late stage disease ( $p=0.0461$ , A). B and C show representative images of stage I and stage IV serous papillary carcinoma respectively.

mTOR and raptor showed no significant changes between epithelial or germ cell tumours or when comparing grade or stage of tumour (Figures 5.11, 5.12, 5.13, 5.18 and 5.19). Although not significant, raptor did show a trend towards increasing protein expression with deteriorating stage of ovarian cancer (Figure 5.19, B). DEPTOR also showed no significant difference in protein expression between epithelial and germ tumours (Figure 5.14); however, a significant but subtle decrease was noted between grade II and grade III tumours (Figure 5.15,  $p=0.05$ ). A significant decrease in DEPTOR expression was detected in late stage disease in comparison to early stage (Figure 5.16,  $p=0.0109$ ). No significant change in rictor expression was detected in different grades of disease (Figure 5.17). p70S6 kinase expression was significantly higher in epithelial tumours than in germ cell tumours (Figure 5.20,  $p=0.0389$ ) but showed no significant change between grades (Figure 5.21, A). A significant increase in p70S6 kinase expression was detected in late stage disease in comparison to early stage (Figure 5.22,  $p=0.0461$ ).

### **5.3.5 *In silico* analysis of survival in relation to mTOR pathway component biomarker expression**

We used the Kaplan-Meier Plotter to assess how the expression of mTOR pathway components mTOR and DEPTOR relate to patient survival. The Kaplan-Meier Plotter ([kmplot.com](http://kmplot.com)) is an online resource allowing for the assessment of biomarker expression in relation to survival. The Kaplan-Meier Plotter combines Affymetrix microarray data from the Gene Expression Omnibus (GEO), the European Genome-phenome Archive (EGA) and The Cancer Genome Atlas (TCGA) to provide survival data in relation to biomarkers in breast, ovarian, lung and gastric cancers (Győrffy *et al.*, 2013). Unfortunately rictor and raptor are not available for analysis on the Kaplan-Meier Plotter.

### 5.3.5.1 mTOR Overall Survival

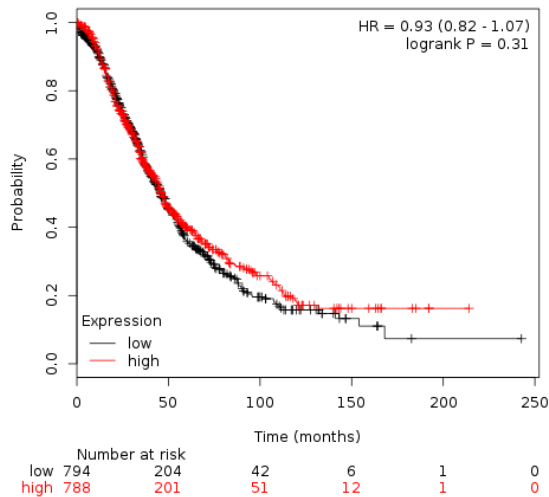


**Figure 5.23** - Kaplan-Meier plot showing overall survival probability of ovarian cancer patients. High (n=788) and low (n=794) expressors of mTOR are shown over a 250 month (20 year) period. There is no significant difference in overall survival between high and low expressors of mTOR (p=0.31).

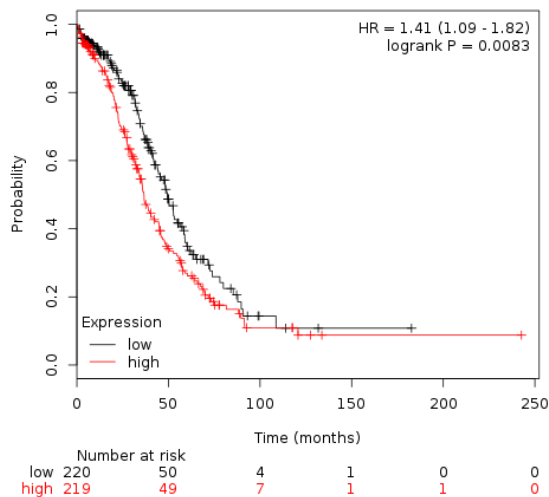


**Figure 5.24** - Kaplan-Meier plot showing overall survival probability of ovarian cancer patients. High (n=219) and low (n=220) expressors of mTOR with TP53 mutation are shown over a 250 month (20 year) period. There is greater overall survival in low mTOR expressors when TP53 is mutated (p=0.0083).

No correlation between mTOR expression and overall survival is seen (Figure 5.20). However, patients with low expression of mTOR have a significantly greater chance of overall survival when the TP53 gene is mutated (Figure 5.21, p=0.0083).

### 5.3.5.2 DEPTOR Overall Survival

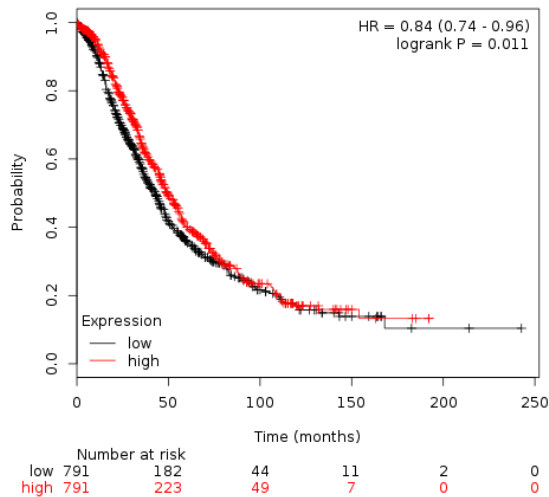


**Figure 5.25** - Kaplan-Meier plot showing overall survival probability of ovarian cancer patients. High ( $n=791$ ) and low ( $n=791$ ) expressors of DEPTOR are shown over a 250 month (20 year) period. High DEPTOR expressors show a significant improvement in survival than low DEPTOR expressors ( $p=0.011$ ).

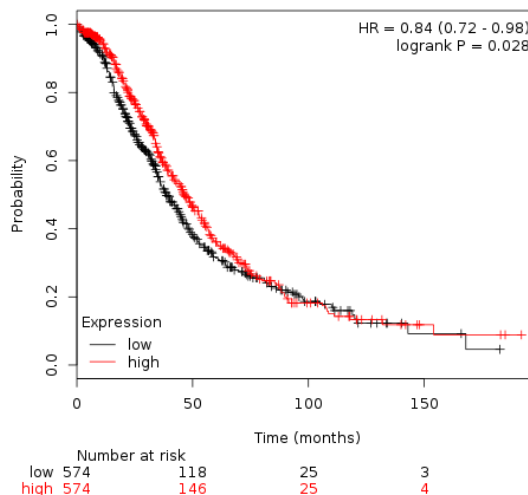


**Figure 5.26** - Kaplan-Meier plot showing overall survival probability of stage III and IV ovarian cancer patients. High ( $n=574$ ) and low ( $n=574$ ) expressors of DEPTOR are shown over a 250 month (20 year) period. High DEPTOR expressors show a significant improvement in survival than low DEPTOR expressors ( $p=0.028$ ).

Consistent with its role as an mTOR pathway inhibitor, high expression of DEPTOR was related to greater overall survival (Figure 5.25,  $p=0.011$ ). This was particularly evident for stage III and IV ovarian cancer patients (Figure 5.26,  $p=0.028$ ).



## 5.4 Discussion

In this chapter we studied the expression of mTOR components at gene and protein level in clinical samples. No change was seen in mTOR expression in ovarian cancer, fibroids or endometrial cancer by qPCR and OncoPrint patient analysis showed a small (1.122-1.166 fold) increase in mTOR expression in ovarian carcinoma in comparison to normal ovarian surface epithelium. These data agree with previous research which showed that mTOR gene expression levels did not change between ovarian cancer, benign ovarian tumours and normal ovarian tissue (Laudański *et al.*, 2011). In addition, it has been shown that expression of phosphorylated mTOR has no bearing on prognosis in epithelial ovarian cancer tissue (No *et al.*, 2011). Kaplan-Meier plots revealed that mTOR does not affect survival except in ovarian cancers with *TP53* mutation, where patients with low mTOR expression showed greater survival. The *TP53* gene product, p53, is a tumour suppressor protein which controls the expression of PTEN, a lipid phosphatase that dephosphorylates PIP<sub>3</sub> to the inactive form PIP<sub>2</sub> and thereby downregulates mTOR signalling via PI3 kinase (Weng *et al.*, 1999; Leslie *et al.*, 2000; Sun *et al.*, 1999; Thorpe *et al.*, 2015). In the absence of p53, the attenuating effects of PTEN on mTOR signalling is lost and it may follow that increased mTOR expression would augment mTOR signalling and result in an unfavourable prognosis in these cases. This is further supported by data showing that phosphorylated S6, a target of p70S6 kinase, is increased in p53 knockout mice (Leontieva *et al.*, 2013).

Ovarian cancer is most often epithelial in origin (CRUK, 2014b) but can also develop from germ and stromal cells. We were able to compare mTOR, DEPTOR, raptor and phosphorylated p70S6 kinase protein expression in ovarian cancers of both epithelial and germ cell origin. In the cases of mTOR, DEPTOR and raptor, no significant difference was detected between epithelial and germ cell tumours but phosphorylated p70S6 kinase was significantly decreased in germ cell tumours in comparison to epithelial cell tumours. Patients with germ cell tumours typically have a better prognosis than those with epithelial tumours with five year survival being up to 97.4% in comparison to 46% for epithelial ovarian cancer

(Chatchotikawong *et al.*, 2015; Neeyalavira and Suprasert, 2014; Saber *et al.*, 2014; CRUK, 2015h). These data support this in showing that mTORC1 signalling is decreased in germ cell tumours suggesting that the growth and proliferative effects of mTORC1 signalling are decreased in these cases.

Ovarian cancer patients expressed increased DEPTOR in comparison to unaffected controls and these data were supported by Oncomine analysis. DEPTOR is an mTOR interacting protein that is inhibitory to both mTORC1 and mTORC2. DEPTOR loss increases both mTORC1 (p70S6 kinase/4EBP1) and mTORC2 (Akt) signalling consistent with its role as an mTOR inhibitor; however, overexpression of DEPTOR causes overactivation of mTORC2 signalling (Peterson *et al.*, 2009; Kazi *et al.*, 2011). This may be because inhibition of mTORC1 relieves a negative feedback loop directed towards the upstream PI3 kinase. This then overcomes mTORC2 inhibition by DEPTOR which in turn hyperactivates mTORC2 signalling (Peterson *et al.*, 2009) and suggests that inhibition of mTORC2 by DEPTOR is not as robust as that of mTORC1. DEPTOR has been shown to be underexpressed in many cancers including that of the prostate, bladder and cervix but it is overexpressed in multiple myelomas, thyroid cancers and taxol resistant ovarian cancer cell lines (Peterson *et al.*, 2009; Foster *et al.*, 2010; Pei *et al.*, 2011). An increase in DEPTOR expression may represent a transformation in the balance of signalling from mTORC1 to mTORC2. The mTORC2 complex activates Akt which is known to promote cell survival (Dudek *et al.*, 1997) and mTORC2 dependent phosphorylation of Akt has been shown to be increased in ovarian cancer tissue in comparison to control tissue (De Marco *et al.*, 2013). If ovarian cancer progression is driven predominantly by mTORC2, mTORC1 targeting drug therapies would be ineffective in the treatment of this disease. Indeed, rapalogues, which robustly inhibit mTORC1 signalling but have little effect on mTORC2 signalling have not demonstrated the advance in cancer treatment that was expected from them with only few licenced uses for malignancy (Laplane and Sabatini, 2012).

An increase in phosphorylated p70S6 kinase expression was detected in later stages of ovarian cancer. p70S6 kinase is a downstream effector of the mTOR pathway

which is active when phosphorylated by mTORC1 (Isotani *et al.*, 1999; Burnett *et al.*, 1998). Phosphorylation of p70S6 kinase leads to activation of translation initiation factors which cause protein translation and cell growth (Ma and Blenis, 2009; Holz *et al.*, 2005). These data show that phosphorylation of p70S6 kinase and therefore the downstream growth effects of mTORC1 signalling are more active as ovarian cancer progresses and that increased mTORC1 signalling, which is responsible for p70S6 kinase activation, confers an unfavourable prognosis. These data support previous findings that p70S6 kinase overexpression is related to an increase in recurrence and metastasis in breast cancer and metastasis in ovarian cancer (van der Hage *et al.*, 2004; Ip *et al.*, 2014). In addition, DEPTOR protein expression was shown to decrease in higher grade and later stage ovarian cancers. Ovarian cancer grading and staging is a method of classifying ovarian cancer based on its differentiation, location and metastasis; higher grade and later stage ovarian cancers are considered more severe as the degree of differentiation of cells decreases and metastasis increases (CRUK, 2014a). This may suggest a switch in mTOR mediated responses in ovarian cancer; initial malignancy is mediated by mTORC2 and mTORC1 signalling predominates in later stages. However, it should be noted that ovarian cancer is not a homogenous disease, therefore these changes in signalling pathways may be subtype, stage or grade related.

In endometriosis, there was no significant change in rictor expression over all; however, when patients were compared based on age and disease grade, a significant increase was seen in younger patients (20-29 years compared to 30-39 years) and patients with higher disease grade score (>50 compared to <50). Differential expression of mTOR, DEPTOR and raptor was not seen based on age or disease grade in endometriosis. Endometriosis grade represents severity of disease based on location and infiltration of adhesions (American Society for Reproductive Medicine, 1997). Endometriosis is primarily a pre-menopausal condition as endometrium proliferates in response to oestrogen. As women age and enter a menopausal state, oestrogen is no longer produced by the ovaries and the endometrium no longer proliferates and sheds with menstrual cycles. This translates to a decrease in severity of endometriosis symptoms with increasing age.

A more pronounced expressional change seen in rictor in younger patients may be related to the effect of oestrogen. Indeed, oestrogen has previously been shown to interact with the mTOR pathway, with oestrogen treatment causing phosphorylation of mTOR, p70S6 kinase and 4EBP1 (Sudhagar *et al.*, 2011) and the oestrogen receptor has been shown to bind to the P85 $\alpha$  regulatory subunit of PI3 kinase in response to oestrogen stimulation (Simoncini *et al.*, 2000). Because oestrogen secretion decreases with menopause, higher rictor expression in younger patients may be explained by increased levels of oestrogen in premenopausal cases. Given that the influence of oestrogen on the development and progression of ovarian cancer remains unclear, it will be of interest to study the impact of sex hormones on mTOR signalling in ovarian cancer cells. Martin *et al.*, found that rictor expression was higher in oestrogen receptor positive breast cancers in comparison to oestrogen receptor negative breast cancers (Martin *et al.*, 2014). In addition to this, mouse models of ovarian cancer which involve KRAS activation and PTEN deletion and result in increased mTOR, Akt and p70S6 kinase phosphorylation show high levels of oestrogen receptor expression (Dinulescu *et al.*, 2005). There was also an increase in raptor observed in endometriosis. An increase in mTOR combined with raptor expression in endometriosis suggests that mTOR pathway signalling is more heavily weighted to the mTORC1 complex in this condition as raptor is a component unique to mTORC1 (Hara *et al.*, 2002). An increase in mTORC1 signalling has been observed in many conditions including intellectual disability, tuberous sclerosis and diabetes (Troca-Marín *et al.*, 2012; Wataya-Kaneda, 2015; Nyman *et al.*, 2014).

The data in this study present the differential regulation of mTOR signalling components in malignancies and borderline conditions. Collectively, our data suggests that a transformation from mTORC1 to mTORC2 signalling may occur in the progression from endometriosis to ovarian cancer and that DEPTOR status may be responsible for this. It may be useful to study the phosphorylation statuses of Akt, NDRG1 or PKC $\alpha$  to determine if mTORC2 signalling is altered in different disease states. More detailed analysis of mTORC1 and mTORC2 signalling must be carried out to fully elucidate the extent to which each pathway is active in ovarian

cancer and endometriosis and provide appropriate druggable targets. Interpatient variation as well as the alleviation of the negative feedback loop to PI3 kinase which occurs with mTORC1 inhibition and the paradoxical effects of DEPTOR expression makes predicting changes in mTOR pathway signalling difficult and this must be fully understood to effectively develop methods of diagnosing and treating these conditions.

# ***Chapter 6***

## ***Development of a PoCT platform for ovarian cancer***

### **6.1 Introduction**

PoCT is the implementation of a full suite of diagnostic procedures (obtaining a sample, sample preparation, testing and diagnosis) in a single visit to a primary or secondary health care provider (NHS, 2014). Many PoCTs are routinely used by the National Health Service (NHS) in the UK. For example blood gas analysis, blood glucose monitors and HIV tests (NHS, 2015c). Advantages of PoCT include decreased wait time, improved and more rapid treatment, reduced visits to a healthcare provider, reduced hospitalisation burden and decreased costs (NHS, 2015e). qPCR, a method of amplifying and quantifying genetic material, is a fundamental procedure in both research and medical laboratories. qPCR allows for accurate quantification of gene transcripts in real time and has eliminated the need for end-point analysis with the addition of fluorescent probes or DNA binding dyes (Tania Nolan, 2013; Stephen A. Bustin, 2014). qPCR is well established as a diagnostic tool and a range of 'off the shelf' tests for pathogen detection are available (Cepheid, 2015); however, a typical 40-cycle qPCR test can take up to two hours to complete (Tania Nolan, 2013). In pathogen detection, for example, speed is of critical importance, not only to isolate the pathogen but to ensure rapid treatment, and could be the difference between life and death in some cases. Historically, the limiting factors in the speed of qPCR experiments have been the sample preparation time and the 'ramping rate' or time taken to move between the required temperatures in a cycle (i.e. from 95°C to 60°C to 72°C). The length of a qPCR test must be improved if it is to become a useful tool in PoCT.

qPCR machines, which function to cycle samples through temperatures 40 times or more, have typically used a peltier and conductive block system; however, some

more recently developed products have attempted to overcome the speed and accuracy limitations by using alternative methods of heating. Namely, heated air (Rotor-Gene® Q, Qiagen) and resistive heating (xxpress®, BJS Biotechnologies). However, increasing speed has the potential to compromise thermal uniformity, an important factor affecting the accuracy and reproducibility of a qPCR test (Tania Nolan, 2013). xxpress® by BJS Biotechnologies is a prototype thermal cycler that claims to be the fastest and most thermally active available. The xxpress® technology employs a technique known as resistive heating to achieve active and multizonal thermal control over the sample area. In conventional peltier based thermal cyclers the sample plate is a separate unit to the conductive block which is heated and cooled to apply temperature changes to the samples. The xxpress® system combines the conductive component and sample plate into one consumable item, allowing for close contact (approximately 10µM) (BJS Biotechnologies, 2015a) between the reagents and the heating source and therefore allowing the sample to closely mimic the desired temperature (Figure 6.1) (BJS Biotechnologies, 2015b).

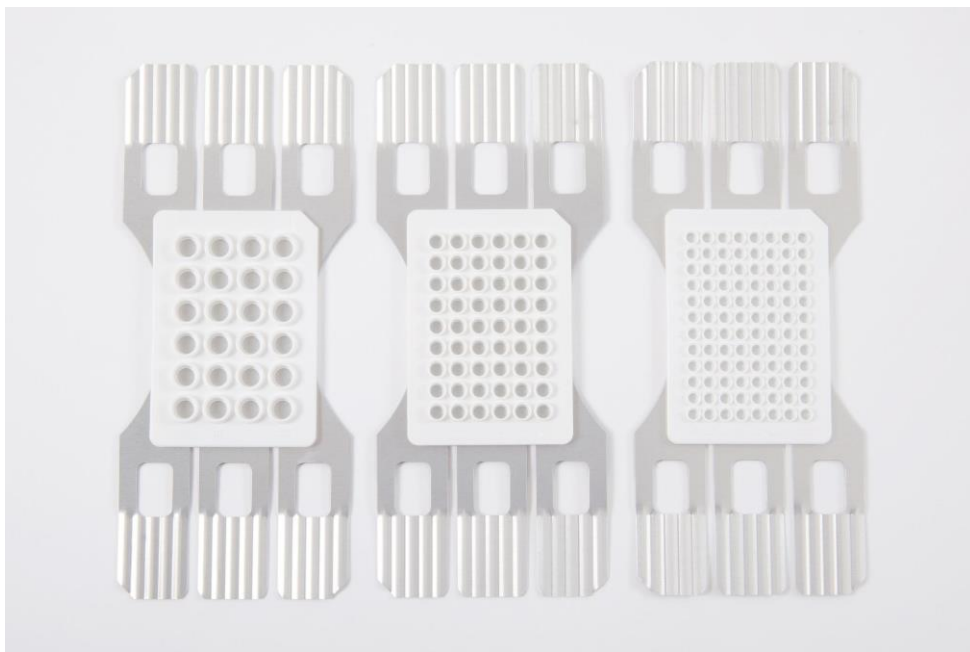


**Figure 6.1** - An image of the three xxplate™ well configurations available (24, 54 and 96 wells) showing the unique design of the xxpress® consumable. Image courtesy of BJS Biotechnologies.

The use of resistive heating as an alternative to peltiers translates to a significant speed advantage for the xpress® thermal cycler. Six electrical contact points allow the passage of current through the element (Figure 6.2). The element is made of very thin aluminium and so has reduced thermal mass in comparison to typical blocks. Because of this, heat can be driven in at a much faster rate meaning a 40-cycle qPCR experiment can be completed in less than 10 minutes (Tania Nolan, 2013). In addition to speed, accuracy is also important to provide reliable and reproducible data. If the thermal uniformity across the sample plate is low, samples will experience different thermal environments and, as important factors such as primer binding are reliant on accuracy of temperature, the integrity of the experiment is lost. The xxplate™ is designed so that thermal control of the sample area can be multizonal to adjust for greater heat loss at the edges (Figure 6.3). The software algorithm uses 12 different routes for current to travel through the conductive component (Figure 6.3) to deliver heat to specific areas meaning that the thermal uniformity across the sampling area can be within 0.3°C. The temperature of the sample area is measured 100 times a second by nine non-contact infra-red sensors resulting in temperature that is under active control and can be rapidly adjusted to maintain uniformity (Tania Nolan, 2013).



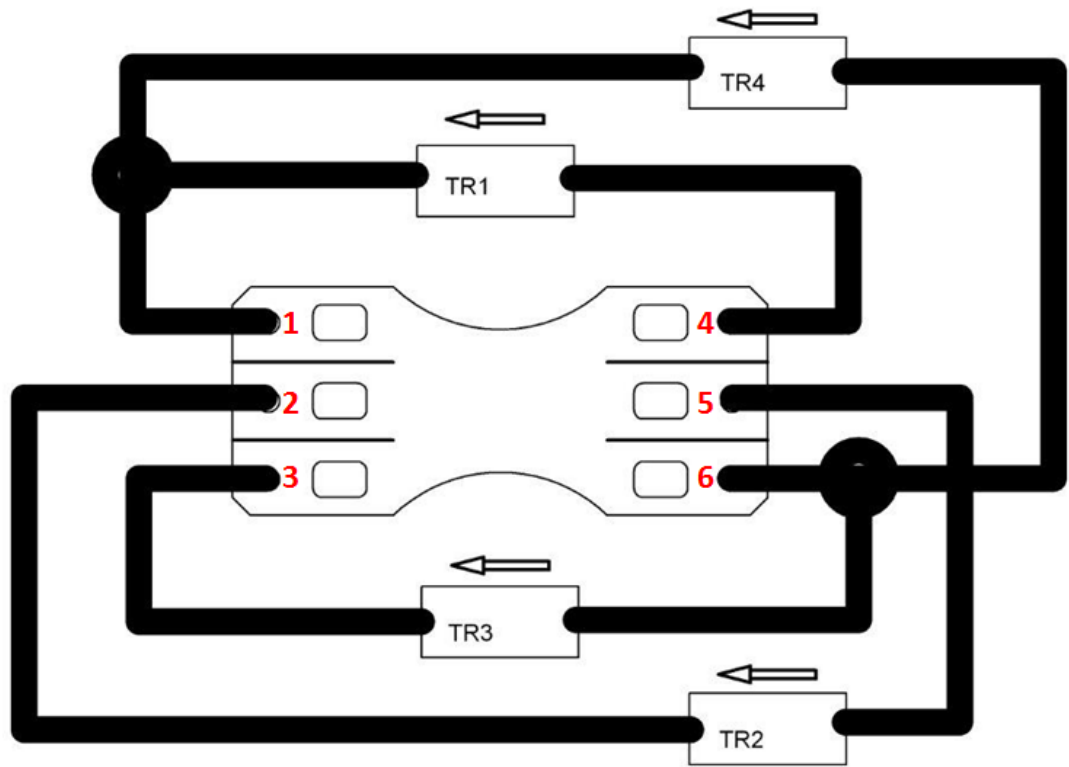


**Figure 6.2** - The xxplate™ design has six electrical contact points and allows for multizonal thermal control of the sample area by modulating the route of current through the conductive element. TR refers to toroidal transformer. Image courtesy of BJS Biotechnologies.

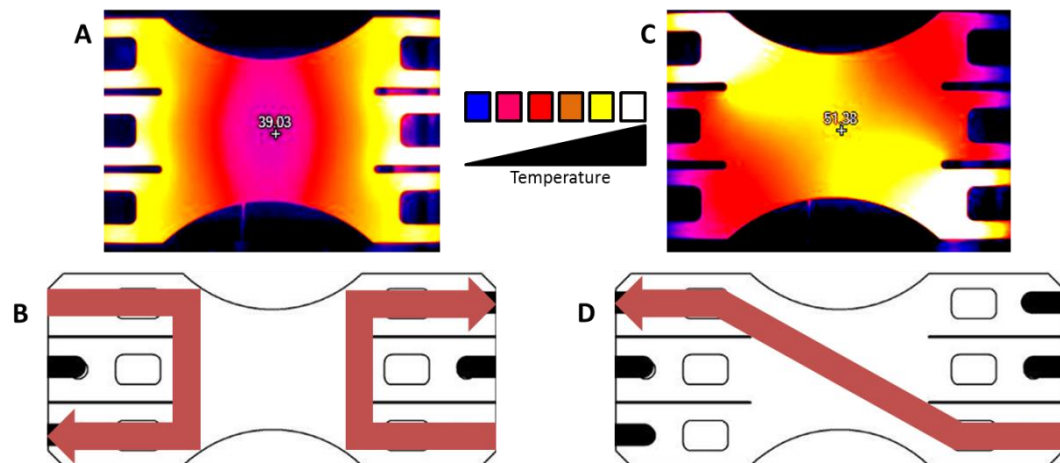


**Figure 6.3** - Infra-red images of multizonal heating of the xxplate™ under two different current configurations. Image A shows a heatmap of the sample area on an xxplate™ according to the circuit paths illustrated in diagram B and image C shows the sample area on an xxplate™ according to the circuit path illustrated in diagram D. Image generated in conjunction with BJS Biotechnologies.

## 6.2 Objectives

-To compare speed, efficiency and variability of four current, commercially available qPCR thermal cyclers, two of which use the industry standard peltier/block system and two of which use novel heating systems.

-To assess how the xpress® (BJS Biotechnologies) compares to industry standard thermal cyclers and which, if any, are suitable for development into a platform for rapid diagnostic clinical testing.

-To assess instrument usability in terms of level of training needed and adaptability to a PoCT scenario.

-To develop a proof of principle assay to demonstrate PoC biomarker detection in ovarian cancer for development on xpress® technology.

## 6.3 Results

### 6.3.1 Reaction Efficiency and Time

Company	qPCR Platform	Thermal System	Advertised Fastest Ramp Rate	Advertised Thermal Uniformity
Bio-Rad	CFX96™	Block/Peltier	2.5°C per second	±0.4°C
BJS Biotechnologies	xpress®	Resistive heating/active control	10°C per second	±0.3°C
Life Technologies	7900HT Fast	Block Peltier	3°C per second	±0.5°C
Qiagen	Rotor-Gene® Q	Heated Air	15°C per second	±0.02°C

**Table 6.1** - A summary of the qPCR thermal cyclers compared.

We first sought to assess qPCR reaction efficiency across four different thermal cycler platforms. 18S rRNA amplification in commercially available human DNA was assessed and compared by qPCR using CFX96™ (Bio-Rad), xpress® (BJS Biotechnologies), 7900HT Fast (Life Technologies) and Rotor-Gene® Q (Qiagen) thermal cyclers (Table 6.1).

A dilution series of hgDNA was created to include 100, 10, 1, 0.1 and 0.01ng/μL (final concentrations: 5, 0.5, 0.05, 0.005 and 0.0005ng/μL) in order to generate a standard curve. Previously validated eukaryotic 18S rRNA gene primers (Foster *et al.*, 2010) were used (detailed in Section 2.10.1). KAPA Biosystems' SYBR® FAST qPCR master mix was used across all thermal cyclers (as described in Section 2.10.4) using the following thermal profile:

Temperature	Time	Cycles
95°C	20 seconds	1
95°C	1 second	40
60°C	10 seconds	

**Table 6.2** - Thermal profile for qPCR experiments on hgDNA.

Ramping and cooling rates and all modifiable parameters were used at the manufacturers' pre-set levels. Each concentration of hgDNA was run in triplicate. Speed of experiment was measured from the time the machine was initiated to the time results were obtainable and rounded to the nearest minute.

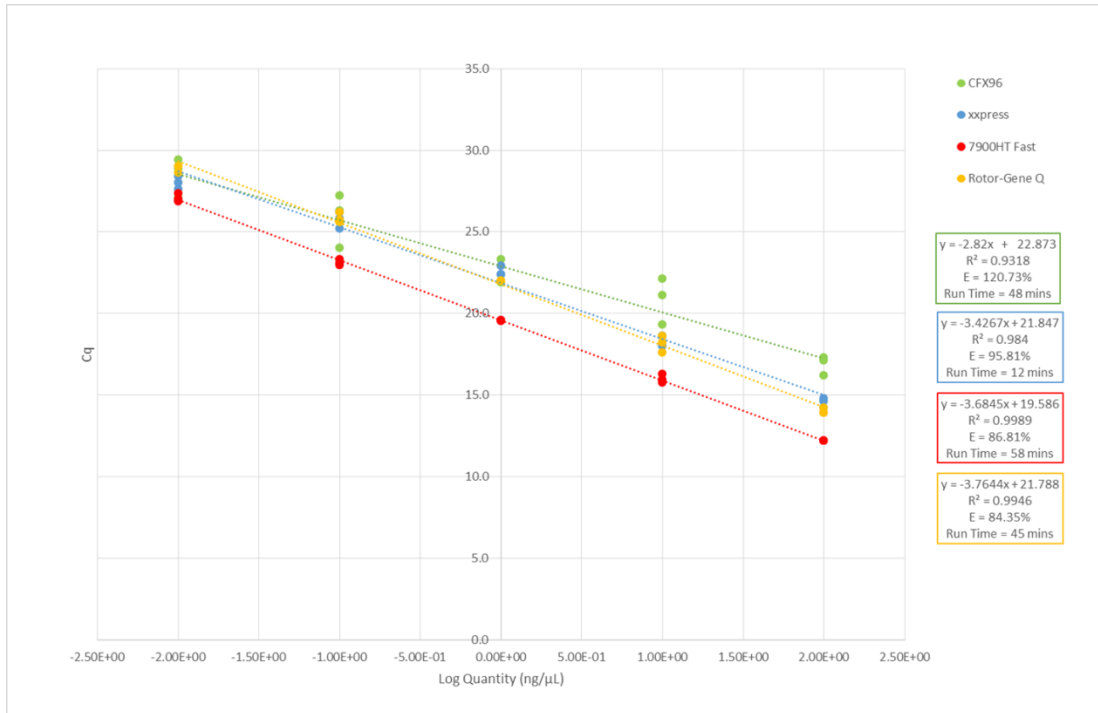


**Figure 6.4** - A dilution series of hgDNA was used to create a standard curve of 18S RNA expression on CFX96™, xxpress®, 7900HT Fast and Rotor-Gene® Q thermal cyclers. Correlation coefficient and efficiency were calculated in addition to protocol run time. Correlation coefficient and efficiency varied between thermal cyclers. All thermal cyclers were able to operate over the same linear dynamic range.

Figure 6.4 shows the amplification efficiency of each thermal cycler. In the  $\Delta$  or  $\Delta\Delta$  quantification cycle ( $C_q$ ) qPCR analysis methods, amplification efficiency is assumed to be equal across GOIs and reference genes. An amplification efficiency of 100% indicates that the PCR product is doubling with every cycle. Efficiency is calculated as follows (Kennedy and Oswald, 2011):

$$E = 10^{(1-\text{slope})-1}$$

An efficiency in the range of 90-110% is considered acceptable (Kennedy and Oswald, 2011). The only thermal cycler to achieve an efficiency within the acceptable range was the xxpress® (BJS Biotechnologies) at 95.81%. Correlation coefficient ( $R^2$ ), a measurement of linear correlation, depicts how well the individual data points relate to their slope. An  $R^2$  value of 0.975 or higher is considered acceptable for qPCR experiments (Kennedy and Oswald, 2011). The

only thermal cycler to not achieve an acceptable  $R^2$  value was the CFX96™ at 0.918. The time to complete a 40-cycle experiment varied between machines. The fastest machine by a marked amount was the xpress® (BJS Biotechnologies) at 12 minutes. The rest of the cyclers ranged from 45 to 58 minutes (Table 6.3). Each machine was able to operate over the same linear dynamic range.

Thermal Cycler	Time to complete 40 cycles (minutes)	Acceptable efficiency	Acceptable correlation coefficient
CFX96™	48	X	X
xpress®	12	✓	✓
7900HT	58	X	✓
Rotor-Gene® Q	45	X	✓

**Table 6.3** - A summary of time, efficiency and correlation coefficients for 18S RNA expression assay in human gDNA carried out on four thermal cyclers.

### 6.3.2 Reaction Uniformity

We next assessed the uniformity of qPCR reactions across the sample area of each thermal cycler consumable. Reaction uniformity was assessed using qPCR by measuring amplification of 18S rRNA in a selection of wells with covering all areas of the sample plate on CFX96™ (Bio-Rad), xpress® (BJS Biotechnologies), 7900HT Fast (Life Technologies) and Rotor-Gene® Q (Qiagen) thermal cyclers. Human DNA at 100ng/μL (final concentration of 5ng/μL) was used in all wells with the thermal protocol detailed above.

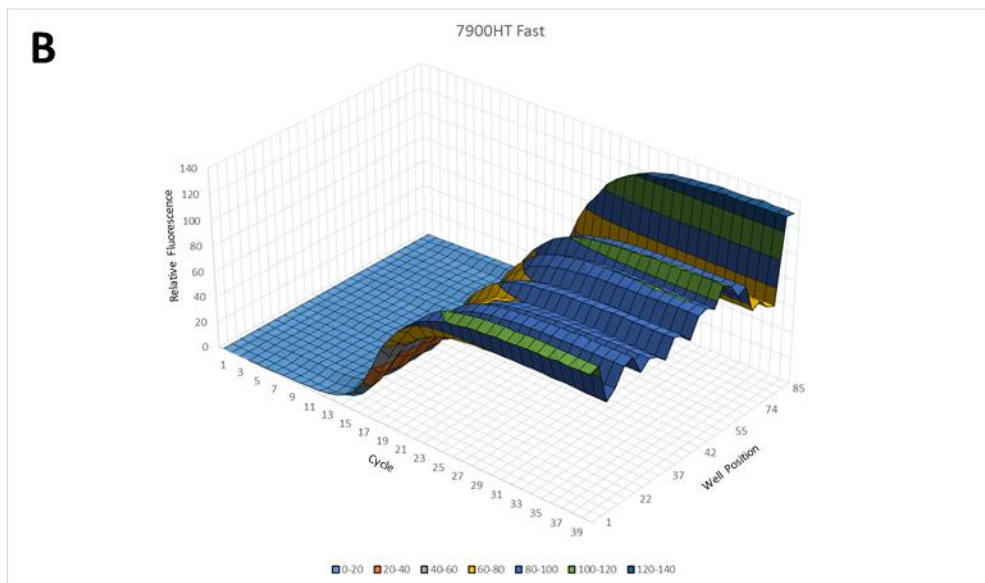
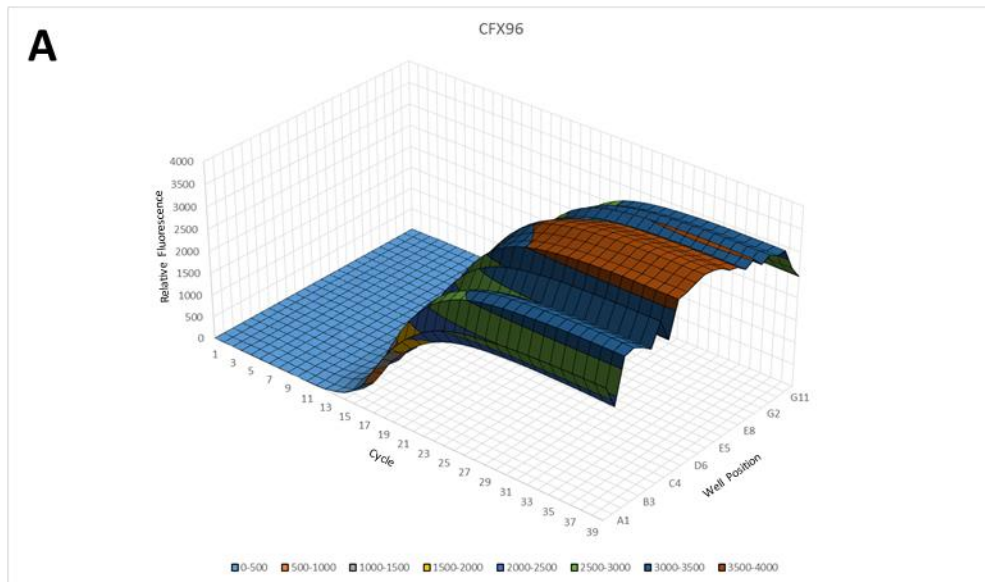


**Figure 6.5** - qPCR with a fixed template concentration of 5ng/ $\mu$ L hgDNA was carried out for 18S RNA in a selection of wells covering all areas of the sample plate on each thermal cycler to investigate if the sample location on the plate affects fluorescence and  $C_q$ . Figure 6.5 demonstrates the fluorescence variability across the sampling areas of the CFX96™ and 7900 HT Fast thermal cyclers at each cycle of the protocol. The CFX96™ showed a doming effect over the well rows (A). The 7900HT Fast appears to experience a substantial edge effect on the bottom row of the sample plate (B).

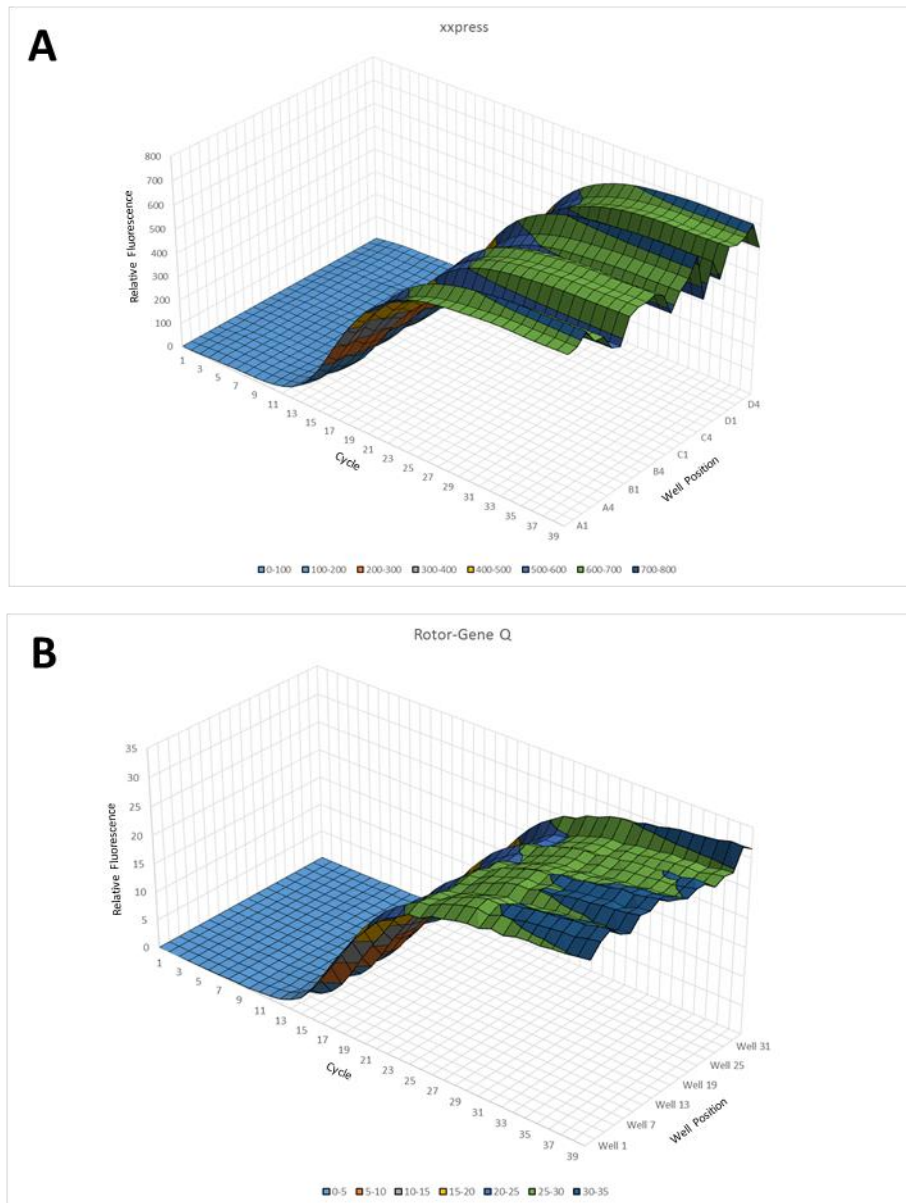


**Figure 6.6** - qPCR with a fixed template concentration of  $5\text{ng}/\mu\text{L}$  hgDNA was carried out for 18SRNA in a selection of wells covering all areas of the sample plate on each thermal cycler to investigate if the sample location on the plate affects fluorescence and  $C_q$ . Figure 6.6 demonstrates the fluorescence variability across the sampling areas of the *xxpress*<sup>®</sup> (**A**) and *Rotor-Gene*<sup>®</sup> Q (**B**) thermal cyclers at each cycle of the protocol. All thermal cyclers demonstrated a level of variability but the *xxpress*<sup>®</sup> showed the lowest deviation of  $C_q$  value.

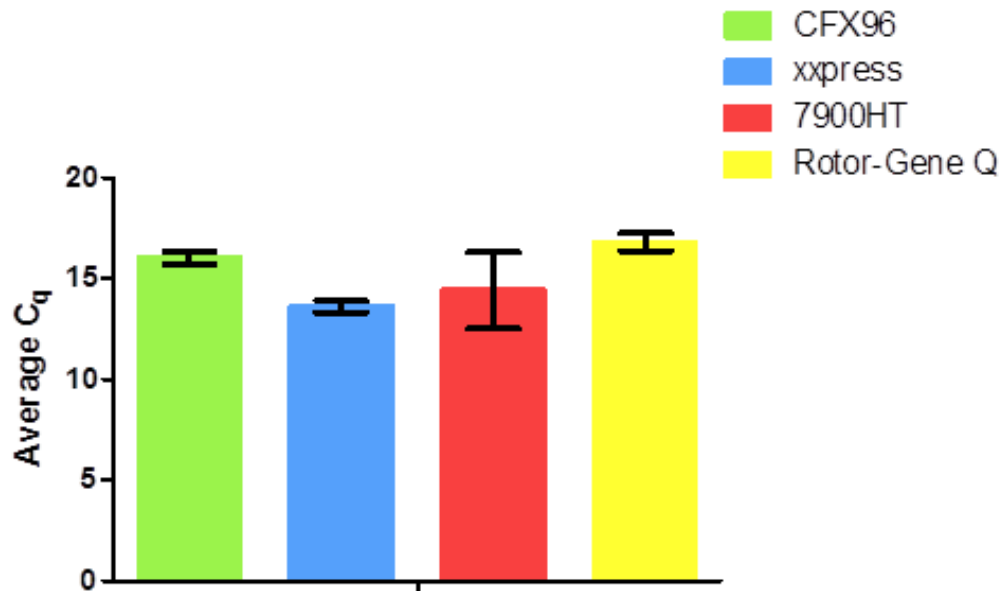


**Figure 6.7** - qPCR with a fixed template concentration of 5ng/ $\mu$ L hgDNA was carried out for 18SRNA in a selection of wells covering all areas of the sample plate on each thermal cycler to give an indication of how the sample location on the plate can affect fluorescence and  $C_q$ . Figure 6.7 shows the average  $C_q$  value among technical replicates for each of the thermal cyclers. Error bars depict standard deviation.

Figures 6.5 and 6.6 show the fluorescence uniformity across the sample area of each sample plate. Each uniformity graph provides a visual representation of the level of variation across each sample area. Figure 6.7 shows the average  $C_q$  value for each of the thermal cyclers with error bars depicting standard deviation (SD). The SD of  $C_q$  values within identical reactions on a sample plate indicates the repeatability of an assay. Without extraneous variables the fluorescence for technical replicates would be identical at each cycle; however thermal and optical variation can cause fluorescence outputs to fluctuate. This fluctuation can cause  $C_q$  variation in what should otherwise be stable values. In this experiment, the 7900HT Fast (Life Technologies) showed the greatest  $C_q$  variation with a value of 1.91 (Figure 6.7). xpress® showed the least variation with a value of 0.29 (Figure 6.7). Although MIQE guidelines state that intra-assay variation as a measure of repeatability should be reported for all qPCR experiments, no parameters of acceptable variation have been described.



### 6.3.3 Biomarker Detection in Whole Blood

PoC detection of biomarkers is not currently a routine procedure in primary or secondary healthcare. As we have previously demonstrated DEPTOR upregulation in ovarian cancer, we investigated if DEPTOR gene expression changes could be detected in whole blood of ovarian cancer patients in comparison to unaffected controls. RNA was extracted from whole blood of 7 ovarian cancer patients and 6 unaffected controls using the QIAamp® RNA Blood Mini Kit (Qiagen, Section 2.6.3). cDNA was synthesised from extracted RNA using the nanoScript™ 2 cDNA synthesis kit (Primerdesign). qPCR was performed on cDNA using primers for DEPTOR and 18S RNA (section 2.10.1). Power SYBR® Master Mix was used on a 7900HT Fast thermal cycler (Life Technologies, described in Section 2.10.3). Three technical replicates were performed for each sample.

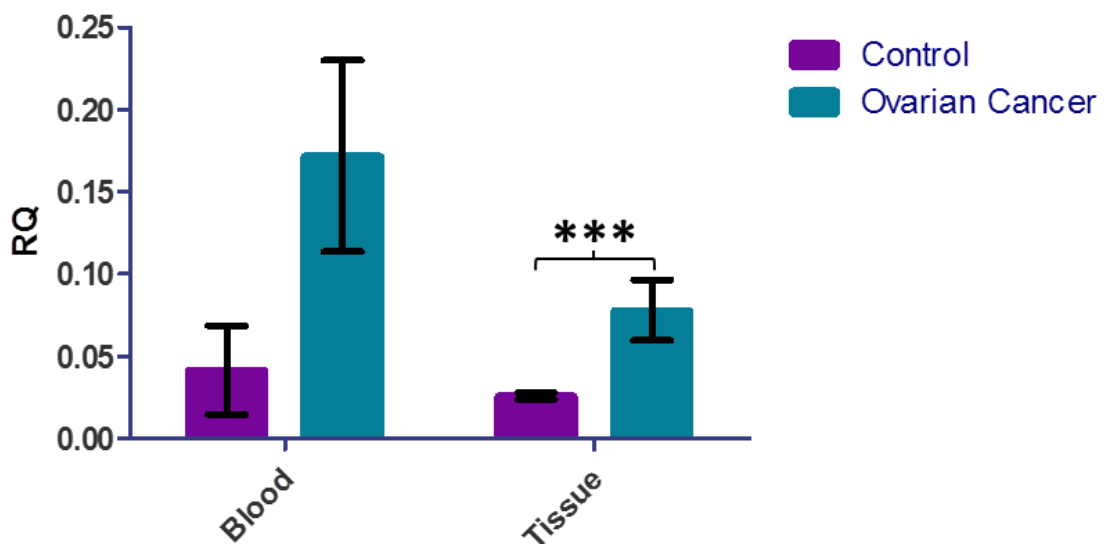


**Figure 6.8** - Relative DEPTOR expression was measured by qPCR in the whole blood of ovarian cancer patients and unaffected controls and ovarian tissue of ovarian cancer patients and unaffected controls. cDNA was synthesised from extracted RNA and data were analysed using the  $\Delta C_q$  method. An RQ value calculated by  $2^{-\Delta C_q}$ . An F-test was performed to assess variance between groups and a two-tailed, unpaired Student's t-tests was performed to assess significance. Error bars depict standard error and asterisks denote significance. DEPTOR expression was increased in ovarian cancer patients in comparison to controls; this change did not achieve significance ( $p=0.0817$ ). As previously shown, DEPTOR expression was also increased in ovarian cancer patients in comparison to controls ( $p=0.0007$ ).

DEPTOR mRNA was detected in greater quantity in the whole blood of ovarian cancer patients in comparison to unaffected controls although this change did not reach statistical significance. These findings are in concordance with detection of significantly greater levels of DEPTOR in ovarian tumour tissue in comparison to unaffected controls (Figure 6.8).

#### **6.4 Discussion**

In this chapter we assessed the performance of qPCR instrumentation and investigated if gene expression changes are detectable in whole blood by qPCR. As rapid developments are made in PoCT, it is essential that the pitfalls and drawbacks of this technique are understood. It is often the case that machinery operators have a disconnected relationship with the equipment they are using and may not fully understand the restraints on the data they have generated. In a healthcare setting, it is not only speed and accuracy of qPCR that are of consideration. Thought must be given to the operator of the test who is unlikely to have laboratory training (NHS, 2015d). Ideally, the machine would be intuitive, recognise samples (i.e. through barcodes or other means that avoid user input) and guide the user through the set-up process with little chance of error. Many commercially available pieces of laboratory instrumentation are unusable without at least some level of training which, in a low resource environment, is not always practical.

The 7900HT Fast by Life Technologies is an industry standard machine, the sample tray is placed in a metal block which is heated and cooled using a peltier (ThermoFisher Scientific, 2015). The CFX96™ by Bio-Rad has improved the block design by reducing its thermal mass to allow faster heat transfer and an improved ramp rate (Bio-Rad, 2015). In addition to being a relatively slow method of heating and cooling, block/sample tray methods have an added disadvantage of creating a large thermal barrier between sample and heat source (caused, in part, by the thick plastic sample tray). This can result in a disparity between temperature of block and temperature of sample and can lead to discrepancy between the desired

temperature and the actual temperature of the sample. Furthermore, block based systems often experience what is known as the 'edge effect' in which the rate of heat transfer is greatest around the edges of the block. This results in the lower temperatures at the peripheral areas of the sample plate (Kennedy and Oswald, 2011). The Rotor-Gene® Q and xpress® have made attempts to overcome these issues with novel heating and cooling methods. The Rotor-Gene® Q by Qiagen uses a centrifugal system by which samples are arranged in a ring formation and are rotated through heated or cooled air (Qiagen, 2015). As samples are not fixed in place, they are able to experience the same temperatures without variability arising from the edge effect. xpress® by BJS Biotechnologies employs a different heating method again, resistive heating. The consumable in this case consists of both the sample tray and the heat source with 10µm of polymer separating the two (BJS Biotechnologies, 2015a). Electricity is passed through the block component of the PCR plate whose temperature is monitored in real-time and is therefore under active control. With this technology, any thermal uniformity issues can be quickly corrected by passing more or less current through specific sample areas (BJS Biotechnologies, 2015a). Despite xpress® technology having a fixed, block-based sampling area, the lack of thermal uniformity usually noted in these models should be eliminated due to active control heating. This has been confirmed in this study; xpress® had lowest standard deviation in  $C_q$  value of all four machines studied.

An acceptable reaction efficiency was achieved only by the xpress® thermal cycler. Common methods of qPCR analysis do not account for variations in efficiency between reactions (Bustin *et al.*, 2009). In research settings where qPCR experiments are designed by the user, efficiency is not always assessed prior to the commencement of data generation. This assessment has shown that efficiency cannot be assumed to be within acceptable limits and that optimisation may be required; this may include adjusting thermal or time parameters, and template and primer concentration. For the purpose of comparison, experimental design, template and primer concentrations and thermal protocol were kept constant between each thermal cycler; however, with optimisation, it may be possible to

achieve efficiency within acceptable parameters on each of the thermal cyclers tested. This highlights the importance of instrument specific optimisation.

Variability in fluorescence may also be due to the optical system in place within the thermal cycler (i.e. the excitation source and method of fluorescence detection). It would be advantageous to design an experiment to distinguish between these two variables. For example, a thermochromic material which will change colour at different temperatures could be used to assess temperature variations across the plate. In addition to this, measuring fluorescence from a fluorophore without applying temperature will demonstrate optical fluctuations.

Despite using novel thermal techniques which stray from the industry standard, the xpress<sup>®</sup> and Rotor-Gene<sup>®</sup> Q thermal cyclers demonstrated that they can compete with, and in some cases exceed, the CFX96<sup>™</sup> and 7900HT Fast instruments. The speed of the xpress<sup>®</sup> instrument's ramp rate, due to resistive heating, did not compromise the efficiency of the reaction and the close contact between the reaction and the heat source may have provided an improvement; making the xpress<sup>®</sup> thermal cycler a potential candidate for a PoCT system. Moreover, the xpress<sup>®</sup> user interface could be easily adapted to be operated by non-technical users.

An accelerated qPCR test in the research lab is a useful improvement, but in healthcare settings where an infectious pathogen may be present, the advantages of a fast and reliable test can not be overstated. For example, in the case of sepsis, a life threatening inflammatory condition caused by bacterial or fungal infection, the time between onset of infection and serious illness can be short and over 50% of sepsis patients die of their disease (Engel *et al.*, 2007). Patients are often treated for sepsis before a positive test result is returned; however, appropriate treatment which covers the specific microbe can greatly improve survival in sepsis patients (Hanon *et al.*, 2002). A rapid diagnosis resulting in swift and appropriate treatment

can mean the difference between life and death for some and could save costs in preemptive and erroneous treatment before a confirmed diagnosis.

As previously mentioned, there is currently no effective screening method available for ovarian cancer. Ovarian cancer biomarkers such as CA125 have been proven to be ineffective for many reasons including low specificity (Buys *et al.*, 2011; Menon *et al.*, 2015). Current diagnostic methods for ovarian cancer are time consuming and invasive; with the emergence of circulating tumour cells (CTCs), readily available in the blood, there is renewed hope of developing a tool that may serve as a surrogate biomarker. CTCs are cells that have detached from a primary or metastatic tumour and migrated into the circulatory system (Azevedo *et al.*, 2015). We hypothesised therefore, that if CTCs have entered circulation from the primary tumour, their gene profile would resemble the one of the tissue they came from. Since we have shown that DEPTOR is upregulated in the tissue of ovarian cancer patients, we sought to investigate if the same readout could be detected in RNA extracted from whole blood. Upregulation of DEPTOR gene expression was evident in the blood of ovarian cancer patients compared to unaffected controls, mimicking our previous data obtained from ovarian cancer tissue. Detection of CTCs by blood extraction (known as a liquid biopsy) holds potential as a minimally invasive method of screening for ovarian cancer which could improve prognosis by detecting malignancy at an earlier stage and prompting earlier commencement of treatment.

# **Chapter 7**

## **General Discussion and Concluding Remarks**

### **7.1 Why is this research important?**

The advances made in cancer treatment have not mirrored other diseases; chemotherapeutic treatments are often poorly tolerated and paradoxically carcinogenic. Ovarian cancer is particularly lethal due to ambiguous symptoms and lack of reliable biomarkers leading to late stage diagnosis and unfavourable prognosis. To date, there is no discrete, non-invasive screening method to detect ovarian cancer. Currently, CA125 and transvaginal ultrasound are used when ovarian cancer is suspected, at which point the majority of cancers have reached stages III or IV (Buys *et al.*, 2011). In addition to this, using CA125 as a screening marker has shown low specificity which increases the risk of screening related harms such as unnecessary surgery and no improvement in survival (Buys *et al.*, 2011). Daily, nineteen women are diagnosed with ovarian cancer in the UK; more than twelve of these are expected to have died of their disease after 10 years (CRUK, 2015g). If improvements are to be made in the prognosis of ovarian cancer, efforts must be focussed on the development of effective screening methods. Disease detected at stage I benefits from a 98% survival rate (CRUK, 2015h) and an effective and fast, single point screening assay would increase the amount of ovarian cancers detected at this stage.

### **7.2 How is the mTOR pathway implicated in ovarian cancer?**

The mTOR pathway is responsible for the control of growth and proliferation in response to cellular and extracellular cues (Laplante and Sabatini, 2012). mTOR pathway deregulation has been shown in patients as well as *in vivo* and *in vitro* studies of ovarian cancer and the mTOR pathway represents a potential target in the treatment of this disease (Castellvi *et al.*, 2006; No *et al.*, 2011; Zhang *et al.*,

2015; Masoumi-Moghaddam *et al.*, 2015; De Marco *et al.*, 2013; Zhou and Wong, 2006; Meng *et al.*, 2006; Pon *et al.*, 2008; Bian *et al.*, 2010; Ip *et al.*, 2014; Im-aram *et al.*, 2013; Foster *et al.*, 2010). We showed that the mTOR pathway components show differential patterns of expression in ovarian cancer and endometriosis. We used fibroids and endometrial cancer as a benign and malignant comparison of conditions unrelated to ovarian cancer and showed that neither condition resembles ovarian cancer in terms of mTOR complex component expression profile. We showed that mTOR complex inhibitor DEPTOR is increased in tumour tissue and blood from ovarian cancer patients but decreased in later stage and higher grade disease when phosphorylation of p70S6 kinase increases, indicating increased mTORC1 signalling. *In silico* cancer survival analysis by Kaplan-Meier plot showed that mTOR component expression plays a role in survival. High expression of DEPTOR relates to improved overall survival. mTOR is not related to survival unless the *TP53* gene, encoding the p53 tumour suppressor gene is mutated. In these cases, survival is improved for patients who express lower levels of mTOR. Collectively, these data present strong evidence of DEPTOR modulation in the progression of ovarian cancer.

### **7.3 What role does mTOR pathway inhibition play in the treatment of ovarian cancer?**

In this study we showed that SKOV3 and MDAH-2774 cells have no apoptotic response to mTOR pathway inhibition by demonstrating no caspase pathway activation and no increase in dead cell number in response to Rapamycin, rapalogues, Resveratrol or NVP BEZ-235. However, we were able to show that Rapamycin, rapalogues and dual inhibitors exert a cytostatic effect on these cells. Previous studies have shown that rapalogues can potentiate the cytotoxic effects of DNA damaging agents such as Tamoxifen, Doxorubicin, UCN-01 and Cisplatin, even at levels below their usual efficacy (Treeck *et al.*, 2006; Avellino *et al.*, 2005; Hahn *et al.*, 2005; Beuvink *et al.*, 2005), providing evidence that mTOR pathway inhibition is an effective combinatorial approach to the treatment of ovarian cancer. At the time of writing, a vast number of clinical trials investigating the use of combinatorial

mTOR pathway inhibitors in ovarian cancer are underway; a number of these are detailed in Table 7.1.

<b>mTOR Pathway Inhibitor(s)</b>	<b>Title of Study</b>
<b>Rapamycin</b>	Vaccine Therapy With or Without Sirolimus in Treating Patients With NY-ESO-1 Expressing Solid Tumors
<b>Everolimus</b>	Single Arm Trial With Combination of Everolimus and Letrozole in Treatment of Platinum Resistant Relapse or Refractory or Persistent Ovarian Cancer/Endometrial Cancer
<b>Deforolimus</b>	Carboplatin/Taxol/Ridaforolimus in Endometrial, Ovarian and Solids
<b>Temsirolimus</b>	Temsirolimus, Carboplatin, and Paclitaxel as First-Line Therapy in Treating Patients With Newly Diagnosed Stage III-IV Clear Cell Ovarian Cancer

**Table 7.1** - Examples of currently active clinical trials using rapalogues in the treatment of ovarian cancer (Table adapted from [clinicaltrials.gov](http://clinicaltrials.gov)).

Despite the vast heterogeneity detected in ovarian cancers, there is no divergence in therapeutic techniques. In demonstrating that MDAH-2774 cells are more resistant to mTOR pathway inhibition, we have highlighted the need for personalised medicine in the treatment of different ovarian cancer subtypes. Tumour heterogeneity must be accounted for in ovarian cancer therapeutics.

#### **7.4 How could CTCs form the basis of a PoCT for ovarian cancer?**

CTCs are tumour cells which have dissociated from a primary or metastatic tumour and are present in the circulatory system (Azevedo *et al.*, 2015). CTCs have been detected in many cancers including breast, ovarian and prostate (Engel *et al.*, 1999; Lowes *et al.*, 2015). CTCs are thought to be a major cause of metastasis although little is known of the mechanism by which they enter the bloodstream or colonise



new locations (Azevedo *et al.*, 2015). Despite this, CTCs represent a useful, minimally invasive source of cancer RNA, known as a liquid biopsy, for biomarker detection by qPCR. We have demonstrated a preliminary proof of principle assay showing that DEPTOR RNA is upregulated in the blood of ovarian cancer patients and can be detected by qPCR. Genetic analysis by liquid biopsy could provide a window into a PoC diagnostic test for ovarian cancer. Further work needs to expand this study with a larger cohort of patients in order to confirm our findings.

### **7.5 What are the limitations of this research?**

Interpatient variation is likely to mask trends in gene and protein changes, particularly if they are subtle, that may be seen in respective cancer types. In this study, cDNA synthesised from clinical samples was used to assess the expressional change of mTOR signalling component genes; paraffin embedded tissue samples were used to visualise protein expression of these components. Samples were taken from individual patient tumours (or unaffected tissue) and specific gene aberrations are unlikely to be identical to any other patient in the cohort; ovarian cancer is recognised as a strikingly heterogenous condition. The higher standard deviation of RQ values and percentage of positively stained cells seen in this study may be due to interpatient variation and may translate to a lack of statistical significance in some of the changes seen. For example, in the cases of fibroids and endometrial cancer, a marked decrease in raptor gene expression can be seen; however, no statistical significance can be garnered from the change. High interpatient variation in ovarian cancer, due to individual differences, provides an additional hurdle in the quest for a suitable method of early diagnosis and prognostic prediction (Jordan *et al.*, 2003; Prado *et al.*, 2014).

Tumour composition can also be highly heterogenous and recent developments in single-cell analytics have shown that cells from the same tumour may be geno- and phenotypically different from one another. Single cells taken from tumour tissue have shown modulations in oncogenic, proliferative and immune signalling, differential response to UVB irradiation and chemotherapeutics, differences in PI3

kinase mutation and gene expression of multiple transcripts including *ERBB2*, growth factor receptors and *KRAS* (Miwa *et al.*, 2015; Kim *et al.*, 2015; Janiszewska *et al.*, 2015; Shalek *et al.*, 2014; Patel *et al.*, 2014). This type of heterogeneity has also been noted in cultured cells (Shalek *et al.*, 2013; Bai *et al.*, 2015) and the SKOV3 cell line has been shown to contain cells with high and low invasive and migratory potential (Bai *et al.*, 2015). SKOV3 cells with increased and decreased invasive potential differ in their proliferative rate (higher in highly invasive cells), apoptotic rate (lower in highly invasive cells), response to cisplatin and taxol (lower in highly invasive cells) and tumourigenicity in nude mice (higher in highly invasive cells) (Bai *et al.*, 2015). SKOV3 cells also showed differential expression of mTOR pathway components including higher gene and protein expression of *PIK3CA* and *mTOR* and lower gene and protein expression of *PTEN* in highly invasive cells (Bai *et al.*, 2015). These data present evidence of previously uncharacterised diversity between cells within the same culture. This may provide an explanation of the high level of variability seen in experiments involving SKOV3 and MDAH-2774 cell lines.

In addition to inter-patient variation, another cause for increased variability in immunohistochemical analysis is the variable nature of the analysis method. As mentioned, ovarian tumours can be highly heterogenous and different cell types within a tumour may express mTOR pathway components to different extents. Each tissue sample was taken from an unspecified area of a tumour and may have contained multiple tissue types that were phenotypically different. Three areas of each tissue sample were selected at random and total and positive number of cells were counted. The amount of positively stained cells may have varied from area to area depending on the area of tumour being observed. Immunohistochemistry by DAB staining is a semi-quantitative method of analysis; number of cells showing expression are counted but expression levels cannot be determined using this method as DAB does not follow Beer-Lambert's law (there is not a direct relationship between staining intensity and protein expression) (van der Loos, 2008). This may account for discrepancies between gene and protein expression. RNA was extracted from a large tissue sample which was likely to contain multiple tumour cell types; however, only three small areas of tissue were samples for

protein expression. It is less likely that analysis of protein expression would have taken into account as many areas of the tumour as RNA expression analysis did and therefore may have excluded areas containing cells expressing high or low levels of mTOR, DEPTOR, rictor, raptor and phosphorylated p70S6 kinase, masking any significant increases or decreases in expression.

On a wider scale, tumour heterogeneity may present a barrier to effective treatment. Ovarian cancer has a low survival rate in part due to a high rate of chemotherapy resistance. A tumour which appears primarily responsive to chemotherapy often develops resistance and recurrence rate is high. This may be due to a subpopulation of resistant cells which remain and continue to proliferate after treatment.

## **7.6 What are the future directions of this work?**

### **7.6.1 Increase sample size**

We have investigated expression of mTOR pathway components in ovarian tumour tissue samples (n=13) and whole blood (n=7) from ovarian cancer patients. In future, these results must be expanded to include a larger clinical cohort in order to confirm the changes seen in this study. The differences seen between stages, grades and types of ovarian cancer should be further characterised in a larger population of patients as this could be used to better understand prognostic factors. As aspects such as ethnicity can affect gene expression (Knappskog *et al.*, 2014), patients from a wide range of backgrounds should be included. In addition to this, immunohistochemical staining should also be performed on unaffected control tissues in order to further dissect the changes that occur in mTOR, DEPTOR, rictor, raptor and p70S6 kinase expression in ovarian cancer patients.

### 7.6.2 Optimise PoC blood assay

We were able to demonstrate an increase in DEPTOR mRNA in the blood of ovarian cancer patients by qPCR. This assay should be optimised for use on a fast thermal cycler such as xpress® for development for use as a PoCT. Below is a flow diagram depicting a proposed screening method for ovarian cancer patients. The majority of ovarian cancers present over the age of 50 years (CRUK, 2012) however, patients with familial *BRCA* mutation are at high risk of ovarian cancer under this age (Ingham *et al.*, 2013; Mavaddat *et al.*, 2013). We propose that patients over 50 and high risk patients are screened annually. A negative result should be accompanied by information on the symptoms of ovarian cancer (i.e. abdominal distension, early satiety, irritable bowel syndrome-like symptoms) for self-monitoring. A positive result can initiate further testing such as transvaginal ultrasound to confirm diagnosis and more prompt commencement of treatment (Figure 7.1).

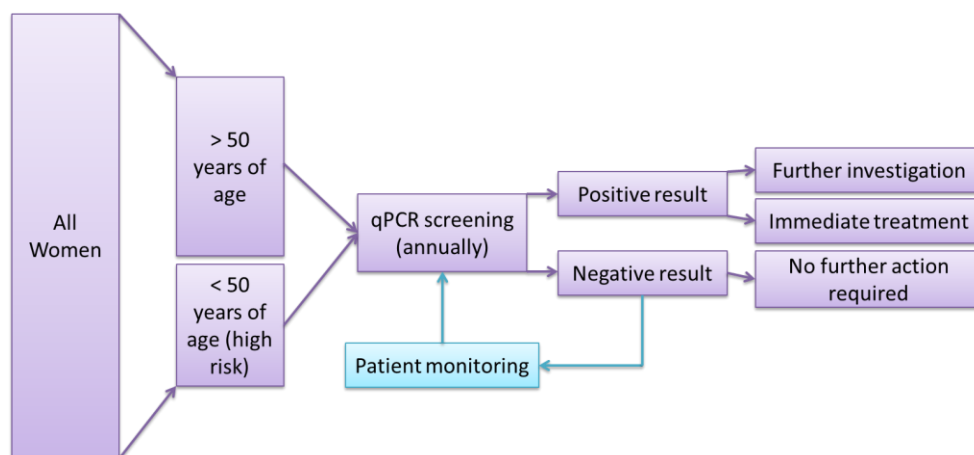


**Figure 7.1** - Suggested patient screening stream. Patients over 50 years of age and high risk patients should be screened annually for ovarian cancer biomarkers such as DEPTOR. A positive result prompts further confirmation such as transvaginal ultrasound and earlier commencement of treatment.

### 7.6.3 Further elucidate the cytostatic effects of mTOR pathway inhibition

We observed cytostatic effects exerted by mTOR pathway inhibitors in SKOV3 and MDAH-2774 cell lines. Future work should look at cell cycle progression markers

such as the expression of cyclin B1 and phosphorylation of cyclin dependent kinase 1 (CDK1) which are increased at G<sub>2</sub>/M transition (Porter and Donoghue, 2003) and proliferating cell nuclear antigen (PCNA) which increases at the G<sub>1</sub>/S transition (Stewart and Dell'orco, 1992) by qPCR and western blot in order to further examine cell cycle arrest in these cells. Further understanding of how mTOR pathway inhibitors cause cytostatic effects will allow greater exploitation of their benefits.

#### **7.6.4 Use additional *in vitro* models to study the effects of mTOR pathway inhibition**

This study used two epithelial ovarian adenocarcinoma cell lines as *in vitro* models of ovarian cancer. The cell lines differed in their cells of origin, SKOV3 cells are clear cell derived and MDAH-2774 are endometrioid. Using these cell lines we were able to study the two forms of malignancy most associated with endometriosis (Pearce *et al.*, 2012; Brinton *et al.*, 2005; Merritt *et al.*, 2008). However, a useful addition to this comparison may have been a non-malignant ovarian surface epithelial cell line such as the IOSE (immortalised ovarian surface epithelial) cell line or TIOSE (telomerase immortalised ovarian surface epithelial) cell line (Lanitis *et al.*, 2012; Zorn *et al.*, 2003). In addition to non-malignant ovarian surface epithelial cells, a human endometriosis cell line such as FbEM-1 cell line (Bouquet de Jolinière *et al.*, 1997) would have provided a useful insight into how proliferation, mTOR pathway activation, apoptosis and wound healing differ in endometriosis, a strong ovarian cancer risk factor.

#### **7.6.5 Investigate the role of MAP kinase signalling in ovarian cancer**

We demonstrated that MDAH-2774 cells have a higher proliferative capacity, increased mTOR and raptor expression and are less responsive to mTOR pathway inhibition than SKOV3 cells and suggest that this may be due to MAP kinase pathway upregulation. The MAP kinase pathway is an upstream regulator of mTOR signalling (Ma and Blenis, 2009) and additional inhibition of this pathway may provide a supplementary source of mTOR inhibition and anticancer therapy in the

subset of ovarian cancer patients with *KRAS* and *BRAF* mutation. The effects of inhibitors such as UO126 (MEK1/2 inhibitor), 6H05 (K-Ras inhibitor) and AZ 628 (B-Raf inhibitor) on proliferation should be studied in combination with mTOR and PI3 kinase inhibitors in cell lines both with and without MAP kinase pathway mutation to determine if this pathway does indeed play a role in increasing mTOR signalling and if it could provide a target for anticancer therapy.

#### **7.6.6 Elucidate the subcellular localisation of mTOR complexes**

Currently, little is known of the location of mTOR complexes within cells and reports have located it in mitochondria of mouse embryonic fibroblasts (3T3) (Desai *et al.*, 2002), at the cellular membranes of cervical cancer cells (HeLa) (Sabatini *et al.*, 1999), in the nuclei of rhabdomyosarcoma cell lines (Rh1, Rh30 and Rh41), colon carcinoma cell lines (HCT8, HCT29 and HCT116) and normal human fibroblasts (IMR90) and in the cytoplasm of human embryonic kidney (HEK293) and ovarian cancer (SKOV3) cells (Zhang *et al.*, 2002; Foster *et al.*, 2010). One report has suggested that mTOR may migrate between the cytoplasm and nucleus and that this shuttling is required for activation of mTOR downstream effectors p70S6 kinase and 4EBP1 (Kim and Chen, 2000). Given the wide functional range of the mTOR pathway, it is unsurprising that the subcellular localisation of mTOR complexes varies. The localisation of mTOR is likely to be cell and context specific and may have implications in therapeutic targeting of the mTOR pathway. Future work should focus on clarifying mTOR location in ovarian cancer cell lines in order to further understand how this affects mTOR pathway function. It would also be interesting to investigate if mTOR localisation or shuttling behaviour is changed in response to treatment with pathway inhibitors. Further understanding of this may allow us to fully discern how mTOR inhibition exerts downstream effects.

#### **7.6.7 Investigate the stoichiometry of the DEPTOR/mTOR interaction**

DEPTOR interacts with mTOR and is an mTORC1 and mTORC2 inhibitor which can be down or upregulated in cancer. We have shown that DEPTOR expression is a

positive prognostic marker in ovarian cancer and is increased in response to mTOR pathway inhibition, indicating that it functions as a tumour suppressor gene. Conversely, we have also shown that DEPTOR expression is upregulated in the tumour tissue and blood of ovarian cancer patients and decreased in higher grade disease, suggesting oncogenic properties. As described previously, DEPTOR depletion activates both mTORC1 and mTORC2 activity but paradoxically, DEPTOR overexpression can upregulate mTORC2 activity in a range of cell lines (Peterson *et al.*, 2009). This suggests that inhibition of mTORC2 by DEPTOR is not as robust as that of mTORC1 and indicates that DEPTOR does not interact with each mTOR complex identically. By modifying DEPTOR expression in ovarian cancer cell lines and assessing activation of mTORC1 (p70S6 kinase Thr<sup>389</sup>, 4EBP1 Thr<sup>37/46</sup>) or mTORC2 (Akt Ser<sup>473</sup>) specific downstream effectors, the specific effects of DEPTOR in ovarian cancer cells can be studied. In addition, performing colocalisation experiments on DEPTOR with mTORC1 and mTORC2 components under basal conditions and in the presence of mTOR inhibitors will allow us to further understand the stoichiometry of DEPTOR within the mTOR complexes.

The mTOR complexes differ in their accessory components and there is evidence mTORC1 and mTORC2 signalling is in competition (Martin *et al.*, 2014). We have demonstrated evidence that components specific to each complex are deregulated in gynaecological disease. It would be useful to further elucidate the process by which the cell selects for mTOR complexes to increase understanding of the balance of mTORC1 and mTORC2 signalling in order to discern how these pathways are affected in disease states.

## **7.7 Concluding Remarks**

The exact causes of both ovarian cancer and endometriosis remains elusive with often conflicting data. The mTOR pathway represents a potential connection between endometriosis and ovarian cancer and a possible indication as to the high incidence of ovarian cancer in endometriosis patients. In addition, the mTOR pathway may represent a druggable target in the treatment of ovarian cancer and

endometriosis. Efficacy of mTOR pathway inhibition has thus far been low, in part due to lack of knowledge of the feedback mechanisms present within the mTOR pathway which serve to overcome inhibition. More work must be done to elucidate the activity of the mTOR pathway within ovarian cancer and endometriosis and to understand in full the effects of mTOR pathway component inhibition on overall activity.

PoCT is the ultimate goal in the development of diagnostics. Due to the inefficacious diagnosis of ovarian cancer resulting from a lack of early physical symptoms, and the invasive procedures currently used to diagnose endometriosis, it is crucial to determine detectable biomarkers in both conditions with a view to better detecting and treating them. Both conditions would benefit greatly from PoCT.



# Chapter 8

## Bibliography

Acién, P., Velasco, I., Acién, M., Capello, C., Vela, P. (2015) Epithelial ovarian cancers and endometriosis. *Gynecologic and Obstetric Investigation*. **79**(2), 126–135.

AddexBio (2015) MDAH-2774 Cells. *AddexBio*. [online]. Available from: <http://www.addexbio.com/productdetail?pid=57>.

Afshar, Y., Hastings, J., Roqueiro, D., Jeong, J.-W., Giudice, L.C., Fazleabas, A.T. (2013) Changes in eutopic endometrial gene expression during the progression of experimental endometriosis in the baboon, *Papio anubis*. *Biology of Reproduction*. **88**(2), 44.

Akane, A., Matsubara, K., Nakamura, H., Takahashi, S., Kimura, K. (1994) Identification of the heme compound copurified with deoxyribonucleic acid (DNA) from bloodstains, a major inhibitor of polymerase chain reaction (PCR) amplification. *Journal of Forensic Sciences*. **39**(2), 362–372.

Alessi, D.R., James, S.R., Downes, C.P., Holmes, A.B., Gaffney, P.R., Reese, C.B., Cohen, P. (1997) Characterization of a 3-phosphoinositide-dependent protein kinase which phosphorylates and activates protein kinase Balpha. *Current Biology*. **7**(4), 261–269.

Alexandre, J., Ray-Coquard, I., Selle, F., Floquet, A., Cottu, P., Weber, B., Falandry, C., Lebrun, D., Pujade-Lauraine, E., GINECO (2010) Mucinous advanced epithelial ovarian carcinoma: clinical presentation and sensitivity to platinum–paclitaxel-based chemotherapy, the GINECO experience. *Annals of Oncology*. **21**(12), 2377–2381.

Amato, R., Menniti, M., Agosti, V., Boito, R., Costa, N., Bond, H.M., Barbieri, V., Tagliaferri, P., Venuta, S., Perrotti, N. (2007) IL-2 signals through Sgk1 and inhibits proliferation and apoptosis in kidney cancer cells. *Journal of Molecular Medicine*. **85**(7), 707–721.

Amemiya, S., Sekizawa, A., Otsuka, J., Tachikawa, T., Saito, H., Okai, T. (2004) Malignant transformation of endometriosis and genetic alterations of K-ras and microsatellite instability. *International Journal of Gynecology & Obstetrics*. **86**(3), 371–376.

American Society for Reproductive Medicine (1997) Revised American Society for Reproductive Medicine classification of endometriosis: 1996. *Fertility and Sterility*. **67**(5), 817–821.

Aoyama, T., Matsui, T., Novikov, M., Park, J., Hemmings, B., Rosenzweig, A. (2005) Serum and glucocorticoid-responsive kinase-1 regulates cardiomyocyte survival and hypertrophic response. *Circulation*. **111**(13), 1652–1659.

Arumugam, A., Parada, J., Rajkumar, L. (2012) Mammary cancer promotion by ovarian hormones involves IGFR/AKT/mTOR signaling. *Steroids*. **77**(7), 791–797.

ATCC (2014) SK-OV-3 [SKOV-3; SKOV3] (ATCC® HTB-77™). ATCC. [online]. Available from: <http://www.lgcstandards-atcc.org/Products/All/HTB-77.aspx>.

Avellino, R., Romano, S., Parasole, R., Bisogni, R., Lamberti, A., Poggi, V., Venuta, S., Romano, M.F. (2005) Rapamycin stimulates apoptosis of childhood acute lymphoblastic leukemia cells. *Blood*. **106**(4), 1400–1406.

Azevedo, S., Follain, G., Patthabhiraman, S., Harlepp, S., Goetz, J.G. (2015) Metastasis of circulating tumor cells: favorable soil or suitable biomechanics, or both? *Cell Adhesion & Migration*. **9**(5), 345–356.

Bai, H., Li, H., Li, W., Gui, T., Yang, J., Cao, D., Shen, K. (2015) The PI3K/AKT/mTOR pathway is a potential predictor of distinct invasive and migratory capacities in human ovarian cancer cell lines. *Oncotarget*. **6**(28), 25520–25532.

Baskin, R., Sayeski, P.P. (2012) Angiotensin II mediates cell survival through upregulation and activation of the serum and glucocorticoid inducible kinase 1. *Cellular Signalling*. **24**(2), 435–442.

Beaufort, C.M., Helmijr, J.C.A., Piskorz, A.M., Hoogstraat, M., Ruigrok-Ritstier, K., Besselink, N., Murtaza, M., van IJcken, W.F.J., Heine, A.A.J., Smid, M., Koudijs, M.J., Brenton, J.D., Berns, E.M.J.J., Helleman, J. (2014) Ovarian Cancer Cell Line Panel (OCCP): Clinical Importance of In Vitro Morphological Subtypes. *PLoS ONE*. **9**(9), e103988.

Benjamin, D., Colombi, M., Moroni, C., Hall, M.N. (2011) Rapamycin passes the torch: a new generation of mTOR inhibitors. *Nature Reviews. Drug Discovery*. **10**(11), 868–880.

Beral, V., Million Women Study Collaborators, Bull, D., Green, J., Reeves, G. (2007) Ovarian cancer and hormone replacement therapy in the Million Women Study. *Lancet*. **369**(9574), 1703–1710.

Berek, J.S. (2007) *Berek & Novak's Gynecology*. Lippincott Williams & Wilkins.

Beuvink, I., Boulay, A., Fumagalli, S., Zilbermann, F., Ruetz, S., O'Reilly, T., Natt, F., Hall, J., Lane, H.A., Thomas, G. (2005) The mTOR inhibitor RAD001 sensitizes tumor cells to DNA-damaged induced apoptosis through inhibition of p21 translation. *Cell*. **120**(6), 747–759.

- Bian, C.-X., Shi, Z., Meng, Q., Jiang, Y., Liu, L.-Z., Jiang, B.-H. (2010) P70S6K 1 regulation of angiogenesis through VEGF and HIF-1alpha expression. *Biochemical and Biophysical Research Communications*. **398**(3), 395–399.
- Bio-Rad (2015) CFX96 Real-Time PCR Detection System. [online]. Available from: [http://www.bio-rad.com/webroot/web/pdf/lsr/literature/Bulletin\\_5589.pdf](http://www.bio-rad.com/webroot/web/pdf/lsr/literature/Bulletin_5589.pdf).
- BJS Biotechnologies (2015a) The xpress direct resistive heating system. [online]. Available from: <http://xpresspcr.com/technology/>.
- BJS Biotechnologies (2015b) xpress PCR. *xpress*. [online]. Available from: <http://xpresspcr.com/>.
- Blommaart, E.F., Luiken, J.J., Blommaart, P.J., van Woerkom, G.M., Meijer, A.J. (1995) Phosphorylation of ribosomal protein S6 is inhibitory for autophagy in isolated rat hepatocytes. *The Journal of Biological Chemistry*. **270**(5), 2320–2326.
- Böhm, A., Aichberger, K.J., Mayerhofer, M., Herrmann, H., Florian, S., Krauth, M.-T., Derdak, S., Samorapoompichit, P., Sonneck, K., Vales, A., Gleixner, K.V., Pickl, W.F., Sperr, W.R., Valent, P. (2009) Targeting of mTOR is associated with decreased growth and decreased VEGF expression in acute myeloid leukaemia cells. *European Journal of Clinical Investigation*. **39**(5), 395–405.
- Bonome, T., Levine, D.A., Shih, J., Randonovich, M., Pise-Masison, C.A., Bogomolny, F., Ozbun, L., Brady, J., Barrett, J.C., Boyd, J., Birrer, M.J. (2008) A gene signature predicting for survival in suboptimally debulked patients with ovarian cancer. *Cancer Research*. **68**(13), 5478–5486.
- Borgfeldt, C., Andolf, E. (2004) Cancer risk after hospital discharge diagnosis of benign ovarian cysts and endometriosis. *Acta Obstetrica Et Gynecologica Scandinavica*. **83**(4), 395–400.
- Bouquet de Jolinière, J., Validire, P., Canis, M., Doussau, M., Levardon, M., Gogusev, J. (1997) Human endometriosis-derived permanent cell line (FbEM-1): establishment and characterization. *Human Reproduction Update*. **3**(2), 117–123.
- Brana, I., Berger, R., Golan, T., Haluska, P., Edenfield, J., Fiorica, J., Stephenson, J., Martin, L.P., Westin, S., Hanjani, P., Jones, M.B., Almhanna, K., Wenham, R.M., Sullivan, D.M., Dalton, W.S., Gunchenko, A., Cheng, J.D., Siu, L.L., Gray, J.E. (2014) A parallel-arm phase I trial of the humanised anti-IGF-1R antibody dalotuzumab in combination with the AKT inhibitor MK-2206, the mTOR inhibitor ridaforolimus, or the NOTCH inhibitor MK-0752, in patients with advanced solid tumours. *British Journal of Cancer*. **111**(10), 1932–1944.
- Brinton, L.A., Gridley, G., Persson, I., Baron, J., Bergqvist, A. (1997) Cancer risk after a hospital discharge diagnosis of endometriosis. *American Journal of Obstetrics and Gynecology*. **176**(3), 572–579.

- Brinton, L.A., Lamb, E.J., Moghissi, K.S., Scoccia, B., Althuis, M.D., Mabie, J.E., Westhoff, C.L. (2004) Ovarian cancer risk associated with varying causes of infertility. *Fertility and Sterility*. **82**(2), 405–414.
- Brinton, L.A., Sakoda, L.C., Sherman, M.E., Frederiksen, K., Kjaer, S.K., Graubard, B.I., Olsen, J.H., Mellekjaer, L. (2005) Relationship of benign gynecologic diseases to subsequent risk of ovarian and uterine tumors. *Cancer Epidemiology, Biomarkers & Prevention*. **14**(12), 2929–2935.
- Brock, T.D., Freeze, H. (1969) *Thermus aquaticus* gen. n. and sp. n., a Nonsporulating Extreme Thermophile. *Journal of Bacteriology*. **98**(1), 289–297.
- Brown, E.J., Albers, M.W., Shin, T.B., Ichikawa, K., Keith, C.T., Lane, W.S., Schreiber, S.L. (1994) A mammalian protein targeted by G1-arresting rapamycin-receptor complex. *Nature*. **369**(6483), 756–758.
- Brown, E.J., Beal, P.A., Keith, C.T., Chen, J., Shin, T.B., Schreiber, S.L. (1995) Control of p70 s6 kinase by kinase activity of FRAP in vivo. *Nature*. **377**(6548), 441–446.
- Brugarolas, J., Lei, K., Hurley, R.L., Manning, B.D., Reiling, J.H., Hafen, E., Witters, L.A., Ellisen, L.W., Kaelin, W.G. (2004) Regulation of mTOR function in response to hypoxia by REDD1 and the TSC1/TSC2 tumor suppressor complex. *Genes & Development*. **18**(23), 2893–2904.
- Brünner-Kubath, C., Shabbir, W., Saferding, V., Wagner, R., Singer, C.F., Valent, P., Berger, W., Marian, B., Zielinski, C.C., Grusch, M., Grunt, T.W. (2011) The PI3 kinase/mTOR blocker NVP-BEZ235 overrides resistance against irreversible ErbB inhibitors in breast cancer cells. *Breast Cancer Research and Treatment*. **129**(2), 387–400.
- Budanov, A.V., Karin, M. (2008) p53 target genes sestrin1 and sestrin2 connect genotoxic stress and mTOR signaling. *Cell*. **134**(3), 451–460.
- Burnett, P.E., Barrow, R.K., Cohen, N.A., Snyder, S.H., Sabatini, D.M. (1998) RAFT1 phosphorylation of the translational regulators p70 S6 kinase and 4E-BP1. *Proceedings of the National Academy of Sciences of the United States of America*. **95**(4), 1432–1437.
- Burney, R.O., Lathi, R.B. (2009) Menstrual bleeding from an endometriotic lesion. *Fertility and Sterility*. **91**(5), 1926–1927.
- Bustin, S.A., Benes, V., Garson, J.A., Hellemans, J., Huggett, J., Kubista, M., Mueller, R., Nolan, T., Pfaffl, M.W., Shipley, G.L., Vandesompele, J., Wittwer, C.T. (2009) The MIQE guidelines: minimum information for publication of quantitative real-time PCR experiments. *Clinical Chemistry*. **55**(4), 611–622.
- Buys, S.S., Partridge, E., Black, A., Johnson, C.C., Lamerato, L., Isaacs, C., Reding, D.J., Greenlee, R.T., Yokochi, L.A., Kessel, B., Crawford, E.D., Church, T.R., Andriole, G.L., Weissfeld, J.L., Fouad, M.N., Chia, D., O'Brien, B., Ragard, L.R., Clapp, J.D., Rathmell,

- J.M., Riley, T.L., Hartge, P., Pinsky, P.F., Zhu, C.S., Izmirlian, G., Kramer, B.S., Miller, A.B., Xu, J.-L., Prorok, P.C., Gohagan, J.K., Berg, C.D., PLCO Project Team (2011) Effect of screening on ovarian cancer mortality: the Prostate, Lung, Colorectal and Ovarian (PLCO) Cancer Screening Randomized Controlled Trial. *JAMA*. **305**(22), 2295–2303.
- Cafferkey, R., Young, P.R., McLaughlin, M.M., Bergsma, D.J., Koltin, Y., Sathe, G.M., Faucette, L., Eng, W.K., Johnson, R.K., Livi, G.P. (1993) Dominant missense mutations in a novel yeast protein related to mammalian phosphatidylinositol 3-kinase and VPS34 abrogate rapamycin cytotoxicity. *Molecular and Cellular Biology*. **13**(10), 6012–6023.
- Callahan, M.J., Crum, C.P., Medeiros, F., Kindelberger, D.W., Elvin, J.A., Garber, J.E., Feltmate, C.M., Berkowitz, R.S., Muto, M.G. (2007) Primary Fallopian Tube Malignancies in BRCA-Positive Women Undergoing Surgery for Ovarian Cancer Risk Reduction. *Journal of Clinical Oncology*. **25**(25), 3985–3990.
- Campbell, I.G., Russell, S.E., Choong, D.Y.H., Montgomery, K.G., Ciavarella, M.L., Hooi, C.S.F., Cristiano, B.E., Pearson, R.B., Phillips, W.A. (2004) Mutation of the PIK3CA gene in ovarian and breast cancer. *Cancer Research*. **64**(21), 7678–7681.
- Campbell, L., Jasani, B., Edwards, K., Gumbleton, M., Griffiths, D.F.R. (2008) Combined expression of caveolin-1 and an activated AKT/mTOR pathway predicts reduced disease-free survival in clinically confined renal cell carcinoma. *British Journal of Cancer*. **98**(5), 931–940.
- Carpenter, C.L., Duckworth, B.C., Auger, K.R., Cohen, B., Schaffhausen, B.S., Cantley, L.C. (1990) Purification and characterization of phosphoinositide 3-kinase from rat liver. *The Journal of Biological Chemistry*. **265**(32), 19704–19711.
- Carpten, J.D., Faber, A.L., Horn, C., Donoho, G.P., Briggs, S.L., Robbins, C.M., Hostetter, G., Boguslawski, S., Moses, T.Y., Savage, S., Uhlik, M., Lin, A., Du, J., Qian, Y.-W., Zeckner, D.J., Tucker-Kellogg, G., Touchman, J., Patel, K., Mousset, S., Bittner, M., Schevitz, R., Lai, M.-H.T., Blanchard, K.L., Thomas, J.E. (2007) A transforming mutation in the pleckstrin homology domain of AKT1 in cancer. *Nature*. **448**(7152), 439–444.
- Carracedo, A., Ma, L., Teruya-Feldstein, J., Rojo, F., Salmena, L., Alimonti, A., Egia, A., Sasaki, A.T., Thomas, G., Kozma, S.C., Papa, A., Nardella, C., Cantley, L.C., Baselga, J., Pandolfi, P.P. (2008) Inhibition of mTORC1 leads to MAPK pathway activation through a PI3K-dependent feedback loop in human cancer. *The Journal of Clinical Investigation*. **118**(9), 3065–3074.
- Carracedo, A., Pandolfi, P.P. (2008) The PTEN-PI3K pathway: of feedbacks and cross-talks. *Oncogene*. **27**(41), 5527–5541.
- Castellvi, J., Garcia, A., Rojo, F., Ruiz-Marcellan, C., Gil, A., Baselga, J., Ramon y Cajal, S. (2006) Phosphorylated 4E binding protein 1: a hallmark of cell signaling that correlates with survival in ovarian cancer. *Cancer*. **107**(8), 1801–1811.

- Cepheid (2015) Cepheid | Healthcare Associated Infections. *Cepheid*. [online]. Available from: <http://www.cepheid.com/us/cepheid-solutions/clinical-ivd-tests/healthcare-associated-infections> [Accessed August 30, 2015].
- Chatthotikawong, U., Ruengkachorn, I., Leelaphatanadit, C., Phithakwatchara, N. (2015) 8-year analysis of the prevalence of lymph nodes metastasis, oncologic and pregnancy outcomes in apparent early-stage malignant ovarian germ cell tumors. *Asian Pacific journal of cancer prevention: APJCP*. **16**(4), 1609–1613.
- Chen, H., Yang, X., Feng, Z., Tang, R., Ren, F., Wei, K., Chen, G. (2015) Prognostic value of Caspase-3 expression in cancers of digestive tract: a meta-analysis and systematic review. *International Journal of Clinical and Experimental Medicine*. **8**(7), 10225–10234.
- Chen, J., Holguin, N., Shi, Y., Silva, M.J., Long, F. (2015) mTORC2 Signaling Promotes Skeletal Growth and Bone Formation in Mice. *Journal of bone and mineral research : the official journal of the American Society for Bone and Mineral Research*. **30**(2), 369–378.
- Chen, J., Zheng, X.F., Brown, E.J., Schreiber, S.L. (1995) Identification of an 11-kDa FKBP12-rapamycin-binding domain within the 289-kDa FKBP12-rapamycin-associated protein and characterization of a critical serine residue. *Proceedings of the National Academy of Sciences of the United States of America*. **92**(11), 4947–4951.
- Chiaffarino, F., Parazzini, F., Bosetti, C., Franceschi, S., Talamini, R., Canzonieri, V., Montella, M., Ramazzotti, V., Franceschi, S., La Vecchia, C. (2007) Risk factors for ovarian cancer histotypes. *European Journal of Cancer*. **43**(7), 1208–1213.
- Cho, K.R. (2009) Ovarian cancer update: lessons from morphology, molecules, and mice. *Archives of Pathology & Laboratory Medicine*. **133**(11), 1775–1781.
- Claffey, K.P., Robinson, G.S. (1996) Regulation of VEGF/VPF expression in tumor cells: consequences for tumor growth and metastasis. *Cancer Metastasis Reviews*. **15**(2), 165–176.
- Collaborative Group on Epidemiological Studies of Ovarian Cancer (2012) Ovarian cancer and body size: individual participant meta-analysis including 25,157 women with ovarian cancer from 47 epidemiological studies. *PLoS medicine*. **9**(4), e1001200.
- COSMIC (2015) COSMIC. *COSMIC: Cancer Browser*. [online]. Available from: <http://cancer.sanger.ac.uk/cosmic/browse/tissue>.
- CRUK (2015a) Bevacizumab (Avastin). *Cancer Research UK*. [online]. Available from: <http://www.cancerresearchuk.org/about-cancer/cancers-in-general/treatment/cancer-drugs/bevacizumab> [Accessed August 18, 2015].

CRUK (2015b) Bowel cancer survival statistics. *Cancer Research UK*. [online]. Available from: <http://www.cancerresearchuk.org/health-professional/cancer-statistics/statistics-by-cancer-type/bowel-cancer/survival> [Accessed September 23, 2015].

CRUK (2015c) Breast cancer survival statistics. *Cancer Research UK*. [online]. Available from: <http://www.cancerresearchuk.org/health-professional/cancer-statistics/statistics-by-cancer-type/breast-cancer/survival> [Accessed August 18, 2015].

CRUK (2015d) Cervical cancer survival statistics. *Cancer Research UK*. [online]. Available from: <http://www.cancerresearchuk.org/health-professional/cancer-statistics/statistics-by-cancer-type/cervical-cancer/survival> [Accessed September 23, 2015].

CRUK (2015e) Drugs used for ovarian cancer. *Cancer Research UK*. [online]. Available from: <http://www.cancerresearchuk.org/about-cancer/type/ovarian-cancer/treatment/drugs-used-for-ovarian-cancer> [Accessed August 18, 2015].

CRUK (2012) Ovarian cancer incidence statistics. *Cancer Research UK*. [online]. Available from: <http://www.cancerresearchuk.org/cancer-info/cancerstats/types/ovary/incidence/uk-ovarian-cancer-incidence-statistics#source12> [Accessed November 30, 2012].

CRUK (2015f) Ovarian cancer risk factors. *Cancer Research UK*. [online]. Available from: <http://www.cancerresearchuk.org/health-professional/cancer-statistics/statistics-by-cancer-type/ovarian-cancer/risk-factors> [Accessed August 24, 2015].

CRUK (2015g) Ovarian cancer statistics. *Cancer Research UK*. [online]. Available from: <http://www.cancerresearchuk.org/health-professional/cancer-statistics/statistics-by-cancer-type/ovarian-cancer> [Accessed September 23, 2015].

CRUK (2015h) Ovarian cancer survival statistics. *Cancer Research UK*. [online]. Available from: <http://www.cancerresearchuk.org/health-professional/cancer-statistics/statistics-by-cancer-type/ovarian-cancer/survival> [Accessed August 16, 2015].

CRUK (2015i) Prostate cancer survival statistics. *Cancer Research UK*. [online]. Available from: <http://www.cancerresearchuk.org/health-professional/cancer-statistics/statistics-by-cancer-type/prostate-cancer/survival> [Accessed September 23, 2015].

CRUK (2014a) Stages of ovarian cancer. *Cancer Research UK*. [online]. Available from: <http://www.cancerresearchuk.org/about-cancer/type/ovarian-cancer/treatment/stages-of-ovarian-cancer> [Accessed July 26, 2015].

CRUK (2014b) Types of ovarian cancer. *Cancer Research UK*. [online]. Available from: <http://www.cancerresearchuk.org/about-cancer/type/ovarian-cancer/about/types-of-ovarian-cancer> [Accessed July 25, 2015].

CRUK (2015j) Types of treatment for ovarian cancer. *Cancer Research UK*. [online]. Available from: <http://www.cancerresearchuk.org/about-cancer/type/ovarian-cancer/treatment/which-treatment-for-ovarian-cancer> [Accessed August 18, 2015].

CRUK (2015k) Uterine cancer survival statistics. *Cancer Research UK*. [online]. Available from: <http://www.cancerresearchuk.org/health-professional/cancer-statistics/statistics-by-cancer-type/uterine-cancer/survival> [Accessed September 23, 2015].

Das, F., Ghosh-Choudhury, N., Bera, A., Dey, N., Abboud, H.E., Kasinath, B.S., Choudhury, G.G. (2013) Transforming Growth Factor  $\beta$  Integrates Smad 3 to Mechanistic Target of Rapamycin Complexes to Arrest Deptor Abundance for Glomerular Mesangial Cell Hypertrophy. *The Journal of Biological Chemistry*. **288**(11), 7756–7768.

Datta, K., Bellacosa, A., Chan, T.O., Tsichlis, P.N. (1996) Akt Is a Direct Target of the Phosphatidylinositol 3-Kinase ACTIVATION BY GROWTH FACTORS, v-src and v-Ha-ras, IN Sf9 AND MAMMALIAN CELLS. *Journal of Biological Chemistry*. **271**(48), 30835–30839.

De Brabander, M., Geuens, G., Nuydens, R., Willebrords, R., De Mey, J. (1981) Taxol induces the assembly of free microtubules in living cells and blocks the organizing capacity of the centrosomes and kinetochores. *Proceedings of the National Academy of Sciences of the United States of America*. **78**(9), 5608–5612.

De Marco, C., Rinaldo, N., Bruni, P., Malzoni, C., Zullo, F., Fabiani, F., Losito, S., Scrima, M., Marino, F.Z., Franco, R., Quintiero, A., Agosti, V., Viglietto, G. (2013) Multiple genetic alterations within the PI3K pathway are responsible for AKT activation in patients with ovarian carcinoma. *PLoS One*. **8**(2), e55362.

Demir Weusten, A.Y., Groothuis, P.G., Dunselman, G.A., de Goeij, A.F., Arends, J.W., Evers, J.L. (2000) Morphological changes in mesothelial cells induced by shed menstrual endometrium in vitro are not primarily due to apoptosis or necrosis. *Human Reproduction*. **15**(7), 1462–1468.

Desai, B.N., Myers, B.R., Schreiber, S.L. (2002) FKBP12-rapamycin-associated protein associates with mitochondria and senses osmotic stress via mitochondrial dysfunction. *Proceedings of the National Academy of Sciences of the United States of America*. **99**(7), 4319–4324.

DeYoung, M.P., Horak, P., Sofer, A., Sgroi, D., Ellisen, L.W. (2008) Hypoxia regulates TSC1/2-mTOR signaling and tumor suppression through REDD1-mediated 14-3-3 shuttling. *Genes & Development*. **22**(2), 239–251.



- D'Hooghe, T.M., Debrock, S. (2002) Endometriosis, retrograde menstruation and peritoneal inflammation in women and in baboons. *Human Reproduction Update*. **8**(1), 84–88.
- Di Cosimo, S., Sathyanarayanan, S., Bendell, J.C., Cervantes, A., Stein, M.N., Braña, I., Roda, D., Haines, B.B., Zhang, T., Winter, C.G., Jha, S., Xu, Y., Frazier, J., Klinghoffer, R.A., Leighton-Swayze, A., Song, Y., Ebbinghaus, S., Baselga, J. (2015) Combination of the mTOR inhibitor ridaforolimus and the anti-IGF1R monoclonal antibody dalotuzumab: preclinical characterization and phase I clinical trial. *Clinical Cancer Research*. **21**(1), 49–59.
- Dinulescu, D.M., Ince, T.A., Quade, B.J., Shafer, S.A., Crowley, D., Jacks, T. (2005) Role of K-ras and Pten in the development of mouse models of endometriosis and endometrioid ovarian cancer. *Nature Medicine*. **11**(1), 63–70.
- Dong, Q., Zheng, S., Hu, Y., Chen, G., Ding, J.-Y. (2005) Evaluation of ST13 gene expression in colorectal cancer patients. *Journal of Zhejiang University. Science. B*. **6**(12), 1170–1175.
- Dowling, R.J.O., Topisirovic, I., Alain, T., Bidinosti, M., Fonseca, B.D., Petroulakis, E., Wang, X., Larsson, O., Selvaraj, A., Liu, Y., Kozma, S.C., Thomas, G., Sonenberg, N. (2010) mTORC1-mediated cell proliferation, but not cell growth, controlled by the 4E-BPs. *Science*. **328**(5982), 1172–1176.
- Dudek, H., Datta, S.R., Franke, T.F., Birnbaum, M.J., Yao, R., Cooper, G.M., Segal, R.A., Kaplan, D.R., Greenberg, M.E. (1997) Regulation of neuronal survival by the serine-threonine protein kinase Akt. *Science*. **275**(5300), 661–665.
- Dumont, F.J., Staruch, M.J., Koprak, S.L., Melino, M.R., Sigal, N.H. (1990) Distinct mechanisms of suppression of murine T cell activation by the related macrolides FK-506 and rapamycin. *Journal of Immunology*. **144**(1), 251–258.
- Dun, E.C., Taylor, R.N., Wieser, F. (2010) Advances in the genetics of endometriosis. *Genome medicine*. **2**(10), 75.
- Engel, C., Brunkhorst, F.M., Bone, H.-G., Brunkhorst, R., Gerlach, H., Grond, S., Gruendling, M., Huhle, G., Jaschinski, U., John, S., Mayer, K., Oppert, M., Olthoff, D., Quintel, M., Ragaller, M., Rossaint, R., Stuber, F., Weiler, N., Welte, T., Bogatsch, H., Hartog, C., Loeffler, M., Reinhart, K. (2007) Epidemiology of sepsis in Germany: results from a national prospective multicenter study. *Intensive Care Medicine*. **33**(4), 606–618.
- Engel, H., Kleespies, C., Friedrich, J., Breidenbach, M., Kallenborn, A., Schöndorf, T., Kolhagen, H., Mallmann, P. (1999) Detection of circulating tumour cells in patients with breast or ovarian cancer by molecular cytogenetics. *British Journal of Cancer*. **81**(7), 1165–1173.
- European Medicines Agency (2015a) European Medicines Agency - Abraxane. *European Medicines Agency*. [online]. Available from:

[http://www.ema.europa.eu/ema/index.jsp?curl=pages/medicines/human/medicines/000778/human\\_med\\_000620.jsp&mid=WC0b01ac058001d124](http://www.ema.europa.eu/ema/index.jsp?curl=pages/medicines/human/medicines/000778/human_med_000620.jsp&mid=WC0b01ac058001d124).

European Medicines Agency (2015b) European Medicines Agency - Afinitor. [online]. Available from:

[http://www.ema.europa.eu/ema/index.jsp?curl=pages/medicines/human/medicines/001038/human\\_med\\_000633.jsp&mid=WC0b01ac058001d124](http://www.ema.europa.eu/ema/index.jsp?curl=pages/medicines/human/medicines/001038/human_med_000633.jsp&mid=WC0b01ac058001d124).

European Medicines Agency (2015c) European Medicines Agency - Rapamune. *European Medicines Agency - Rapamune*. [online]. Available from:

[http://www.ema.europa.eu/ema/index.jsp?curl=pages/medicines/human/medicines/000273/human\\_med\\_001010.jsp&mid=WC0b01ac058001d124](http://www.ema.europa.eu/ema/index.jsp?curl=pages/medicines/human/medicines/000273/human_med_001010.jsp&mid=WC0b01ac058001d124).

European Medicines Agency (2015d) European Medicines Agency - Torisel. [online]. Available from:

[http://www.ema.europa.eu/ema/index.jsp?curl=pages/medicines/human/medicines/000799/human\\_med\\_001098.jsp&mid=WC0b01ac058001d124](http://www.ema.europa.eu/ema/index.jsp?curl=pages/medicines/human/medicines/000799/human_med_001098.jsp&mid=WC0b01ac058001d124).

Faber, M.T., Kjær, S.K., Dehlendorff, C., Chang-Claude, J., Andersen, K.K., Høgdall, E., Webb, P.M., Jordan, S.J., Australian Cancer Study (Ovarian Cancer), Australian Ovarian Cancer Study Group, Rossing, M.A., Doherty, J.A., Lurie, G., Thompson, P.J., Carney, M.E., Goodman, M.T., Ness, R.B., Modugno, F., Edwards, R.P., Bunker, C.H., Goode, E.L., Fridley, B.L., Vierkant, R.A., Larson, M.C., Schildkraut, J., Cramer, D.W., Terry, K.L., Vitonis, A.F., Bandera, E.V., Olson, S.H., King, M., Chandran, U., Kiemeny, L.A., Massuger, L.F.A.G., van Altena, A.M., Vermeulen, S.H., Brinton, L., Wentzensen, N., Lissowska, J., Yang, H.P., Moysich, K.B., Odunsi, K., Kasza, K., Odunsi-Akanji, O., Song, H., Pharaoh, P., Shah, M., Whittemore, A.S., McGuire, V., Sieh, W., Sutphen, R., Menon, U., Gayther, S.A., Ramus, S.J., Gentry-Maharaj, A., Pearce, C.L., Wu, A.H., Pike, M.C., Risch, H.A., Jensen, A., Ovarian Cancer Association Consortium (2013) Cigarette smoking and risk of ovarian cancer: a pooled analysis of 21 case-control studies. *Cancer causes & control*. **24**(5), 989–1004.

Faghihzadeh, F., Adibi, P., Rafiei, R., Hekmatdoost, A. (2014) Resveratrol supplementation improves inflammatory biomarkers in patients with nonalcoholic fatty liver disease. *Nutrition Research*. **34**(10), 837–843.

Fagone, P., Donia, M., Mangano, K., Quattrocchi, C., Mammana, S., Coco, M., Libra, M., McCubrey, J.A., Nicoletti, F. (2013) Comparative study of rapamycin and temsirolimus demonstrates superimposable anti-tumour potency on prostate cancer cells. *Basic & Clinical Pharmacology & Toxicology*. **112**(1), 63–69.

Fan, W., Yang, H., Xue, H., Sun, Y., Zhang, J. (2015) ELMO3 is a novel biomarker for diagnosis and prognosis of non-small cell lung cancer. *International Journal of Clinical and Experimental Pathology*. **8**(5), 5503–5508.

Feng, Z., Zhang, H., Levine, A.J., Jin, S. (2005) The coordinate regulation of the p53 and mTOR pathways in cells. *Proceedings of the National Academy of Sciences of the United States of America*. **102**(23), 8204–8209.

- Ferrero, S., Alessandri, F., Racca, A., Leone Roberti Maggiore, U. (2015) Treatment of pain associated with deep endometriosis: alternatives and evidence. *Fertility and Sterility*. **104**(4), 771–792.
- Fingar, D.C., Richardson, C.J., Tee, A.R., Cheatham, L., Tsou, C., Blenis, J. (2004) mTOR controls cell cycle progression through its cell growth effectors S6K1 and 4E-BP1/eukaryotic translation initiation factor 4E. *Molecular and Cellular Biology*. **24**(1), 200–216.
- Folga, A., Filipiak, K.J., Mamcarz, A., Obrebska-Tabaczka, E., Opolski, G. (2012) Simultaneous predictive value of NT-proBNP and CA-125 in patients newly diagnosed with advanced heart failure: preliminary results. *Archives of Medical Science*. **8**(4), 637–643.
- Forbes, S.A., Beare, D., Gunasekaran, P., Leung, K., Bindal, N., Boutselakis, H., Ding, M., Bamford, S., Cole, C., Ward, S., Kok, C.Y., Jia, M., De, T., Teague, J.W., Stratton, M.R., McDermott, U., Campbell, P.J. (2015) COSMIC: exploring the world's knowledge of somatic mutations in human cancer. *Nucleic Acids Research*. **43**(D1), D805–D811.
- Foster, H., Coley, H.M., Goumenou, A., Pados, G., Harvey, A., Karteris, E. (2010) Differential Expression of mTOR Signalling Components in Drug Resistance in Ovarian Cancer. *Anticancer Research*. **30**(9), 3529–3534.
- Fox, H.L., Kimball, S.R., Jefferson, L.S., Lynch, C.J. (1998) Amino acids stimulate phosphorylation of p70S6k and organization of rat adipocytes into multicellular clusters. *The American Journal of Physiology*. **274**(1 Pt 1), C206–213.
- Franke, T.F., Yang, S.-I., Chan, T.O., Datta, K., Kazlauskas, A., Morrison, D.K., Kaplan, D.R., Tsichlis, P.N. (1995) The protein kinase encoded by the Akt proto-oncogene is a target of the PDGF-activated phosphatidylinositol 3-kinase. *Cell*. **81**(5), 727–736.
- Freedman, R.S., Pihl, E., Kusyk, C., Gallager, H.S., Rutledge, F. (1978) Characterization of an ovarian carcinoma cell line. *Cancer*. **42**(5), 2352–2359.
- Fröjdö, S., Cozzone, D., Vidal, H., Pirola, L. (2007) Resveratrol is a class IA phosphoinositide 3-kinase inhibitor. *The Biochemical Journal*. **406**(3), 511–518.
- Gaetje, R., Winnekendonk, D.W., Ahr, A., Kaufmann, M. (2002) Ovarian cancer antigen CA 125 influences adhesion of human and mammalian cell lines in vitro. *Clinical and Experimental Obstetrics & Gynecology*. **29**(1), 34–36.
- Gaetje, R., Winnekendonk, D.W., Scharl, A., Kaufmann, M. (1999) Ovarian cancer antigen CA 125 enhances the invasiveness of the endometriotic cell line EEC 145. *Journal of the Society for Gynecologic Investigation*. **6**(5), 278–281.
- Ganley, I.G., Lam, D.H., Wang, J., Ding, X., Chen, S., Jiang, X. (2009) ULK1.ATG13.FIP200 complex mediates mTOR signaling and is essential for autophagy. *The Journal of Biological Chemistry*. **284**(18), 12297–12305.

Gao, D., Inuzuka, H., Tan, M.-K.M., Fukushima, H., Locasale, J.W., Liu, P., Wan, L., Zhai, B., Chin, Y.R., Shaik, S., Lyssiotis, C.A., Gygi, S.P., Toker, A., Cantley, L.C., Asara, J.M., Harper, J.W., Wei, W. (2011) mTOR drives its own activation via SCF $\beta$ -TRCP-dependent degradation of the mTOR inhibitor DEPTOR. *Molecular cell*. **44**(2), 290–303.

García-Martínez, J.M., Alessi, D.R. (2008) mTOR complex 2 (mTORC2) controls hydrophobic motif phosphorylation and activation of serum- and glucocorticoid-induced protein kinase 1 (SGK1). *The Biochemical Journal*. **416**(3), 375–385.

Gebauer, F., Hentze, M.W. (2004) Molecular mechanisms of translational control. *Nature Reviews. Molecular Cell Biology*. **5**(10), 827–835.

Giannakouros, P., Comamala, M., Matte, I., Rancourt, C., Piché, A. (2014) MUC16 mucin (CA125) regulates the formation of multicellular aggregates by altering  $\beta$ -catenin signaling. *American Journal of Cancer Research*. **5**(1), 219–230.

Groothuis, P.G., Koks, C.A., de Goeij, A.F., Dunselman, G.A., Arends, J.W., Evers, J.L. (1999) Adhesion of human endometrial fragments to peritoneum in vitro. *Fertility and Sterility*. **71**(6), 1119–1124.

Grunt, T.W., Mariani, G.L. (2013) Novel approaches for molecular targeted therapy of breast cancer: interfering with PI3K/AKT/mTOR signaling. *Current Cancer Drug Targets*. **13**(2), 188–204.

Guertin, D.A., Stevens, D.M., Saitoh, M., Kinkel, S., Crosby, K., Sheen, J.-H., Mullholland, D.J., Magnuson, M.A., Wu, H., Sabatini, D.M. (2009) mTOR complex 2 is required for the development of prostate cancer induced by Pten loss in mice. *Cancer Cell*. **15**(2), 148–159.

Guertin, D.A., Stevens, D.M., Thoreen, C.C., Burds, A.A., Kalaany, N.Y., Moffat, J., Brown, M., Fitzgerald, K.J., Sabatini, D.M. (2006) Ablation in mice of the mTORC components raptor, rictor, or mLST8 reveals that mTORC2 is required for signaling to Akt-FOXO and PKC $\alpha$ , but not S6K1. *Developmental cell*. **11**(6), 859–871.

Guo, J., Gao, J., Yu, X., Luo, H., Xiong, X., Huang, O. (2015) Expression of DJ-1 and mTOR in eutopic and ectopic endometria of patients with endometriosis and adenomyosis. *Gynecologic and Obstetric Investigation*. **79**(3), 195–200.

Guseh, S.H., Rauh-Hain, J.A., Tambouret, R.H., Davis, M., Clark, R.M., Boruta, D.M., Goodman, A., Growdon, W.B., Schorge, J.O., del Carmen, M.G. (2014) Transitional cell carcinoma of the ovary: A case–control study. *Gynecologic Oncology*. **132**(3), 649–653.

Gutierrez, L., Mauriat, M., Guénin, S., Pelloux, J., Lefebvre, J.-F., Louvet, R., Rusterucci, C., Moritz, T., Guerineau, F., Bellini, C., Van Wuytswinkel, O. (2008) The lack of a systematic validation of reference genes: a serious pitfall undervalued in reverse transcription-polymerase chain reaction (RT-PCR) analysis in plants. *Plant Biotechnology Journal*. **6**(6), 609–618.

Gwinn, D.M., Shackelford, D.B., Egan, D.F., Mihaylova, M.M., Mery, A., Vasquez, D.S., Turk, B.E., Shaw, R.J. (2008) AMPK phosphorylation of raptor mediates a metabolic checkpoint. *Molecular Cell*. **30**(2), 214–226.

Gyórfy, B., Surowiak, P., Budczies, J., Lánczky, A. (2013) Online survival analysis software to assess the prognostic value of biomarkers using transcriptomic data in non-small-cell lung cancer. *PLoS One*. **8**(12), e82241.

van der Hage, J.A., van den Broek, L.J.C.M., Legrand, C., Clahsen, P.C., Bosch, C.J.A., Robanus-Maandag, E.C., van de Velde, C.J.H., van de Vijver, M.J. (2004) Overexpression of P70 S6 kinase protein is associated with increased risk of locoregional recurrence in node-negative premenopausal early breast cancer patients. *British Journal of Cancer*. **90**(8), 1543–1550.

Hahn, M., Li, W., Yu, C., Rahmani, M., Dent, P., Grant, S. (2005) Rapamycin and UCN-01 synergistically induce apoptosis in human leukemia cells through a process that is regulated by the Raf-1/MEK/ERK, Akt, and JNK signal transduction pathways. *Molecular Cancer Therapeutics*. **4**(3), 457–470.

Hamada, Y., Mizoguchi, M., Suzuki, S.O., Iwaki, T. (1998) Accumulation of class I mutant p53 and apoptosis induced by carboplatin in a human glioma cell line. *Brain Tumor Pathology*. **15**(2), 77–82.

Hanon, F.-X., Monnet, D.L., Sørensen, T.L., Mølbak, K., Pedersen, G., Schönheyder, H. (2002) Survival of patients with bacteraemia in relation to initial empirical antimicrobial treatment. *Scandinavian Journal of Infectious Diseases*. **34**(7), 520–528.

Hara, K., Maruki, Y., Long, X., Yoshino, K., Oshiro, N., Hidayat, S., Tokunaga, C., Avruch, J., Yonezawa, K. (2002) Raptor, a binding partner of target of rapamycin (TOR), mediates TOR action. *Cell*. **110**(2), 177–189.

Hara, K., Yonezawa, K., Weng, Q.P., Kozlowski, M.T., Belham, C., Avruch, J. (1998) Amino acid sufficiency and mTOR regulate p70 S6 kinase and eIF-4E BP1 through a common effector mechanism. *The Journal of Biological Chemistry*. **273**(23), 14484–14494.

Harrington, L.S., Findlay, G.M., Gray, A., Tolkacheva, T., Wigfield, S., Rebholz, H., Barnett, J., Leslie, N.R., Cheng, S., Shepherd, P.R., Gout, I., Downes, C.P., Lamb, R.F. (2004) The TSC1-2 tumor suppressor controls insulin-PI3K signaling via regulation of IRS proteins. *The Journal of Cell Biology*. **166**(2), 213–223.

Havrilesky, L.J., Elbendary, A., Hurteau, J.A., Whitaker, R.S., Rodriguez, G.C., Berchuck, A. (1995) Chemotherapy-induced apoptosis in epithelial ovarian cancers. *Obstetrics and Gynecology*. **85**(6), 1007–1010.

Heitman, J., Movva, N.R., Hall, M.N. (1991) Targets for cell cycle arrest by the immunosuppressant rapamycin in yeast. *Science*. **253**(5022), 905–909.

- Hemminki, K., Sundquist, J., Brandt, A. (2011) Incidence and mortality in epithelial ovarian cancer by family history of any cancer. *Cancer*. **117**(17), 3972–3980.
- Hisamatsu, T., Mabuchi, S., Matsumoto, Y., Kawano, M., Sasano, T., Takahashi, R., Sawada, K., Ito, K., Kurachi, H., Schilder, R.J., Testa, J.R., Kimura, T. (2013) Potential Role of mTORC2 as a Therapeutic Target in Clear Cell Carcinoma of the Ovary. *Molecular cancer therapeutics*. **12**(7), 1367–1377.
- Holz, M.K., Ballif, B.A., Gygi, S.P., Blenis, J. (2005) mTOR and S6K1 mediate assembly of the translation preinitiation complex through dynamic protein interchange and ordered phosphorylation events. *Cell*. **123**(4), 569–580.
- Hosokawa, N., Hara, T., Kaizuka, T., Kishi, C., Takamura, A., Miura, Y., Iemura, S., Natsume, T., Takehana, K., Yamada, N., Guan, J.-L., Oshiro, N., Mizushima, N. (2009) Nutrient-dependent mTORC1 association with the ULK1-Atg13-FIP200 complex required for autophagy. *Molecular Biology of the Cell*. **20**(7), 1981–1991.
- Hsu, C.-Y., Bristow, R., Cha, M.S., Wang, B.G., Ho, C.-L., Kurman, R.J., Wang, T.-L., Shih, I.-M. (2004) Characterization of Active Mitogen-Activated Protein Kinase in Ovarian Serous Carcinomas. *Clinical Cancer Research*. **10**(19), 6432–6436.
- Hsu, P.P., Kang, S.A., Rameseder, J., Zhang, Y., Ottina, K.A., Lim, D., Peterson, T.R., Choi, Y., Gray, N.S., Yaffe, M.B., Marto, J.A., Sabatini, D.M. (2011) The mTOR-regulated phosphoproteome reveals a mechanism of mTORC1-mediated inhibition of growth factor signaling. *Science*. **332**(6035), 1317–1322.
- Hudson, C.C., Liu, M., Chiang, G.G., Otterness, D.M., Loomis, D.C., Kaper, F., Giaccia, A.J., Abraham, R.T. (2002) Regulation of hypoxia-inducible factor 1 $\alpha$  expression and function by the mammalian target of rapamycin. *Molecular and Cellular Biology*. **22**(20), 7004–7014.
- Im-aram, A., Farrand, L., Bae, S.-M., Song, G., Song, Y.S., Han, J.Y., Tsang, B.K. (2013) The mTORC2 component rictor contributes to cisplatin resistance in human ovarian cancer cells. *PLoS One*. **8**(9), e75455.
- Ingham, S.L., Warwick, J., Buchan, I., Sahin, S., O’Hara, C., Moran, A., Howell, A., Evans, D.G. (2013) Ovarian cancer among 8,005 women from a breast cancer family history clinic: no increased risk of invasive ovarian cancer in families testing negative for BRCA1 and BRCA2. *Journal of Medical Genetics*. **50**(6), 368–372.
- Inoki, K., Li, Y., Zhu, T., Wu, J., Guan, K.-L. (2002) TSC2 is phosphorylated and inhibited by Akt and suppresses mTOR signalling. *Nature Cell Biology*. **4**(9), 648–657.
- Inoki, K., Zhu, T., Guan, K.-L. (2003) TSC2 mediates cellular energy response to control cell growth and survival. *Cell*. **115**(5), 577–590.
- Ip, C.K.M., Yung, S., Chan, T.-M., Tsao, S.-W., Wong, A.S.T. (2014) p70 S6 kinase drives ovarian cancer metastasis through multicellular spheroid-peritoneum

interaction and P-cadherin/b1 integrin signaling activation. *Oncotarget*. **5**(19), 9133–9149.

Ireland, C.M., Pittman, S.M. (1995) Tubulin alterations in taxol-induced apoptosis parallel those observed with other drugs. *Biochemical Pharmacology*. **49**(10), 1491–1499.

Isotani, S., Hara, K., Tokunaga, C., Inoue, H., Avruch, J., Yonezawa, K. (1999) Immunopurified mammalian target of rapamycin phosphorylates and activates p70 S6 kinase alpha in vitro. *The Journal of Biological Chemistry*. **274**(48), 34493–34498.

Jacinto, E., Facchinetti, V., Liu, D., Soto, N., Wei, S., Jung, S.Y., Huang, Q., Qin, J., Su, B. (2006) SIN1/MIP1 maintains rictor-mTOR complex integrity and regulates Akt phosphorylation and substrate specificity. *Cell*. **127**(1), 125–137.

Jacinto, E., Loewith, R., Schmidt, A., Lin, S., Ruegg, M.A., Hall, A., Hall, M.N. (2004) Mammalian TOR complex 2 controls the actin cytoskeleton and is rapamycin insensitive. *Nature Cell Biology*. **6**(11), 1122–1128.

Jacob, F., Guertler, R., Naim, S., Nixdorf, S., Fedier, A., Hacker, N.F., Heinzelmann-Schwarz, V. (2013) Careful selection of reference genes is required for reliable performance of RT-qPCR in human normal and cancer cell lines. *PLoS One*. **8**(3), e59180.

Janiszewska, M., Liu, L., Almendro, V., Kuang, Y., Paweletz, C., Sakr, R.A., Weigelt, B., Hanker, A.B., Chandarlapaty, S., King, T.A., Reis-Filho, J.S., Arteaga, C.L., Park, S.Y., Michor, F., Polyak, K. (2015) In situ single-cell analysis identifies heterogeneity for PIK3CA mutation and HER2 amplification in HER2-positive breast cancer. *Nature Genetics*. **47**(10), 1212–1219.

Jervis, S., Song, H., Lee, A., Dicks, E., Tyrer, J., Harrington, P., Easton, D.F., Jacobs, I.J., Pharoah, P.P.D., Antoniou, A.C. (2014) Ovarian cancer familial relative risks by tumour subtypes and by known ovarian cancer genetic susceptibility variants. *Journal of Medical Genetics*. **51**(2), 108–113.

Jiang, H., Shang, X., Wu, H., Gautam, S.C., Al-Holou, S., Li, C., Kuo, J., Zhang, L., Chopp, M. (2009) Resveratrol downregulates PI3K/Akt/mTOR signaling pathways in human U251 glioma cells. *Journal of experimental therapeutics & oncology*. **8**(1), 25–33.

Jiang, S., Zou, Z., Nie, P., Wen, R., Xiao, Y., Tang, J. (2015) Synergistic Effects between mTOR Complex 1/2 and Glycolysis Inhibitors in Non-Small-Cell Lung Carcinoma Cells. *PLoS One*. **10**(7), e0132880.

Jia, W., Wu, Y., Zhang, Q., Gao, G.E., Zhang, C., Xiang, Y. (2015) Expression profile of circulating microRNAs as a promising fingerprint for cervical cancer diagnosis and monitoring. *Molecular and Clinical Oncology*. **3**(4), 851–858.

- Johnson, C.C., Kessel, B., Riley, T.L., Ragard, L.R., Williams, C.R., Xu, J.-L., Buys, S.S., Prostate, Lung, Colorectal and Ovarian Cancer Project Team (2008) The epidemiology of CA-125 in women without evidence of ovarian cancer in the Prostate, Lung, Colorectal and Ovarian Cancer (PLCO) Screening Trial. *Gynecologic oncology*. **110**(3), 383–389.
- Jordan, S.D., Poole, C.J., Archer, V.R., Steven, N.M., Burton, A. (2003) A retrospective evaluation of the feasibility of inpatient dose escalation as appropriate methodology for dose-ranging studies for combination cytotoxic regimens. *Cancer Chemotherapy and Pharmacology*. **52**(2), 113–118.
- Jung, C.H., Jun, C.B., Ro, S.-H., Kim, Y.-M., Otto, N.M., Cao, J., Kundu, M., Kim, D.-H. (2009) ULK-Atg13-FIP200 complexes mediate mTOR signaling to the autophagy machinery. *Molecular Biology of the Cell*. **20**(7), 1992–2003.
- Karthik, G.-M., Ma, R., Lövrot, J., Kis, L.L., Lindh, C., Blomquist, L., Fredriksson, I., Bergh, J., Hartman, J. (2015) mTOR inhibitors counteract tamoxifen-induced activation of breast cancer stem cells. *Cancer Letters*. **367**(1), 76–87.
- Kastan, M.B., Onyekwere, O., Sidransky, D., Vogelstein, B., Craig, R.W. (1991) Participation of p53 protein in the cellular response to DNA damage. *Cancer Research*. **51**(23 Pt 1), 6304–6311.
- Kawada, J., Ito, Y., Iwata, S., Suzuki, M., Kawano, Y., Kanazawa, T., Siddiquey, M.N.A., Kimura, H. (2014) mTOR inhibitors induce cell-cycle arrest and inhibit tumor growth in Epstein-Barr virus-associated T and natural killer cell lymphoma cells. *Clinical Cancer Research*. **20**(21), 5412–5422.
- Kay, J.E., Kromwel, L., Doe, S.E., Denyer, M. (1991) Inhibition of T and B lymphocyte proliferation by rapamycin. *Immunology*. **72**(4), 544–549.
- Kazi, A.A., Hong-Brown, L., Lang, S.M., Lang, C.H. (2011) Deptor knockdown enhances mTOR Activity and protein synthesis in myocytes and ameliorates disuse muscle atrophy. *Molecular Medicine*. **17**(9-10), 925–936.
- Kenerson, H.L., Aicher, L.D., True, L.D., Yeung, R.S. (2002) Activated mammalian target of rapamycin pathway in the pathogenesis of tuberous sclerosis complex renal tumors. *Cancer Research*. **62**(20), 5645–5650.
- Kennedy, A.W., Markman, M., Biscotti, C.V., Emery, J.D., Rybicki, L.A. (1999) Survival Probability in Ovarian Clear Cell Adenocarcinoma. *Gynecologic Oncology*. **74**(1), 108–114.
- Kennedy, S., Oswald, N. eds. (2011) *PCR Troubleshooting and Optimization: The Essential Guide*. Norfolk, UK: Caister Academic Press.
- Kim, D.-H., Sarbassov, D.D., Ali, S.M., King, J.E., Latek, R.R., Erdjument-Bromage, H., Tempst, P., Sabatini, D.M. (2002) mTOR interacts with raptor to form a nutrient-sensitive complex that signals to the cell growth machinery. *Cell*. **110**(2), 163–175.



Kim, D.-H., Sarbassov, D.D., Ali, S.M., Latek, R.R., Guntur, K.V., Erdjument-Bromage, H., Tempst, P., Sabatini, D.M. (2003) GβL, a Positive Regulator of the Rapamycin-Sensitive Pathway Required for the Nutrient-Sensitive Interaction between Raptor and mTOR. *Molecular Cell*. **11**(4), 895–904.

Kim, E., Goraksha-Hicks, P., Li, L., Neufeld, T.P., Guan, K.-L. (2008) Regulation of TORC1 by Rag GTPases in nutrient response. *Nature Cell Biology*. **10**(8), 935–945.

Kim, J.E., Chen, J. (2000) Cytoplasmic-nuclear shuttling of FKBP12-rapamycin-associated protein is involved in rapamycin-sensitive signaling and translation initiation. *Proceedings of the National Academy of Sciences of the United States of America*. **97**(26), 14340–14345.

Kim, J.E., Chen, J. (2004) Regulation of peroxisome proliferator-activated receptor-γ activity by mammalian target of rapamycin and amino acids in adipogenesis. *Diabetes*. **53**(11), 2748–2756.

Kim, K.-T., Lee, H.W., Lee, H.-O., Kim, S.C., Seo, Y.J., Chung, W., Eum, H.H., Nam, D.-H., Kim, J., Joo, K.M., Park, W.-Y. (2015) Single-cell mRNA sequencing identifies subclonal heterogeneity in anti-cancer drug responses of lung adenocarcinoma cells. *Genome Biology*. **16**, 127.

Kjaer, T.N., Ornstrup, M.J., Poulsen, M.M., Jørgensen, J.O.L., Hougaard, D.M., Cohen, A.S., Neghabat, S., Richelsen, B., Pedersen, S.B. (2015) Resveratrol reduces the levels of circulating androgen precursors but has no effect on, testosterone, dihydrotestosterone, PSA levels or prostate volume. A 4-month randomised trial in middle-aged men. *The Prostate*. **75**(12), 1255–1263.

Knappskog, S., Gansmo, L.B., Dibirova, K., Metspalu, A., Cybulski, C., Peterlongo, P., Aaltonen, L., Vatten, L., Romundstad, P., Hveem, K., Devilee, P., Evans, G.D., Lin, D., Van Camp, G., Manolopoulos, V.G., Osorio, A., Milani, L., Ozelik, T., Zalloua, P., Mouzaya, F., Bliznetz, E., Balanovska, E., Pocheshkova, E., Kučinskas, V., Atramentova, L., Nymadawa, P., Titov, K., Lavryashina, M., Yusupov, Y., Bogdanova, N., Koshel, S., Zamora, J., Wedge, D.C., Charlesworth, D., Dörk, T., Balanovsky, O., Lønning, P.E. (2014) Population distribution and ancestry of the cancer protective MDM2 SNP285 (rs117039649). *Oncotarget*. **5**(18), 8223–8234.

Kodaman, P.H. (2015) Current strategies for endometriosis management. *Obstetrics and Gynecology Clinics of North America*. **42**(1), 87–101.

Koks, C.A., Dunselman, G.A., de Goeij, A.F., Arends, J.W., Evers, J.L. (1997) Evaluation of a menstrual cup to collect shed endometrium for in vitro studies. *Fertility and Sterility*. **68**(3), 560–564.

Koks, C.A., Groothuis, P.G., Dunselman, G.A., de Goeij, A.F., Evers, J.L. (1999) Adhesion of shed menstrual tissue in an in-vitro model using amnion and peritoneum: a light and electron microscopic study. *Human Reproduction*. **14**(3), 816–822.

- Koo, J., Wang, X., Owonikoko, T.K., Ramalingam, S.S., Khuri, F.R., Sun, S.-Y. (2015) GSK3 is required for rapalogs to induce degradation of some oncogenic proteins and to suppress cancer cell growth. *Oncotarget*. **6**(11), 8974–8987.
- Kovacina, K.S., Park, G.Y., Bae, S.S., Guzzetta, A.W., Schaefer, E., Birnbaum, M.J., Roth, R.A. (2003) Identification of a Proline-rich Akt Substrate as a 14-3-3 Binding Partner. *Journal of Biological Chemistry*. **278**(12), 10189–10194.
- Kumar, N. (1981) Taxol-induced polymerization of purified tubulin. Mechanism of action. *The Journal of Biological Chemistry*. **256**(20), 10435–10441.
- Kurian, A.W., Balise, R.R., McGuire, V., Whittemore, A.S. (2005) Histologic types of epithelial ovarian cancer: have they different risk factors? *Gynecologic Oncology*. **96**(2), 520–530.
- Lalwani, N., Prasad, S.R., Vikram, R., Shanbhogue, A.K., Huettnner, P.C., Fasih, N. (2011) Histologic, molecular, and cytogenetic features of ovarian cancers: implications for diagnosis and treatment. *Radiographics*. **31**(3), 625–646.
- Lamouille, S., Connolly, E., Smyth, J.W., Akhurst, R.J., Derynck, R. (2012) TGF- $\beta$ -induced activation of mTOR complex 2 drives epithelial–mesenchymal transition and cell invasion. *Journal of Cell Science*. **125**(5), 1259–1273.
- Lanitis, E., Dangaj, D., Hagemann, I.S., Song, D.-G., Best, A., Sandaltzopoulos, R., Coukos, G., Powell, D.J., Jr (2012) Primary Human Ovarian Epithelial Cancer Cells Broadly Express HER2 at Immunologically-Detectable Levels. *PLoS ONE*. **7**(11), e49829.
- Laplane, M., Sabatini, D.M. (2012) mTOR Signaling in Growth Control and Disease. *Cell*. **149**(2), 274–293.
- Laudański, P., Kowalczyk, O., Klasa-Mazurkiewicz, D., Milczek, T., Rysak-Luberowicz, D., Garbowicz, M., Baranowski, W., Charkiewicz, R., Szamatowicz, J., Chyczewski, L. (2011) Selective gene expression profiling of mTOR-associated tumor suppressor and oncogenes in ovarian cancer. *Folia Histochemica Et Cytobiologica*. **49**(2), 317–324.
- Leconte, M., Nicco, C., Ngô, C., Chéreau, C., Chouzenoux, S., Marut, W., Guibourdenche, J., Arkwright, S., Weill, B., Chapron, C., Dousset, B., Batteux, F. (2011) The mTOR/AKT inhibitor temsirolimus prevents deep infiltrating endometriosis in mice. *The American journal of pathology*. **179**(2), 880–889.
- Lee, L.G., Connell, C.R., Bloch, W. (1993) Allelic discrimination by nick-translation PCR with fluorogenic probes. *Nucleic Acids Research*. **21**(16), 3761–3766.
- Lee, M., Wiedemann, T., Gross, C., Leinhäuser, I., Roncaroli, F., Braren, R., Pellegata, N.S. (2015) Targeting PI3K/mTOR Signaling Displays Potent Antitumor Efficacy against Nonfunctioning Pituitary Adenomas. *Clinical Cancer Research*. **21**(14), 3204–3215.

- Leontieva, O.V., Novototskaya, L.R., Paszkiewicz, G.M., Komarova, E.A., Gudkov, A.V., Blagosklonny, M.V. (2013) Dysregulation of the mTOR pathway in p53-deficient mice. *Cancer Biology & Therapy*. **14**(12), 1182–1188.
- Leslie, N.R., Gray, A., Pass, I., Orchiston, E.A., Downes, C.P. (2000) Analysis of the cellular functions of PTEN using catalytic domain and C-terminal mutations: differential effects of C-terminal deletion on signalling pathways downstream of phosphoinositide 3-kinase. *Biochemical Journal*. **346**(Pt 3), 827–833.
- Leung, E.Y., Askarian-Amiri, M., Finlay, G.J., Rewcastle, G.W., Baguley, B.C. (2015) Potentiation of Growth Inhibitory Responses of the mTOR Inhibitor Everolimus by Dual mTORC1/2 Inhibitors in Cultured Breast Cancer Cell Lines. *PLoS ONE*. **10**(7), e0131400.
- Levine, D.A., Bogomolny, F., Yee, C.J., Lash, A., Barakat, R.R., Borgen, P.I., Boyd, J. (2005) Frequent mutation of the PIK3CA gene in ovarian and breast cancers. *Clinical Cancer Research: An Official Journal of the American Association for Cancer Research*. **11**(8), 2875–2878.
- Liang, X.H., Jackson, S., Seaman, M., Brown, K., Kempkes, B., Hibshoosh, H., Levine, B. (1999) Induction of autophagy and inhibition of tumorigenesis by beclin 1. *Nature*. **402**(6762), 672–676.
- Liedtke, C., Rody, A., Gluz, O., Baumann, K., Beyer, D., Kohls, E.-B., Lausen, K., Hanker, L., Holtrich, U., Becker, S., Karn, T. (2015) The prognostic impact of age in different molecular subtypes of breast cancer. *Breast Cancer Research and Treatment*. **152**(3), 667–673.
- Li, S., Brown, M.S., Goldstein, J.L. (2010) Bifurcation of insulin signaling pathway in rat liver: mTORC1 required for stimulation of lipogenesis, but not inhibition of gluconeogenesis. *Proceedings of the National Academy of Sciences of the United States of America*. **107**(8), 3441–3446.
- Li, S., Ogawa, W., Emi, A., Hayashi, K., Senga, Y., Nomura, K., Hara, K., Yu, D., Kasuga, M. (2011) Role of S6K1 in regulation of SREBP1c expression in the liver. *Biochemical and Biophysical Research Communications*. **412**(2), 197–202.
- Liu, K., Zhou, R., Wang, B., Mi, M.-T. (2014) Effect of resveratrol on glucose control and insulin sensitivity: a meta-analysis of 11 randomized controlled trials. *The American Journal of Clinical Nutrition*. **99**(6), 1510–1519.
- Liu, L., Das, S., Losert, W., Parent, C.A. (2010) mTORC2 regulates neutrophil chemotaxis in a cAMP- and RhoA-dependent fashion. *Developmental Cell*. **19**(6), 845–857.
- Liu, L., Sun, Y., Kargbo, B., Zhang, C., Feng, H., Lu, H., Liu, W., Wang, C., Hu, Y., Deng, Y., Jiang, J., Kang, X., Yang, H., Jiang, Y., Yang, Y., Kargbo, D., Qian, J., Chen, W. (2015) Detection of Zaire Ebola virus by real-time reverse transcription-polymerase chain reaction, Sierra Leone, 2014. *Journal of Virological Methods*. **222**, 62–65.

Liu, M., Wilk, S.A., Wang, A., Zhou, L., Wang, R.-H., Ogawa, W., Deng, C., Dong, L.Q., Liu, F. (2010) Resveratrol inhibits mTOR signaling by promoting the interaction between mTOR and DEPTOR. *The Journal of biological chemistry*. **285**(47), 36387–36394.

Livak, K.J., Flood, S.J., Marmaro, J., Giusti, W., Deetz, K. (1995) Oligonucleotides with fluorescent dyes at opposite ends provide a quenched probe system useful for detecting PCR product and nucleic acid hybridization. *PCR methods and applications*. **4**(6), 357–362.

Li, X., Zhang, Y., Zhao, L., Wang, L., Wu, Z., Mei, Q., Nie, J., Li, X., Li, Y., Fu, X., Wang, X., Meng, Y., Han, W. (2014) Whole-exome sequencing of endometriosis identifies frequent alterations in genes involved in cell adhesion and chromatin-remodeling complexes. *Human Molecular Genetics*. **23**(22), 6008–6021.

van der Loos, C.M. (2008) Multiple Immunoenzyme Staining: Methods and Visualizations for the Observation With Spectral Imaging. *Journal of Histochemistry and Cytochemistry*. **56**(4), 313–328.

Lowes, L.E., Lock, M., Rodrigues, G., D'Souza, D., Bauman, G., Ahmad, B., Venkatesan, V., Allan, A.L., Sexton, T. (2015) The significance of circulating tumor cells in prostate cancer patients undergoing adjuvant or salvage radiation therapy. *Prostate Cancer and Prostatic Diseases*.

Lu, Q., Wang, J., Yu, G., Guo, T., Hu, C., Ren, P. (2015) Expression and clinical significance of mammalian target of rapamycin/P70 ribosomal protein S6 kinase signaling pathway in human colorectal carcinoma tissue. *Oncology Letters*. **10**(1), 277–282.

Mabuchi, S., Altomare, D.A., Cheung, M., Zhang, L., Poulikakos, P.I., Hensley, H.H., Schilder, R.J., Ozols, R.F., Testa, J.R. (2007) RAD001 inhibits human ovarian cancer cell proliferation, enhances cisplatin-induced apoptosis, and prolongs survival in an ovarian cancer model. *Clinical Cancer Research: An Official Journal of the American Association for Cancer Research*. **13**(14), 4261–4270.

Mabuchi, S., Altomare, D.A., Connolly, D.C., Klein-Szanto, A., Litwin, S., Hoelzle, M.K., Hensley, H.H., Hamilton, T.C., Testa, J.R. (2007) RAD001 (Everolimus) delays tumor onset and progression in a transgenic mouse model of ovarian cancer. *Cancer Research*. **67**(6), 2408–2413.

Machado-Linde, F., Sánchez-Ferrer, M.L., Cascales, P., Torroba, A., Orozco, R., Silva Sánchez, Y., Nieto, A., Fiol, G. (2015) Prevalence of endometriosis in epithelial ovarian cancer. Analysis of the associated clinical features and study on molecular mechanisms involved in the possible causality. *European Journal of Gynaecological Oncology*. **36**(1), 21–24.

Magrina, J.F., Espada, M., Kho, R.M., Cetta, R., Chang, Y.-H.H., Magtibay, P.M. (2015) Surgical Excision of Advanced Endometriosis: Perioperative Outcomes and Impacting Factors. *Journal of Minimally Invasive Gynecology*. **22**(6), 944–950.

Maira, S.-M., Stauffer, F., Brueggen, J., Furet, P., Schnell, C., Fritsch, C., Brachmann, S., Chène, P., De Pover, A., Schoemaker, K., Fabbro, D., Gabriel, D., Simonen, M., Murphy, L., Finan, P., Sellers, W., García-Echeverría, C. (2008) Identification and characterization of NVP-BEZ235, a new orally available dual phosphatidylinositol 3-kinase/mammalian target of rapamycin inhibitor with potent in vivo antitumor activity. *Molecular Cancer Therapeutics*. **7**(7), 1851–1863.

Majumder, P.K., Febbo, P.G., Bikoff, R., Berger, R., Xue, Q., McMahon, L.M., Manola, J., Brugarolas, J., McDonnell, T.J., Golub, T.R., Loda, M., Lane, H.A., Sellers, W.R. (2004) mTOR inhibition reverses Akt-dependent prostate intraepithelial neoplasia through regulation of apoptotic and HIF-1-dependent pathways. *Nature Medicine*. **10**(6), 594–601.

Malcolm Coppleson, J.M.M., C. Paul Morrow, M.H.N.T. eds. (1992) Tumors of ovary. In *Gynecologic Oncology*. Churchill Livingstone.

Malpica, A., Deavers, M.T., Lu, K., Bodurka, D.C., Atkinson, E.N., Gershenson, D.M., Silva, E.G. (2004) Grading ovarian serous carcinoma using a two-tier system. *The American Journal of Surgical Pathology*. **28**(4), 496–504.

Manning, B.D., Tee, A.R., Logsdon, M.N., Blenis, J., Cantley, L.C. (2002) Identification of the tuberous sclerosis complex-2 tumor suppressor gene product tuberlin as a target of the phosphoinositide 3-kinase/akt pathway. *Molecular Cell*. **10**(1), 151–162.

Martin, E.C., Rhodes, L.V., Elliott, S., Krebs, A.E., Nephew, K.P., Flemington, E.K., Collins-Burow, B.M., Burow, M.E. (2014) microRNA regulation of mammalian target of rapamycin expression and activity controls estrogen receptor function and RAD001 sensitivity. *Molecular Cancer*. **13**, 229.

Masoumi-Moghaddam, S., Amini, A., Wei, A.-Q., Robertson, G., Morris, D.L. (2015) Vascular endothelial growth factor expression correlates with serum CA125 and represents a useful tool in prediction of refractoriness to platinum-based chemotherapy and ascites formation in epithelial ovarian cancer. *Oncotarget*. **6**(29), 28491–28501.

Masri, J., Bernath, A., Martin, J., Jo, O.D., Vartanian, R., Funk, A., Gera, J. (2007) mTORC2 activity is elevated in gliomas and promotes growth and cell motility via overexpression of rictor. *Cancer Research*. **67**(24), 11712–11720.

Mavaddat, N., Peock, S., Frost, D., Ellis, S., Platte, R., Fineberg, E., Evans, D.G., Izatt, L., Eeles, R.A., Adlard, J., Davidson, R., Eccles, D., Cole, T., Cook, J., Brewer, C., Tischkowitz, M., Douglas, F., Hodgson, S., Walker, L., Porteous, M.E., Morrison, P.J., Side, L.E., Kennedy, M.J., Houghton, C., Donaldson, A., Rogers, M.T., Dorkins, H., Miedzybrodzka, Z., Gregory, H., Eason, J., Barwell, J., McCann, E., Murray, A., Antoniou, A.C., Easton, D.F., EMBRACE (2013) Cancer risks for BRCA1 and BRCA2 mutation carriers: results from prospective analysis of EMBRACE. *Journal of the National Cancer Institute*. **105**(11), 812–822.

Ma, X.M., Blenis, J. (2009) Molecular mechanisms of mTOR-mediated translational control. *Nature Reviews. Molecular Cell Biology*. **10**(5), 307–318.

Maxwell, P.H., Dachs, G.U., Gleadle, J.M., Nicholls, L.G., Harris, A.L., Stratford, I.J., Hankinson, O., Pugh, C.W., Ratcliffe, P.J. (1997) Hypoxia-inducible factor-1 modulates gene expression in solid tumors and influences both angiogenesis and tumor growth. *Proceedings of the National Academy of Sciences of the United States of America*. **94**(15), 8104–8109.

McConechy, M.K., Ding, J., Senz, J., Yang, W., Melnyk, N., Tone, A.A., Prentice, L.M., Wiegand, K., McAlpine, J.N., Shah, S.P., Lee, C.-H., Goodfellow, P.J., Gilks, C.B., Huntsman, D.G. (2014) Ovarian and endometrial endometrioid carcinomas have distinct CTNNB1 and PTEN mutation profiles. *Modern pathology*. **27**(1), 128–134.

Melin, A., Sparén, P., Persson, I., Bergqvist, A. (2006) Endometriosis and the risk of cancer with special emphasis on ovarian cancer. *Human Reproduction*. **21**(5), 1237–1242.

Meng, Q., Xia, C., Fang, J., Rojanasakul, Y., Jiang, B.-H. (2006) Role of PI3K and AKT specific isoforms in ovarian cancer cell migration, invasion and proliferation through the p70S6K1 pathway. *Cellular Signalling*. **18**(12), 2262–2271.

Menon, U., Ryan, A., Kalsi, J., Gentry-Maharaj, A., Dawney, A., Habib, M., Apostolidou, S., Singh, N., Benjamin, E., Burnell, M., Davies, S., Sharma, A., Gunu, R., Godfrey, K., Lopes, A., Oram, D., Herod, J., Williamson, K., Seif, M.W., Jenkins, H., Mould, T., Woolas, R., Murdoch, J.B., Dobbs, S., Amso, N.N., Leeson, S., Cruickshank, D., Scott, I., Fallowfield, L., Widschwendter, M., Reynolds, K., McGuire, A., Campbell, S., Parmar, M., Skates, S.J., Jacobs, I. (2015) Risk Algorithm Using Serial Biomarker Measurements Doubles the Number of Screen-Detected Cancers Compared With a Single-Threshold Rule in the United Kingdom Collaborative Trial of Ovarian Cancer Screening. *Journal of Clinical Oncology*. **33**(18), 2062–2071.

Merritt, M.A., Green, A.C., Nagle, C.M., Webb, P.M., Australian Cancer Study (Ovarian Cancer), Australian Ovarian Cancer Study Group (2008) Talcum powder, chronic pelvic inflammation and NSAIDs in relation to risk of epithelial ovarian cancer. *International Journal of Cancer. Journal International Du Cancer*. **122**(1), 170–176.

Misra, U.K., Pizzo, S.V. (2014) Activated  $\alpha$ 2-Macroglobulin Binding to Cell Surface GRP78 Induces T-Loop Phosphorylation of Akt1 by PDK1 in Association with Raptor. *PLoS ONE*. **9**(2), e88373.

Miwa, S., Yano, S., Kimura, H., Yamamoto, M., Toneri, M., Murakami, T., Hayashi, K., Yamamoto, N., Fujiwara, T., Tsuchiya, H., Hoffman, R.M. (2015) Heterogeneous cell-cycle behavior in response to UVB irradiation by a population of single cancer cells visualized by time-lapse Fucci imaging. *Cell Cycle*. **14**(12), 1932–1937.

Mol, B.W., Bayram, N., Lijmer, J.G., Wiegerinck, M.A., Bongers, M.Y., van der Veen, F., Bossuyt, P.M. (1998) The performance of CA-125 measurement in the detection of endometriosis: a meta-analysis. *Fertility and sterility*. **70**(6), 1101–1108.

Montero, J.C., Chen, X., Ocaña, A., Pandiella, A. (2012) Predominance of mTORC1 over mTORC2 in the regulation of proliferation of ovarian cancer cells: therapeutic implications. *Molecular Cancer Therapeutics*. **11**(6), 1342–1352.

Moraitis, D., Karanikou, M., Liakou, C., Dimas, K., Tzimas, G., Tseleni-Balafouta, S., Patsouris, E., Rassidakis, G.Z., Kouvaraki, M.A. (2014) SIN1, a critical component of the mTOR-Rictor complex, is overexpressed and associated with AKT activation in medullary and aggressive papillary thyroid carcinomas. *Surgery*. **156**(6), 1542–1548; discussion 1548–1549.

Morelon, E., Mamzer-Bruneel, M.F., Peraldi, M.N., Kreis, H. (2001) Sirolimus: a new promising immunosuppressive drug. Towards a rationale for its use in renal transplantation. *Nephrology, Dialysis, Transplantation*. **16**(1), 18–20.

Morotti, M., Remorgida, V., Venturini, P.L., Ferrero, S. (2014) Progestogen-only contraceptive pill compared with combined oral contraceptive in the treatment of pain symptoms caused by endometriosis in patients with migraine without aura. *European Journal of Obstetrics, Gynecology, and Reproductive Biology*. **179**, 63–68.

Nakayama, N., Nakayama, K., Yeasmin, S., Ishibashi, M., Katagiri, A., Iida, K., Fukumoto, M., Miyazaki, K. (2008) KRAS or BRAF mutation status is a useful predictor of sensitivity to MEK inhibition in ovarian cancer. *British Journal of Cancer*. **99**(12), 2020–2028.

Neeyalavira, V., Suprasert, P. (2014) Outcomes of malignant ovarian germ-cell tumors treated in Chiang Mai University Hospital over a nine year period. *Asian Pacific journal of cancer prevention*. **15**(12), 4909–4913.

Neuhaus, P., Klupp, J., Langrehr, J.M. (2001) mTOR inhibitors: An overview. *Liver Transplantation*. **7**(6), 473–484.

NHS (2014) Introduction to Point of Care. *Leeds Pathology*. [online]. Available from: <http://www.pathology.leedsth.nhs.uk/pathology/Departments/BloodSciences/ClinicalBiochemistry/PointofCareTesting.aspx>.

NHS (2015a) NHS Diagnostic Waiting Times and Activity Data, May 2015 Monthly Report.

NHS (2015b) Ovarian Cancer Treatment. *Royal Marsden*. [online]. Available from: <http://www.royalmarsden.nhs.uk/cancer-information/types/ovarian-cancer/pages/treatment.aspx>.

NHS (2015c) Point of Care Testing Devices. *Central Manchester University Hospitals*. [online]. Available from: <http://www.cmft.nhs.uk/info-for-health->

professionals/laboratory-medicine/point-of-care-testing/point-of-care-testing-devices.

NHS (2015d) Point of Care Testing (POCT). *Central Manchester University Hospitals*. [online]. Available from: <http://www.cmft.nhs.uk/info-for-health-professionals/laboratory-medicine/point-of-care-testing>.

NHS (2015e) Point of Care Testing Systems. [online]. Available from: <https://www.supplychain.nhs.uk/product-news/contract-launch-briefs/2013/september/point-of-care-testing-systems/>.

NHS Choices (2015) Endometriosis - NHS Choices. [online]. Available from: <http://www.nhs.uk/conditions/endometriosis/pages/introduction.aspx> [Accessed August 31, 2015].

NHS Choices (2014) Endometriosis - Treatment - NHS Choices. [online]. Available from: <http://www.nhs.uk/Conditions/Endometriosis/Pages/Treatment.aspx> [Accessed August 25, 2015].

NHS Choices (2013) Ovarian cancer - NHS Choices. [online]. Available from: <http://www.nhs.uk/conditions/cancer-of-the-ovary/pages/introduction.aspx> [Accessed July 4, 2013].

NICE (2013) NICE finds advanced ovarian cancer treatment too expensive with not enough benefit | Press and media | News | NICE. [online]. Available from: <https://www.nice.org.uk/news/press-and-media/nice-finds-advanced-ovarian-cancer-treatment-too-expensive-with-not-enough-benefit> [Accessed July 26, 2015].

NICE (2011) Ovarian cancer: The recognition and initial management of ovarian cancer. *Ovarian cancer: The recognition and initial management of ovarian cancer*. [online]. Available from: <https://www.nice.org.uk/guidance/cg122/chapter/guidance> [Accessed August 18, 2015].

No, J.H., Jeon, Y.-T., Park, I.-A., Kim, Y.-B., Kim, J.W., Park, N.-H., Kang, S.-B., Han, J.Y., Lim, J.M., Song, Y.-S. (2011) Activation of mTOR signaling pathway associated with adverse prognostic factors of epithelial ovarian cancer. *Gynecologic Oncology*. **121**(1), 8–12.

Nyman, E., Rajan, M.R., Fagerholm, S., Brännmark, C., Cedersund, G., Strålfors, P. (2014) A single mechanism can explain network-wide insulin resistance in adipocytes from obese patients with type 2 diabetes. *The Journal of Biological Chemistry*. **289**(48), 33215–33230.

Obata, K., Morland, S.J., Watson, R.H., Hitchcock, A., Chenevix-Trench, G., Thomas, E.J., Campbell, I.G. (1998) Frequent PTEN/MMAC mutations in endometrioid but not serous or mucinous epithelial ovarian tumors. *Cancer Research*. **58**(10), 2095–2097.



Orezzoli, J.P., Russell, A.H., Oliva, E., Del Carmen, M.G., Eichhorn, J., Fuller, A.F. (2008) Prognostic implication of endometriosis in clear cell carcinoma of the ovary. *Gynecologic Oncology*. **110**(3), 336–344.

Parness, J., Horwitz, S.B. (1981) Taxol binds to polymerized tubulin in vitro. *The Journal of Cell Biology*. **91**(2 Pt 1), 479–487.

Patel, A.P., Tirosh, I., Trombetta, J.J., Shalek, A.K., Gillespie, S.M., Wakimoto, H., Cahill, D.P., Nahed, B.V., Curry, W.T., Martuza, R.L., Louis, D.N., Rozenblatt-Rosen, O., Suvà, M.L., Regev, A., Bernstein, B.E. (2014) Single-cell RNA-seq highlights intratumoral heterogeneity in primary glioblastoma. *Science*. **344**(6190), 1396–1401.

Pause, A., Belsham, G.J., Gingras, A.C., Donzé, O., Lin, T.A., Lawrence, J.C., Sonenberg, N. (1994) Insulin-dependent stimulation of protein synthesis by phosphorylation of a regulator of 5'-cap function. *Nature*. **371**(6500), 762–767.

Pause, A., Methot, N., Svitkin, Y., Merrick, W.C., Sonenberg, N. (1994) Dominant negative mutants of mammalian translation initiation factor eIF-4A define a critical role for eIF-4F in cap-dependent and cap-independent initiation of translation. *The EMBO Journal*. **13**(5), 1205–1215.

Pearce, C.L., Templeman, C., Rossing, M.A., Lee, A., Near, A.M., Webb, P.M., Nagle, C.M., Doherty, J.A., Cushing-Haugen, K.L., Wicklund, K.G., Chang-Claude, J., Hein, R., Lurie, G., Wilkens, L.R., Carney, M.E., Goodman, M.T., Moysich, K., Kjaer, S.K., Hogdall, E., Jensen, A., Goode, E.L., Fridley, B.L., Larson, M.C., Schildkraut, J.M., Palmieri, R.T., Cramer, D.W., Terry, K.L., Vitonis, A.F., Titus, L.J., Ziogas, A., Brewster, W., Anton-Culver, H., Gentry-Maharaj, A., Ramus, S.J., Anderson, A.R., Brueggmann, D., Fasching, P.A., Gayther, S.A., Huntsman, D.G., Menon, U., Ness, R.B., Pike, M.C., Risch, H., Wu, A.H., Berchuck, A. (2012) Association between endometriosis and risk of histological subtypes of ovarian cancer: a pooled analysis of case-control studies. *The Lancet Oncology*. **13**(4), 385–394.

Pearce, L.R., Huang, X., Boudeau, J., Pawłowski, R., Wullschleger, S., Deak, M., Ibrahim, A.F.M., Gourlay, R., Magnuson, M.A., Alessi, D.R. (2007) Identification of Protor as a novel Rictor-binding component of mTOR complex-2. *The Biochemical journal*. **405**(3), 513–522.

Pecorino, L. (2008) *Molecular Biology of Cancer: Mechanisms, Targets, and Therapeutics*. 2 edition. Oxford ; New York: OUP Oxford.

Pei, L., Xie, P., Zhou, E., Yang, Q., Luo, Y., Tang, Z. (2011) Overexpression of DEP domain containing mTOR-interacting protein correlates with poor prognosis in differentiated thyroid carcinoma. *Molecular Medicine Reports*. **4**(5), 817–823.

Peterson, T.R., Laplante, M., Thoreen, C.C., Sancak, Y., Kang, S.A., Kuehl, W.M., Gray, N.S., Sabatini, D.M. (2009) DEPTOR is an mTOR inhibitor frequently overexpressed in multiple myeloma cells and required for their survival. *Cell*. **137**(5), 873–886.

- Peterson, T.R., Sengupta, S.S., Harris, T.E., Carmack, A.E., Kang, S.A., Balderas, E., Guertin, D.A., Madden, K.L., Carpenter, A.E., Finck, B.N., Sabatini, D.M. (2011) mTOR complex 1 regulates lipin 1 localization to control the SREBP pathway. *Cell*. **146**(3), 408–420.
- Petrillo, M., Paris, I., Vizzielli, G., Amadio, G., Cosentino, F., Salutari, V., Scambia, G., Fagotti, A. (2015) Neoadjuvant Chemotherapy Followed by Maintenance Therapy With or Without Bevacizumab in Unresectable High-Grade Serous Ovarian Cancer: A Case-Control Study. *Annals of Surgical Oncology*.
- Phillips, R.J., Mestas, J., Gharaee-Kermani, M., Burdick, M.D., Sica, A., Belperio, J.A., Keane, M.P., Strieter, R.M. (2005) Epidermal growth factor and hypoxia-induced expression of CXCR4 chemokine receptor 4 on non-small cell lung cancer cells is regulated by the phosphatidylinositol 3-kinase/PTEN/AKT/mammalian target of rapamycin signaling pathway and activation of hypoxia inducible factor-1 $\alpha$ . *The Journal of Biological Chemistry*. **280**(23), 22473–22481.
- Philp, A.J., Campbell, I.G., Leet, C., Vincan, E., Rockman, S.P., Whitehead, R.H., Thomas, R.J., Phillips, W.A. (2001) The phosphatidylinositol 3'-kinase p85 $\alpha$  gene is an oncogene in human ovarian and colon tumors. *Cancer Research*. **61**(20), 7426–7429.
- Plaxe, S.C. (2008) Epidemiology of low-grade serous ovarian cancer. *American Journal of Obstetrics and Gynecology*. **198**(4), 459.e1–459.e9.
- Pon, Y.L., Zhou, H.Y., Cheung, A.N.Y., Ngan, H.Y.S., Wong, A.S.T. (2008) p70 S6 kinase promotes epithelial to mesenchymal transition through snail induction in ovarian cancer cells. *Cancer Research*. **68**(16), 6524–6532.
- Porstmann, T., Santos, C.R., Griffiths, B., Cully, M., Wu, M., Leever, S., Griffiths, J.R., Chung, Y.-L., Schulze, A. (2008) SREBP activity is regulated by mTORC1 and contributes to Akt-dependent cell growth. *Cell Metabolism*. **8**(3), 224–236.
- Porter, L.A., Donoghue, D.J. (2003) Cyclin B1 and CDK1: nuclear localization and upstream regulators. *Progress in Cell Cycle Research*. **5**, 335–347.
- Potter, C.J., Pedraza, L.G., Xu, T. (2002) Akt regulates growth by directly phosphorylating Tsc2. *Nature Cell Biology*. **4**(9), 658–665.
- Prado, C.M.M., Baracos, V.E., Xiao, J., Birdsell, L., Stuyckens, K., Park, Y.C., Parekh, T., Sawyer, M.B. (2014) The association between body composition and toxicities from the combination of Doxil and trabectedin in patients with advanced relapsed ovarian cancer. *Applied Physiology, Nutrition, and Metabolism*. **39**(6), 693–698.
- Presta, L.G., Chen, H., O'Connor, S.J., Chisholm, V., Meng, Y.G., Krummen, L., Winkler, M., Ferrara, N. (1997) Humanization of an anti-vascular endothelial growth factor monoclonal antibody for the therapy of solid tumors and other disorders. *Cancer Research*. **57**(20), 4593–4599.

- Prevot, N., Pyaram, K., Bischoff, E., Sen, J.M., Powell, J.D., Chang, C.-H. (2015) Mammalian Target of Rapamycin Complex 2 Regulates Invariant NKT Cell Development and Function Independent of Promyelocytic Leukemia Zinc-Finger. *The Journal of Immunology*. **194**(1), 223–230.
- Primerdesign (2014) geNorm Reference Gene Selection Kit. [online]. Available from: [http://www.primerdesign.co.uk/assets/files/genorm\\_sybrgreen\\_handbook.pdf?timestamp=1439572558](http://www.primerdesign.co.uk/assets/files/genorm_sybrgreen_handbook.pdf?timestamp=1439572558).
- Qiagen (2015) Rotor-Gene Q. *Qiagen*. [online]. Available from: <https://www.qiagen.com/gb/shop/automated-solutions/detection-and-analysis/rotor-gene-q/#productdetails>.
- Quirk, J.T., Natarajan, N. (2005) Ovarian cancer incidence in the United States, 1992–1999. *Gynecologic Oncology*. **97**(2), 519–523.
- Qu, X., Yu, J., Bhagat, G., Furuya, N., Hibshoosh, H., Troxel, A., Rosen, J., Eskelinen, E.-L., Mizushima, N., Ohsumi, Y., Cattoretti, G., Levine, B. (2003) Promotion of tumorigenesis by heterozygous disruption of the beclin 1 autophagy gene. *The Journal of Clinical Investigation*. **112**(12), 1809–1820.
- Reade, C.J., McVey, R.M., Tone, A.A., Finlayson, S.J., McAlpine, J.N., Fung-Kee-Fung, M., Ferguson, S.E. (2014) The fallopian tube as the origin of high grade serous ovarian cancer: review of a paradigm shift. *Journal of obstetrics and gynaecology*. **36**(2), 133–140.
- Reed, E., Ozols, R.F., Tarone, R., Yuspa, S.H., Poirier, M.C. (1987) Platinum-DNA adducts in leukocyte DNA correlate with disease response in ovarian cancer patients receiving platinum-based chemotherapy. *Proceedings of the National Academy of Sciences of the United States of America*. **84**(14), 5024–5028.
- Reinartz, S., Failer, S., Schuell, T., Wagner, U. (2012) CA125 (MUC16) gene silencing suppresses growth properties of ovarian and breast cancer cells. *European Journal of Cancer*. **48**(10), 1558–1569.
- Rhodes, D.R., Yu, J., Shanker, K., Deshpande, N., Varambally, R., Ghosh, D., Barrette, T., Pandey, A., Chinnaiyan, A.M. (2004) ONCOMINE: A Cancer Microarray Database and Integrated Data-Mining Platform. *Neoplasia*. **6**(1), 1–6.
- Risch, H.A., Marrett, L.D., Jain, M., Howe, G.R. (1996) Differences in risk factors for epithelial ovarian cancer by histologic type. Results of a case-control study. *American Journal of Epidemiology*. **144**(4), 363–372.
- Rizk, B., Fischer, A.S., Lotfy, H.A., Turki, R., Zahed, H.A., Malik, R., Holliday, C.P., Glass, A., Fishel, H., Soliman, M.Y., Herrera, D. (2014) Recurrence of endometriosis after hysterectomy. *Facts, Views & Vision in ObGyn*. **6**(4), 219–227.
- Roos, S., Jansson, N., Palmberg, I., Säljö, K., Powell, T.L., Jansson, T. (2007) Mammalian target of rapamycin in the human placenta regulates leucine transport

and is down-regulated in restricted fetal growth. *The Journal of Physiology*. **582**(Pt 1), 449–459.

Rose, P.G., Piver, M.S., Tsukada, Y., Lau, T. (1989) Metastatic patterns in histologic variants of ovarian cancer. An autopsy study. *Cancer*. **64**(7), 1508–1513.

Rossing, M.A., Cushing-Haugen, K.L., Wicklund, K.G., Doherty, J.A., Weiss, N.S. (2008) Risk of epithelial ovarian cancer in relation to benign ovarian conditions and ovarian surgery. *Cancer causes & control*. **19**(10), 1357–1364.

Rozen-Zvi, B., Hayashida, T., Hubchak, S.C., Hanna, C., Platanias, L.C., William Schnaper, H. (2013) TGF- $\beta$ /Smad3 activates mammalian target of rapamycin complex-1 to promote collagen production by increasing HIF-1 $\alpha$  expression. *American Journal of Physiology - Renal Physiology*. **305**(4), F485–F494.

Rump, A., Morikawa, Y., Tanaka, M., Minami, S., Umesaki, N., Takeuchi, M., Miyajima, A. (2004) Binding of Ovarian Cancer Antigen CA125/MUC16 to Mesothelin Mediates Cell Adhesion. *Journal of Biological Chemistry*. **279**(10), 9190–9198.

Russo, E., Citraro, R., Constanti, A., De Sarro, G. (2012) The mTOR Signaling Pathway in the Brain: Focus on Epilepsy and Epileptogenesis. *Molecular neurobiology*. **46**(3), 662–681.

Sabatini, D.M., Barrow, R.K., Blackshaw, S., Burnett, P.E., Lai, M.M., Field, M.E., Bahr, B.A., Kirsch, J., Betz, H., Snyder, S.H. (1999) Interaction of RAFT1 with gephyrin required for rapamycin-sensitive signaling. *Science*. **284**(5417), 1161–1164.

Saber, M.M., Zeeneldin, A.A., El Gammal, M.M., Salem, S.E., Darweesh, A.D., Abdelaziz, A.A., Monir, M. (2014) Treatment outcomes of female germ cell tumors: the Egyptian National Cancer Institute experience. *Journal of the Egyptian National Cancer Institute*. **26**(2), 103–108.

Sabers, C.J., Martin, M.M., Brunn, G.J., Williams, J.M., Dumont, F.J., Wiederrecht, G., Abraham, R.T. (1995) Isolation of a protein target of the FKBP12-rapamycin complex in mammalian cells. *The Journal of biological chemistry*. **270**(2), 815–822.

Sablina, A.A., Budanov, A.V., Ilyinskaya, G.V., Agapova, L.S., Kravchenko, J.E., Chumakov, P.M. (2005) The antioxidant function of the p53 tumor suppressor. *Nature medicine*. **11**(12), 1306–1313.

Saeed, A.A., Sims, A.H., Prime, S.S., Paterson, I., Murray, P.G., Lopes, V.R. (2015) Gene expression profiling reveals biological pathways responsible for phenotypic heterogeneity between UK and Sri Lankan oral squamous cell carcinomas. *Oral Oncology*. **51**(3), 237–246.

Sainz de la Cuesta, R., Eichhorn, J.H., Rice, L.W., Fuller, A.F., Nikrui, N., Goff, B.A. (1996) Histologic transformation of benign endometriosis to early epithelial ovarian cancer. *Gynecologic Oncology*. **60**(2), 238–244.

- Salani, R., Kurman, R.J., Giuntoli, R., Gardner, G., Bristow, R., Wang, T.-L., Shih, I.-M. (2008) Assessment of TP53 mutation using purified tissue samples of ovarian serous carcinomas reveals a higher mutation rate than previously reported and does not correlate with drug resistance. *International Journal of Gynecological Cancer: Official Journal of the International Gynecological Cancer Society*. **18**(3), 487–491.
- Samaan, M.C., Anand, S.S., Sharma, A.M., Samjoo, I.A., Tarnopolsky, M.A. (2015) Sex differences in skeletal muscle phosphatase and tensin homolog deleted on chromosome 10 (PTEN) levels: a cross-sectional study. *Scientific Reports*. **5**, 9154.
- Sampson, J.A. (1927) Metastatic or Embolic Endometriosis, due to the Menstrual Dissemination of Endometrial Tissue into the Venous Circulation. *The American Journal of Pathology*. **3**(2), 93–110.43.
- Sancak, Y., Bar-Peled, L., Zoncu, R., Markhard, A.L., Nada, S., Sabatini, D.M. (2010) Ragulator-Rag complex targets mTORC1 to the lysosomal surface and is necessary for its activation by amino acids. *Cell*. **141**(2), 290–303.
- Sancak, Y., Thoreen, C.C., Peterson, T.R., Lindquist, R.A., Kang, S.A., Spooner, E., Carr, S.A., Sabatini, D.M. (2007) PRAS40 is an insulin-regulated inhibitor of the mTORC1 protein kinase. *Molecular cell*. **25**(6), 903–915.
- Santillan, A., Kim, Y.W., Zahurak, M.L., Gardner, G.J., Giuntoli, R.L., Shih, I.M., Bristow, R.E. (2007) Differences of chemoresistance assay between invasive micropapillary/low-grade serous ovarian carcinoma and high-grade serous ovarian carcinoma. *International Journal of Gynecological Cancer*. **17**(3), 601–606.
- Sarbassov, D.D., Ali, S.M., Kim, D.-H., Guertin, D.A., Latek, R.R., Erdjument-Bromage, H., Tempst, P., Sabatini, D.M. (2004) Rictor, a novel binding partner of mTOR, defines a rapamycin-insensitive and raptor-independent pathway that regulates the cytoskeleton. *Current biology*. **14**(14), 1296–1302.
- Sarbassov, D.D., Ali, S.M., Sengupta, S., Sheen, J.-H., Hsu, P.P., Bagley, A.F., Markhard, A.L., Sabatini, D.M. (2006) Prolonged rapamycin treatment inhibits mTORC2 assembly and Akt/PKB. *Molecular cell*. **22**(2), 159–168.
- Sarbassov, D.D., Guertin, D.A., Ali, S.M., Sabatini, D.M. (2005) Phosphorylation and regulation of Akt/PKB by the rictor-mTOR complex. *Science*. **307**(5712), 1098–1101.
- Sarwar, S., Siddiqui, N., Ather, S., Hannan, A., Ali Syed, A., Zafar, W. (2014) Outcomes among patients with sex cord stromal tumour of ovary: experience from Pakistan. *Journal of Ayub Medical College*. **26**(3), 389–392.
- Schiff, P.B., Horwitz, S.B. (1980) Taxol stabilizes microtubules in mouse fibroblast cells. *Proceedings of the National Academy of Sciences of the United States of America*. **77**(3), 1561–1565.
- Schmeler, K.M., Sun, C.C., Bodurka, D.C., T. Deavers, M., Malpica, A., Coleman, R.L., Ramirez, P.T., Gershenson, D.M. (2008) Neoadjuvant chemotherapy for low-grade

serous carcinoma of the ovary or peritoneum. *Gynecologic Oncology*. **108**(3), 510–514.

Schneeberger, C., Speiser, P., Kury, F., Zeillinger, R. (1995) Quantitative detection of reverse transcriptase-PCR products by means of a novel and sensitive DNA stain. *PCR methods and applications*. **4**(4), 234–238.

Schrauwen, S., Depreeuw, J., Coenegrachts, L., Hermans, E., Lambrechts, D., Amant, F. (2015) Dual blockade of PI3K/AKT/mTOR (NVP-BEZ235) and Ras/Raf/MEK (AZD6244) pathways synergistically inhibit growth of primary endometrioid endometrial carcinoma cultures, whereas NVP-BEZ235 reduces tumor growth in the corresponding xenograft models. *Gynecologic Oncology*. **138**(1), 165–173.

Sedrani, R., Cottens, S., Kallen, J., Schuler, W. (1998) Chemical modification of rapamycin: the discovery of SDZ RAD. *Transplantation Proceedings*. **30**(5), 2192–2194.

SEER (2015a) SEER Stat Fact Sheets: Breast Cancer. *Surveillance, Epidemiology, and End Results Program*. [online]. Available from: <http://seer.cancer.gov/statfacts/html/breast.html>.

SEER (2015b) SEER Stat Fact Sheets: Colon and Rectum Cancer. *Surveillance, Epidemiology, and End Results Program*. [online]. Available from: <http://seer.cancer.gov/statfacts/html/colorect.html>.

SEER (2015c) SEER Stat Fact Sheets: Ovary Cancer. *Surveillance, Epidemiology, and End Results Program*. [online]. Available from: <http://seer.cancer.gov/statfacts/html/ovary.html>.

SEER (2015d) SEER Stat Fact Sheets: Prostate Cancer. *Surveillance, Epidemiology, and End Results Program*. [online]. Available from: <http://seer.cancer.gov/statfacts/html/prost.html>.

Sehgal, S.N., Baker, H., Vézina, C. (1975) Rapamycin (AY-22,989), a new antifungal antibiotic. II. Fermentation, isolation and characterization. *The Journal of antibiotics*. **28**(10), 727–732.

Seidman, J.D., Horkayne-Szakaly, I., Haiba, M., Boice, C.R., Kurman, R.J., Ronnett, B.M. (2004) The histologic type and stage distribution of ovarian carcinomas of surface epithelial origin. *International Journal of Gynecological Pathology*. **23**(1), 41–44.

Serra, V., Markman, B., Scaltriti, M., Eichhorn, P.J.A., Valero, V., Guzman, M., Botero, M.L., Llonch, E., Atzori, F., Di Cosimo, S., Maira, M., Garcia-Echeverria, C., Parra, J.L., Arribas, J., Baselga, J. (2008) NVP-BEZ235, a dual PI3K/mTOR inhibitor, prevents PI3K signaling and inhibits the growth of cancer cells with activating PI3K mutations. *Cancer Research*. **68**(19), 8022–8030.

Servier (2014) Servier Medical Art. *Servier*. [online]. Available from: <http://www.servier.co.uk/content/servier-medical-art>.

Shahrabi-Farahani, M., Shahbazi, S., Mahdian, R., Amini-Moghaddam, S. (2014) K-Ras 4A Transcript variant is up-regulated in eutopic endometrium of endometriosis patients during proliferative phase of menstrual cycle. *Archives of Gynecology and Obstetrics*. **292**(1), 225–229.

Shalek, A.K., Satija, R., Adiconis, X., Gertner, R.S., Gaublomme, J.T., Raychowdhury, R., Schwartz, S., Yosef, N., Malboeuf, C., Lu, D., Trombetta, J.J., Gennert, D., Gnirke, A., Goren, A., Hacohen, N., Levin, J.Z., Park, H., Regev, A. (2013) Single-cell transcriptomics reveals bimodality in expression and splicing in immune cells. *Nature*. **498**(7453), 236–240.

Shalek, A.K., Satija, R., Shuga, J., Trombetta, J.J., Gennert, D., Lu, D., Chen, P., Gertner, R.S., Gaublomme, J.T., Yosef, N., Schwartz, S., Fowler, B., Weaver, S., Wang, J., Wang, X., Ding, R., Raychowdhury, R., Friedman, N., Hacohen, N., Park, H., May, A.P., Regev, A. (2014) Single-cell RNA-seq reveals dynamic paracrine control of cellular variation. *Nature*. **510**(7505), 363–369.

Shao, Z., Bao, Q., Jiang, F., Qian, H., Fang, Q., Hu, X. (2015) VS-5584, a Novel PI3K-mTOR Dual Inhibitor, Inhibits Melanoma Cell Growth In Vitro and In Vivo. *PLoS ONE*. **10**(7), e0132655.

Shaw, R.J., Kosmatka, M., Bardeesy, N., Hurley, R.L., Witters, L.A., DePinho, R.A., Cantley, L.C. (2004) The tumor suppressor LKB1 kinase directly activates AMP-activated kinase and regulates apoptosis in response to energy stress. *Proceedings of the National Academy of Sciences of the United States of America*. **101**(10), 3329–3335.

Shin, E., Choi, C.M., Kim, H.R., Jang, S.J., Park, Y.S. (2015) Immunohistochemical characterization of the mTOR pathway in stage-I non-small-cell lung carcinoma. *Lung Cancer*. **89**(1), 13–18.

Shu, J., Huang, M., Tian, Q., Shui, Q., Zhou, Y., Chen, J. (2015) Downregulation of angiogenin inhibits the growth and induces apoptosis in human bladder cancer cells through regulating AKT/mTOR signaling pathway. *Journal of Molecular Histology*. **46**(2), 157–171.

Siemer, S., Ørnskov, D., Guerra, B., Boldyreff, B., Issinger, O.-G. (1999) Determination of mRNA, and protein levels of p53, MDM2 and protein kinase CK2 subunits in F9 cells after treatment with the apoptosis-inducing drugs cisplatin and carboplatin. *The International Journal of Biochemistry & Cell Biology*. **31**(6), 661–670.

Simoncini, T., Hafezi-Moghadam, A., Brazil, D.P., Ley, K., Chin, W.W., Liao, J.K. (2000) Interaction of oestrogen receptor with the regulatory subunit of phosphatidylinositol-3-OH kinase. *Nature*. **407**(6803), 538–541.

- Sinaii, N., Cleary, S.D., Ballweg, M.L., Nieman, L.K., Stratton, P. (2002) High rates of autoimmune and endocrine disorders, fibromyalgia, chronic fatigue syndrome and atopic diseases among women with endometriosis: a survey analysis. *Human Reproduction*. **17**(10), 2715–2724.
- Smith, E.M., Finn, S.G., Tee, A.R., Browne, G.J., Proud, C.G. (2005) The tuberous sclerosis protein TSC2 is not required for the regulation of the mammalian target of rapamycin by amino acids and certain cellular stresses. *The Journal of Biological Chemistry*. **280**(19), 18717–18727.
- Smith, H.O., Berwick, M., Verschraegen, C.F., Wiggins, C., Lansing, L., Muller, C.Y., Qualls, C.R. (2006) Incidence and survival rates for female malignant germ cell tumors. *Obstetrics and Gynecology*. **107**(5), 1075–1085.
- Smolle, E., Taucher, V., Pichler, M., Petru, E., Lax, S., Haybaeck, J. (2013) Targeting Signaling Pathways in Epithelial Ovarian Cancer. *International Journal of Molecular Sciences*. **14**(5), 9536–9555.
- Society for Gynecologic Oncology (2014) FIGO Ovarian Cancer Staging. *Society for Gynecologic Oncology*. [online]. Available from: [https://www.sgo.org/wp-content/uploads/2012/09/FIGO-Ovarian-Cancer-Staging\\_1.10.14.pdf](https://www.sgo.org/wp-content/uploads/2012/09/FIGO-Ovarian-Cancer-Staging_1.10.14.pdf).
- Song, R., Tian, K., Wang, W., Wang, L. (2015) P53 suppresses cell proliferation, metastasis, and angiogenesis of osteosarcoma through inhibition of the PI3K/AKT/mTOR pathway. *International Journal of Surgery*. **20**, 80–87.
- Squillace, R.M., Miller, D., Cookson, M., Wardwell, S.D., Moran, L., Clapham, D., Wang, F., Clackson, T., Rivera, V.M. (2011) Antitumor activity of ridaforolimus and potential cell-cycle determinants of sensitivity in sarcoma and endometrial cancer models. *Molecular Cancer Therapeutics*. **10**(10), 1959–1968.
- Stambolic, V., MacPherson, D., Sas, D., Lin, Y., Snow, B., Jang, Y., Benchimol, S., Mak, T.W. (2001) Regulation of PTEN transcription by p53. *Molecular Cell*. **8**(2), 317–325.
- Starup-Linde, J., Karlstad, O., Eriksen, S.A., Vestergaard, P., Bronsveld, H.K., de Vries, F., Andersen, M., Auvinen, A., Haukka, J., Hjellvik, V., Bazelier, M.T., Boer, A. de, Furu, K., De Bruin, M.L. (2013) CARING (CAncer Risk and INsulin analogues): the association of diabetes mellitus and cancer risk with focus on possible determinants - a systematic review and a meta-analysis. *Current Drug Safety*. **8**(5), 296–332.
- Stephen A. Bustin ed. (2014) *The PCR Revolution*. 1st ed.
- Stewart, C.A., Dell'orco, R.T. (1992) Expression of proliferating cell nuclear antigen during the cell cycle of human diploid fibroblasts. *In Vitro Cellular & Developmental Biology - Animal*. **28**(3), 211–214.
- Stewart, L.M., Holman, C.D.J., Aboagye-Sarfo, P., Finn, J.C., Preen, D.B., Hart, R. (2013) In vitro fertilization, endometriosis, nulliparity and ovarian cancer risk. *Gynecologic oncology*. **128**(2), 260–264.



Stokoe, D., Stephens, L.R., Copeland, T., Gaffney, P.R., Reese, C.B., Painter, G.F., Holmes, A.B., McCormick, F., Hawkins, P.T. (1997) Dual role of phosphatidylinositol-3,4,5-trisphosphate in the activation of protein kinase B. *Science*. **277**(5325), 567–570.

Sudhagar, S., Sathya, S., Lakshmi, B.S. (2011) Rapid non-genomic signalling by 17 $\beta$ -oestradiol through c-Src involves mTOR-dependent expression of HIF-1 $\alpha$  in breast cancer cells. *British Journal of Cancer*. **105**(7), 953–960.

Sun, H., Lesche, R., Li, D.-M., Liliental, J., Zhang, H., Gao, J., GavriloVA, N., Mueller, B., Liu, X., Wu, H. (1999) PTEN modulates cell cycle progression and cell survival by regulating phosphatidylinositol 3,4,5,-trisphosphate and Akt/protein kinase B signaling pathway. *Proceedings of the National Academy of Sciences of the United States of America*. **96**(11), 6199–6204.

Tania Nolan, S.A.B. ed. (2013) *PCR Technology: Current Innovations, Third Edition*.

Tee, A.R., Blenis, J. (2005) mTOR, translational control and human disease. *Seminars in Cell & Developmental Biology*. **16**(1), 29–37.

Tee, A.R., Manning, B.D., Roux, P.P., Cantley, L.C., Blenis, J. (2003) Tuberous sclerosis complex gene products, Tuberin and Hamartin, control mTOR signaling by acting as a GTPase-activating protein complex toward Rheb. *Current biology*. **13**(15), 1259–1268.

Tenti, P., Aguzzi, A., Riva, C., Usellini, L., Zappatore, R., Bara, J., Samloff, I.M., Solcia, E. (1992) Ovarian mucinous tumors frequently express markers of gastric, intestinal, and pancreatobiliary epithelial cells. *Cancer*. **69**(8), 2131–2142.

Terry, K.L., Karageorgi, S., Shvetsov, Y.B., Merritt, M.A., Lurie, G., Thompson, P.J., Carney, M.E., Weber, R.P., Akushevich, L., Lo-Ciganic, W.-H., Cushing-Haugen, K., Sieh, W., Moysich, K., Doherty, J.A., Nagle, C.M., Berchuck, A., Pearce, C.L., Pike, M., Ness, R.B., Webb, P.M., Australian Cancer Study (Ovarian Cancer), Australian Ovarian Cancer Study Group, Rossing, M.A., Schildkraut, J., Risch, H., Goodman, M.T., Ovarian Cancer Association Consortium (2013) Genital powder use and risk of ovarian cancer: a pooled analysis of 8,525 cases and 9,859 controls. *Cancer Prevention Research*. **6**(8), 811–821.

The Cancer Genome Atlas (2015) The Cancer Genome Atlas Home Page. *The Cancer Genome Atlas - National Cancer Institute*. [online]. Available from: <http://cancergenome.nih.gov/> [Accessed August 14, 2015].

Thedieck, K., Polak, P., Kim, M.L., Molle, K.D., Cohen, A., Jenö, P., Arriemerlou, C., Hall, M.N. (2007) PRAS40 and PRR5-like protein are new mTOR interactors that regulate apoptosis. *PLoS One*. **2**(11), e1217.

ThermoFisher Scientific (2015) 7900HT Fast Real-Time PCR System with Fast 96-Well Block Module. *ThermoFisher Scientific*. [online]. Available from: <http://www.thermofisher.com/order/catalog/product/4351405>.

- Thorpe, L.M., Yuzugullu, H., Zhao, J.J. (2015) PI3K in cancer: divergent roles of isoforms, modes of activation and therapeutic targeting. *Nature Reviews. Cancer.* **15**(1), 7–24.
- Tortora, G.J., Derrickson, B. (2005) *Principles of Anatomy and Physiology*. 11th Edition. Hoboken, NJ: John Wiley & Sons.
- Treeck, O., Wackwitz, B., Haus, U., Ortmann, O. (2006) Effects of a combined treatment with mTOR inhibitor RAD001 and tamoxifen in vitro on growth and apoptosis of human cancer cells. *Gynecologic Oncology.* **102**(2), 292–299.
- Treins, C., Giorgetti-Peraldi, S., Murdaca, J., Semenza, G.L., Van Obberghen, E. (2002) Insulin stimulates hypoxia-inducible factor 1 through a phosphatidylinositol 3-kinase/target of rapamycin-dependent signaling pathway. *The Journal of Biological Chemistry.* **277**(31), 27975–27981.
- Trimbos, J.B., Vergote, I., Bolis, G., Vermorken, J.B., Mangioni, C., Madronal, C., Franchi, M., Tateo, S., Zanetta, G., Scarfone, G., Giurgea, L., Timmers, P., Coens, C., Pecorelli, S., Collaborators, F. the E.-A. (2003) Impact of Adjuvant Chemotherapy and Surgical Staging in Early-Stage Ovarian Carcinoma: European Organisation for Research and Treatment of Cancer–Adjuvant ChemoTherapy in Ovarian Neoplasm Trial. *Journal of the National Cancer Institute.* **95**(2), 113–125.
- Troca-Marín, J.A., Alves-Sampaio, A., Montesinos, M.L. (2012) Deregulated mTOR-mediated translation in intellectual disability. *Progress in neurobiology.* **96**(2), 268–282.
- Truong, M., Cook, M.R., Pinchot, S.N., Kunnimalaiyaan, M., Chen, H. (2011) Resveratrol induces Notch2-mediated apoptosis and suppression of neuroendocrine markers in medullary thyroid cancer. *Annals of Surgical Oncology.* **18**(5), 1506–1511.
- Tsoref, D., Welch, S., Lau, S., Biagi, J., Tonkin, K., Martin, L.A., Ellard, S., Ghatage, P., Elit, L., Mackay, H.J., Allo, G., Tsao, M.-S., Kamel-Reid, S., Eisenhauer, E.A., Oza, A.M. (2014) Phase II study of oral ridaforolimus in women with recurrent or metastatic endometrial cancer. *Gynecologic Oncology.* **135**(2), 184–189.
- Tung, K.-H., Goodman, M.T., Wu, A.H., McDuffie, K., Wilkens, L.R., Kolonel, L.N., Nomura, A.M.Y., Terada, K.Y., Carney, M.E., Sobin, L.H. (2003) Reproductive factors and epithelial ovarian cancer risk by histologic type: a multiethnic case-control study. *American Journal of Epidemiology.* **158**(7), 629–638.
- Tzatsos, A., Kandrór, K.V. (2006) Nutrients suppress phosphatidylinositol 3-kinase/Akt signaling via raptor-dependent mTOR-mediated insulin receptor substrate 1 phosphorylation. *Molecular and Cellular Biology.* **26**(1), 63–76.
- Um, S.H., Frigerio, F., Watanabe, M., Picard, F., Joaquin, M., Sticker, M., Fumagalli, S., Allegrini, P.R., Kozma, S.C., Auwerx, J., Thomas, G. (2004) Absence of S6K1

protects against age- and diet-induced obesity while enhancing insulin sensitivity. *Nature*. **431**(7005), 200–205.

Unger, F.T., Klasen, H.A., Tchartchian, G., de Wilde, R.L., Witte, I. (2009) DNA damage induced by cis- and carboplatin as indicator for in vitro sensitivity of ovarian carcinoma cells. *BMC cancer*. **9**, 359.

Vang, R., Shih, I.-M., Kurman, R.J. (2009) OVARIAN LOW-GRADE AND HIGH-GRADE SEROUS CARCINOMA: Pathogenesis, Clinicopathologic and Molecular Biologic Features, and Diagnostic Problems. *Advances in anatomic pathology*. **16**(5), 267–282.

Veras, E., Mao, T.-L., Ayhan, A., Ueda, S., Lai, H., Hayran, M., Shih, I.-M., Kurman, R.J. (2009) Cystic and adenofibromatous clear cell carcinomas of the ovary: distinctive tumors that differ in their pathogenesis and behavior: a clinicopathologic analysis of 122 cases. *The American Journal of Surgical Pathology*. **33**(6), 844–853.

Vézina, C., Kudelski, A., Sehgal, S.N. (1975) Rapamycin (AY-22,989), a new antifungal antibiotic. I. Taxonomy of the producing streptomycete and isolation of the active principle. *The Journal of antibiotics*. **28**(10), 721–726.

Wang, G.L., Jiang, B.H., Rue, E.A., Semenza, G.L. (1995) Hypoxia-inducible factor 1 is a basic-helix-loop-helix-PAS heterodimer regulated by cellular O<sub>2</sub> tension. *Proceedings of the National Academy of Sciences of the United States of America*. **92**(12), 5510–5514.

Wang, Y., Fei, D., Vanderlaan, M., Song, A. (2004) Biological activity of bevacizumab, a humanized anti-VEGF antibody in vitro. *Angiogenesis*. **7**(4), 335–345.

Wataya-Kaneda, M. (2015) Mammalian target of rapamycin and tuberous sclerosis complex. *Journal of Dermatological Science*. **79**(2), 93–100.

Weiss, N.S., Homonchuk, T., Young, J.L. (1977) Incidence of the histologic types of ovarian cancer: the U.S. Third National Cancer Survey, 1969-1971. *Gynecologic Oncology*. **5**(2), 161–167.

Weng, L.-P., Smith, W.M., Dahia, P.L.M., Ziebold, U., Gil, E., Lees, J.A., Eng, C. (1999) PTEN Suppresses Breast Cancer Cell Growth by Phosphatase Activity-dependent G1 Arrest followed by Cell Death. *Cancer Research*. **59**(22), 5808–5814.

Wilson, M.A., Zhao, F., Khare, S., D'Andrea, K., Wubbenhorst, B., Roszik, J., Woodman, S.E., Rimm, D.L., Kirkwood, J.M., Kluger, H.M., Schuchter, L.M., Lee, S.J., Flaherty, K.T., Nathanson, K.L. (2015) Copy number changes are associated with response to treatment with carboplatin, paclitaxel, and sorafenib in melanoma. *Clinical Cancer Research*.

Wu, A.H., Pearce, C.L., Tseng, C.-C., Templeman, C., Pike, M.C. (2009) Markers of inflammation and risk of ovarian cancer in Los Angeles County. *International Journal of Cancer*. **124**(6), 1409–1415.

- Wu, J., Yin, R.-X., Guo, T., Lin, Q.-Z., Shen, S.-W., Sun, J.-Q., Shi, G.-Y., Wu, J.-Z., Yang, D.-Z., Lin, W.-X. (2015) Gender-specific association between the cytoplasmic poly(A) binding protein 4 rs4660293 single nucleotide polymorphism and serum lipid levels. *Molecular Medicine Reports*. **12**(3), 3476–3486.
- Xu, M., Bu, L.-M., Wu, K., Lu, L.-G., Wang, X.-P. (2015) Rapamycin inhibits the proliferation of SW1990 pancreatic cancer cell. *European Review for Medical and Pharmacological Sciences*. **19**(16), 3072–3079.
- Yang, H.-J., Liu, V.W.S., Wang, Y., Tsang, P.C.K., Ngan, H.Y.S. (2006) Differential DNA methylation profiles in gynecological cancers and correlation with clinico-pathological data. *BMC cancer*. **6**, 212.
- Yip, C.K., Murata, K., Walz, T., Sabatini, D.M., Kang, S.A. (2010) Structure of the human mTOR complex I and its implications for rapamycin inhibition. *Molecular Cell*. **38**(5), 768–774.
- Yoon, D., Pastore, Y.D., Divoky, V., Liu, E., Mlodnicka, A.E., Rainey, K., Ponka, P., Semenza, G.L., Schumacher, A., Prchal, J.T. (2006) Hypoxia-inducible factor-1 deficiency results in dysregulated erythropoiesis signaling and iron homeostasis in mouse development. *The Journal of Biological Chemistry*. **281**(35), 25703–25711.
- Yoshihara, K., Tajima, A., Komata, D., Yamamoto, T., Kodama, S., Fujiwara, H., Suzuki, M., Onishi, Y., Hatae, M., Sueyoshi, K., Fujiwara, H., Kudo, Y., Inoue, I., Tanaka, K. (2009) Gene expression profiling of advanced-stage serous ovarian cancers distinguishes novel subclasses and implicates ZEB2 in tumor progression and prognosis. *Cancer Science*. **100**(8), 1421–1428.
- Young, J., Povey, S. (1998) The genetic basis of tuberous sclerosis. *Molecular Medicine Today*. **4**(7), 313–319.
- Yue, Z., Jin, S., Yang, C., Levine, A.J., Heintz, N. (2003) Beclin 1, an autophagy gene essential for early embryonic development, is a haploinsufficient tumor suppressor. *Proceedings of the National Academy of Sciences of the United States of America*. **100**(25), 15077–15082.
- Zhang, G.Y., Ahmed, N., Riley, C., Oliva, K., Barker, G., Quinn, M.A., Rice, G.E. (2005) Enhanced expression of peroxisome proliferator-activated receptor gamma in epithelial ovarian carcinoma. *British Journal of Cancer*. **92**(1), 113–119.
- Zhang, X., Shu, L., Hosoi, H., Murti, K.G., Houghton, P.J. (2002) Predominant nuclear localization of mammalian target of rapamycin in normal and malignant cells in culture. *The Journal of Biological Chemistry*. **277**(31), 28127–28134.
- Zhang, X., Wang, X., Xu, T., Zhong, S., Shen, Z. (2015) Targeting of mTORC2 may have advantages over selective targeting of mTORC1 in the treatment of malignant pheochromocytoma. *Tumour Biology*. **36**(7), 5273–5281.

- Zhong, H., Chiles, K., Feldser, D., Laughner, E., Hanrahan, C., Georgescu, M.M., Simons, J.W., Semenza, G.L. (2000) Modulation of hypoxia-inducible factor 1 $\alpha$  expression by the epidermal growth factor/phosphatidylinositol 3-kinase/PTEN/AKT/FRAP pathway in human prostate cancer cells: implications for tumor angiogenesis and therapeutics. *Cancer Research*. **60**(6), 1541–1545.
- Zhou, C., Chen, Z., Dong, J., Li, J., Shi, X., Sun, N., Luo, M., Zhou, F., Tan, F., He, J. (2015) Combination of serum miRNAs with Cyfra21-1 for the diagnosis of non-small cell lung cancer. *Cancer Letters*. **367**(2), 138–146.
- Zhou, H.Y., Wong, A.S.T. (2006) Activation of p70S6K induces expression of matrix metalloproteinase 9 associated with hepatocyte growth factor-mediated invasion in human ovarian cancer cells. *Endocrinology*. **147**(5), 2557–2566.
- Zinzalla, V., Stracka, D., Oppliger, W., Hall, M.N. (2011) Activation of mTORC2 by association with the ribosome. *Cell*. **144**(5), 757–768.
- Zipper, H., Brunner, H., Bernhagen, J., Vitzthum, F. (2004) Investigations on DNA intercalation and surface binding by SYBR Green I, its structure determination and methodological implications. *Nucleic Acids Research*. **32**(12), e103.
- Zito, G., Luppi, S., Giolo, E., Martinelli, M., Venturin, I., Di Lorenzo, G., Ricci, G. (2014) Medical treatments for endometriosis-associated pelvic pain. *BioMed Research International*. **2014**, 191967.
- Zitzmann, K., Rüden, J. von, Brand, S., Göke, B., Lichtl, J., Spöttl, G., Auernhammer, C.J. (2010) Compensatory activation of Akt in response to mTOR and Raf inhibitors - a rationale for dual-targeted therapy approaches in neuroendocrine tumor disease. *Cancer Letters*. **295**(1), 100–109.
- Zorn, K.K., Jazaeri, A.A., Awtrey, C.S., Gardner, G.J., Mok, S.C., Boyd, J., Birrer, M.J. (2003) Choice of Normal Ovarian Control Influences Determination of Differentially Expressed Genes in Ovarian Cancer Expression Profiling Studies. *Clinical Cancer Research*. **9**(13), 4811–4818.
- Zwart, J., Geisler, J.P., Geisler, H.E. (1998) Five-year survival in patients with endometrioid carcinoma of the ovary versus those with serous carcinoma. *European Journal of Gynaecological Oncology*. **19**(3), 225–228.

# ***Chapter 9***

## ***Appendix***

### **9.1 qPCR**

qPCR (quantitative polymerase chain reaction) is a method of amplifying and quantifying genetic material in real-time using gene-specific primers, DNA polymerase and fluorescent reporter dyes. The following section describes qPCR methods and chemistry including experimental design and post-amplification controls.

### **9.2 Experimental Design**

Prior to a qPCR experiment, a number of preliminary procedures are required. Sources of amplicon, the template DNA used in a qPCR experiment, are wide and varied, whether it be animal or plant, from tissue, blood or cultured cells, the nucleic acid must be prepared before it is suitable for use in a qPCR experiment. The nucleic acid must first be extracted from its source. There are a number of ways to do this including phenol-chloroform extraction by TRI reagent and silica membrane extraction by spin column. The method chosen will depend on type and amount of starting material.

One of the most common applications of qPCR is examining gene expression by the amount of messenger ribonucleic acid (mRNA) transcript. mRNA is transcribed from a specific gene and is responsible for providing a template by which to make proteins. mRNA may be extracted under basal conditions or following different treatment variables. As RNA is single stranded, it is not possible to use it directly in a qPCR reaction. Due to this, mRNA is converted into cDNA using a process called reverse transcription. Reverse transcription creates a DNA molecule copy of the mRNA sequence which can be directly used in a qPCR reaction.

qPCR primers are short (~20 base pairs) sequences of nucleotides designed to be complementary to the 5' end of the gene of interest (GOI) on the sense (forward) and antisense (reverse) strands of DNA. Primers provide a base from which the polymerase enzyme can begin synthesising the complementary strand of DNA. qPCR experiments may utilise probes or SYBR® Green as methods of reporting DNA amplification by fluorescence. Non-probe based qPCR includes the addition of SYBR® Green ([2-[N-(3-dimethylaminopropyl)-N-propylamino]-4-[2,3-dihydro-3-methyl-(benzo-1,3-thiazol-2-yl)-methylidene]-1-phenyl-quinolinium]<sup>+</sup>) cyanine reporter dye, an intercalating DNA dye which fluoresces when bound to double stranded DNA (Zipper *et al.*, 2004; Schneeberger *et al.*, 1995). qPCR probes are short (~20 base pairs) sequences of nucleic acids designed to be complementary to an area between the primer and the end of the GOI and which are conjugated to a fluorophore. The probe also usually contains a quencher which absorbs emitted fluorescence when in close contact with the fluorophore. Probe based qPCR can use a number of methods to dissociate the fluorophore from the quencher, allowing it to fluoresce. Some probes, known as TaqMan probes, take advantage of the nucleolytic activity of DNA polymerase which cleaves and disassembles nucleotides as it is creating a new strand. The probe is cleaved in the process of the reaction, separating the fluorophore from the quencher and allowing its emitted fluorescence to be detected (Lee *et al.*, 1993; Livak *et al.*, 1995).

SYBR® Green will bind to all double stranded DNA, whether or not it is the amplified GOI and so is less specific than using probe based chemistries which can only fluoresce when bound to the sequence they were designed for. Probes, however, are costly and a number of methods designed to ensure that SYBR® Green fluorescence measured is as a result of GOI amplification will be described later. In addition to SYBR® Green or probes, qPCR experiments involve three main reagents: target genetic material to be amplified (amplicon), the enzyme, usually a derivative of *Taq* polymerase, and dNTPs. Commercially available reagent master mixes such as Power SYBR® Master Mix (Life Technologies) or KAPA SYBR® FAST Master Mix

(KAPA) usually contains ready optimised concentrations of polymerase enzyme,  $Mg^{2+}$  to maintain efficient enzyme activity and dNTPs. In addition to this, master mixes may also contain a passive ROX™ dye for fluorescence normalisation. Master mixes designed for primer, as opposed to probe, based qPCR experiments will also contain the reporter dye SYBR® Green. qPCR reactions are formulated to contain the optimal concentrations of reagents and should be developed to account for the specific conditions of the experiment; however a typical formulation for one 20µL reaction may be as follows (Table 8.1):

Reagent	Volume
2X qPCR master mix	10µL
Primer (forward and reverse)	2µL
Template	1µL
Pure H <sub>2</sub> O	7µL
Total	20µL

**Table 9.1** - An example of a typical qPCR reaction formulation.

### 9.3 Amplification

In recent years, *Taq* polymerase derivatives have been modified to improve stability. Enzymes are usually conjugated to an inhibitor, such as an antibody, which blocks activity until heated. This type of enzyme developed the ‘hot start’ method of qPCR which requires an extended incubation of around 95°C before thermal cycling begins. Enzyme inactivity at low temperatures allows for ambient set up of qPCR experiments and greater specificity of results.

After a hot start incubation for a time and temperature specific to the enzyme within the master mix, qPCR reactions are subjected to rounds of thermal cycling. Each cycle is completed in three steps: dissociation of amplicon strands, primer annealing and extension (Figure 8.1). Dissociation happens at around 95°C and separates the double stranded amplicon into single strands. This makes way for



primer binding which is optimised for the specific primers or probes in use (usually 55-60°C). dNTPs then build onwards from the primers, adding complementary nucleosides and creating two new double stranded copies of the gene, each copy containing one strand of the original template (Figure 8.2).

The efficiency of a qPCR reaction is an important determinant when comparing results. An efficiency of 100% implies that the amplicon is doubled with each thermal cycle. If the efficiencies of two reactions are dissimilar, results cannot be compared. Efficiency is assessed by creating a standard curve graph using a dilution series of the nucleic acid input and plotting log concentration against  $C_q$ . The gradient of the trend line can be used to calculate efficiency. The correlation coefficient ( $R^2$ ) of the data points must also be taken into account with an  $R^2$  value of  $\geq 0.975$  considered acceptable (Kennedy and Oswald, 2011). The commonly used  $\Delta$  (delta) and  $\Delta\Delta C_q$  methods of qPCR analysis make an assumption of 100% efficiency within their calculations (i.e. generated amplicon is  $2^n$  when cycle number is  $n$ ). However, without optimisation, efficiency may fall below acceptable levels (90-110%) and concentration of reagents or thermal protocol may need to be modified to improve it.

Although qPCR reactions occur in three stages, thermal cycling itself may have two or three steps. As enzyme activity is improving, it is becoming more common to combine primer binding and extension into one temperature incubation step. Typical two or three step thermal protocols are shown in Table 8.2 and 8.3 respectively.

Step	Temperature	Time	Repeats
Hot Start	95°C	10 minutes	1 X
Denaturation	95°C	15 seconds	40 X
Annealing/Extension	60°C	60 seconds	
Fluorescence Measurement			

**Table 9.2** - A typical two step qPCR thermal protocol where annealing and extension have been combined into one step.

Step	Temperature	Time	Repeats
Hot Start	95°C	10 minutes	1 X
Denaturation	95°C	15 seconds	40 X
Annealing	60°C	30 seconds	
Extension	72°C	30 seconds	
Fluorescence Measurement			

**Table 9.3** - A typical three step qPCR thermal protocol.

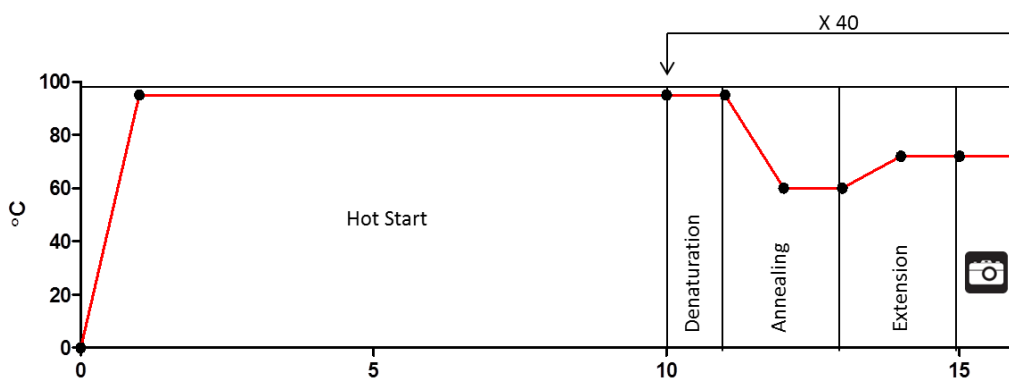


**Figure 9.1** - The thermal profile of a typical three-step qPCR reaction. The 95°C hot start step dissociates the enzyme from its inhibitor. 40 cycles of 95°C-60°C-72°C follow the hot start. A fluorescence measurement is taken at the end of each cycle.

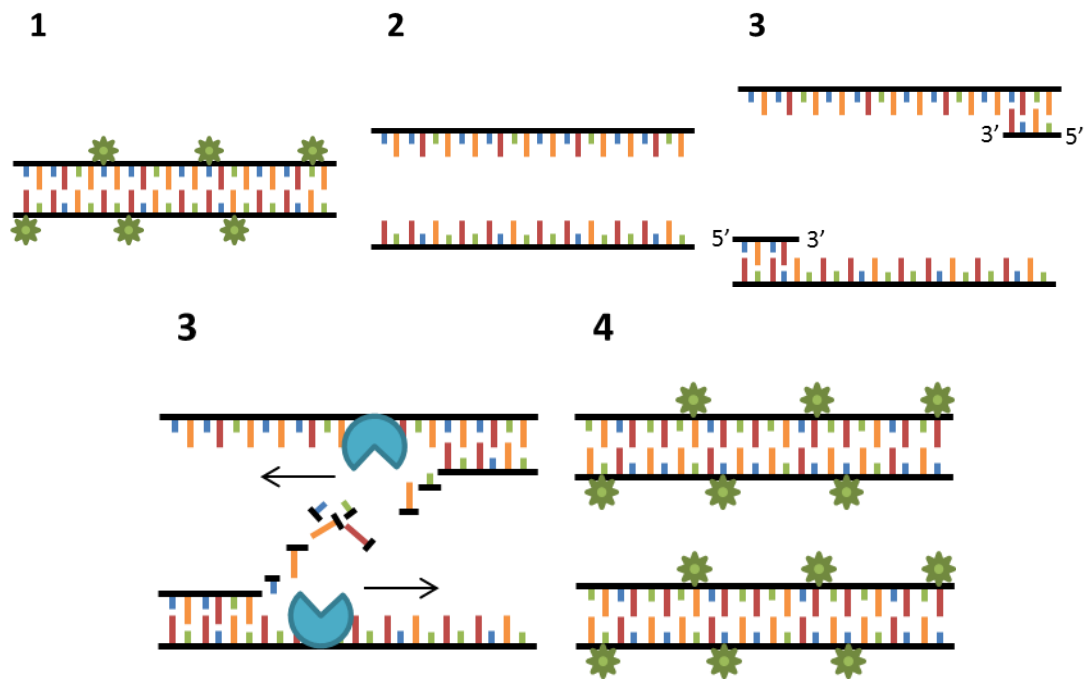


**Figure 9.2** - The process of one DNA strand during one thermal cycle of a qPCR reaction using primers and SYBR® Green. (1) Double stranded DNA with fluorescing SYBR® Green bound to the minor groove. (2) Denaturation: The denaturation stage (95°C) causes the two strands of DNA to dissociate, in turn causing the dissociation and cessation of fluorescence of SYBR® Green. (3) Annealing: The annealing stage (60°C) allows the primers to bind to their complementary sequences but does not allow dissociated DNA strands to reassociate. (4) Extension: DNA polymerase catalyses the addition of dNTPs to their complementary bases to create a new strand of DNA. (5) Two double stranded DNA molecules have been created from one starting template. SYBR® Green is able to bind and double the amount of fluorescence is emitted than at the beginning of the cycle.

As each thermal cycle is completed, a fluorescence image is captured. Fluorescence increases when the GOI is amplified as more probe conjugated fluorophores are unquenched or as more double stranded DNA is created for SYBR® Green to bind to. Fluorescence readings are plotted against cycle number on a graph to create a sigmoidal amplification curve (Figure 8.3). A quantification cycle ( $C_q$ ) value can be obtained by creating a fluorescence threshold above background fluorescence and determining at which cycle or cycle fraction the threshold was reached. An increase in amplicon translates to a higher level of fluorescence and therefore a lower  $C_q$  value.

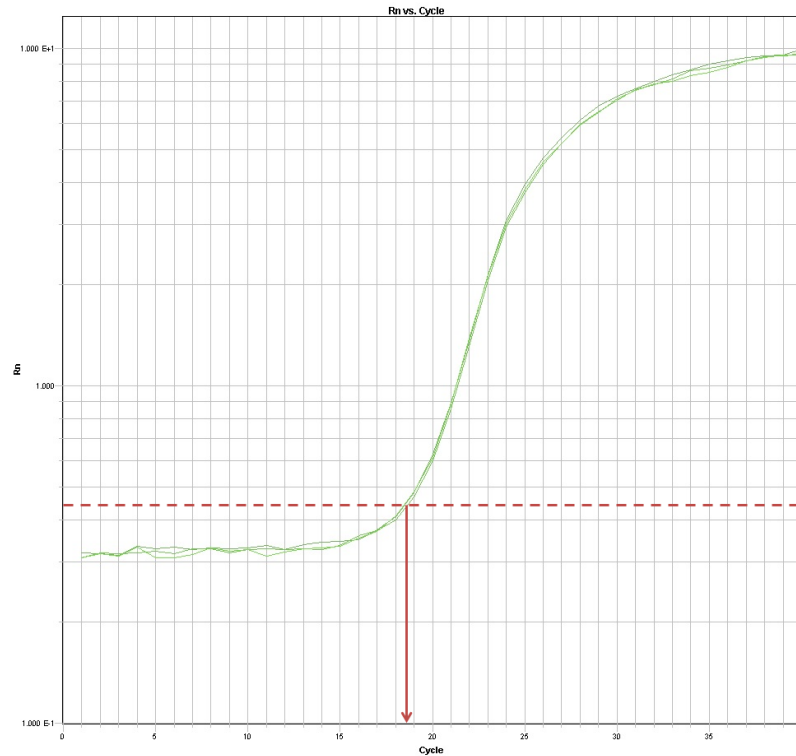


**Figure 9.3** - An example of three technical replicate amplification curves. Curves show a sigmoidal shape with a lag, exponential and plateau stage. Cq value is calculated from a defined threshold.

#### 9.4 Post-Amplification Controls

As SYBR® Green is a non-specific double stranded DNA dye, a number of post-amplification methods can be taken to ensure that the fluorescence measured is as a result of amplification of the GOI. A dissociation curve, also referred to as a melt curve, is a thermal protocol often programmed to begin immediately after amplification. The qPCR reaction is heated and a fluorescence measurement taken stepwise, either by degree or fraction of degree Celsius, usually from 60 to 95°C. As the amplified product strands dissociate from one another, SYBR® Green dissociates and ceases to fluoresce. The temperature at which the strands dissociate is dependent on the amount of base pairs in the product; a longer amplicon will dissociate at a higher temperature due to a higher number of hydrogen bonds present between the bases in each strand. By plotting the rate of change in fluorescence against temperature (Figure 8.4) and knowing the expected melt temperature ( $T_m$ ) of the amplicon, one is able to check if the product is at least the

expected size and if any nucleic acid contaminants of different  $T_m$ s have been amplified. The size of qPCR products can also be validated by agarose gel electrophoresis. Separating PCR products in a gel with a DNA ladder reference is able to show the size of all amplified nucleic acids and can serve as a method of assessing specificity of fluorescence. Although neither of these methods can verify with certainty that measured fluorescence is as a result of specific GOI amplification, they go some way to demonstrating that it is likely.

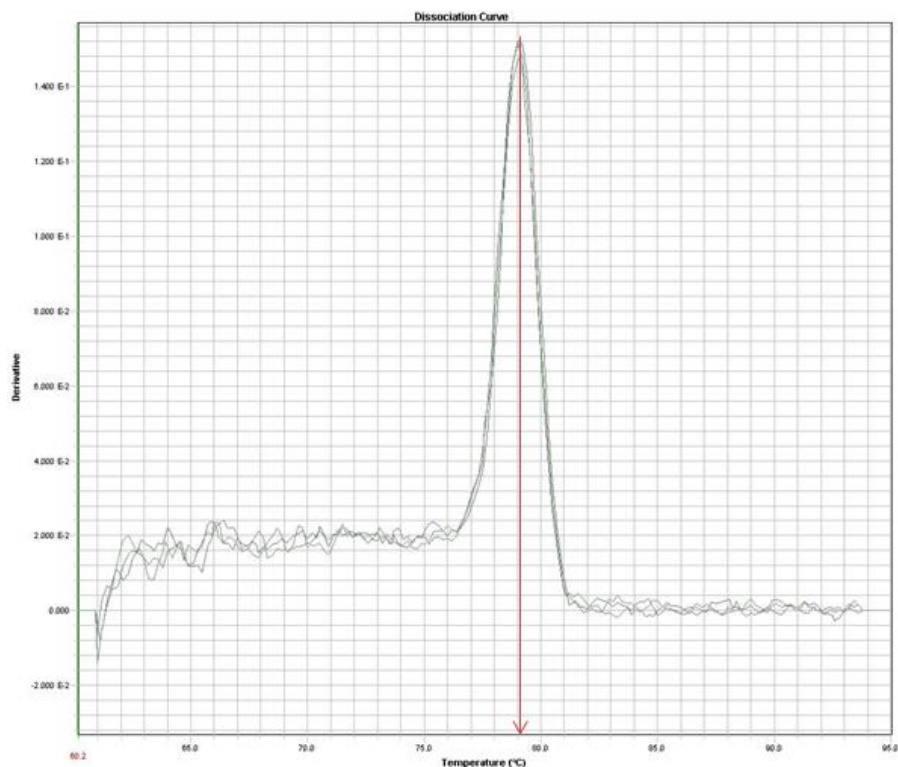


**Figure 9.4** - An example of three technical replicate dissociation curves. Replicates mimic each other well and only one peak is observed, indicating that the  $T_m$  is 79°C and there are no products of other sizes present.

Contamination can present a major problem in qPCR experiments. The inherent nature of an amplification experiment means that even the smallest amount of nucleic acid contamination can be represented in the data to a similar degree as the amplicon. For this reason, non-template controls (NTCs), where template is replaced with sterile water, should be included with every experiment to validate that amplification is a result of the template and not reagent contamination.